

Assessing the Role of Solution Chemistry and Organic Matter in the Genesis of the Dengying
Formation Dolostones at Sichuan Basin, China

By
Bryan J. Rodriguez-Colon

B.S. Geology and B.S. Biology, University of Puerto Rico at Mayagüez, 2017.
© 2020

Submitted to the graduate degree in Geology and the Graduate Faculty of the University of
Kansas in partial fulfillment of the requirements of the degree of Master of Science.

Chair: Jennifer Roberts

Alison Olcott

Randy Stotler

Date Defended: 12/3/2020

The thesis committee of Bryan J. Rodriguez-Colon certifies that this is the
approved version of the following thesis:

Assessing the Role of Solution Chemistry and Organic Matter in the Genesis of the
Dengying Formation Dolostones at Sichuan Basin, China.

Chair: Jennifer Roberts

Date Approved: 12/3/2020

Abstract

The role that microorganisms play in low-temperature dolomite formation is still unresolved. Given the scarcity of dolomite in modern low-temperature depositional settings, controls on its formation remain unclear. Textural evidence from modern and ancient geomicrobiological dolomite-forming environments, combined with laboratory experiments that produce dolomite phases associated with microbial surfaces and metabolism, support a microbial model for dolomite formation. However, more research is needed to substantiate this model. This study here aims to clarify the role of organic matter abundance and solution chemistry in a putative microbial dolomite: the Neoproterozoic dolomite of the Dengying Formation, Sichuan Basin, China. Researchers debate the origin of dolomite with different data supporting a microbial model conflicting with late-state hydrothermal dolomite. This study tested the microbial model for dolomite formation in the Dengying using controlled laboratory experiments constructed to emulate Ediacaran seawater chemistry (ESW) with abundant microbial mats. The constructed Ediacaran solution chemistry accounted for alkalinity, pH, temperature, and dissolved sulfate. Experimental variables included differing Mg:Ca (1:1) ratios, the presence of dissolved silica in solution (ESW no silica), and presence/absence of synthetic organic matter (in the form of carboxyl microspheres).

Solution pH, alkalinity and dolomite saturation index decreased through the incubation period in all solutions. Further, aragonite and Mg-calcite (with mol % of Mg ranging from 15-25% MgCO_3) precipitates were the main mineral suite of the ESW solution, while calcite and small yields of aragonite predominated in the 1:1 solution. Further, microscopy analysis shows an association between magnesium ions and dissolved silica, the presence of spheroidal precipitates associated with the microspheres and possible Mg-carbonate precipitation in the carboxylated

surfaces. Despite trends in the literature that suggest both silica and organic carbon play crucial roles in the availability of Mg for the dolomite reaction, our results did not document dolomite nucleation and precipitation from any of the studied solutions. Our summarized results suggest parallelisms with likely initial stages of carbonate precipitation in the Ediacaran prior to early or late stage dolomitization processes. While results from this study do not substantiate a microbial model of dolomite formation nor do they abrogate this possibility, our data underscore the complex interactions between solution chemistry and surface nucleation and their interaction to produce dolomite at low temperature.

Acknowledgements

First of all, I would like to extend my thanks to my advisor, Dr. Jennifer Roberts, for her endless support during my master's degree endeavor. She has been there for me since day one and have been supporting me during these years. Thank you for your patience, support and knowledge, Jen. To my masters committee, Alison Olcott and Randy Stotler, many thanks for your support, recommendations and great discussions throughout these years. I could not have chosen a better masters committee.

I would also want to thank to Adam Yoerg. Adam's help and guidance during my first semester in the laboratory was crucial for me and the project, and for that I will be eternally grateful. To my lab mates, Shawn Dunaway, Zijie Gao and Marissa Duckett, thanks for your help and great memories in the laboratory. To Adrienne Seiden, thank you for your insights on the project as well.

I would also extend my gratitude to the faculty members, such as Luis Gonzalez, David Fowle, Bob Goldstein, Gwen Macpherson, Noah McLean, Craig Marshall, Andreas Moeller and Gene Rankey, who gave me insightful recommendations through my academic journey. I would also like to thank Eduardo Rosa-Molinar, Noraida, Irma, Prem and the rest of the MAI team for your incredible help and teaching with the electron microscopy tools. In that line, many thanks to Victor and Zach Day for the training and help with the XRD machine and data analysis. I would like to thank the department of Geology, PetroChina and KICC for their financial support throughout during my research.

To my undergraduate advisors, Edgard Rivera-Valentin and Wilson Ramirez, I would also like to thank you for continuing advising and supporting me throughout these years. To Leila, I want to thank you for your endless help and also for helping me settle in my new life at Lawrence. And

to the incredible people I met and the new friends I made in Lawrence, thank you for the great time here.

Finally, I would like to dedicate this thesis to my mom, my grandparents, my dad and my best friends: Pedro, Sharlyn, Alejandro, Wilfredo, Rudy, Lola, Carolina, Julio, Giovanna and Hector. Without you all, this journey would had been more difficult. You all gave me the strength to continue. Thank you for being always there for me, in the bright days but also in the dark ones.

Table of Contents

Abstract.....	iii
Acknowledgements	v
List of Tables	ix
List of Figures.....	ix
Introduction.....	1
Background	3
<i>Models for Dolomite Formation</i>	4
<i>Late-Diagenetic Dolomites</i>	4
<i>Early-Diagenetic Dolomite Formation</i>	5
<i>Ancient Dolomitic Microbialites</i>	7
<i>Dengying Formation and Ediacaran Seawater Chemistry</i>	8
Methods.....	10
<i>Laboratory Batch Reactors and Solution Chemistry</i>	10
<i>Testing the role of Mg:Ca ratio and the presence of dissolved silica</i>	12
<i>Aqueous Geochemistry</i>	13
<i>Mineralogy and Microscopy of Bulk Sediment</i>	13
Results	15
<i>Ediacaran seawater solution (ESW)</i>	15
<i>Effect of the Mg:Ca ratio</i>	17
<i>Effect of the Silica content</i>	18
<i>Effect of the organic matter abundance</i>	19
Discussion.....	21
<i>Dolomite precipitation from Ediacaran seawater</i>	21
<i>The role of Mg:Ca ratios</i>	23
<i>The role of temperature</i>	25
<i>The role of dissolved SO₄</i>	26
<i>The role of dissolved silica</i>	27
<i>The role of organic matter</i>	31
<i>Implications for Dengying Formation</i>	35
Conclusion	41
Tables	1
Figures.....	45

References	62
Appendix A	70
Appendix B: PhreeqC models.....	85
<i>Model for ESW original solution chemistry.....</i>	<i>85</i>
<i>ESW NoSi solution chemistry:.....</i>	<i>127</i>
<i>Model ESW** 93-day solution model:</i>	<i>166</i>
<i>ESW11 solution model:.....</i>	<i>192</i>

List of Tables

Table 1: Solution chemistry corresponded to the studied solutions.

Table 2: MgCO₃ mol % in Mg-calcites from the 6.1:1 solutions.

List of Figures

Figure 1: pH and alkalinity evolution on the 15-day batch experiments.

Figure 2: pH and alkalinity evolution on the 93-day batch experiments.

Figure 3: Mg:Ca ratio evolution.

Figure 4: Saturation Indices for ESW and ESW with no silica (ESWNoSi) of dolomite through the 15-day batch experiments.

Figure 5: Saturation Indices for ESW and ESW11 of dolomite through the 93-day batch solutions.

Figure 6: X-Ray diffraction analysis for the ESW precipitates after 5, 10 and 15 days.

Figure 7: X-Ray diffraction analysis for the ESW solution precipitates after 14 days and 93 days.

Figure 8: ESW control batches for 5 days and 15 days.

Figure 9: ESW control batches for 15 day and 93-day experiments.

Figure 10: X-Ray diffraction analysis for the ESW11 solution precipitates after 15 and 93 days.

Figure 11: ESW11 control solutions for 15 days and 93 days.

Figure 12: X-Ray diffraction analysis for the EWS with no silica precipitates after 5, 10 and 15 days.

Figure 13: ESW solution with no silica control precipitates for 5 days, 10 days and 15 days.

Figure 14: A Mg-Ca precipitate is spotted in the ESW solids with no silica present.

Figure 15: The presence of small (~0.2-0.3 nm) spherical precipitates are shown in all batch solutions and in association with the carboxylic microspheres.

Figure 16: ESW seeded solution precipitates (day 15).

Figure 17: Transmission Electron Microscopy throughout a microsphere surface (day 15). Line scan using TEM.

Figure Ap.1: Calcium and magnesium evolution through the 15-day batch experiments.

Figure Ap.2: Saturation Indices of calcite (15 days) through time.

Figure Ap.3: Saturation Indices of aragonite (15 days) through time.

Figure Ap.4: Calcium and magnesium evolution through the 93-day batch experiments.

Figure Ap.5: Saturation Indices of calcite (93-days) through time.

Figure Ap.6: Saturation Indices of aragonite (93 days) through time.

Figure Ap.7: EDS spectra for Figure 8

Figure Ap.8: Elemental spectra for ESW control (Figure 9; A-14 days, B-93 days) and (C) experimental solution precipitates (Figure 16).

Figure Ap.9: ESW precipitates after 10 days of incubation

Figure Ap.10: Elemental spectra for the SW11 control.

Figure Ap.11: Elemental spectra for the TEM data (Figure 17)

Figure Ap.12: SEM captures of ESW precipitates.

Figure Ap.13: SEM captures of ESW non-silica batch precipitates.

Figure Ap.14: TEM captures of spheres with precipitates in the surface on ESW 6:1 solution.

Figure Ap.15: Close up of TEM captures of spheres with precipitates in the surface on ESW 6:1 solution.

Introduction

Biogeochemical processes at low-temperature (<80°C) and surface conditions can significantly influence mineral formation in natural systems. In particular, the role of microorganisms in facilitating the rates of dolomite [MgCa(CO₃)₂] formation has received substantial attention in the last twenty years (e.g., *Petrash et al. 2017*). Unlike other carbonate phases (e.g., calcite and aragonite, [CaCO₃] polymorphs), dolomite is scarce in modern-depositional settings due to a kinetic inhibition to precipitation at low temperature. The presence of naturally occurring dolomite in present-days settings are constrained to environments with high microbial activity or related to geomicrobial systems such as microbial mats and microbialites (*Bontognali et al. 2010*). This interconnection between the presence of authigenic dolomite and microbially-active systems has not only been observed in present day conditions, but also throughout geologic time, as many ancient microbialite carbonate formations are associated with dolostone formations (*Peters et al., 2017*).

One example of these ancient systems is the Neoproterozoic dolomites in the Sichuan Basin in central China (*Chen et al. 2017; Lin et al. 2017; Wang et al., 2020*). More specifically, the Dengying Formation (~552-541 Ma), which is part of the Sinian Yangtze region, is of special interest in ancient microbial dolomite studies. Petrographical, textural and isotopic evidence suggests that some of the geologic units from this formation could have a microbial origin (*Peng et al. 2014; Lin et al. 2017; Wang et al., 2020*). Furthermore, it has been shown that some of the dolomites could have formed in syngenetic and penecontemporaneous stages, which is consistent with modern depositional stages of precipitation in microbial mats throughout present-day depositional systems (*Bontognali et al. 2010; Lin et al. 2017; Chen et al. 2017*). However, the presence of hydrothermal alteration, high-temperature dolomite phases such as saddle dolomite

and fluid inclusion analysis within some of these geologic units has posed a debate on the origin of the Dengying Formation dolostones (*Feng et al., 2017*).

This study will test the hypothesis the low-temperature, organogenic model for Dengying Formation dolostones using laboratory-controlled experiments supersaturated with respect to dolomite and seeded with synthetic organic matter. Results from these experiments will give insight into the origin of putative low-temperature dolomites, such as those in the Dengying, and further inform the varying roles of solution chemistry and surface nucleation in dolomite formation.

Background

Dolomite [$\text{CaMg}(\text{CO}_3)_2$] is a common mineral observed in a variety of carbonate depositional systems through time. Together with calcite and aragonite (CaCO_3 polymorphs), dolomite is an important building block in many ancient carbonate rock formations around the world (*Machel, 2004; Peters et al., 2017*). Earth science researchers frequently use dolomite to constrain geochemical parameters (e.g., seawater chemistry, sea-level changes, climate), underscoring its importance as a proxy for environmental parameters such as temperature within fields such as paleoclimatology (*Vasconcelos et al., 2005; Vandeginste and John, 2012; Diaz-Pulido et al., 2014; Meng et al., 2015*). Further, many productive carbonate petroleum reservoirs (for oil and gas) around the world are composed of dolomite, in part, due to its preservation of porosity upon burial compared to limestone reservoirs (*Noris, 1957; Walton and Neill, 1963; Cantrell et al., 2001; Machel, 2004; Shen et al., 2016*). Therefore, the study of the formation and later diagenetic alteration of dolomite is significant for both interpreting geologic history as well as understanding this mineral's role as a petroleum and natural gas resource.

Dolomite is defined by its crystal structure, which requires ordered layering of Mg and Ca within the lattice, and an Mg:Ca ratio of 1 (e.g., ordered, stoichiometric dolomites; *Gregg et al., 2015*). Disordered Mg:Ca carbonates with very high Mg content ($\sim\text{Mg:Ca}=1$) retain the calcite crystal structure and therefore are referred to as very high Mg-calcite (VHMC), although these are colloquially referred to as proto-dolomites or disordered dolomites (*see Gregg et al., 2015*). While dolomite is widespread in ancient carbonate formations, it rarely forms in modern low-temperature carbonate depositional settings (*Machel, 2004*) despite the fact the modern seawater is supersaturated with respect to dolomite (*Coggon et al., 2010*). Previous studies have attempted to synthesize dolomite under abiotic low-temperature controlled laboratory conditions; however,

none of these attempts have been successful (*e.g.*, Land, 1998; Yoerg, 2018). The dichotomy between dolomite’s ubiquity in ancient rocks and its scarcity in modern-day systems, ostensibly due to a kinetic inhibition of formation at low temperature (<80°C), is often characterized as the “Dolomite Problem” (Fairbridge, 1957; McKenzie, 1991; Arvidson and Mackenzie, 1999).

Models for Dolomite Formation

Despite the scarcity of dolomite formation in modern sedimentary environments, dolostones are abundant in ancient rocks, and their genesis is described by several models based on the depositional, petrographic, morphologic, and geochemical evidence observed in dolostone formations (Adams and Rhodes, 1960; Land, 1973; McKenzie et al., 1980; Machel, 2004). These models are divided according to two types of dolomites (Machel, 2004). Most models for low-temperature dolomite formation are relevant for synsedimentary environments, in which primary dolomite is formed (*see Eq. 1*), while many of these specifically describe the more extensive occurrence of dolomite formation through dolomitization, in which pre-existing limestone is transformed into dolostone through interaction with Mg-rich fluids (*e.g. Eq. 2*; Adams and Rhodes, 1960; Land, 1973; McKenzie et al., 1980).



Late-Diagenetic Dolomites

Dolomite can form as a diagenetic product. A common model for late-diagenetic secondary dolomites is constrained to hydrothermal settings (Machel, 2004; Davies, 1997). In high temperature, hydrological systems, fluids often migrate through fractures and faulting zones, resulting in the alteration and dolomitization of pre-existing limestone formations (Davies, 1997; Lonnee and Machel, 2004). Dolomites of this category present distinct morphological features,

such as the presence of saddle dolomite (*Davies, 1997*). It is estimated that many ancient dolomites observed in nature are a byproduct of this type of dolomitization (*Goldsmith, 1980*). Furthermore, it is well known that high-temperature dolomites are less constrained in nature than their low-temperature counterparts (*Goldsmith, 1980*).

Early-Diagenetic Dolomite Formation

Several models for dolomite formation focus on low-temperature dolomite, as many ancient dolomites bear isotopic signatures that suggest dolomite was formed syndepositionally. The mixing zone dolomite model, for example, refers to environments in which seawater, supersaturated with magnesium, mixes with subsurface meteoritic waters in a marine carbonate platform (*Land, 1970*). As a result, these meteoritic hydrological systems can promote the dissolution of other carbonate minerals such as calcite and aragonite, followed by the precipitation of dolomite in solution throughout the mixing boundary of the seawater/freshwater interface (*Land, 1970*). However, it has also been suggested that these processes would not be replicated in natural settings given thermodynamic constraints (*Hardi, 1987; Machel, 2004; Li et al., 2013*).

The reflux model for dolomite formation involves the evaporation of saline fluids with high concentrations of magnesium. High evaporation rates cause dense brines to move downward into the platform subsurface, resulting in the formation of dolomite as an early diagenetic byproduct from pre-existing limestone (*Adams and Rhodes, 1960; Deffeyes et al., 1965*). Sabkha and alkaline lacustrine settings have been proposed as syndepositional dolomite forming environments, as they present similar mechanisms to those of the reflux model (*McKenzie et al., 1980*). Similarly, other environments for dolomite formation in association with silica gels in lacustrine settings (resulting from the formation of extensive Mg-silicates such as stevensite), have been suggested as additional models for dolomite synthesis (e.g., the pre-salt carbonate formations; *Wright, 2012*).

Across modern carbonate depositional settings, the detection of naturally occurring dolomite and VHMC mineral phases has been constrained to environments associated with microbially-active systems such as microbial mats, microbialites, and organic-rich sediments (Warren, 1990; Vasconcelos and McKenzie, 1997; Kenward et al., 2009; Bontognali et al. 2010; Last et al., 2012; Brauchli et al., 2015; Pace, et al., 2016; Samylina and Zaytseva, 2018; Sanz-Monteto et al., 2019; Diloreto et al., 2019; Rodriguez-Colon et al., 2019). This has led to the formulation of another model for authigenic dolomite formation, called the microbial dolomite model (Vasconcelos and McKenzie, 1997; Wright, 1999; Kenward et al., 2009; Bontognali et al. 2010). Controlled laboratory experiments have further supported this model by reporting the formation of authigenic ordered dolomites and disordered VHMC precipitates in association with microorganisms such as sulfate-reducing bacteria, methanogens, fermenters, halophilic archaea, and anoxygenic phototrophs (Vasconcelos et al. 1995; Roberts et al. 2004; Wright and Wacey, 2005; Sanchez-Roman et al. 2009; Kenward et al., 2009; Daye et al., 2019). These studies have found that actively-metabolizing microbial communities can play a role in the synthesis of carbonate minerals by altering the micro-environment surrounding the microbes, thus creating the geochemical conditions necessary for dolomite to form (e.g., dolomite saturation, sulfate depletion, changes in Mg:Ca ratios, pH and increase alkalinity; Petrash et al., 2017). Other studies, however, have suggested that the presence of organic matter in the form of microbial surfaces and complex biofilms—not necessarily active metabolism—are satisfactory for dolomite to form (Braissant et al. 2007; Roberts et al. 2013; Bontognali et al. 2014; Sanz-Monteto et al., 2019). Indeed, much about the genesis and timing of dolomite formation in ancient rocks remains contested. Certainly, modes of low-temperature dolomite formation are not well validated in modern carbonate settings or with laboratory experiments, and ancient rocks may have multiple

generations of diagenesis that may blur the mode of dolomite genesis. Nevertheless, there are abundant examples of dolomites with observed microbial textures within the geologic record, suggesting that more research is needed to elucidate whether the association between dolomite and microbial communities is indeed causal.

Ancient Dolomitic Microbialites

The geologic record contains numerous examples of dolomite associated with textures and fabrics attributed to microorganisms (*Grotzinger, 1990; Shan et al. 2017; Lin et al. 201; Meister et al., 2013; Peters et al., 2017; You et al. 2018*). In fact, previous research has demonstrated a positive correlation between the occurrence of putative microbialite systems in carbonate rocks with the abundance of dolomite that span geologic time (*Peters et al., 2017*). For example, in the Tarim Basin of northwestern China, microscopy observations indicate the presence of dolomitic spheroids within stromatolitic fabrics (*You et al. 2018*). Previous studies have also shown correlation between the dolomites in Alpine Triassic Units with penecontemporaneous stages of formation (i.e., syndimentary), thus suggesting these dolomites could have formed in low-temperature environments with active microbial processes (*Meister et al., 2013*). Further, diagenetic features of the Alpine dolomites, combined with the documentation of possible microbial fabrics (e.g., laminated dolostone units), suggests this type of dolomite formed in a shallow marine or evaporitic setting (*Meister et al., 2013*).

Precambrian units are of special interest in the study of the relation between microbial processes and the formation of dolomites (*Harwood and Sumner, 2011; Grotzinger and Al-Rawahi, 2014; Chen et al. 2017; Peters et al., 2017*). Microbial mats, preserved as microbialites, are the earliest complex ecosystems in Earth's geologic and biologic history (*Grotzinger, 1990; Des Maris, 1990*). Moreover, an interrelation between microbial carbonate formations and the

occurrence of dolostones has been observed through the geologic time, including the Precambrian (*Peters et al., 2017*). The role of microbial systems in the origin of ancient dolostones is still a matter of debate, though specific locations can elucidate important findings related to this ongoing investigation.

Dengying Formation and Ediacaran Seawater Chemistry

One of the best examples of Precambrian dolomite units with a possible microbial origin are the Late Neoproterozoic dolostones of Sichuan Basin, central China (*Shan et al. 2017; Lin et al. 2017*). These dolostones, which include the Dengying Formation (which is part of the Sinian Yangtze region), date to the Ediacaran Period (~552-541 Ma). The dolomites of the Dengying Formation contain extensive microbial fabrics, which are observed throughout the units. Specifically, the second and fourth units of this system have shown distinct stromatolitic macrofabrics and other geobiological-related structures such as well-developed laminar microbial mats, stromatolitic systems, and thrombolite and leolite structures (*Chen et al. 2017; Lin et al. 2017; Wang et al., 2020*). These two units contain characteristics typical of tidal flat and hypersaline lagoon depositional systems, which is consistent with the formation of microbial communities such as microbial mats and stromatolites. Other structures present in the units, such as botryoidal textures, have also been associated with biogenic origin (*Lei and Zhu, 1992; Peng et al. 2014; Wang et al, 2020*).

The proposed microbial origin of these dolostones suggests a crucial relation with the seawater chemistry in the Ediacaran Period (ESW), which is distinct from modern seawater in several important ways. Previous fluid inclusion studies of halite deposits from the Ara Formation in Oman have shown that the total molar concentration of $[Mg^{2+}]$ and $[Ca^{2+}]$ in seawater during the Late Neoproterozoic, Ediacaran, and Early Phanerozoic periods had higher Mg:Ca ratios

(approximately 6.1:1) than those observed in modern seawater (approximately 5:1). Data indicate that $[\text{Mg}^{2+}]$ and $[\text{Ca}^{2+}]$ in the Late Neoproterozoic also correspond to higher values than those observed in present-day seawater chemistry, while values of dissolved sulfate $[\text{SO}_4^{2-}]$ were lower in Ediacaran seawater (ESW) than modern values (*Horita et al., 2001*). Previous research also suggests the lack of marine silica-biomineralized organisms during the Ediacaran Period resulted in differences in the silica cycle in surface marine waters compared to modern conditions, and therefore impacted the presence of dissolved silica in Precambrian seawater (*Siever, 1992*). Unlike modern values, it is proposed that silica values in ESW were ~ 60 times higher than those observed in modern seawater (*Siever, 1992*). The suggestion that the dolostones of the Dengying Formation formed in penecontemporaneous (i.e., syndimentary) stages related to subtidal intraplatform microbial reef system is consistent with modern depositional stages of dolomite precipitation in microbial systems (*Peng et al., 2014; Lin et al. 2017; Chen et al. 2017*).

Indeed, the extensive presence of preserved microbial relics within the Dengying Formation, coupled with isotopic analysis, support the hypothesis of a microbial origin for these dolomite formations. Yet other hypotheses offer alternative explanations for the dolomitization of these rocks. For example, the presence of saddle dolomite, which is a prominent dolomitic morphology observed in hydrothermal dolomite formations, has been documented in some units in the Dengying Formation (*Feng et al., 2017*), suggesting a more complicated genesis of dolomite. Further, fluid inclusion analysis and isotopic fractionation data suggest that some of the dolomites observed in the Dengying Formation units were formed in the presence of high temperature fluids (*Feng et al., 2017*). Other studies have described many of the facies throughout the units as microbial in origin, with latter diagenetic changes that resulted in hydrothermal features (*Chen et*

al., 2017). In general, these findings (both the microbial and the hydrothermal evidence) make the Dengying Formation a disputed location in terms of dolomite genesis.

Taking into consideration the role of the Dengying formation as an important natural gas reservoir in China, it is essential to understand the primary mechanisms of the formation of these dolomitic reservoirs in order to better comprehend the diagenetic and pore evolution of the system (*Zhang et al.*, 2017). This study further examines the organogenic model as a plausible explanation for the development of dolomites in the Dengying Formation by investigating the presence of organic matter and the role of Mg:Ca ratios on dolomite formation in solutions that simulate Ediacaran seawater conditions as well as considering other geochemical factors (e.g., the presence of dissolved silica) that may contribute to dolomite formation or its precursors at low-temperature.

Methods

The genesis of putative low-temperature dolomite in Dengying Formation dolostones was investigated using batch laboratory experiments. Experiments were conducted under conditions that simulated those present in seawater during the Late Neoproterozoic; specifically, the water chemistry conditions during the Sinian sequence, which is part of the Ediacaran Period (635-541 Ma) (*Horita et al.* 2002; *Meng et al.* 2011; *Lin et al.* 2017; *Walker et al.*, 2018). Experiments utilized solutions supersaturated with respect to dolomite and monitored the formation of dolomite or Mg-bearing Ca-carbonates as a function of solution chemistry and the presence of carboxylated organic matter.

Laboratory Batch Reactors and Solution Chemistry

Controlled laboratory batch reactors contained solutions were prepared from stock reagents (NaCl, Na₂CO₃, CaCl₂*2H₂O, MgCl₂*6H₂O, Na₂SO₄ and Na₂SiO₃) to simulate the chemical conditions of ESW. Salinity was adjusted to slightly higher than normal seawater, or slightly

evaporated seawater consistent with near-shore environments, such as those observed in Shark bay stromatolite systems at Hamelin Pool, Australia, and thus simulating a subtidal intraplatform system like those interpreted in Dengying (*Chen et al., 2017; Babilonia et al., 2018*). The mass of each salt, measured in grams, was calculated using a constructed digital calculator in Excel (*Yoerg, 2018*) to achieve values that corresponded with the geochemical data for ESW (e.g., Mg:Ca ratios, salinity, alkalinity, and concentrations of dissolved sulfate and silica; e.g., *Siever, 1992; Horita et al., 2001*). The complete solution composition is presented in **Table 1**.

PHREEQC (v. 3.4 for MacOS; *Parkhurst and Appelo, 2013*) was used to speciate solutions and calculate ionic strength, theoretical solution alkalinity, and saturation indices (SI) for carbonate minerals (aragonite, calcite, dolomite) and silicate phases (e.g., sepiolite and talc). Because the solution ionic strengths were greater than 1 mol kg⁻¹ (*see Table 1*), Pitzer equations were used to calculate the saturation indices using the Pitzer.dat database. Unlike other databases, the Pitzer model gives more accurate values for solutions with high salinities (< 1 mol kg⁻¹) (*Plummer et al., 1988*).

Batch reactors were prepared using autoclaved Milli-q 18 M Ω deionized water. In order to achieve complete dissolution of the salts without any reaction prior to the experiment period, two separate bottles (one with the magnesium and calcium source and the other with the sulfate, carbonate and silica source) were prepared separately. Following the mixture, an instantaneous precipitation reaction was observed, which persisted during the solution preparation. Following solution preparation and mixture, the pH was fixed to 8.5 by bubbling the solution with CO_{2(g)} under normal atmospheric conditions (pCO₂ of 10^{-3.5} atm), which corresponds to pH values that have been detected in modern lacustrine systems in which microbial Mg-carbonate precipitation

occurs (*Vasconcelos and Mckenzie, 1997; Casillas-Martinez et al., 2005; Paul et al., 2016; Bouton et al., 2016; Rodriguez-Colon et al., 2019*).

Following the adjustment of pH, the solution was separated into sterile, 100 mL borosilicate serum bottles. Each experiment consisted of two experimental vessels and one control vessel. Experimental vessels were seeded with functionalized polystyrene microspheres (©Bang Laboratories, Inc.) to a concentration of 6×10^{12} R-COO⁻ groups L⁻¹ (*see Table I*). These microspheres, made of polyester latex, are embedded with carboxyl groups (with a R-COO⁻ density of 796 µeq/g); thus, they enable the investigation of the role of microbial surfaces and biofilms in the nucleation of carbonate minerals such as dolomite (e.g., *Roberts et al., 2013; Kenward et al., 2013*). This was achieved by adding 1.2 µl of the microsphere solution to 100ml of the study solution. The batch reactors were then sealed with butyl rubber caps and placed in shaker incubators at 75 rpm and 40°C. This temperature is within the range of the suggested temperature values of global seawater during the Ediacaran Period (*Meng et al., 2011*).

Testing the role of Mg:Ca ratio and the presence of dissolved silica

In addition to creating the ESW solution and investigating the role of organic matter in the formation of low-temperature dolomite, two other sets of experiments were performed to investigate the role of 1) Mg:Ca ratios and 2) dissolved silica on dolomite formation. For this investigation, 15-day and 93-day batch experiments were conducted. For the 15-day experiments, control and experimental ESW solution batches were examined every five days to a maximum of 15 days (i.e., T=5 d, T=10 d, T=15 d). Further, an ESW solution experiment with no silica (named ESWNoSi) was also tested for a duration of 15 days. For the 93-day batch experiments, batches were examined only on day 14 and after three months (day 93). These batch experiments used a similar solution chemistry of ESW, except with an Mg:Ca ratio of 1:1 (named ESW11), which

was also investigated for 93 days to see how the molar ratios of $[\text{Mg}^{2+}]$ and $[\text{Ca}^{2+}]$ affect the process of dolomite formation (*see Table 1*).

Aqueous Geochemistry

Immediately after the solutions were created and thoroughly mixed (and before incubation), a 60 mL sample of bulk solution was collected and filtered (0.45 μm) and the alkalinity, pH, and cation concentrations were analyzed. Samples were also sacrificed at the end of the incubation period for geochemical and mineralogical analysis (T=5, 10, 15 d; T=14; 93 d). pH was measured using an Orion Sat A211 pH meter (©Thermo Scientific) with a calibrated pH electrode. For alkalinity, the solution was titrated with 0.1 M HCl using a Metrohm automatic titrator with an 807 Dosing Unit on a 0.45 μm filtered sample (~25-30 mL) and alkalinity was then calculated using Tiamo v 1.2 software. Cations were characterized on 0.45 μm filtered samples acidified to 2% using ultrapure concentrated HNO_3 and Inductively Coupled Plasma Optical Emission Spectrometry (ICP-OES).

Mineralogy and Microscopy of Bulk Sediment

The resulting precipitate was filtered, rinsed 3x with MilliQ DI 18M Ω water (to extract halite) and air-dried overnight in a hood. The dry powder was then divided, and subsamples were analyzed to determine mineralogy and characterized using electron microscopy. For mineralogy, Powder X-Ray-Diffraction analysis (PXRD) was performed on air-dried samples. The analysis was performed on a Bruker D2 Phaser powder x-ray diffractometer equipped with a 1D mode Lynxeye detector. X-rays (CoK α radiation, $\lambda = 1.79026 \text{ \AA}$) were conducted using a sealed tube operating at a voltage of 30 kV and 10 mA (300 W). Given the small amount of yield, the powder was held by a thin layer of oil/grease spread on a 24.6 mm x 1.0 mm Zero Diffraction Silica crystal plate (©MTI Corp) inserted into the standard D2 Phaser sample discs. Scan results were analyzed using

JADE software (©Materials Data, Inc). Since a cobalt radiation source was used to collect the data and most literature PXRD results are recorded with copper radiation, the spectra and results were converted to their copper counterparts using JADE software. Data visualization was performed using MATLAB v. R2019a software (©MathWorks, Inc). The mole percentage of MgCO₃ content in the Mg-carbonate precipitates was quantified using calculations from *Arvidson and Mackenzie, 1999*, where $\text{mol \% MgCO}_3 = -363.96 * (\text{d-spacing}) + 1104.5$. These calculations were made using a digital calculator in Excel with the X-Ray diffraction data for each sample.

Electron microscopy was used to examine the morphological features of the minerals formed in solution and to determine if precipitates were associated with the carboxylated microspheres. Air-dried samples were mounted on individual 12.7 mm aluminum stubs with carbon tape (©SPI supplies) for image acquisition. Samples were analyzed in the Microscopy and Analytical Imaging Laboratory at the University of Kansas. Before imaging, all samples were sputter-coated with approximately 10-35 μm gold using an EMS Quorum 150RS sputter coater. Images were captured on a Cold Field Emission Scanning Electron Microscope (Hitachi High Technologies, SU8230 series) with a secondary electron detector (SE) at accelerating voltages ranging from 5.0 to 10.0 kV, aperture 2 (80 μm diameter) and a working distance between 6.5 to 8.0 mm. Coupled with imaging, energy dispersive spectroscopy (EDX) was used to analyze major elemental components and their distributions throughout the precipitates. Element content spectra and distribution maps were collected at 10 kV using the Aztec software (Oxford 11 instruments).

For transmission electron microscopy, the air-dried sample was mounted on a copper mesh grid with lacey carbon film and examined using a FEI Tecnai™ G2 transmission electron microscope/scanning transmission electron microscope (TEM-S/TEM) at an electron acceleration

voltage of 200 kV. The morphology, size, electron beam diffraction patterns, lattice spacing, and elemental composition were determined by TEM-S/TEM and EDX.

Results

Ediacaran seawater solution (ESW)

Following the incubation period, batch reactors were opened, and fluids and precipitates were characterized. Both solution pH and alkalinity decreased during the first 15 days of incubation (**Figure 1**). Solution pH initially declined from 8.52 to ~7.54 during the first five days of incubation, then stabilized to ~7.57 for the remainder of incubation (with the exception of a slight increase on day 15). Alkalinity gradually decreased over the period of the experiment (from ~8.29 down to ~6.6 mmol L⁻¹).

The evolution of the solution pH and alkalinity for the 93-day experiments, shown in **Figure 2**, were similar to those observed in the 15-day experiments. Solution pH initially decreased by ~0.5 pH units (from ~8.5 to 8.0) during the first 15 days of incubation, then stabilized from day 15 to day 93, remaining at ~8.0. Similarly, alkalinity decreased from ~10.40 mmol L⁻¹ to ~8.47 mmol L⁻¹ in the first 15 days and then remained stable through the remaining experiment duration.

The differential evolution of [Ca²⁺] and [Mg²⁺] with respect to time (**Appendix A, Figure Ap.1**) facilitated changes in Mg:Ca molar ratios (**Figure 3**). Relative decreases in [Ca²⁺] concentration compared to [Mg²⁺] resulted in an increase of Mg:Ca ratios in the fluid throughout the incubation period compared to the modeled Mg:Ca ratio of the solution (**Table 1**). This was observed during the 15-day incubation, when the Mg:Ca ratio increased just after the experimental preparation (from a modeled ratio of 6.1:1 to ~17:1), followed by an increase in increments up to ~24:1 by day 15. For the 93-day experiments, an increase in the ratio is shown (up to ~50:1); however, the Mg:Ca ratio decrease was observed from day 15 (~50:1) to the day 93 (~43:1).

For both experiment durations, calcite, aragonite, and dolomite were all initially supersaturated in the fluid, and saturation indices decreased for all minerals (**Figures 4, Figure 5 and Appendix A, Figures Ap.2 and Ap.3**; for *PhreeqC* models, see **Appendix B**). The dolomite saturation index during the 15-day experiments decreased from ~4 to ~2.25 for the first five days, with no further changes during the following 10 days (**Figure 4**). For the 93-day experiments, a step decrease in the dolomite saturation index occurred, similar to what was observed in the 15-day experiments (from ~3.70 to ~2.60). The calcite SI initial supersaturation for the 15-day run decreased and stabilized at values close to equilibrium (~0.39). Although aragonite was initially supersaturated (**Appendix A, Figure Ap.5 and Ap.6**), it was undersaturated (down to -0.35) by the end of the experiment run 15-day run. Of note is that while the 15-day and 93-day batch experiments had different $[Ca^{2+}]$ and $[Mg^{2+}]$ concentrations in their initial solution chemistry (**Table 1**), the results from both runs showed similar trends.

The mineralogical analysis of the resulting precipitates is shown in **Figures 6 and 7**. X-Ray diffraction analysis revealed that aragonite was the principal mineral present in both the 15-day and 93-day experiments. A smaller C-104 ordering peak, which corresponds to Mg-calcite, was observed in all of the runs (*see sub-boxes in Figures 6 and 7*) (Gregg *et al.*, 2015). Mol % of Mg for all Mg-calcites formed in the solutions are shown in **Table 2**. In general, most of the Mg-calcites observed here showed high mol % of magnesium (~15-23 mol % of $MgCO_3$). Although the solutions were rinsed in deionized water, some halite residue was observed on day 10, which was interpreted to be an artifact of the drying process. Although the solution contained silica, no silicate minerals were detected in the clay mineral diffraction region (**Figure 6**).

Electron microscopy photomicrographs revealed three distinct morphologies of the precipitates produced from ESW (**Figures 8-9**). SEM coupled with EDX analysis revealed calcium

rich precipitates with dumbbell-shaped and spherulite-shaped morphologies (with an average size of $\sim 5 \mu\text{m}$). Closer inspection showed that the dumbbells were mainly composed of hexagonal crystals with an acicular growth pattern (**Figure 8D**). Smaller precipitates ($\sim 3\text{-}5 \mu\text{m}$) with an oblong shape were also detected. Elemental mapping indicated these solids were a mixture of calcium, magnesium, and silica (**Figure 8C**). The third type of observed morphology was amorphous (**Figure 8C and Figure 9**). Elemental mapping showed this amorphous morphology was composed of silica and magnesium (*see Figure 9*).

Effect of the Mg:Ca ratio

ESW reactors were compared to a similar solution recipe with a Mg:Ca ratio adjusted to 1:1 (referred to here as ESW11). The fluid evolution of this solution (compared with the ESW) is shown in **Figure 2**. Similar to what was observed for ESW, pH decreased (from ~ 8.39 to ~ 7.42) in batch solutions with ESW11 chemistry during the first 15 days of the incubation. However, unlike ESW solutions, the ESW11 pH slightly increased after 15 days, from ~ 7.42 to ~ 7.49 . Although both solution models had similar initial alkalinity values (**Table 1**), there were differences in the initial measured alkalinity values between ESW and ESW11. The initial value for alkalinity (in mmol L^{-1} of $[\text{CO}_3^{2-}]$) for ESW was $\sim 10.4 \text{ mmol L}^{-1}$, with a final value of 8.5 mmol L^{-1} . ESW11 alkalinity values were lower, measuring at 3 and 1.5 mmol L^{-1} respectively.

The evolution of Ca^{2+} in solution and the resulting Mg:Ca for ESW11 are very similar to ESW (**Appendix A, Figure Ap.4**). Overall, the data shows an incremental increase in the Mg:Ca ratio through the incubation period for ESW11 right before solution preparation, with values close to ~ 2.37 relative to the initial 1:1 ratio. However, no apparent changes are shown during the incubation period (**Figure 3**). Saturation indices for dolomite, calcite, and aragonite are shown in **Figure 5 and Appendix A, Figures Ap.5 and Ap.6**. A decrease in the saturation index of dolomite

from 3.31 to ~1.50 was documented. For calcite, values decreased almost to equilibrium (~0.45), while values for the aragonite saturation index decreased to values within the range of 0.16 and 0.26.

The mineralogical components of ESW11 are shown in **Figure 10**. In contrast to the ESW solids, Low-Mg-calcite is the dominant mineral (based on the peak intensity), with small yields of aragonite detected. Microscopy analysis coupled with EDX showed two distinct morphologies: 1) relatively big (~8-9 μm) calcium-rich spherulites composed of rhombohedral crystal aggregates and 2) an amorphous Si-Mg rich solid similar to those shown in the original ESW solution (**Figure 11**).

Effect of the Silica content

The fluid evolution of pH and alkalinity in ESW solutions with and without silica (ESWNoSi) are shown in **Figure 1**. Solutions with silica displayed a slower rate of change in pH and alkalinity compared to the original ESW solution. In contrast to solutions with Si, a faster rate of change in pH and alkalinity were observed during the first five days, when no silica was present. Solution pH decreased from ~8.50 to ~6.85 in ESWNoSi solutions, then increased to ~7 by day 15. Alkalinity decreased from 14.14 mmol L^{-1} to 9.05 mmol L^{-1} during the first five days, following a slow decrease down to 8.68 mmol L^{-1} at day 15.

The Mg^{2+} and Ca^{2+} evolution in ESWNoSi solutions is shown in **Appendix A (Figure Ap.1)**. A decrease in magnesium and calcium was observed during the first 15 days of incubation when silica was not present, whereas no step changes in magnesium were seen with silica in solution. A general increase in Mg:Ca ratios was observed in ESWNoSi solutions during the first 15 days of incubation, ranging from ~11:1 to ~26.1 (although a small decrease from ~20:1 to ~18:1 occurred between day five and ten) (**Figure 4A**). For the dolomite saturation index, a broader range in

saturation with respect to dolomite was observed when no silica was present in solution (between ~4.95 and ~1.43), compared to the original ESW solution (between ~3.98 and ~2.33). A steeper decrease in the dolomite saturation index was observed during the first five days when no silica was present (with ~1.63), followed by stabilization for the remaining 10 days of incubation time (**Figure 4**). An undersaturation of aragonite (~-0.23) was observed following day five, with a continued decrease down to ~-0.39 by the end of the run, whereas calcite was shown to be undersaturated on day 15 (with ~-0.07) (*see Appendix A, Figures Ap.2 and Ap.3*).

Solutions without silica presented no differences in the primary mineral components from those observed in the original ESW solution, with aragonite as the principal mineral and small yields of Mg-calcite (as shown in the c-104 ordering peak; *mol % of Mg is shown in Table 2*) (**Figure 12**). Microscopy analysis, however, did not detect the amorphous solid composed of silica and magnesium observed in ESW solutions in ESWNoSi solutions. Nevertheless, calcium-rich spherulites (~5-7 μm) composed of hexagonal crystals with an acicular growth were observed and no magnesium was detected (**Figure 13**). Lastly, one Mg-Ca precipitate (~3-5 μm) with an oblong shape was detected (**Figure 14**).

Effect of the organic matter abundance

All experimental solutions were examined in the presence of organic matter. The fluid evolution of the organic matter-seeded batch experiments for all solutions showed that seeded solutions present a similar behavior to the control experiments. 15-day batch solutions documented the difference in behavior between the control and seeded experiments, regardless of silica content (**Figures 1, 2, 3, 4 and 5**). In terms of pH evolution, a similar decrease was reported for the seeded solutions (~7.57) relative to their ESW control counterpart (**Figure 1**). However, solutions without silica (ESWNoSi) reported a lower decrease in pH after five days when organic matter was present

(~7) relative to the control solution (~6.85). Alkalinity values were slightly lower in the ESWNoSi solution for the first five days when organic matter was present (~9.27 mmol L⁻¹); however, values remained similar to the control values at day 10 (~8.90-8.95 mmol L⁻¹), followed by a gentle decrease of 8.81 mmol L⁻¹ relative to the control solution (~8.68 mmol L⁻¹). Mg:Ca ratios were very similar in both the control and seeded solutions for ESW; however, a lower ratio was reported for the seeded ESWNoSi solution at day 15 (~23:1) compared to the control solution (~26:1). The dolomite saturation index for the seeded solutions in ESW were shown to be very similar to the control (with a range between ~3.98 and ~2.30), whereas a higher saturation index (~4.95-1.72) was reported when organic matter was present in the ESWNoSi solutions. Dolomite saturation indices for the 93-days solutions show a higher depletion in dolomite saturation when organic matter is present, from ~3.72 to ~2.03 for the first 15 days, compared to the ~2.59 in the control values (with a final value of ~1.7 compared with the ~2.65 for the control solutions during day 93; *see Figure 5*). When taking the molar ratio into consideration, ESW11 experiments show no difference between the control and seeded solutions, with higher pH values occurring at day 15 and 93 compared to the control solutions (~7.54 and ~7.63, respectively) (*Figure 1, 3, 5*). Similarly, alkalinity values in ESW11 were close to the values observed in the control solution (between 2.9 and 1.75 mmol L⁻¹). Although no changes were observed in the Mg:Ca ratios for ESW11 with organic matter (~2:1) relative to the control solution, the dolomite saturation was higher compared to the control (down to ~1.67 at day 93 versus 1.43 for the control) (*Figure 2 and 5*).

The overall solid abundance in the seeded solutions did not notably differ from the ones observed in the control solutions. Further, there was no apparent change in the crystal size throughout all experiment runs when organic matter was present (*Appendix A, Figures Ap.12 and*

Ap.13). However, in all experimental treatments with organic matter (regardless of the silica content or Mg:Ca ratio), small (~0.2 µm) spherical precipitates were observed in association with the microspheres (*Figure 15*). Electron microscopy coupled with EDS documented a high abundance of silica and magnesium in the surface of the microspheres compared to the calcium content. Elemental mapping on SEM images also showed this association (*Figure 15*). Detailed TEM photomicrographs further confirmed this relationship, showing a higher abundance of silica and magnesium on the microsphere surface relative to calcium (*Figure 16 and Appendix A, Figure Ap.11*). EDX Line scan analysis showed a similar trend for the magnesium and silica, with higher counts closer to the surface of the microsphere. Calcium, on the other hand, had lower counts in proximity to the microsphere surface.

Discussion

Dolomite precipitation from Ediacaran seawater

Dolomitic formations with microbial relics through time can present ideal scenarios to unveil the role of microbial communities and the presence of organic matter in the genesis and early diagenetic changes of dolomite systems. Previous works have shown the possible microbial origins for the Sinian Dengying Formation dolostones, giving us an opportunity to investigate this further (*Wang et al., 2016; Chen et al. 2017; Lin et al., 2017*). In particular, isotopic analysis from rock samples on the fourth unit of the Dengying formation suggests that these dolomites formed near shore at low temperature conditions (*Chen et al. 2017*). Further, microbial relics throughout these geologic units are consistent with this interpretation (*Chen et al. 2017; Lin et al., 2017; Hu et al., 2020, Wang et al., 2020*). Therefore, we tested several scenarios that may impact dolomite formation at low temperature using the theoretical seawater chemistry from the time these microbialites systems were alive (i.e., Ediacaran seawater, ESW).

None of the experimental parameters in this study resulted in the formation of dolomite; however, some of the experimental treatments resulted in Mg-Calcite. Calcium carbonate minerals did form in all experiments as evidenced by, not only, mineralogical analysis, but commensurate evolution of fluid geochemistry. In batch solutions, the pH was adjusted to a slightly basic starting value (~8.5), approximating environmental conditions within the microbial systems (similar to those observed in Dengying Formation, e.g. *Bao et al., 2008; Ohnemüller, 2014; Ohnemüller et al., 2014; Halevy and Bachan, 2017*). In general, all the experimental runs experienced a decrease in pH during the incubation time. In ESW solutions, for example, pH values dropped from 8.50 to ~7.54 for those first 15 days of incubation. Similarly, alkalinity also decreases. Within the first 15 days of the ESW solution run, alkalinity decreases from 10.2 mmol L⁻¹ to 8.47 mmol L⁻¹. Both parameters are essential for carbonate mineral formation and pH is also essential for the saturation and stabilization of authigenic carbonate minerals (*Feely et al., 2009*). The decrease in alkalinity and pH during our incubation period translates for the depletion of carbonate ions out of solution as precipitation takes place. Yet, although batch experiments were created to be supersaturated with respect to dolomite, no dolomite detection was observed in the bulk sediment. Previous work by *Yoerg, 2018* showed that solutions with extremely high alkalinity and pH values (as those observed in alkaline lake systems), lead to the formation of a variety of Mg-bearing carbonate minerals, linking the increase in the saturation state of the minerals (relative to alkalinity and availability metals in solution) with the successful removal of magnesium out of solution. Although experiments in this study contained elevated values of alkalinity compared to modern oceans, it is still lower compared to the alkaline geochemical model studied by *Yoerg, 2018* and to what is observed in modern microbialite-forming systems (*Vasconcelos and McKenzie, 1997; Bontognali et al. 2010; Samylina and Zaytseva, L. V. 2018*).

The role of Mg:Ca ratios

Bulk mineralogical analysis of ESW batch experiments indicates that aragonite and small amounts of Mg-calcite (~18.28-25.28 mol %MgCO₃; *calculations based on Arvidson and Mackenzie, 1999; see Table 2*) are shown to be the main minerals in the bulk precipitate. SEM/EDX confirms these observations, main carbonate precipitates with spherulite-shaped morphologies (~5 μm) composed of calcium-rich hexagonal crystals with an acicular pattern, and smaller (~3-5 μm) precipitates with oblong shape mainly composed of calcium with small traces of magnesium (*see Figure 8b and Figure 14*). These results are typical of a mineralogy precipitated under high Mg:Ca (*Lowenstein et al., 2001*). In present-day marine carbonate depositional systems, for example, Mg:Ca ratios of 5.1:1 favor aragonite as the primary and more stable carbonate mineral to form (*Lowenstein et al., 2001*). In ocean waters with Mg:Ca ratios higher than two (e.g., Ediacaran Period, late Paleozoic to mid Mesozoic and late Cenozoic to present), for example, aragonite and Mg-calcite will dominate, since excess of magnesium ions in solution can inhibit the formation of the calcite polymorph, resulting in a favoring to the aragonite polymorph (*Lowenstein et al., 2001*). In contrast, experiments performed with Mg:Ca ratios of ~1 (ESW11), produced calcite and very small amounts of aragonite (*see Figure 10*), with SEM/EDX data showing spherulitic calcium-rich precipitates composed of rhombohedral crystals aggregates (*see Figure 11*). Ocean chemistries with a Mg:Ca ratio closer to one (e.g., early and mid-Paleozoic and Late Mesozoic) favor calcite to be the main mineral polymorph (*Lowenstein et al., 2001*), and dolomite. One thing to consider with both experiments is that both experimental solutions (with Mg:Ca of 6.1:1 and 1:1) were formulated to be saturated with respect to dolomite (*see Table 1*). Therefore, the inhibition of the formation of dolomite in these experiments, and by extension in marine carbonate systems, is not caused by a lack of supersaturation; rather, there is a kinetic

barrier that plays a role, as is shown by previous works (*i.e.*, Land, 1998). Nevertheless, results from the experiments taken together are consistent with the geologic record, which documents Mg:Ca ratios in ocean water through time correlated to dominant carbonate polymorph (*i.e.*, aragonite and calcite; Wilkinson and Given, 1986).

It is also necessary to point out that the evolution of solution chemistry over the course of the experiment resulted in changes in both saturation state and Mg:Ca. This had an effect on the saturation index of the main carbonate minerals (calcite, aragonite and dolomite) with respect to time. A decrease in dolomite saturation indices, for example, during the 15-day ESW batch incubation time, with values depleting from ~ 4 to ~ 2.25 (*see Figure 4 and Figure 5*) occur as calcium carbonates are precipitated. Similarly, results show a decrease in aragonite and calcite saturation indices, with values as low as ~ 0.39 for calcite and even in the range of undersaturation for aragonite (~ -0.35). This depletion coincides with other works, where saturation indices of these three minerals does indeed decrease through the experimental running in solutions simulating Silurian seawater (close to $\sim 1:1$) and Modern seawater ($\sim 5:1$); thus, these results are expected under the proposed solution chemistry on this study (Roberts *et al.*, 2013). One thing to consider is the difference between the modeled solution chemistry and the tested experimental solution before incubation ($T=0$). The formation of an instantaneous reaction right after the experimental batch preparation could be the cause of this difference. Both our original ESW solution and the 1:1 Mg:Ca solution (ESW11) were initially made with higher concentrations of magnesium relative to calcium (*see Table 1*). An instantaneous reaction accounted for the up-take of calcium (relative to magnesium) out of solution, drastically depleting the concentration of calcium available for the experiment run. This depletion is also observed in the alkalinity, where a difference between the modeled values and experimental solution is shown. In result, this change

in Mg:Ca ratio (and alkalinity) during the experiment preparation would have dictated the evolution behavior of the solution chemistry throughout the incubation time. Previous works have reported how this Mg:Ca evolution in the solution can even affect the mineral suite of the bulk precipitate over time. *Tutolo and Tosca, 2018*, for example, reported mineralogical transitions from calcite nucleation to aragonite as the Mg:Ca increase through the incubation period. This coincides with the mineralogical data for our ESW11 solution, where more aragonite is detected after 93 days of incubation compared to 15 days.

The role of temperature

Temperature is another crucial parameter controlling carbonate mineral equilibria. In fact, higher temperatures ($\sim 40^{\circ}\text{C}$) coincide with the abundance of dolostone rocks during the Ediacaran (*Tucker, 1992*). The incubation temperature used in our study coincided with the literature regarding Ediacaran seawater surface temperatures (*e.g., Meng et al., 2011*). In general, our mineralogical data is consistent with the expected mineral suite from our ESW seawater model at 40°C , with Mg-calcite and aragonite as the observed phases for the original ESW solution and calcite and aragonite for the 1:1 batch solutions (*see Figure 6, 7 and 10; for PhreeqC models, see Appendix B*). It has been estimated, by using fluid inclusion homogenization temperature analysis, that maximum global ocean temperatures during the Ediacaran were higher ($\sim 40^{\circ}\text{C}$) than those observed in modern day seawater conditions (*Meng et al., 2011*). It has been estimated that temperature fluctuations in shallow waters, as those were Dengying microbialites formed, during that time ranged close to Phanerozoic values (*Meng et al., 2011*). However, paleomagnetic analysis shows that the microbialites of the Dengying formation could have formed close to the equator; thus, tropical temperatures could be assumed here, indicating warmer temperatures than global seawater (*Yang et al., 2004*). These values also can be observed in modern microbial systems on

which there is active carbonate precipitation (*i.e.*, *Bontognali et al. 2010; Rodriguez-Colon et al., 2019*). However, although dolomite is saturated in the models, the batch experiments did not produce detectable dolomite. Instead of mimicking the mineralogy of the Dengying formation, results from precipitation experiments with Ediacaran-like fluid precipitates are consistent with what is observed in modern low-temperature (<55°C) carbonate depositional systems, where dolomite is less kinetically favorable to precipitate relative to calcite and aragonite (*i.e.*, *Land, 1998; Roberts et al., 2013*).

The role of dissolved SO₄

Another seawater component that differs between Ediacaran and modern seawater is the concentration of dissolved sulfate [SO₄²⁻]. In our study, 23 mmol L⁻¹ of sulfate (in the form of Na₂SO₄) was added to simulate the interpreted concentration of this component in Ediacaran seawater as shown by fluid inclusion analysis (*e.g.*, *Horita et al., 2001*). Neither of the experimental runs made in our study produced dolomite in the bulk precipitate, however it is unclear if dissolved sulfate in solution had an inhibitory effect in the process. Previous studies have debated the role of sulfate in the formation of dolomite (*Baker and Kantsner, 1981; Sanchez-Roman et al., 2009; Roberts et al., 2013*). Sulfate has been posited as an inhibitor of dolomite given the strong Mg²⁺ complexation with sulfate ions (MgSO₄⁰), limiting the availability of this metal in solution (*Baker and Kantsner, 1981*). In particular, solutions with low concentrations (*e.g.*, ~5 mmol L⁻¹) have shown inhibitory properties in the dolomite synthesis process (*Morrow and Ricketts, 1988; Brady et al., 1996*). One thing to take in consideration, however, is that the experimental approach in *Baker and Kantsner, 1981* and *Morrow and Ricketts, 1988*, for example, did not consider the formation of authigenic dolomite under low-temperature conditions, but rather it shows the effects of sulfate ions in high temperature geochemical models. In contrast, sulfate

has been shown to be a catalyst for dolomite to form under high sulfate concentrations (~10 times higher, relative to Mg in solution) (Jones, 1966; Brady *et al.*, 1996). Nevertheless, recent studies have documented the presence of disordered dolomite crystals under laboratory-controlled experiments and low-temperature conditions (similar to experiments performed here) in the presence of different concentrations of sulfate in solution (Sánchez-Román *et al.*, 2009). This latter work documented the formation of dumbbell-shape dolomite crystals (~1-2µm) in solutions with no dissolved sulfate present and as high as 56 mmol L⁻¹ in solutions in the presence of sulfate reducing-bacteria (Sánchez-Román *et al.*, 2009). The study suggests that although the interrelation between sulfate-reducing bacteria communities with the formation of dolomite might have been associated in regards to the depletion of sulfate out of solution by the microbial communities (hence, eliminating the inhibition barrier), the production of alkalinity by these communities could be a more important factor (Sánchez-Román *et al.*, 2009). Similarly, Roberts *et al.* (2013) documented the synthesis of dolomite nanocrystals in the presence of organic matter (in the form of carboxylated microspheres) under Silurian seawater chemistry conditions (11 mmol L⁻¹ of [SO₄²⁻]). These two studies show that sulfate might not be in fact a key player for the synthesis of dolomite. Indeed, other geochemical factors (such as Mg:Ca ratios and alkalinity) might play a bigger role and could explain the lack of dolomite in our studies.

The role of dissolved silica

The role of the dissolved silica is particularly important in our simulated Ediacaran seawater solutions. Here, we used 2.2 mmol L⁻¹ of dissolved silica (in the form of Na₂SiO₃), in order to achieve the hypothesized values for marine surface waters during the Ediacaran (Siever, 1992). Further, to test how the presence of silica could affect the solution, another batch reactor without silica was made. Evolution of solution chemistry over the period of the experiment shows that the

presence of silica impacted solution pH and Mg sequestered in the solid phase. In the ESW solution without silica, for example, pH decreases (from ~8.50 to ~6.85) more than those experiments that contain silica (~8.52 to ~7.54; *see Figure 1 and Figure 2*). Similarly, alkalinity shows a steeper decline when no silica is in solution. These abrupt changes in pH and alkalinity for the nonsilicated solutions shows that the presence of dissolved silica is likely buffering pH, as the solution pH is ~1.5 pH units for the pKa of H₄SiO₄ (i.e., pka 9.8; *Belton et al., 2012*). Moreover, although alkalinity values decreased in the silicated ESW solutions, less was precipitated from solution than in the nonsilicated solutions (*see Figure 1*). This effect is also shown in the elemental analysis of solution geochemistry (*see Figure Ap.1*), where in nonsilicated ESW solutions, the concentrations of magnesium and calcium decrease over time; however, magnesium and calcium evolution show to be lesser to almost no change when silica is present. It should be noted that although the evolution of Mg concentration when silica is present does not change through time, there is indeed a small depletion in calcium concentration. Therefore, there is still carbonate precipitation, but to a lesser extent when no silica is present. SEM/EDX data corroborates this, showing an intrinsic relationship between the dissolved silica and the magnesium ions and the formation of calcium-rich carbonates in solution (*see Figure 8-9*). Microscopy data shows the presence of Si-Mg rich amorphous solids alongside calcium-rich precipitates. Furthermore, EDX data reveals that the affinity of silica and magnesium does not occurred with silica and calcium.

The preferential association between Mg²⁺ ions and dissolved silica is observed in previous works (*e.g., Tosca and Masterson, 2014*). Removal of dissolved silica from industrial water is a well-known method that uses this affinity by adding magnesium soluble salts for to solution for silica extraction (by Mg-silicate solids formation) (*e.g., Lataur et al., 2015*). However, specific mechanisms that could explain this association between magnesium and silica remain unknown

(*Tosca and Masterson, 2014*). Although the complexation of calcium and silicate has been documented, the solubility of calcium silicate solids is higher than Mg-silicates ones; hence, amorphous Mg-silicate will be more stable in solution (*Lataur et al., 2015*). Our SEM data is consistent with these findings, as no calcium-silicate was detected in the bulk sediment. Preferential binding of dissolved silica to magnesium compared to calcium could be attributed to differences in atomic radii and electronegativity between magnesium and calcium atoms, because magnesium ions tend to be more electronegative than calcium ions given their smaller atomic radii. Indeed, fast kinetics in the binding and stable complexation of magnesium with silica (similar to what is observed with magnesium and sulfate) could result in the removal of $[Mg^{2+}]$ out of solution and preventing further binding with $[Ca^{2+}]$ and $[CO_3^{2-}]$ to form dolomite.

A positive correlation between the formation of amorphous silicate precipitates in the presence of magnesium has been found to be more kinetically favorable in high pH environments (>9.5) and as concentrations of magnesium were changed in solution, with a positive catalytic effect as concentrations increase from as low as $0.082 \text{ mmol L}^{-1}$ to $\sim 0.410 \text{ mmol L}^{-1}$ (*Demadis et al., 2012; Lataur et al., 2015; Tosca and Masterson, 2014*). Under pH ranges in this study ($\sim 8.5-7$), silicic acids tend to be in a stable form (as pK_a values for orthosilicic acids is close to 9.8). However, it has been shown that when concentrations of dissolved silica in solution are higher than its solubility threshold, orthosilicic acid can undergo autopolycondensation (*Belton et al., 2012*). Oligomers (polymers of orthosilicic acids) larger than 1 nm will tend to have charge negative surfaces above pH of 6.8, as the silanol groups (i.e., hydroxyl groups attached to silicon atoms) are deprotonated above this pH value (*Belton et al., 2012*). Thus, our observations from SEM/EDX suggested that dissolved silica in our solution reacted to form large oligomers with negative charged surfaces, which in return served as nucleation sites for magnesium to attach given the

deprotonated hydroxyl groups. In fact, this effect has been shown with silicate minerals as well, as it has been suggested to play a potential role in dolomite formation by acting as nucleation sites (Liu *et al.*, 2019). Findings by Liu *et al.*, (2019) show that some clay mineral surfaces (e.g., illite and montmorillonite), would account for negatively charged hydroxyl surfaces that could bind magnesium ions by dehydration and complexation.

Past studies have debated the role of the co-precipitation process between silica and magnesium as precursors for clay minerals (such as Mg-silicates) (Tosca and Masterson, 2016; Tutolo and Tosca, 2018). Previous works have shown that amorphous silicate nucleation is more kinetically favorable than the subsequent steps that lead to clay mineral synthesis (Tosca and Masterson, 2016; Tutolo and Tosca, 2018). Therefore, for Mg-silicate amorphous precipitates, a solution chemistry similar to what is observed in extremely alkaline lacustrine settings (high pH solutions) would potentially further the reaction to produce more stoichiometric clay minerals, like sepiolite $[\text{Si}_{12}\text{Mg}_8\text{O}_{30}(\text{OH})_4(\text{OH}_2)*4.8\text{H}_2\text{O}]$ or stevensite $[(\text{Ca},\text{Na})_x\text{Mg}_{3-x}(\text{Si}_4\text{O}_{10})(\text{OH})_2]$, with respect to time (Tosca and Masterson, 2016; Tutolo and Tosca, 2018). PhreeqC modeling of data in this study indicates supersaturation with respect to clay minerals such as sepiolite or stevensite. Yet, our mineralogy data do not detect peaks in the clay mineral region, probably as a result of the low pH values used on this study; hence, supporting the observations made by the Tosca team (Tosca and Masterson, 2016; Tutolo and Tosca, 2018). The formation of Mg-silicates has also been implicated as potential diagenetic contributors for carbonate dolomitization (Tosca and Wright, 2015). Pore characterization of lacustrine carbonate reservoirs in the pre-salt Barra Velha formations have shown that Mg-silicate dissolution (as a result of microbial activity) contributed to the dolomitization of carbonate systems in the pre-salt formations (Tosca and Wright, 2015).

The role of organic matter

While solution chemistry is crucial to defining the composition of precipitates that form, nucleation surfaces are key in facilitating mineral nucleation and formation. In these experiments, we used a synthetic organic matter in the form of carboxylated microspheres as a representation that approximates organic matter present in microbial surfaces and mats. Our overall data shows that the presence of organic matter did not significantly affect the geochemical evolution of the solution over the course of the experiment compared to experiments without organic carbon (*see Figure 1*). Instead, the data shows a similar pattern between the control and their seeded counterparts in all batch solutions. However, minimal specific differences can be seen in the solution chemistry of some of the solutions. For example, a lower value of Mg:Ca ratio was reported for the seeded nonsilicated ESW solution at day 15 (~23:1) compared the control solution (~26:1), suggesting that more magnesium is being precipitated in carbonate minerals or sorbed to sphere surfaces when no silica is available and organic matter is present. This effect can also be seen in the 93-days dolomite saturation evolution, with lower values in saturation index reported when organic matter is in solution (~1.7 compared to ~2.65 in the control solutions during the day 93; *see Figure 5*). The saturation indices in Mg:Ca 1:1 solutions are lower in the control experiments compared to the seeded solutions (*see Figure 6*). One thing to consider is the possible effects of the solution chemistry at these early stages of the solution preparation and incubation, which could be dictating the behavior of the fluid evolution; however, these results show that indeed the carboxylated spheres present in the solution are impacting the behavior of $[Mg^{2+}]$ over the time period of the experiments.

SEM data shows precipitates with spherulitic morphologies in both ESW experiments and our 1:1 experiment as well. In the original ESW solutions, the spherulites are composed of

aggregations of hexagonal crystals growing in an acicular pattern, while those in with the 1:1 solution is shown to be aggregations of rhombohedral crystals. These morphologies have been shown to be associated with microbial activity and controlled by the presence of organic matter (e.g., Braissant, 2003; Mercedes-Martin et al., 2016). In particular, Mercedes-Martin et al., (2016) reported the formation of calcitic spherulites composed of rhombohedral crystals in alkaline solutions with organic matter (in the form of alginates). Nevertheless, previous works by Tutolo and Tosca (2018) reported the formation of these similar morphological features in precipitates from solutions that mimic alkaline lacustrine settings poor in organic matter. These observations suggest that solution chemistry might have a larger effect in the final morphology of the precipitate, contradicting results from Mercedes-martin et al., (2016.) Indeed, these results coincide with bulk precipitates from all our studied solutions, suggesting that solution chemistry could alone control the morphological features in the bulk precipitates. Here, spherulites were observed in both control and seeded solutions, suggesting that no mediation by carboxylated organic matter was necessary. Moreover, it should be noted that before the desired pH was reached during the solution preparation, our solution reported high pH values (close to ~10) before they were adjusted to 8.5 using CO_{2(g)}, with an instantaneous reaction recorded during the pH adjustment period, meaning that the precipitation observed might not have formed all under the final desire solution, but rather some of the crystals formed during the preparation process (at high pH values). This is similar to what is observed in the experiments by Mercedes-martin et al., (2016.) As shown in **Figure Ap.11 and Ap.12**, most of bulk precipitates from the corresponded solutions are formed in the instantaneous reaction mentioned above (before organic matter inoculation). Therefore, these observations in our SEM data supports the interpretation for the formation of the precipitates, on which the main precipitates observed in our solutions (i.e., the aragonite hexagonal crystals in the

ESW batch, the calcite rhombohedral precipitates in the 1:1 solution and the amorphous Mg-silica precipitates) were not controlled by presence of the organic matter, but rather resulted from the solution chemistry; thus, coinciding with the data from *Tutolo and Tosca, (2018)*. However, as mentioned above, fluid evolution shows depletion of calcium, alkalinity and magnesium over time (and decreasing in saturation, presumably through precipitation); thus, there is an effect during the incubation time that could be attribute with the presence of organic matter in solution.

Aside from the precipitates observed in the bulk sediment, small spheroidal precipitates (~0.2 μm) are found in association with the carboxylated microspheres and are shown to be ubiquitous throughout all the types of studied solutions on this study (see *Figure 15*). These observations coincide with the findings made by *Roberts et al., (2013)* and *Yoerg, (2018)*, where similar precipitates are documented in association with microspheres. Although EDX mapping in the scanning electron microscope does not show a distinct elemental distribution through precipitates that associate with the spheres, *Roberts et al., 2013* and *Yoerg, 2018* have suggested that these are indeed carbonate in nature with a mineralogy dictated by the solution chemistry (e.g., Mg:Ca ratio of the solution), and with a further favored growth assisted by the carboxylated surfaces (*Roberts et al. 2013; Yoerg, 2018*). Moreover, *Yoerg, (2018)* documented a preferential distribution of the magnesium and calcium in the carbonate precipitates in the control solutions, with these occurring as discrete phases, whereas solutions containing organic matter documented an even distribution of magnesium and calcium ions in the precipitates. *Yoerg, (2018)* suggests this discrete distribution observed in the control solutions was a product of the kinetics barriers described for magnesium, where calcium will precipitate first and, with enough alkalinity (carbonate ions), magnesium will follow. Thus, organic matter will reduce kinetic barrier; hence, the even distribution in the seeded solutions. Our results, however, did not show any differences in the distribution of these two metals

between the control and the seeded solutions. Higher resolution analysis of the elemental distribution in the precipitates is needed to confirm this distribution in our data.

In-detail analytical microscopy methods, such as TEM-EDX, give us more information on the metal distribution in the carboxylated surface. TEM imagery from one of our ESW solutions shows precipitation close to the surface of the microspheres similar to the observations made by *Roberts et al., 2013 (see Figure Ap. 14 and Ap.15)*. Further elemental analysis (TEM/EDX) on some of these precipitates associated with the microspheres documented a distinct relationship between the magnesium and the silica with the microsphere (*see Figure 17*). As mentioned previously, a preferential association between magnesium and silica was shown in the SEM analysis and was inferred from the solution chemistry data (*see previous section*). Our results also indicated that the Mg-Si complexes tends to be preferentially attached to the carboxylated surface relative to the calcium (*see Figure 17*). The interrelation between silica and organic matter has been investigated in the field of biosilification and has been documented in association with surfaces of *Bacillus subtilis* (*e.g., Fein and Nelson, 2002*). The latter study shows that for dissolved silica present in solution, its affinity with metal ions (or in the form of iron or aluminum oxides) can enhance the sorption capacity of the silica into the bacterial surfaces (*Fein and Nelson, 2002*). Taking in consideration the nature of our amorphous silica solids (*see previous section; Demadis et al., 2012*), our data coincides with the results observed by *Fein and Nelson, (2002)*, suggesting that magnesium could have a similar mediating function as observed with the Fe-oxides in *Fein and Nelson, (2002)*. The fact that very low amounts of calcium was detected by TEM-EDX throughout the carboxylated surface in our study may suggest an affinity towards magnesium and silica that was not spotted under the SEM-EDX imagery. This affinity could be attributed to the stabilization constant of Ca-carboxyl complexes compared to Mg-carboxyl complex, on which

there is a differential complexation strength between carboxyl groups and magnesium relative to calcium (*Bunting and Thong, 1970*). This data also coincides with findings from *Bontognali et al., (2010)*, which showed Mg-Si amorphous precipitates in association biofilms in microbial mats, and with no calcium present. Dolomitic phases with calcium but no silica present close to the Mg-Ca precipitates were also detected, leading to the hypothesis that these two phases resulted from the same process, on which the Mg-Si precipitates attached to the organic matter and latter evolve into the dolomites shown here (*Bontognali et al., 2010*). Thus, the complexation of Mg with the amorphous silica observed in our results could further facilitate interactions between the attached magnesium with carbonate ions and calcium in solution (overcoming the kinetic barrier); which could lead to the formation of Mg-bearing carbonates such as dolomite (*Bontognali et al., 2010*). Dissolution of these Mg-Si precipitates (and Mg-silicates) could also contribute to the dolomitization of pre-existing carbonate formations (*Tosca and Wright, 2015*). On the contrary, this complexation could also inhibit the bonding of calcium and carbonate ions into magnesium ions, since the magnesium strongly complexed with the silica and the organic matter. Since our solutions formed the Mg-Si precipitates together with calcium-rich precipitates, it could suggest that these are two separate phases and not subsequent mineral phases. Nevertheless, these findings could have implications for the processes that could have promoted the formation of these dolomitic formations in the Dengying microbialite systems.

Implications for Dengying Formation

The solution chemistry studied here attempted to emulate the seawater chemistry of the Ediacaran Period, on which the Dengying Formation (which is interpreted as “microbial dolomite”) was formed; thus, testing the microbial dolomite model as a potential process for the genesis of these carbonate deposits. Our solution chemistry took into account the presence of high

concentrations of magnesium relative to calcium (with Mg:Ca ratios of 6.1:1), alkalinity, the concentrations of dissolved sulfate and the presence of dissolved silica. Further, synthetic organic matter was used to emulate the presence of the microbial mat systems and their potential roles as catalysts for dolomite synthesis in these terminal Ediacaran formations. This period, which occurred after the last global glaciation of the Cryogenian Period (i.e., Marionan glaciation; ~650-635 Ma), shows significant evidence of important atmospheric and ocean chemistry changes in the planet (*Seilacher et al., 2003; Kasemann et al., 2014; Halevy and Bachan, 2017; Penman and Rooney, 2019*). Several works pointed out the correlation of atmospheric and chemical conditions in global ocean changes, such as changes in O_{2(g)} and CO_{2(g)} levels in the seawater, with weathering processes and changes in element cycling, with drastic changes that could have contributed to the complex seawater chemistry that was modeled on this study (*Fike et al., 2006; Seilacher et al., 2003; Kasemann et al., 2014; Halevy and Bachan, 2017; Penman and Rooney, 2019*).

This study took into consideration the resulted composition from this ocean chemistry evolution estimated for the Ediacaran after the global deglaciation. Given the extensive amounts of dolomite units in this Period, such as the microbialites observed in the Dengying Formation, the proposed experimental setup was constructed to be supersaturated with respect to dolomite. Yet, our proposed recipe for ESW did not succeed in precipitating dolomite out of solution. Indeed, our results could suggest that, 1) our proposed solution chemistry needs to be revised, 2) more high resolution transmission microscopy is needed to confirm the presence of dolomitic crystals associated with the microspheres surfaces or 3) that the dolomites from Dengying formation are not “microbial” in origin, but a result of later-diagenetic processes that lead to the dolomitization of these systems.

The mineralogy results from the constructed ESW solution (i.e., with Mg:Ca of 6.1:1) in this study align with the accepted mineralogy in oceans under this Mg:Ca ratio (i.e., “aragonite seas”). Previous works have suggested that the dolomites from Dengying Formation are a product of aragonite and Mg-calcite dolomitization and not from primary dolomite precipitation, as evidence for these precursor phases have been observed (*Feng et al., 2017; Hu et al., 2020*). Thus, the Dengying Formation could have formed under an “aragonite sea”, on which aragonite and Mg-calcite were the dominant carbonate phases, and later diagenetic processes promoted dolomitization of these rocks. Petrographic evidence shows the presence of hydrothermal minerals such as quartz, fluorite, pyrite and saddle dolomite throughout some of Dengying Formation units, suggesting this dolomitization process took place under hydrothermal conditions after burial (*Feng et al., 2017*). These observations are supported by fluid inclusion analysis, which shows that these saddle dolomites were formed from high temperature fluids (with values close to $\sim 176^{\circ}\text{C}$) (*Feng et al., 2017*). Other works, however, have pointed out that petrographic analysis in botryoidal and stromatolitic dolomites with no apparent to low alteration have shown that some of the dolomites observed on these units are not a product of mimetic dolomitization from aragonite or Mg-calcite, but indeed are syndepositional in nature (*Wang et al., 2020*). Textural features and cements within these botryoidal dolomites, such as rhombic dolomite and radial slow dolomite, are shown to be evidence of primary dolomite formation or early stage of mimetic dolomitization from precursor phases. These observations are also shown in samples from the fourth unit of Dengying, where small dolomitic spherulite precipitates (with sizes close to $\sim 10\ \mu\text{m}$) with low degree of ordering were detected (*Chen et al., 2017*). Isotopic analysis from these samples shows negative $\delta^{18}\text{O}$ values expected in an early-stage diagenetic environment origin (*Chen et al., 2017*). Thus, there is clear evidence that syndepositional dolomite formation happened within these microbial systems as

well, with later high-temperature diagenetic alteration that led to the formation of other phases such as saddle dolomite (*Chen et al., 2017*).

Indeed, the results from our study could represent the first stages prior to the early-diagenetic changes that could have resulted in the formation of geologic formations at Sichuan Basin, as. Further, the presence of carboxylated organic matter and dissolved silica played a role in overcoming the kinetic barriers that prevent dolomitic precipitates to form in solution. For example, the presence of spherulitic precipitates in close association with the microspheres could be comparable with the finding made by studies such as *Chen et al., (2017)*. Further, our TEM data shows that mineral precipitation is indeed occurring near the carboxylated surface, similar to the observations documented by *Roberts et al., (2013)* (see **Figure Ap. 14 and Ap.15**). These observations are also shown in the ESW solutions that does not contain silica, on which SEM/EDX analysis spotted a microsphere close to a Mg-calcite precipitate and with magnesium and calcium detected throughout the microsphere surface. It should be noted, however, that a higher resolution analysis is necessary to better understand the distribution of magnesium relative to calcium throughout the carboxylated surface. The relation with dissolved silica and magnesium could also have implications in the occurrence of the dolostones systems in Sichuan Basin. Past studies have shown petrographic evidence of siliceous dolomites in Dengying formation (*Lin et al., 2017; Gao et al., 2020*). As mentioned in the background section of this thesis, the global silica ocean cycle during the Ediacaran Period differed to what is observed in present-day conditions. The lack of biosilification in global oceans (a crucial component in today's silica cycle in surface waters) affected the silica flux into oceans waters and its presence in it (*Siever, 1992; Conley et al., 2017; Gao et al., 2020*). High concentrations of dissolved silica ($\sim 2.2 \text{ mmol L}^{-1}$) were estimated during this period of time and persisted through the terminal Ediacaran, and these high concentrations

could result in the precipitation of silica out of solution, as shown by the presence of chert deposits throughout the Ediacaran-Cambrian boundary (*Gao et al., 2020*). Interestingly, observations on the silicious dolomites from Dengying shows an interrelation with the silicious deposits associated with the stromatolitic textures. The interrelation documented on these rocks coincides with our TEM/EDX observations in the surface of the carboxylated spheres, on which the amorphous Mg-silica precipitate indicates to have a higher affinity to the organic matter than the calcium. Similar to the proposed hypothesis from *Bontognali et al., (2010)*, this affinity could be a crucial step for dolomite formation that might not have been considered, showing that amorphous silica could facilitated the sorption of magnesium in the carboxylated surface and inhibiting calcium to be attached to the organic matter. This process could lead to the formation of Mg-bearing carbonates in the surface on the microsphere surfaces. However, our data does not show a replacement of silica to carbonate and calcium; thus, more works need to be done in understand specific mechanisms that could led to the formation of Mg-bearing minerals facilitated by the silica in solution (*Tosca and Wright, 2015*). Indeed, analytical measurements to study the evolution of dissolved silica in solution should be implemented for future experimental approaches (e.g., Fourier transform spectroscopy, or FTIR), as our experimental data is limited, and the quantification of dissolve silica evolution is lacking.

Other factors to consider in our solution are the presence of sulfate and the alkalinity. Indeed, the presence of these components have shown to have an effect in the processes leading to precipitation of Mg-carbonate minerals. Previous works have shown that sulfate might act an inhibitor for dolomite to form, considering its strong complexation with magnesium ions (MgSO_4^0). Our data shows that under the concentrations of dissolved sulfate used on these solutions ($\sim 23 \text{ mmol L}^{-1}$), no dolomitic phase was detected. However, considering the chemical

mixture used in our solution chemistry, it is not possible to determine the specific effects of this ion in solution compared to other compounds such as dissolved silica and the carboxylated microspheres. Future experimental approaches could address this by testing different concentrations of sulfate with this particular ocean chemistry. Another factor to take into account is that the sulfate concentrations used on this experiment needed to be revised. Although values used here were based on fluid inclusion analysis (e.g., *Horita et al., 2001*), other works have shown possible lower values of this ion in global oceans during the Ediacaran. Sulfate values of $\sim 5 \text{ mmol L}^{-1}$ or less for the early Ediacaran seawater have also been suggested, increasing over time ($\sim 10 \text{ mmol L}^{-1}$) as result of the extensive weathering resulted from post-deglaciation events (*Kah et al., 2004; Algeo et al., 2015; Zhou et al., 2016*). Nevertheless, previous works have shown that the role of sulfate in dolomite inhibition is necessary not case (*Sanchez-Roman et al., 2009*). Instead, other factors, such as high alkalinity, could have a significantly greater impact to the formation of Mg-bearing carbonate minerals than the presence of sulfate in solution.

Some of these findings have posed the idea of “aragonite-dolomite seas” during the terminal Ediacaran, which presents a scenario of extensive aragonite and Mg-calcite precipitation, but with conditions that could trigger either the rapid mimetic dolomitization or even the formation of primary dolomite (*Hood et al., 2011; Hu et al., 2020*). This idea has been supported by REE and U isotopic analysis, suggesting global ocean in shallow waters experienced anoxic conditions (*Hood et al., 2011; Zhang et al., 2018; Hu et al., 2020*). This type of setting in shallow waters could in result favor high microbial activity in the form of sulfate reduction; thus, leading to elevated values in alkalinity and low sulfate concentrations. Together with the high Mg:Ca ratios interpreted for this time, this could support the necessary conditions to trigger either the rapid diagenetic changes of aragonite phases to dolomites or even the direct formation of primary

dolomite (*Hood et al., 2011; Hu et al., 2020; Wang et al., 2020*). Later tectonic processes and high temperature fluids further altered these formations, leading to the formation of the late-diagenetic features shown in some of the rock units (*Feng et al., 2017*). Thus, this shows that the Sinian dolomites from Dengying Formation are not a product of a single process, but a mixture of subsequent processes that lead to what is observed in the geologic record today.

Conclusion

In this study, controlled laboratory experiments were used to emulate the ocean chemistry of the Ediacaran Period, during the time in which the microbialites from Dengying Formation were alive and forming. These microbial dolomite formations, on which genesis of its genesis has been disputed, presents an ideal scenario to show the potential role of microbial communities and the presence of organic matter and in the formation of these dolostone systems. With this in mind, the environmental and hydro-chemical scenario in which the Dengying microbialites could have had formed were emulated here by using controlled laboratory procedures in the presence of carboxylated organic matter; thus, investigating the potential effects of the aqueous geochemistry and the of organic matter abundance on the formation of these geologic systems.

Experiments in this study did not produce dolomite in the bulk precipitate. However, our results indicate that the solution chemistry interpreted for the Ediacaran Period could have indeed promoted the formation of the precursor phases that led to the formation of the extensive dolomites that are now preserved in the Dengying Formation. Although our data does not have conclusive results from the effects of organic matter in the solution chemistry evolution, this study demonstrated that Ca-carbonate precipitation (and possibly Mg-phases) are occurring in close proximity to carboxylated organic matter. Further, other components, such as the presence of dissolved silica, could have played a critical role in facilitating the sorption of magnesium into the

organic surfaces. Further, possible changes in alkalinity and sulfate concentration should be considered for future experimental approaches with this constructed solution chemistry. Results from this work are another step in understanding the specific mechanisms that lead to the formation of these microbial dolomite units.

Tables

Solution Composition	Values				
	15-day solutions		93-day solutions		Modern Seawater (for comparison)
	Ediacaran Seawater (ESW)	ESW without Silica	ESW**	ESW11**	
Temperature	40°C	40°C	40°C	40°C	25°C
pH	8.5	8.5	8.5	8.5	8.2
&%Na ⁺	1271	1272	1271	1272	469
&%Cl ⁻	1294	1311	1294	1311	545
&%Ca ²⁺	11.1	11.1	6.8**	27.2	10.3
&%Mg ²⁺	67.6	67.6	41.3**	29.5	52.8
%Mg:Ca	6.1:1	6.1:1	6.07:1	1.08:1	5.1:1
&HCO ₃ ⁻	9.4	9.4	9.4	9.4	2.4
&%SO ₄ ²⁻	23.1	23.1	23.1	23.1	28
&%Si	2.2	0	2.2	2.2	0.1
#%R-COO ⁻ (0.82µm)	6.0 x10 ¹²	6.0 x10 ¹²	6.0 x10 ¹²	6.0 x10 ¹²	--
*SI _{dol}	4.26	4.62	4.26	4.77	2.46
*SI _{cal}	1.67	1.84	1.67	2.29	0.78
*SI _{arag}	1.35	1.52	1.35	1.97	0.64
*SI _{talc}	13.68	--	13.68	13.26	6.20
*SI _{sepiolite}	5.88	--	5.88	5.60	1.26
*%\$ Ionic Strength	1.66	1.65	1.55	1.58	0.6
%Salinity (wt %)	8.3	8.3	8.0	8.1	3.5
&* Alkalinity	10.28	10.27	10.24	10.26	2
@pCO ₂	10 ^{-3.5}	10 ^{-3.5}	10 ^{-3.5}	10 ^{-3.5}	10 ^{-3.5}

(*) Saturation rates, Ionic Strength and alkalinity were calculated using PhreeqC (K_{sp} for aragonite, calcite and dolomite were 10^{-8.2}, 10^{-8.4}, 10⁻¹⁷, respectively). PhreeqC Percent error is ± 0.64 for ESW and ESW-NoSi. For the ESW** and ESW11 solution was ± 0.67 and ± 0.66, respectively. (&) Concentrations in mmol L⁻¹. (\$) Ionic strength is in mol kg⁻¹. (#) Concentration of carboxyl groups are given as groups L⁻¹, which was acquire by adding 1.2 µl of the microsphere's solution in 100 mL on the solution. (%) Values were obtained from digital calculator. (@) units in atm.

Table 1 | Solution chemistry corresponded to the studied solutions. Based on literature, the solution above is close to the seawater chemistry that occurred during the Ediacaran Period (*see ESW column*). Salinity, alkalinity and pH values of the ESW and similar proposed solutions in this table are based on modern values observed in coastal lacustrine systems in which calcifying microbial mats and microbialites have been spotted. (**) The [Mg²⁺] and [Ca²⁺] on ESW (93 day runs) and ESW11 do not represent Ediacaran-specific concentrations. Only the molar ratio was taken into consideration here.

Batch solution		Mol % MgCO ₃ *	
		Control	Spheres
ESW solution	T = 5 days	20.35 mol %	23.93 mol %
	T = 10 days	18.13 mol %	19.49 mol %
	T = 15 days	22.29 mol %	18.29 mol %
ESW No Silica	T = 5 days	18.28 mol %	19.9 mol %
	T = 10 days	13.28 mol %	17.43 mol %
	T = 15 days	18.9 mol %	15.3 mol %
ESW**	T = 15 days	25.43 mol %	25.28 mol %
	T = 93 days	23.25 mol %	23.19 mol %

Table 2 | MgCO₃ mol % in Mg-calcites from the 6.1:1 solutions. (*) mol % calculations where based on equation from *Arvidson and Mackenzie, 1999*. (**) The [Mg²⁺] and [Ca²⁺] on ESW (93 day runs) and ESW11 do not represent Ediacaran-specific concentrations. Only the molar ratio was taken into consideration here.

Figures

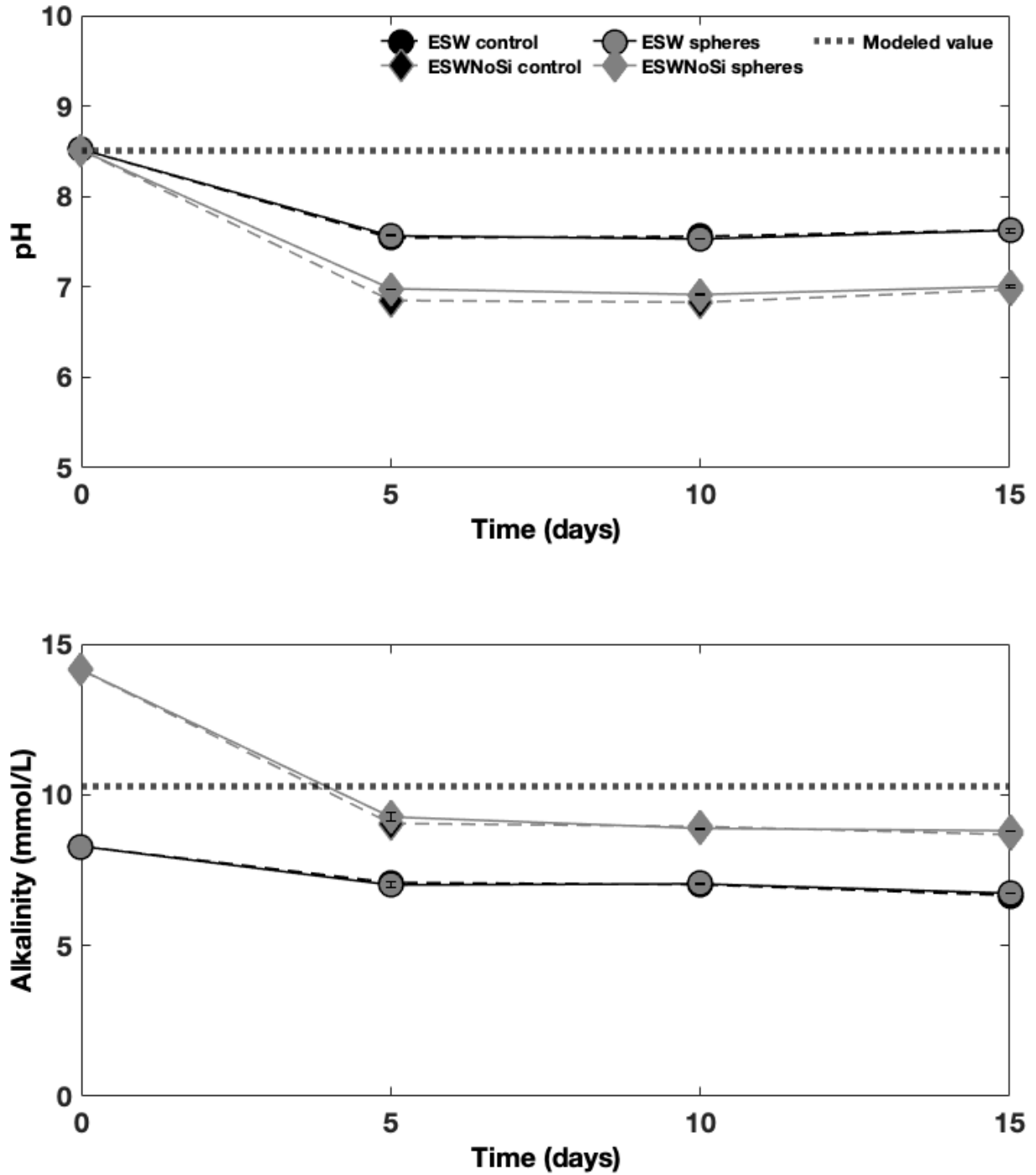


Figure 1 | pH (top) and alkalinity (bottom) evolution on the 15-day batch experiments. Here, the original ESW solution is compared to a batch reactor without silica (ESWNoSi; diamond datapoints).

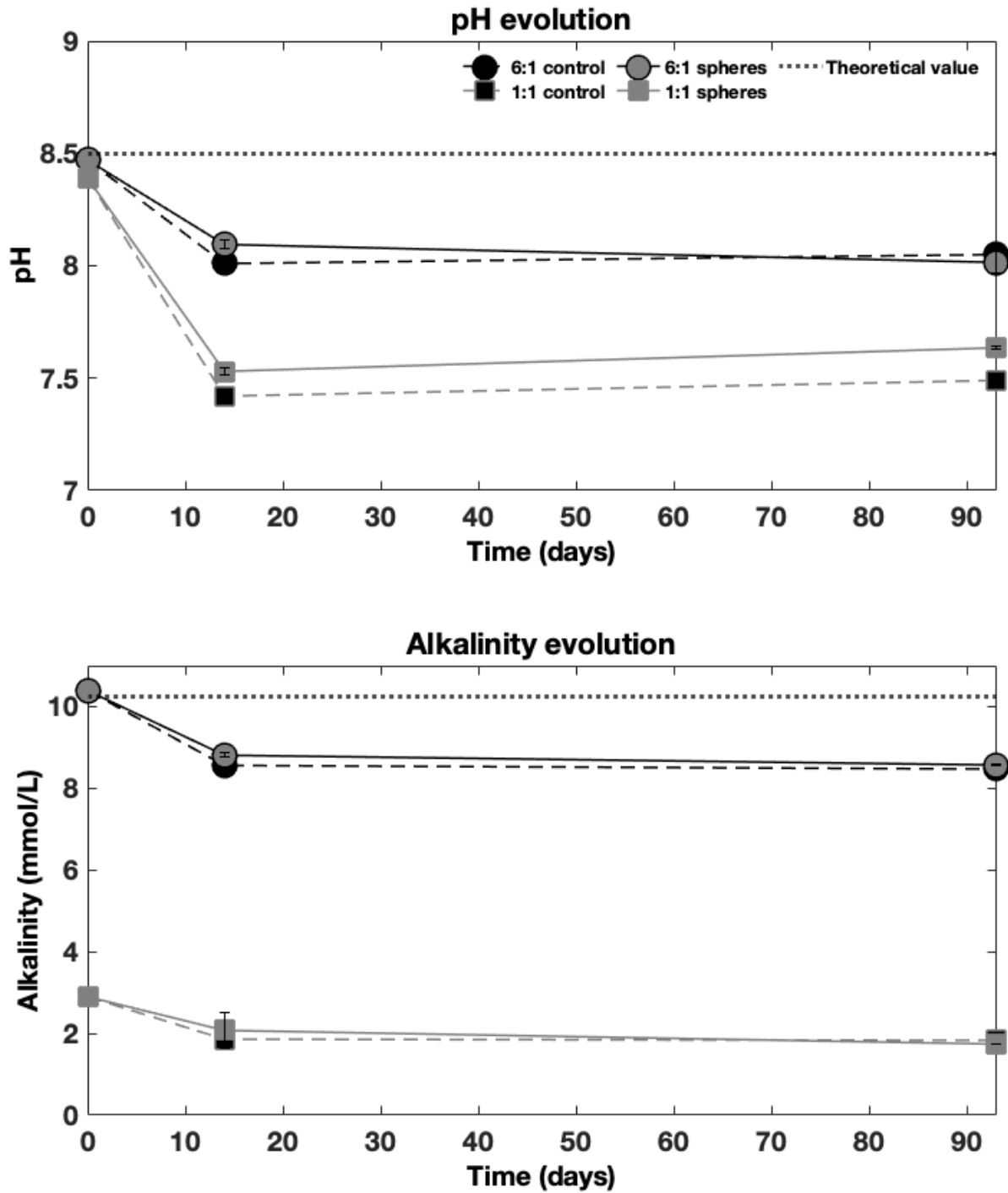


Figure 2 | pH (top) and alkalinity (bottom) evolution on the 93-day batch experiments. Batch solutions with a 1:1 Mg:Ca ratio are shown for comparison (ESW11; squared datapoints).

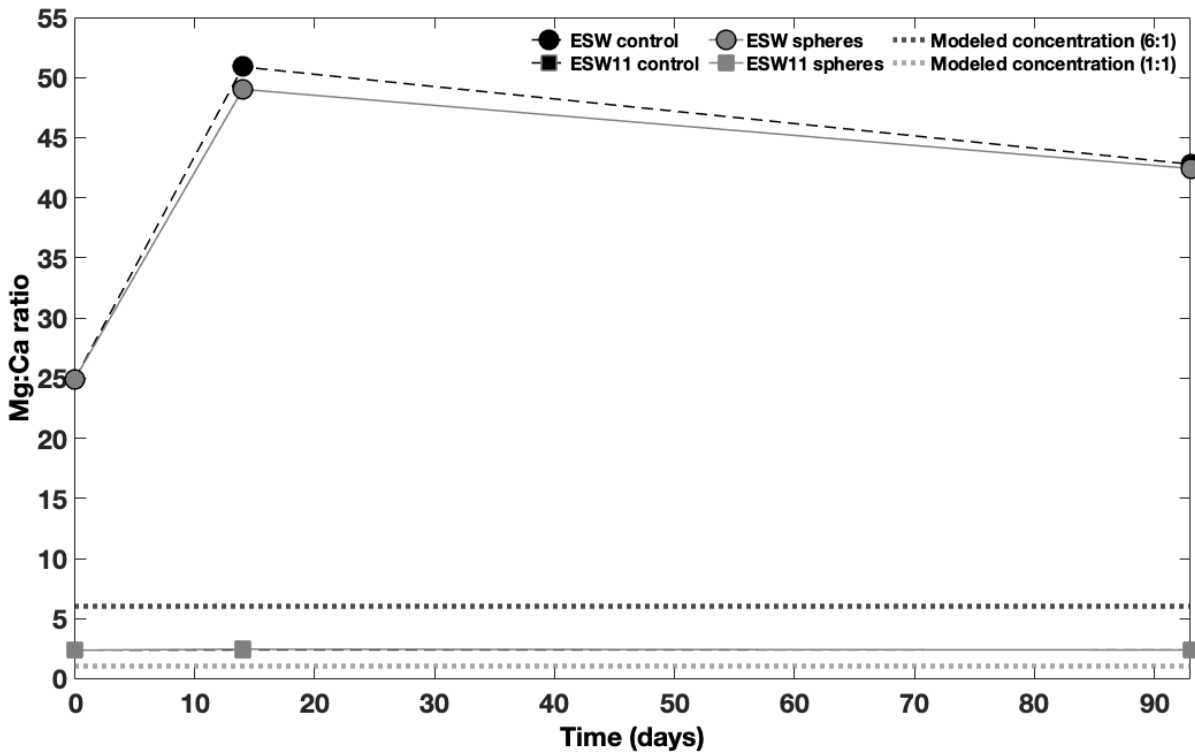
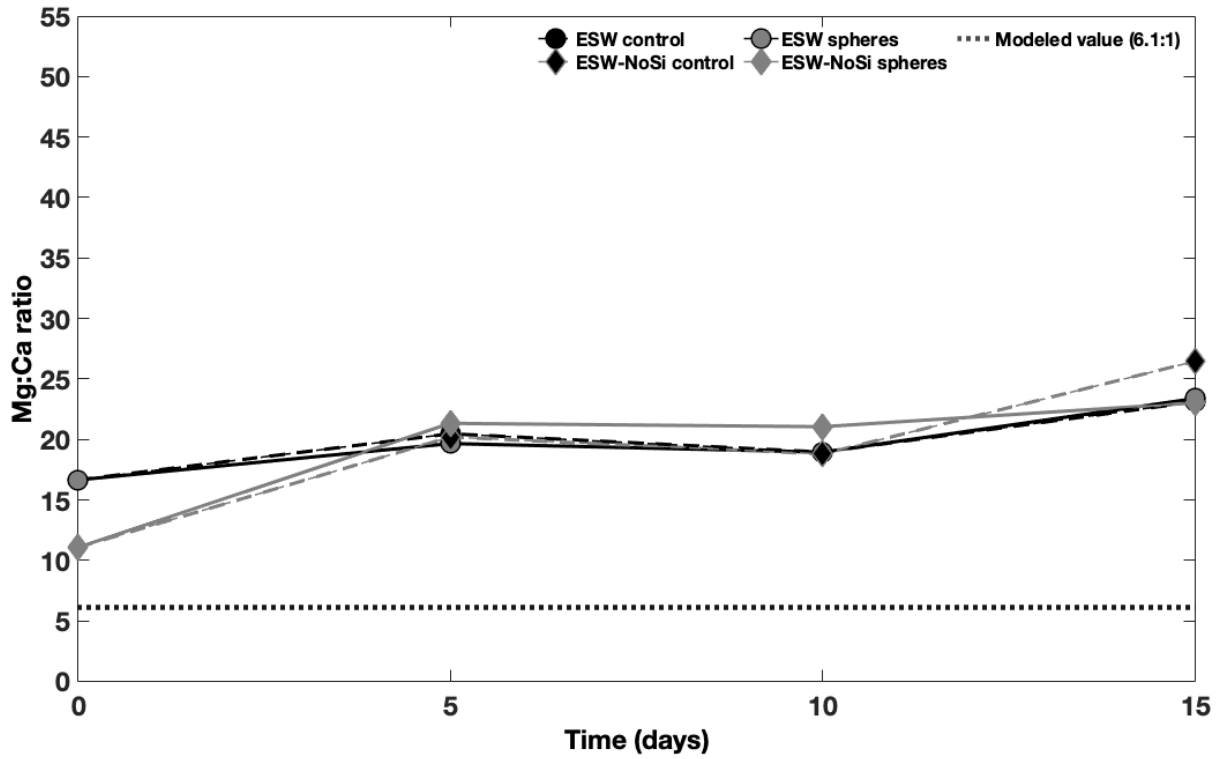


Figure 3 | Mg:Ca ratio evolution. These ratios are based on the $[Mg^{2+}]$ and $[Ca^{2+}]$ evolution in the (top) 15 day and (bottom) 93-day batches throughout the incubation time (see Appendix A for magnesium and calcium evolution).

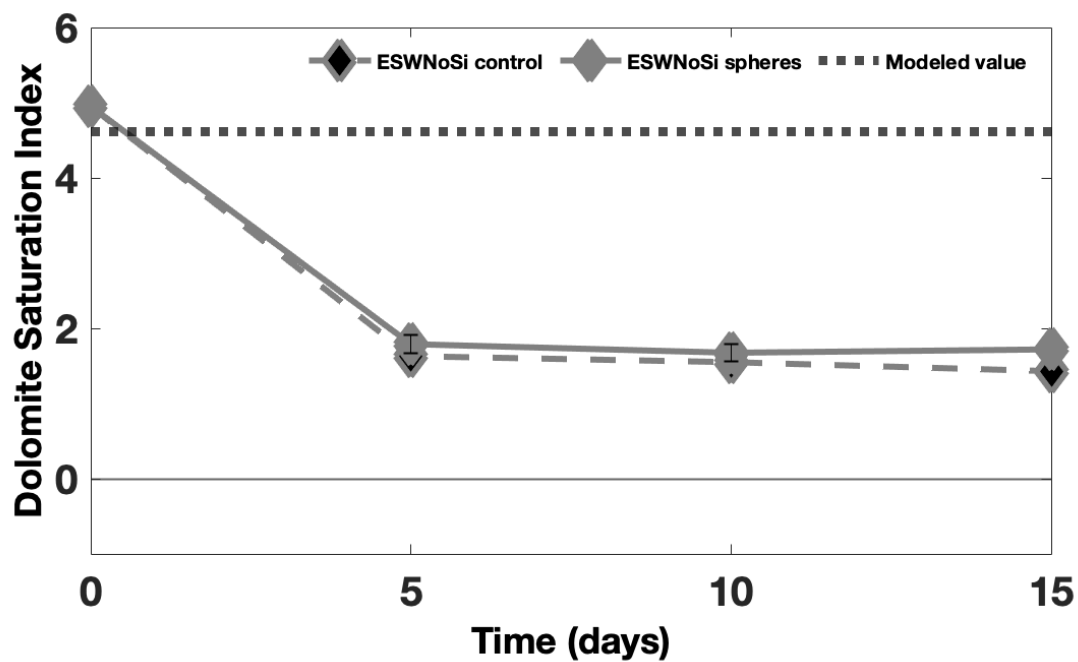
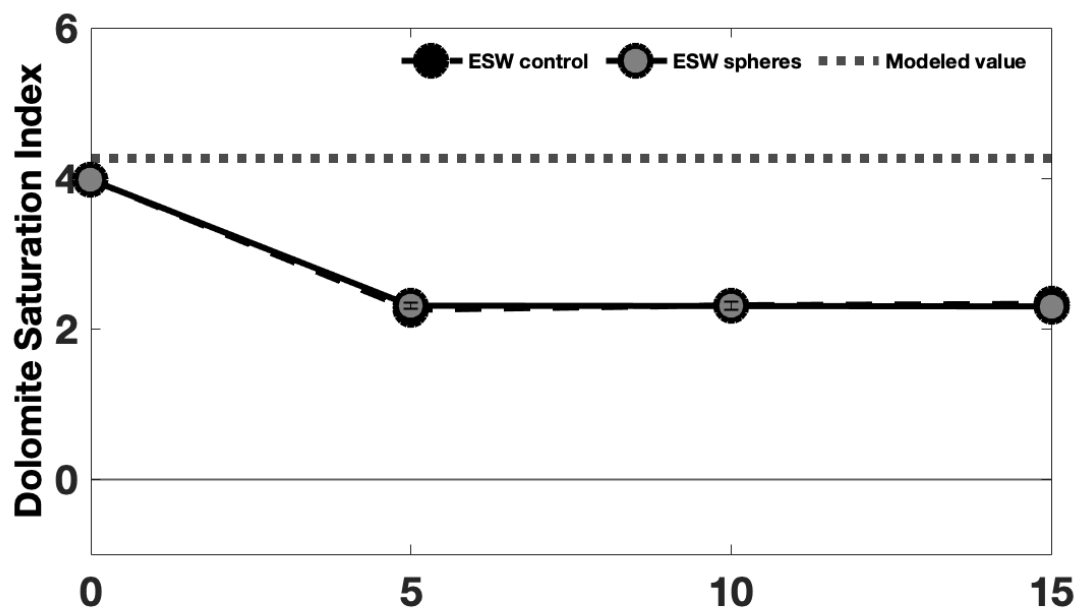


Figure 4 | Saturation Indices for ESW and ESW with no silica (ESWNoSi) of dolomite through the 15-day batch experiments.

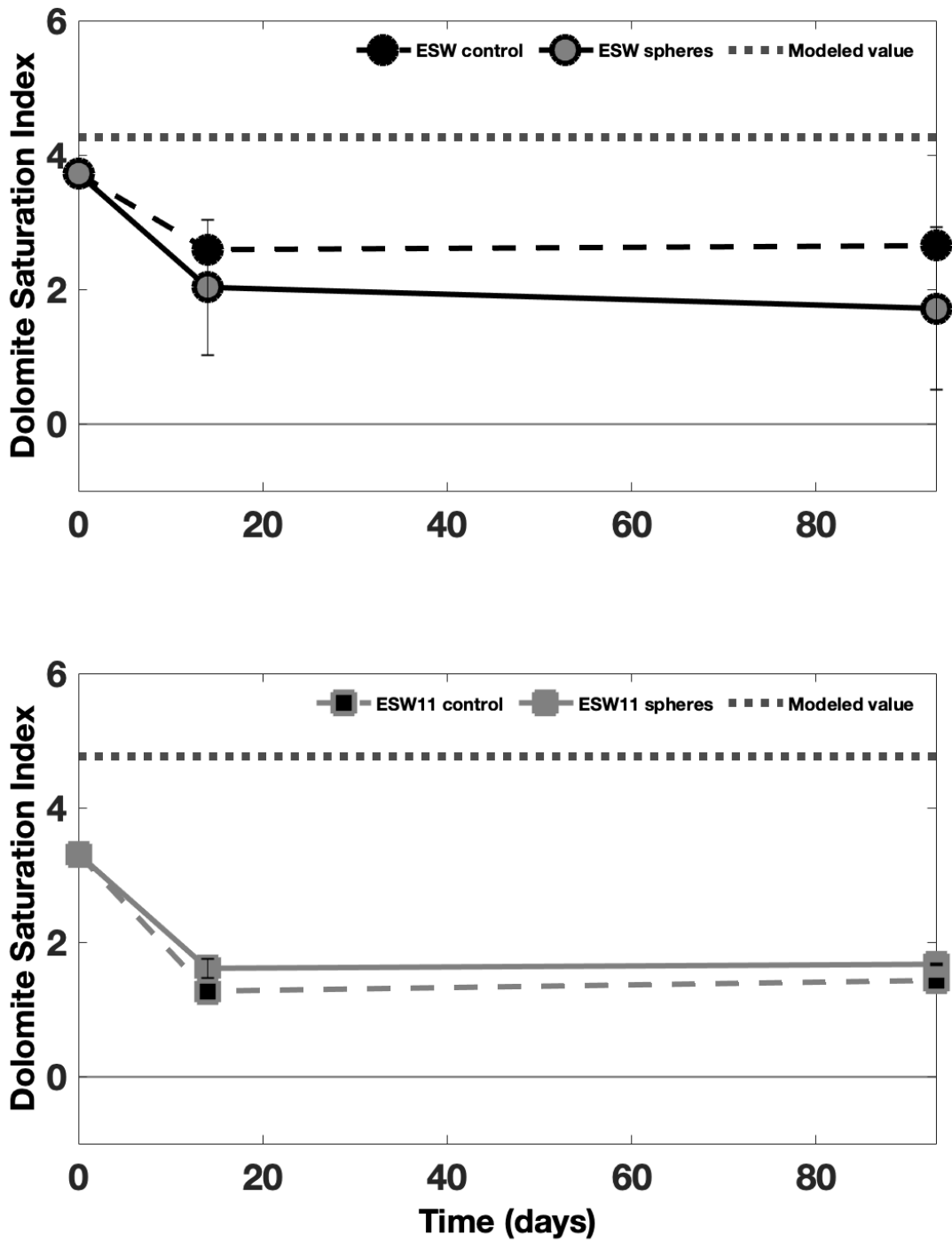


Figure 5 | Saturation Indices for ESW and ESW11 of dolomite through the 93-day batch solutions.

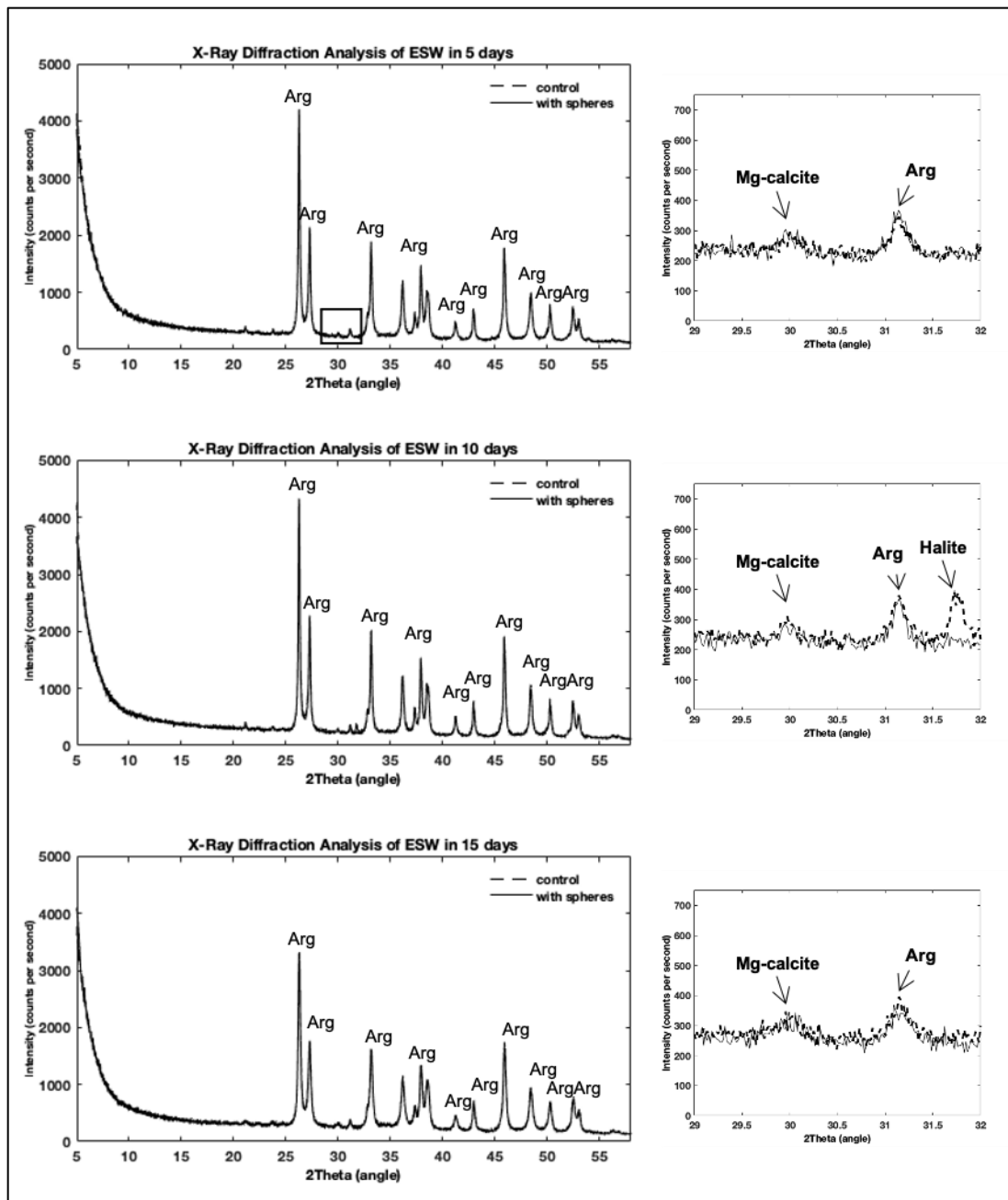


Figure 6 | X-Ray diffraction analysis for the ESW precipitates after 5, 10 and 15 days. In both control and experimental batches, aragonite was the dominant mineral observed. However, a small yield of Mg-calcite was spotted close to its C-104 ordering peak. The small halite peak observed in the close up likely resulted from the drying process. The close-up region is indicated in the first diffractogram (*black rectangle*).

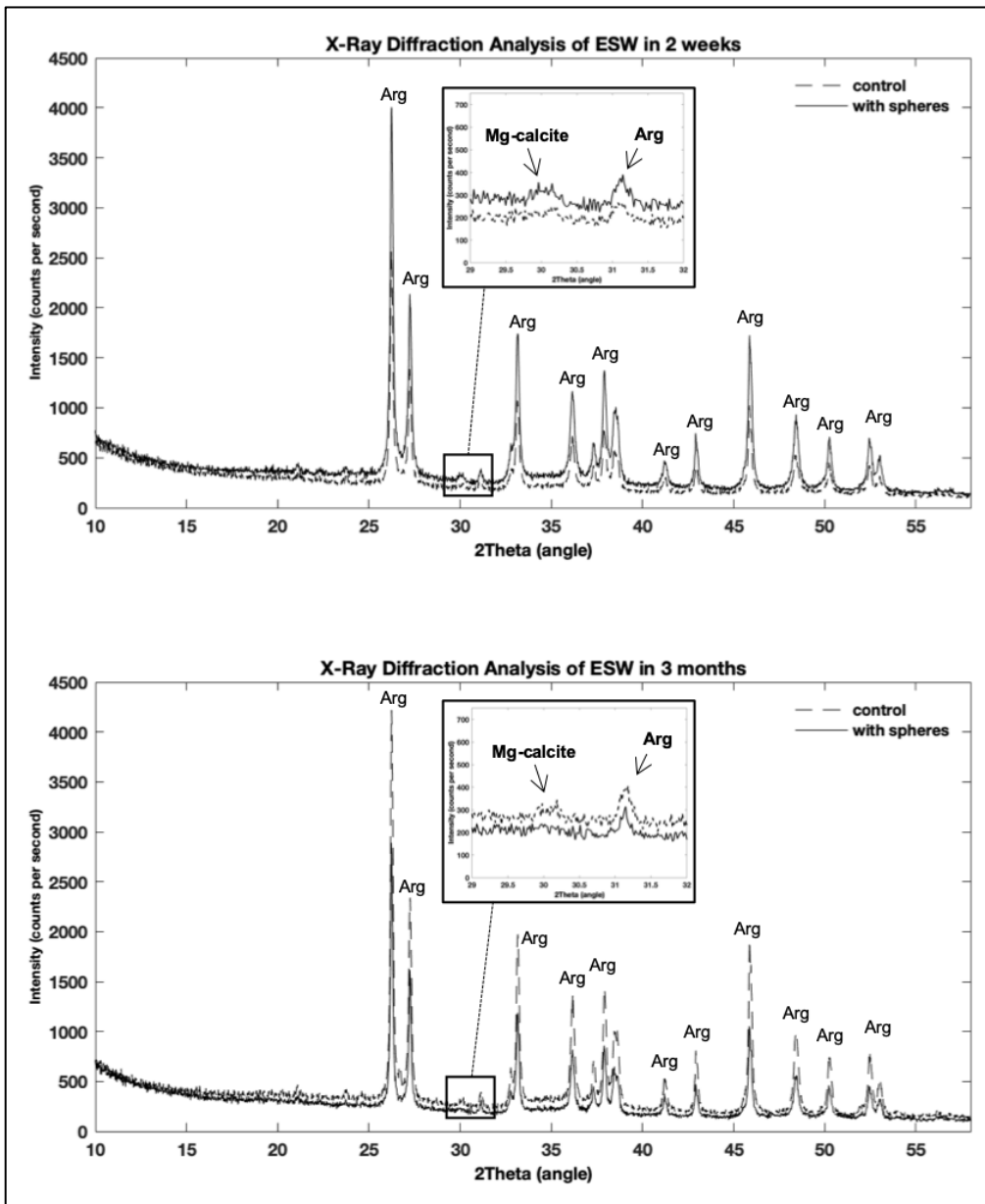


Figure 7 | X-Ray diffraction analysis for the ESW solution precipitates after 14 days and 93 days. Aragonite is the dominate mineral in the ESW solution. However, a small yield of Mg-calcite was also observed.

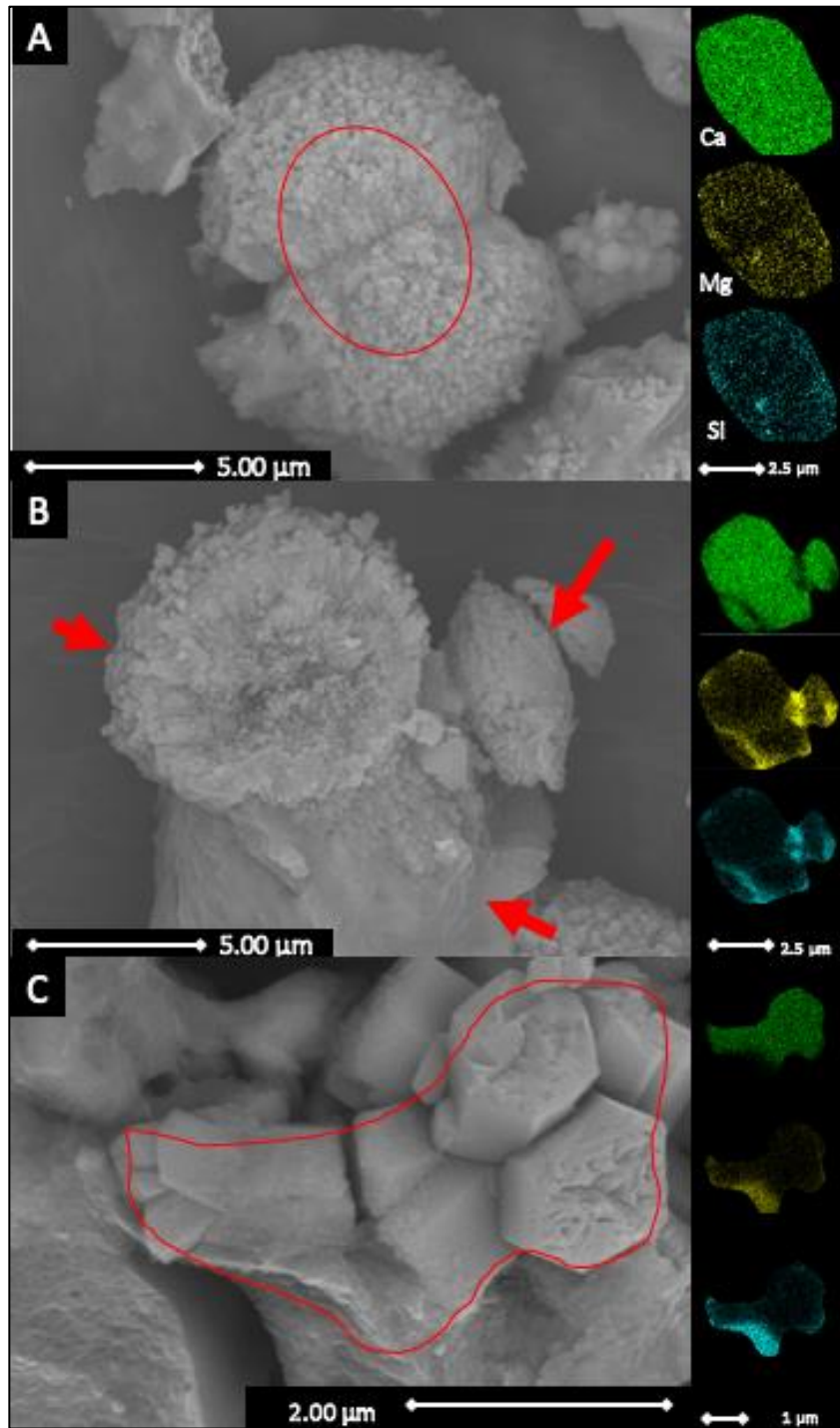


Figure 8 | ESW control batches for 5 days (A) and 15 days (B-C). (A, C) Three main morphologies were observed throughout the incubation time (*red arrows*). (B, D) The precipitates with smooth surfaces showed high levels of silica and magnesium, contrary to the other precipitates, in which calcium dominates. (Green = calcium; yellow = magnesium; blue = silica) (*See Appendix A for spectra; figure ApA7*).

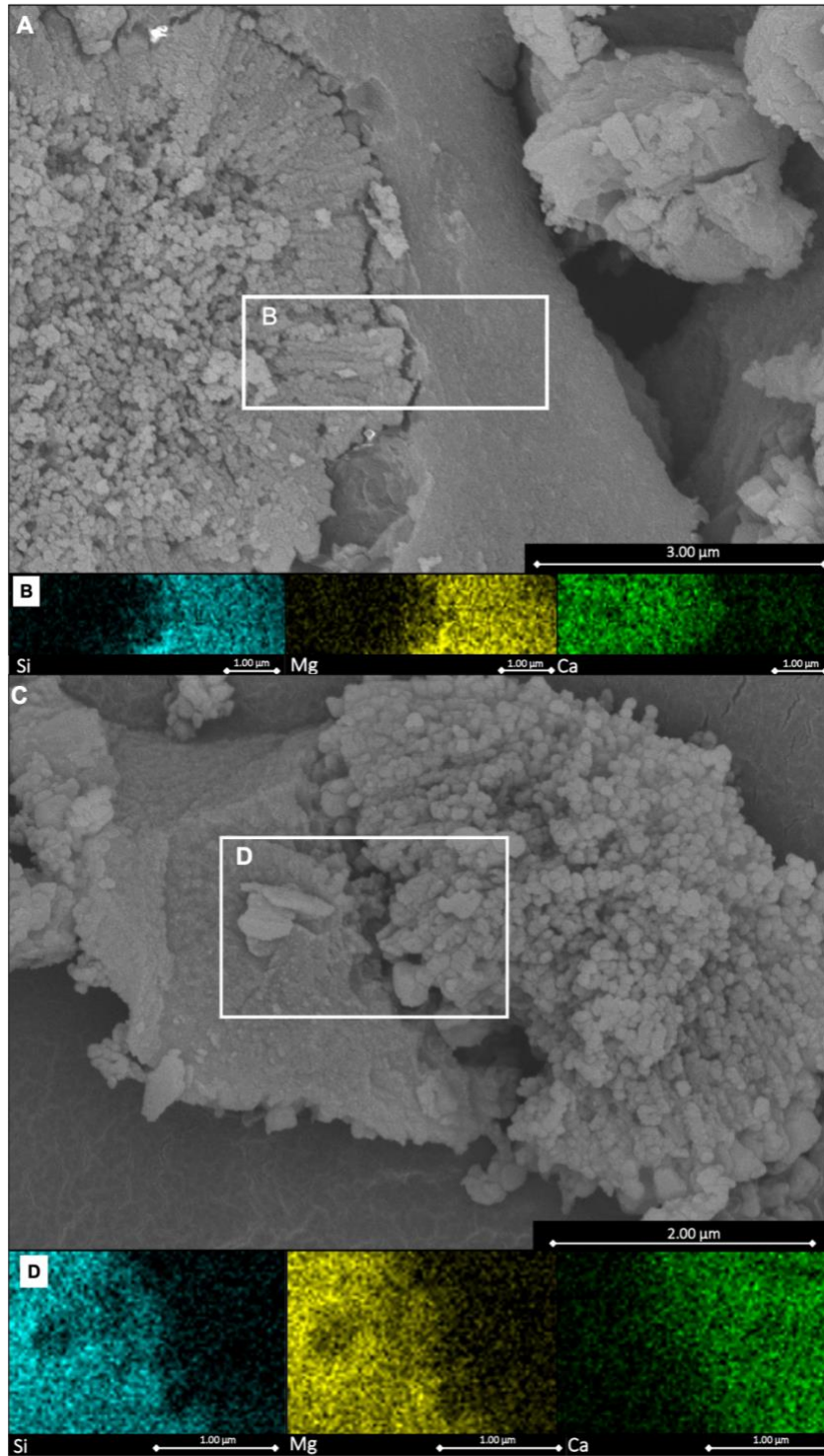


Figure 9 | ESW control batches for 15 day (A-B) and 93 day (C-D) experiments. (A, C) Two main morphologies were observed throughout the incubation time. (B, D) The precipitates with smooth surfaces showed high levels of silica and magnesium, contrary to the other precipitate, in which calcium dominates (*See Appendix A for spectra; figure ApA8*).

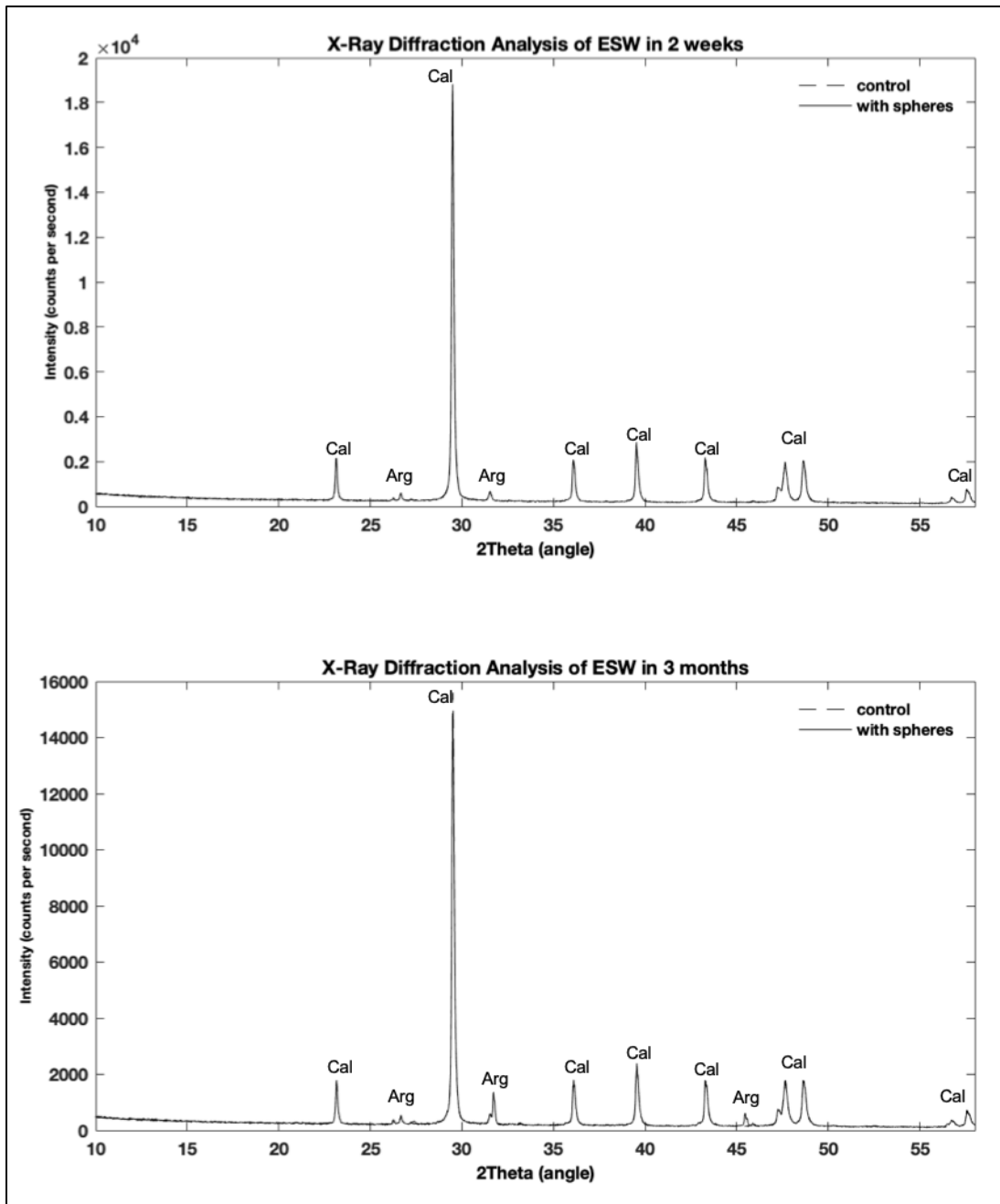


Figure 10 | X-Ray diffraction analysis for the ESW11 solution precipitates after 15 and 93 days. In both control and experimental batches, calcite was the dominant mineral observed in the ESW11 solution precipitate. Small amounts of aragonite were observed as well.

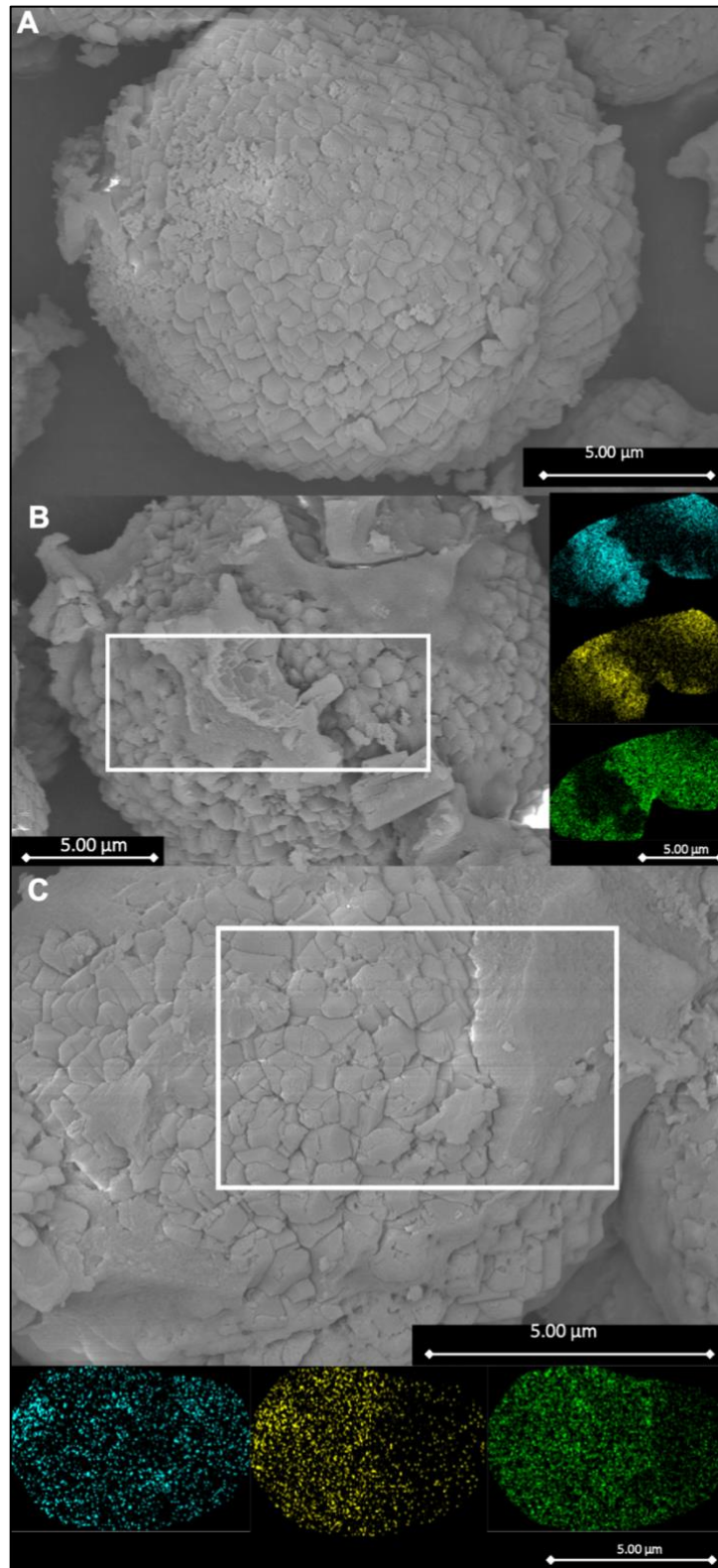


Figure 11 | ESW11 control solutions for 15 days (A-B) and 93 days (C). Here, silica is blue, magnesium is yellow, and calcium is green. (See Appendix A for spectra; figure ApA10).

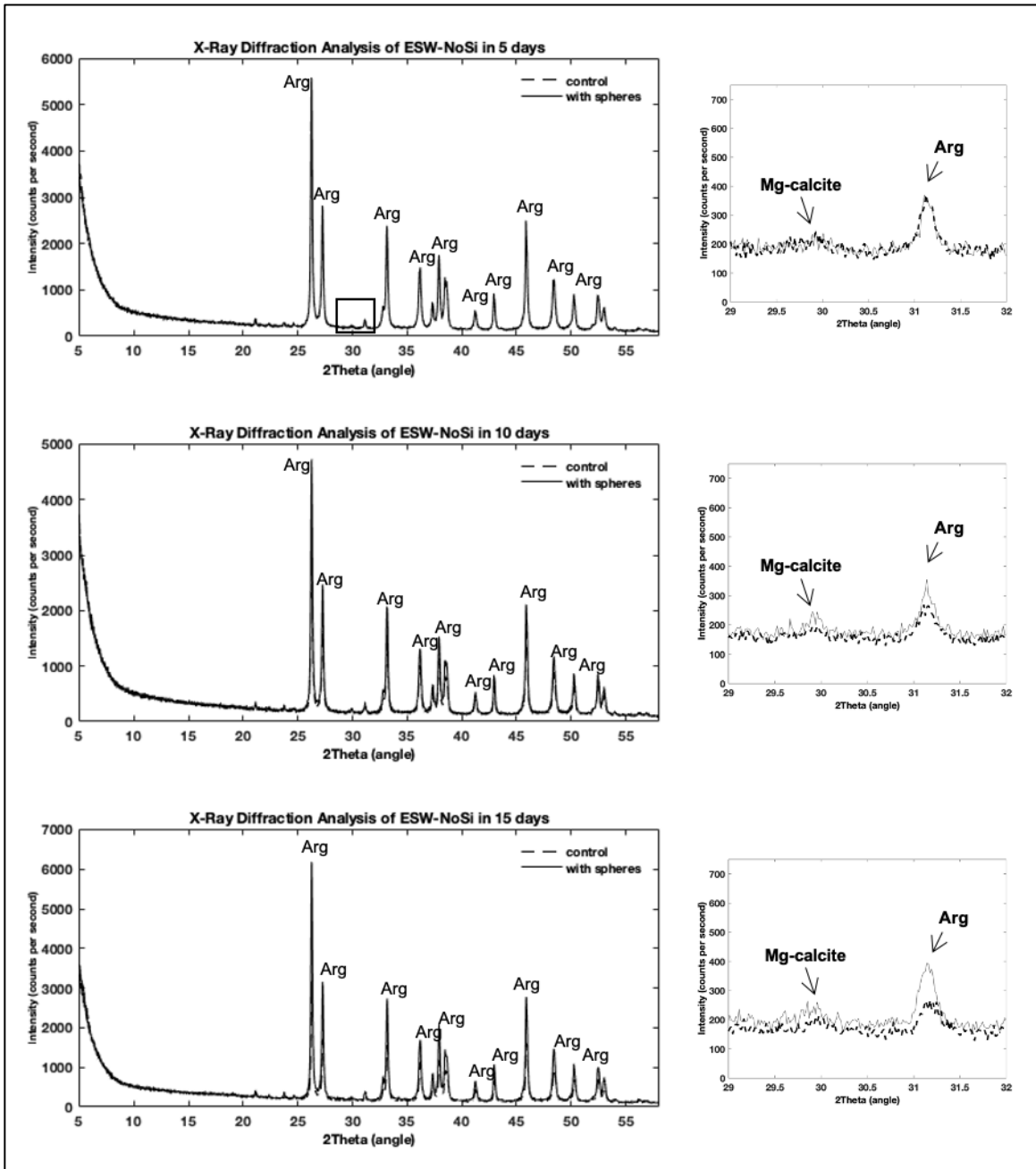


Figure 12 | X-Ray diffraction analysis for the EWS with no silica precipitates after 5, 10 and 15 days. No differences are observed between these batch precipitates and the ones in the original ESW solution solids.

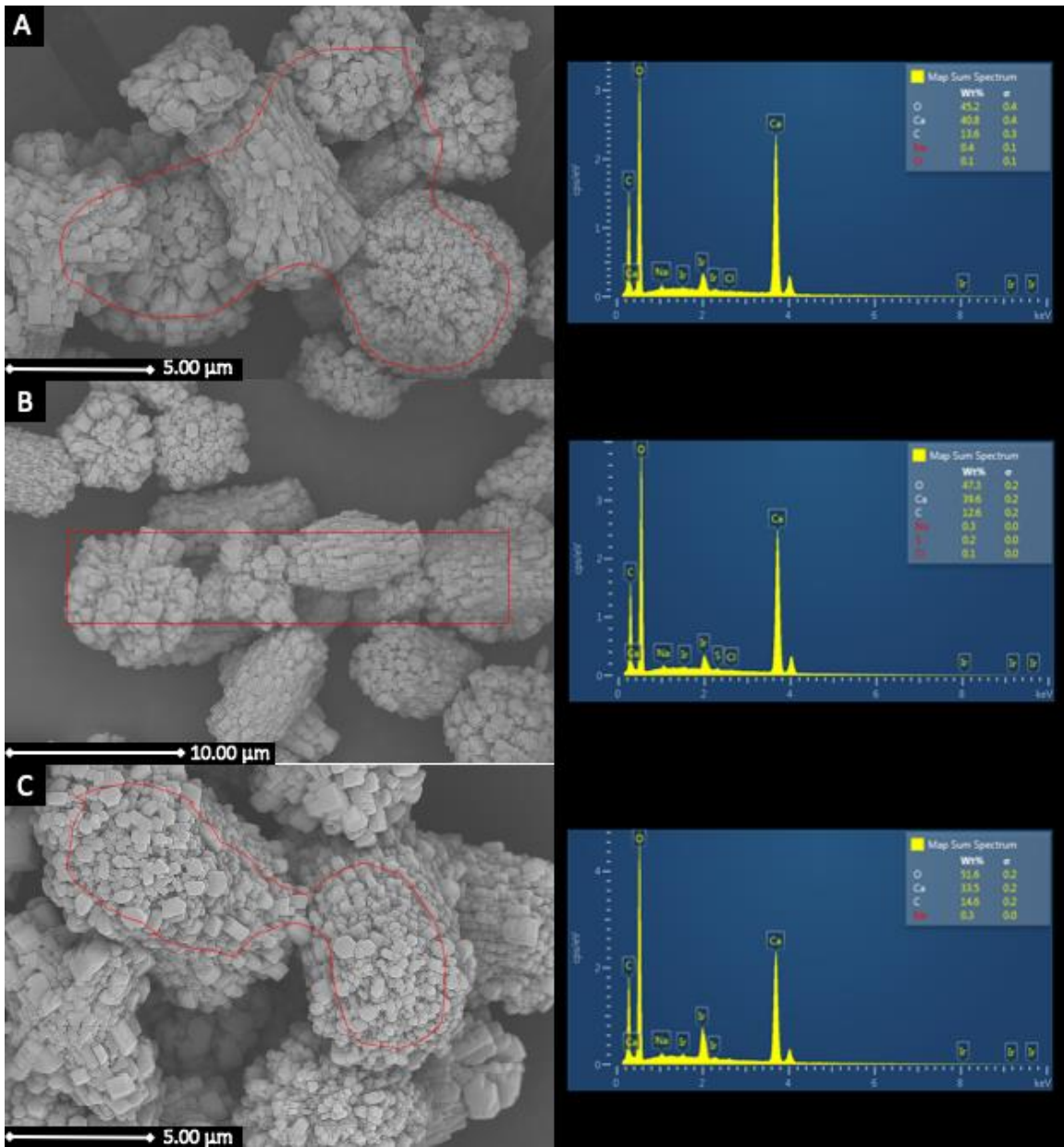


Figure 13 | ESW solution with no silica control precipitates for 5 days (A), 10 days (B) and 15 days (C).

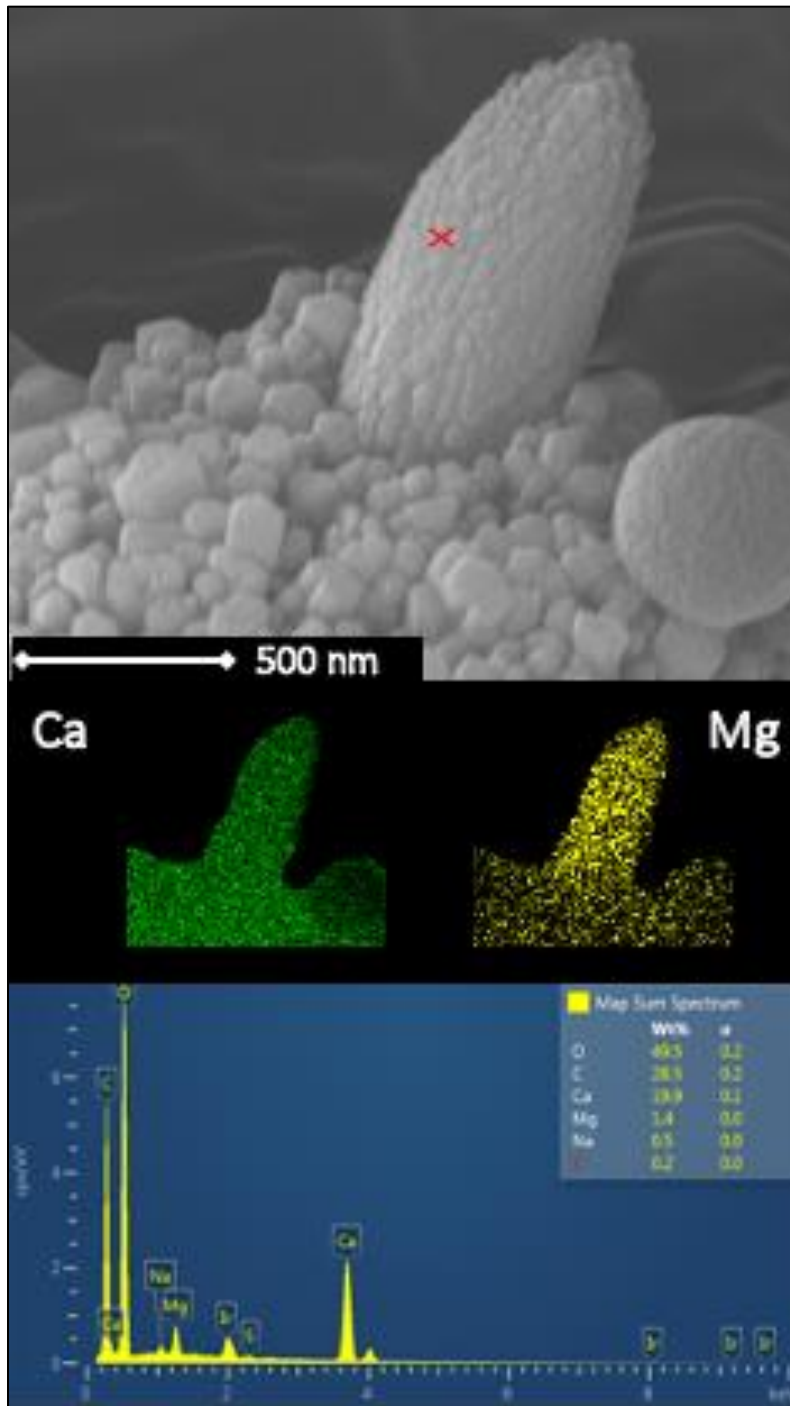


Figure 14 | A Mg-Ca precipitate is spotted in the ESW solids with no silica present. A microsphere is observed on the right side.

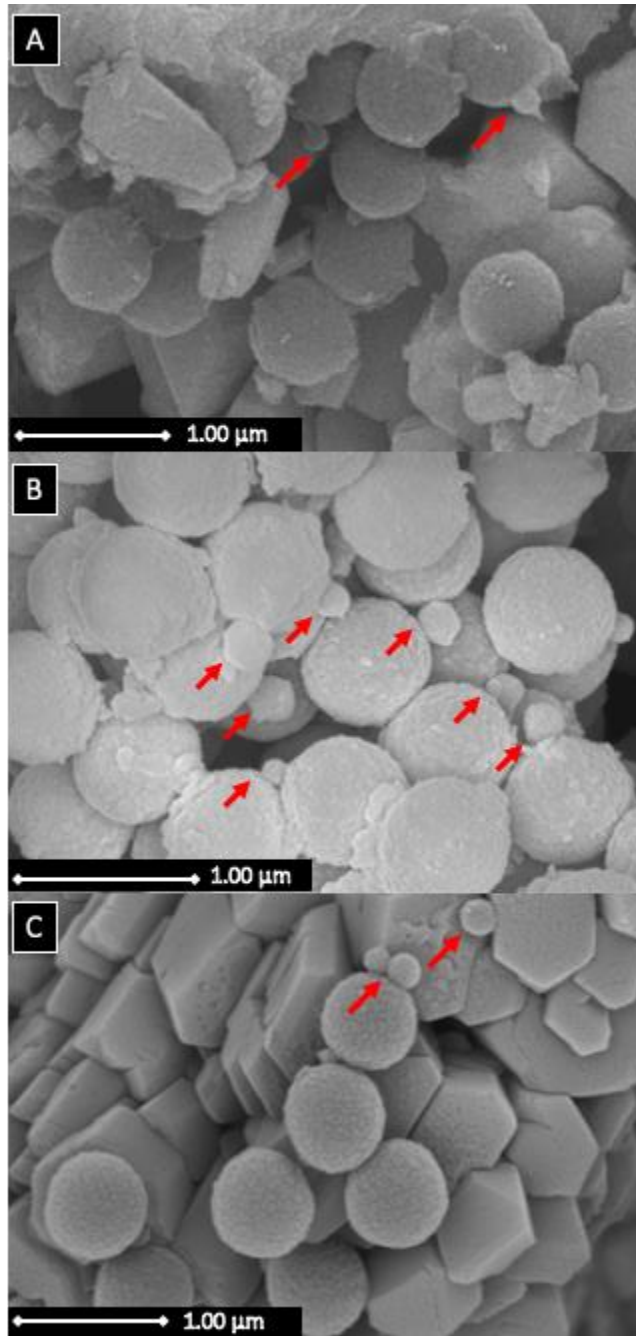


Figure 15 | The presence of small ($\sim 0.2\text{-}0.3$ nm) spherical precipitates are shown in all batch solutions and in association with the carboxylic microspheres (*red arrows*). (A) ESW original solution, (B) ESW11, (C) ESW with no silica.

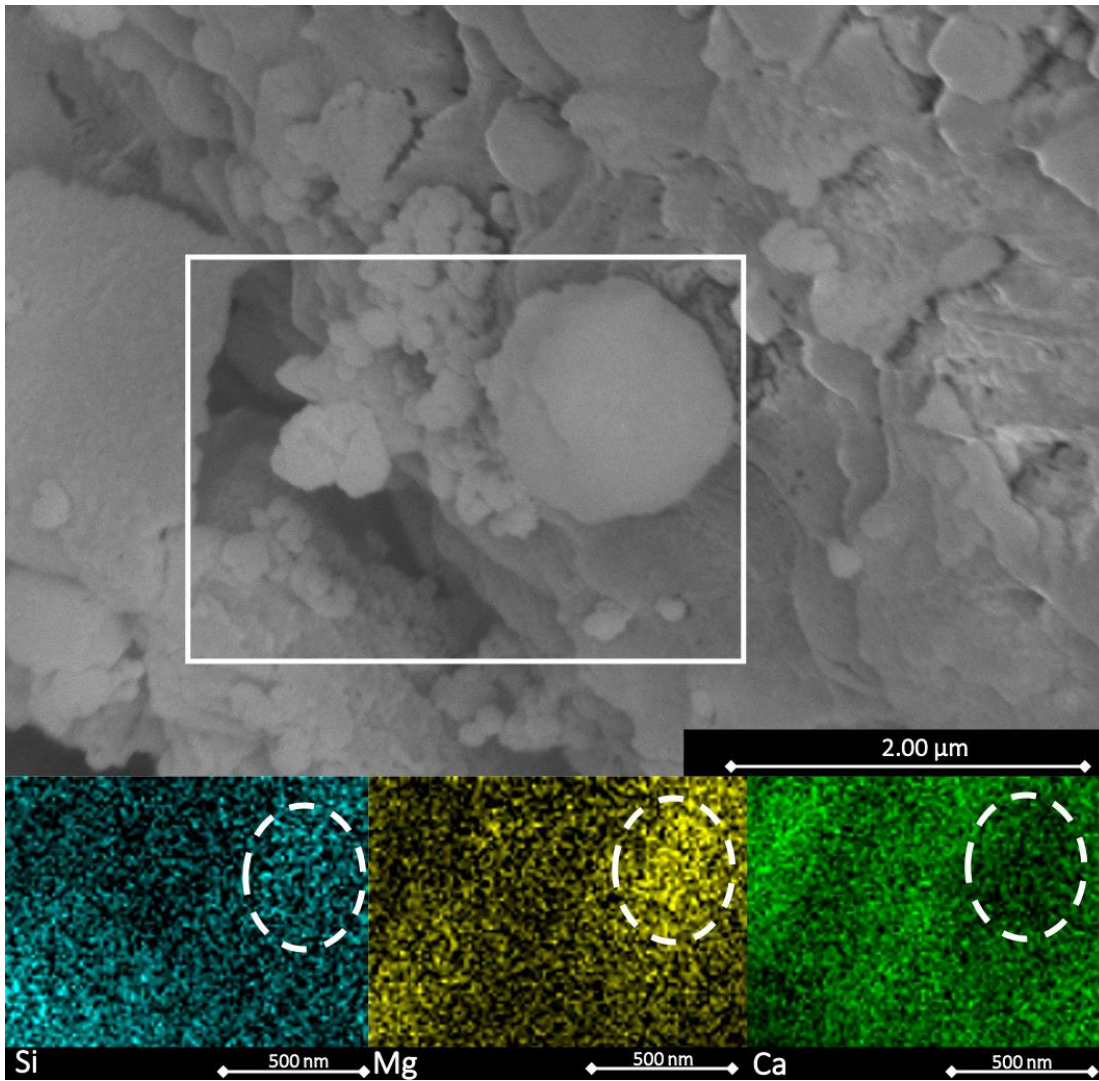


Figure 16 | ESW seeded solution precipitates (day 15). Elemental mapping shows a higher affinity of silica and magnesium, relative to calcium, throughout the surface of the sphere (*See Appendix A for spectra; figure ApA10c*).

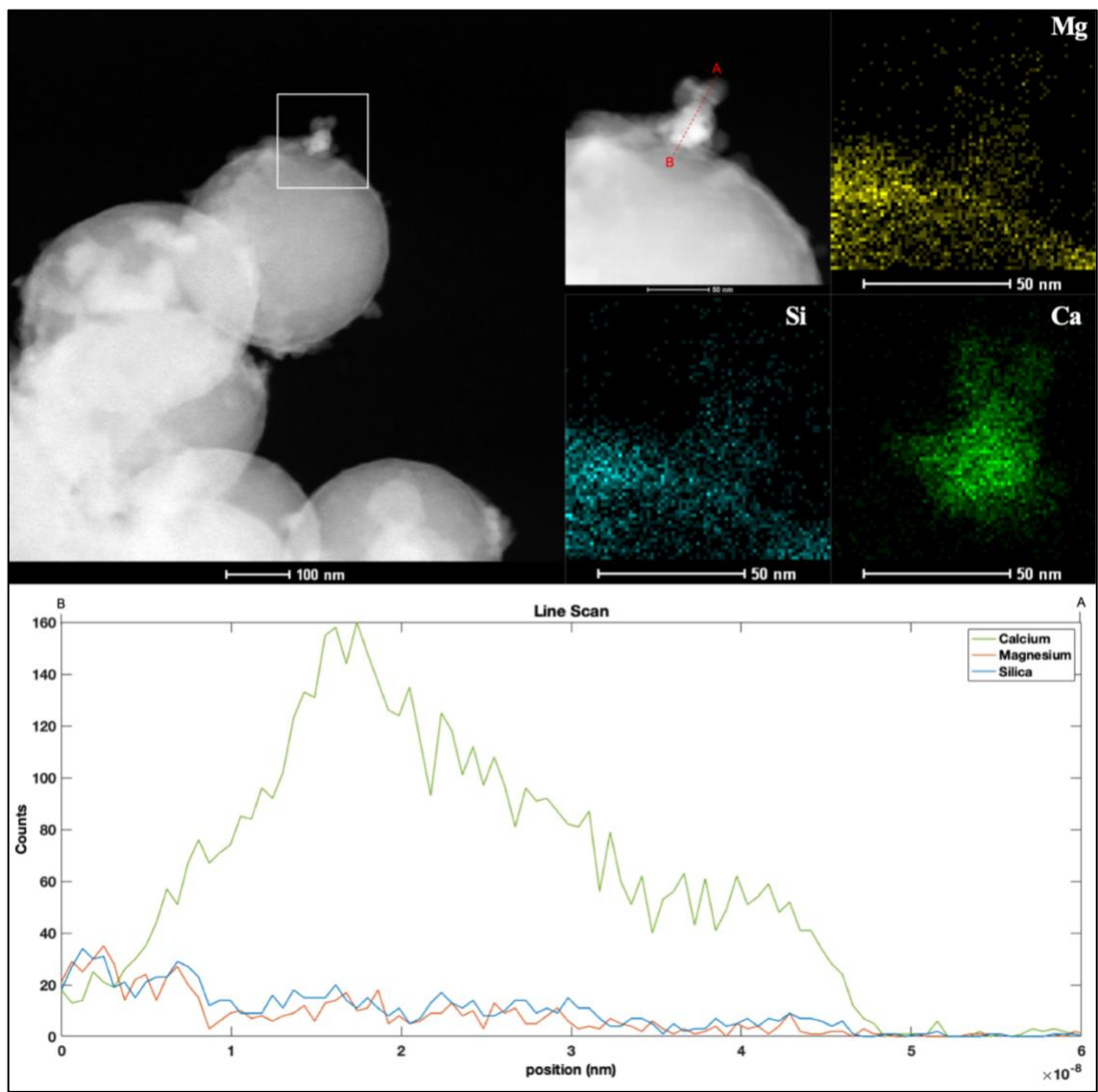


Figure 17 | Transmission Electron Microscopy throughout a microsphere surface (day 15). Line scan using TEM.

References

- Adams, J.E., Rhodes, M.L., 1960, **Dolomitization by Seepage Refluxion: AAPG Bulletin 44**, v. 44, p.1912-1920.
- Algeo, T. J., Luo, G. M., Song, H. Y., Lyons, T. W., Canfield, D. E., 2015, **Reconstruction of secular variation in seawater sulfate concentrations: Biogeosciences**, v. 12, p. 2131-2151.
- Allen, P. A., Hoffman, P. F., 2005, **Extreme winds and waves in the aftermath of a Neoproterozoic glaciation: Nature**, v. 433, p. 123-127.
- Arvidson, R.S., Mackenzie, F.T., 1999, **The dolomite problem; control of precipitation kinetics by temperature and saturation state: American Journal of Science**, v. 299, p. 257–288.
- Babilonia, J., Conesa, A., Casaburi, G., Pereira, C., Louyakis, A. S., Reid, R. P., Foster, J. S., 2018, **Comparative Metagenomics Provides Insight Into the Ecosystem Functioning of the Shark Bay Stromatolites, Western Australia: Frontiers in Microbiology**, v. 9, p. 1-16
- Bao, H., Lyons, J. R., Zhou, C., 2008, **Triple oxygen isotope evidence for elevated CO₂ levels after a Neoproterozoic glaciation: Nature**, v. 453, p. 504-506.
- Belton, D. J., Deschaume, O., and Perry, C. C., 2012, **An overview of the fundamentals of the chemistry of silica with relevance to biosilicification and technological advances: FEBS Journal**, v. 279, p. 1710-1720.
- Bontognali, T. R. R., Mckenzie, J. A., Warthmann, R. J., Vasconcelos, C., 2014, **Microbially influenced formation of Mg-calcite and Ca-dolomite in the presence of exopolymeric substances produced by sulphate-reducing bacteria: Terra Nova**, v. 26, p. 72–77.
- Bontognali, T.R.R., Vasconcelos, C., Warthmann, R.J., Bernasconi, S.M., Dupraz, C., Strohmenger, C.J., Mckenzie, J.A., 2010, **Dolomite formation within microbial mats in the coastal sabkha of Abu Dhabi (United Arab Emirates): Sedimentology**, v. 57, p. 824–844.
- Brady, P. V., Krumhansl, J. L., and Papenguth, H. W., 1996, **Surface complexation clues to dolomite growth: Geochimica Et Cosmochimica Acta**, v. 60, p. 727-731.
- Braissant, O., Cailleau, G., Dupraz, C., and Verrecchia, E.P., 2003, **Bacterially Induced Mineralization of Calcium Carbonate in Terrestrial Environments: The Role of Exopolysaccharides and Amino Acids: Journal of Sedimentary Research**, v. 73, p. 485–490.
- Braissant, O., Decho, A.W., Dupraz, C., Glunk, C., Przekop, K.M., Visscher, P.T., 2007, **Exopolymeric substances of sulfate-reducing bacteria: Interactions with calcium at alkaline pH and implication for formation of carbonate minerals: Geobiology**, v. 5, p. 401–411.
- Brauchli, M., Mckenzie, J. A., Strohmenger, C. J., Sadooni, F., Vasconcelos, C., Bontognali, T. R. R., 2015, **The importance of microbial mats for dolomite formation in the Dohat Faishakh sabkha, Qatar: Carbonates and Evaporites**, v. 31, p. 339–345.
- Bunting, J. W., Thong, K. M., 1970, **Stability constants for some 1:1 metal–carboxylate complexes: Canadian Journal of Chemistry**, v. 48, p. 1654-1656.
- Burne, R. V., Moore, L. S., 1987, **Microbialites: organosedimentary deposits of benthic microbial communities: Palaios**, v. 1, p. 241-254.

- Cantrell, D.L., Swart, P.K., Handford, R.C., Kendall, C.G., Westphal, H., 2001, **Geology and Production Significance of Dolomite Arab-D Reservoir, Ghawar Field, Saudi Arabia:** *GeoArabia*, v. 6, p. 45-60.
- Chen, Y., Shen, A., Pan, L., Zhang, J., Wang, X., 2017, **Features, origin and distribution of microbial dolomite reservoirs: A case study of 4 th Member of Sinian Dengying Formation in Sichuan Basin, SW China:** *Petroleum Exploration and Development*, v. 44, p. 745–757.
- Coggon, R. M., Teagle, D. A. H., Smith-Duque, C. E., Alt, J. C., Cooper, M. J., 2010, **Reconstructing Past Seawater Mg/Ca and Sr/Ca from Mid-Ocean Ridge Flank Calcium Carbonate Veins:** *Science*, v. 327, p. 1114–1117.
- Conley, D.J., Frings, P.J., Fontorbe, G., Clymans, W., Stadmark, J., Hendry, K.R., Marron, A.O. Rocha, C.L.D.L., 2017, **Biosilicification Drives a Decline of Dissolved Si in the Oceans through Geologic Time:** *Frontiers in Marine Science*, v. 4, p. 1-19.
- Davies, G.R., 1997, **Hydrothermal Dolomite (HTD) Reservoir Facies: Global Perspectives on Tectonic-Structural and Temporal Linkage Between MVT and Sedex Pb-Zn Ore Bodies, and Subsurface HTD Reservoir Facies:** *Canadian Society of Petroleum Geologists*, Short Course Notes.
- Daye, M., Higgins, J., Bosak, T., 2019, **Formation of ordered dolomite in anaerobic photosynthetic biofilms:** *Geology*, v. 47, p. 509–512.
- Decho, A. W., 1990, **Microbial exopolymer secretions in ocean environments: their role(s) in food webs and marine processes:** *Oceanography and Marine Biology Annual Review*, v. 28, p. 73–154.
- Defeeyes, K.S., Lucia, F.J. Weyl, P.K., 1965, **Dolomitization of recent and Plio-Pleistocene sediments by marine evaporite waters on Bonaire, Netherlands Antilles.** In: Pray, L.C. and Murray, R.C. (eds) Dolomitization and Limestone Diagenesis: *Society of Economic Paleontologists and Mineralogists, Special Publications*, v. 13, p. 71-88.
- Demadis, K. D., Ketsetzi, A., Sarigiannidou, E., 2012, **Catalytic Effect of Magnesium Ions on Silicic Acid Polycondensation and Inhibition Strategies Based on Chelation:** *Industrial & Engineering Chemistry Research*, v. 51, p. 9032-9040.
- Demico, R.V., Lowenstein, T.K., Hardie, L.A., and Spencer, R.J., 2005, **Model of seawater composition for the Phanerozoic:** *Geology*, v. 33, p. 877.
- Des Marais, D. J., 1990, **Microbial mats and the early evolution of life:** *Trends in ecology & evolution* v. 5, p. 140-144.
- Diaz-Pulido, G., Nash, M. C., Anthony, K. R., Bender, D., Opdyke, B. N., Reyes-Nivia, C., Troitzsch, U., 2014, **Greenhouse conditions induce mineralogical changes and dolomite accumulation in coralline algae on tropical reefs:** *Nature Communications*, v. 5.
- Diloreto, Z. A., Bontognali, T. R. R., Disi, Z. A. A., Al-Kuwari, H. A. S., Williford, K. H., Strohmenger, C. J., ... Dittrich, M., 2019, **Microbial community composition and dolomite formation in the hypersaline microbial mats of the Khor Al-Adaid sabkhas, Qatar:** *Extremophiles*, v. 23, p. 201–218.
- Dupraz, C., Reid, P., Braissant, O., Decho, A.W., Norman, R.S. Visscher, P.T., 2009, **Processes of carbonate precipitation in modern microbial mats:** *Earth-Science Reviews* v. 96, p. 141-162.
- Fairbridge, R.W., 1957, **The Dolomite Question: In: LeBlanc RJ and Breeding JG (eds): Regional Aspects of Carbonate Deposition: A Symposium:** *Society of Economic Paleontologists and Mineralogists*, v. 5, p. 125–178.

- Feely, R., Doney, S. Cooley, S., 2009, **Ocean Acidification: Present Conditions and Future Changes in a High-CO₂ World:** *Oceanography*, v. 22, p. 36–47.
- Fein, J. B., Scott, S., Rivera, N., 2002, **The effect of Fe on Si adsorption by *Bacillus subtilis* cell walls: Insights into non-metabolic bacterial precipitation of silicate minerals:** *Chemical Geology*, v. 182, p. 265-273.
- Fike, D.A., Grotzinger, J.P., Pratt, L.M. Summons, R.E., 2006, **Oxidation of the Ediacaran Ocean:** *Nature*, v. 444, p. 744–747.
- Gao, P., Li, S., Lash, G. G., He, Z., Xiao, X., Zhang, D., Hao, Y., 2020, **Silicification and Si cycling in a silica-rich ocean during the Ediacaran-Cambrian transition:** *Chemical Geology*, v. 552, p. 119787.
- Goldsmith, J.R., 1980, **Thermal stability of dolomite at high temperatures and pressures:** *Journal of Geophysical Research*, v. 85, p. 6949.
- Grotzinger, J., Al-Rawahi, Z., 2014, **Depositional facies and platform architecture of microbialite-dominated carbonate reservoirs, Ediacaran–Cambrian Ara Group, Sultante of Om:** *AAPG Bulletin*, v. 98, p. 1453-1494.
- Grotzinger, J.P., 1990. **Geochemical model for Proterozoic stromatolite decline:** *American Journal of Science*, v. 290, p. 80–103.
- Grotzinger, J.P., Kastig, J.F., 1993, **New Constraints on Precambrian Ocean Composition:** *The Journal of Geology*, v. 101, p. 235–243.
- Halevy, I., Bachan, A., 2017, **The geologic history of seawater pH:** *Science*, v. 355, p. 1069–1071.
- Hardie, L.A., 1987, **Dolomitization: a critical view of some current views:** *Journal of Sedimentary Petrology*, v. 57, p. 166-183.
- Hardie, L.A., 2003, **Secular variations in Precambrian seawater chemistry and the timing of Precambrian aragonite seas and calcite seas:** *Geology*, v. 31, p. 785–788.
- Harwood, C. L., Sumner, D. Y., 2011, **Microbialites of the Neoproterozoic Beck Spring Dolomite, Southern California:** *Sedimentology*, v. 58, p. 1648-1673.
- Higgins, J. A., and Schrag, D. P., 2003, **Aftermath of a snowball Earth:** *Geochemistry, Geophysics, Geosystems*, v. 4, p. 1028.
- Hoffman, P. F., A. J., Halverson, G. P., Schrag, D. P., 1998, **A Neoproterozoic Snowball Earth:** *Science*, v. 281, p. 1342-1346.
- Hoffman, P. F., Schrag, D. P., 2002, **The snowball Earth hypothesis: Testing the limits of global change:** *Terra Nova*, v. 14, p. 129-155.
- Hohl, S. V., Becker, H., Jiang, S., Ling, H., Guo, Q., Struck, U., 2017, **Geochemistry of Ediacaran cap dolostones across the Yangtze Platform, South China: Implications for diagenetic modification and seawater chemistry in the aftermath of the Marinoan glaciation:** *Journal of the Geological Society*, v. 174, p. 893-912.
- Hood, A. V., Wallace, M. W., Drysdale, R. N., 2011, **Neoproterozoic aragonite-dolomite seas? Widespread marine dolomite precipitation in Cryogenian reef complexes:** *Geology*, v. 39, p. 871-874.
- Horita, J., Zimmermann, H., Holland, H. D., 2002, **Chemical evolution of seawater during the Phanerozoic:** *Geochimica et Cosmochimica Acta*, v. 66, p. 3733–3756.
- Hu, Y., Cai, C., Liu, D., Pederson, C.L., Jiang, L., Shen, A., Immenhauser, A., 2020, **Formation, diagenesis and palaeoenvironmental significance of upper Ediacaran fibrous dolomite cements:** *Sedimentology*, v. 67, p. 1161–1187.

- Hurtgen, M.T., Halverson, G.P., Arthur, M.A. Hoffman, P.F., 2006, **Sulfur cycling in the aftermath of a 635-Ma snowball glaciation: Evidence for a syn-glacial sulfidic deep ocean:** *Earth and Planetary Science Letters* v. 245, p. 551–570.
- Jones B. F., 1966, **Geochemical evolution of closed basin water in western Great Basin:** *Proceedings of the Second Symposium on Salt sponsored by the Northern Ohio Geological Society*, v. 1, pp. 181-200.
- Kaczmarek, S.E., Thornton, B.P., 2017. **The effect of temperature on stoichiometry, cation ordering, and reaction rate in high-temperature dolomitization experiments:** *Chemical Geology* v. 468, p. 32–41.
- Kah, L.C., Lyons, T.W., Frank, T.D., 2004, **Low marine sulphate and protracted oxygenation of the Proterozoic biosphere:** *Nature*, v. 431, p. 834–838.
- Kasemann, S. A., Strandmann, P. A., Prave, A. R., Fallick, A. E., Elliott, T., Hoffmann, K., 2014, **Continental weathering following a Cryogenian glaciation: Evidence from calcium and magnesium isotopes:** *Earth and Planetary Science Letters*, v. 396, p. 66-77.
- Kennedy, M., Mrofka, D., Borch, C. V., 2008, **Snowball Earth termination by destabilization of equatorial permafrost methane clathrate:** *Nature*, v. 453, p. 642-645.
- Kenward, P. A., Fowle, D. A., Goldstein, R. H., Ueshima, M., González, L. A., Roberts, J. A., 2013, **Ordered low-temperature dolomite mediated by carboxyl-group density of microbial cell walls:** *AAPG Bulletin*, v. 97, p. 2113-2125.
- Kenward, P. A., Goldstein, R. H., González, L. A., Roberts, J. A., 2009, **Precipitation of low-temperature dolomite from an anaerobic microbial consortium: The role of methanogenic Archaea:** *Geobiology*, v. 7, p. 556–565.
- Land, L. S., 1998, **Failure to precipitate dolomite at 25°C from dilute solution despite 1000-fold oversaturation after 32 years:** *Aquatic Geochemistry*, v. 4, p. 361–368.
- Land, L.S. 1973, **Contemporaneous dolomitization of middle Pleistocene reefs meteoric water, North Jamaica:** *Bulletin of Marine Science*, v. 23, p. 64-92.
- Last, F. M., Last, W. M., Halden, N. M., 2012, **Modern and late Holocene dolomite formation: Manito Lake, Saskatchewan, Canada:** *Sedimentary Geology*, v. 281, p. 222-237.
- Latour, I., Miranda, R., Blanco, A., 2015, **Optimization of silica removal with magnesium chloride in papermaking effluents: Mechanistic and kinetic studies:** *Environmental Science and Pollution Research*, v. 23, p. 3707-3717.
- Lei, H., Zhu, L., 1992, **Study of origin of the Sinuan algal and nonalgal dolostones in Sichuan Basin:** *Acta Sedimentologica Sinica*, v. 10, p. 69-78. (in Chinese with English abstract).
- Li, Z., Goldstein, R. H., Franseen, E. K., 2013, **Ascending Freshwater-Mesohaline Mixing: A New Scenario for Dolomitization:** *Journal of Sedimentary Research*, v. 83, p. 277-283.
- Lin, X., Peng, J., Du, L., Yan, J., Hou, Z., 2017, **Characterization of the Microbial Dolomite of the Upper Sinian Dengying Formation in the Hanyuan Area of Sichuan Province, China:** *Acta Geologica Sinica - English Edition*, v. 91, p. 806–821.
- Liu, D., Xu, Y., Papineau, D., Yu, N., Fan, Q., Qiu, X., Wang, H., 2019, **Experimental evidence for abiotic formation of low-temperature proto-dolomite facilitated by clay minerals:** *Geochimica et Cosmochimica Acta*, v. 247, p. 83–95.
- Lonnee, J. and Machel, H.G., 2004, **Dolomitization by halite-saturated brine and subsequent hydrothermal alteration in the Devonian Slave Point Formation, Clark Lake gas field, British Columbia:** *CSPG-CHOA-CWLS Joint Conference Abstracts*, S013.

- Lowenstein TK, Timofeeff MN, Brennan ST, Hardie LA, Demicco RV, 2001, **Oscillations in Phanerozoic seawater chemistry: evidence from fluid inclusions:** *Science*, v. 294, p. 1086-1088.
- McKenzie, J.A., 1991, **The Dolomite Problem: An Outstanding Controversy** *In* Muller, D.W., McKenzie, J.A., Weissert, H., **Controversies in Modern Geology: Evolution of Geological Theories in Sedimentology, Earth History, and Tectonics:** *Academic Press, Harcourt Brace Jovanovich, Publishers.* New York.
- Mckenzie, J.A., Hsü, K.J., Schneider, J.E., 1980, **Movement of subsurface waters under the sabkha, Abu Dhabi, UAE, and its relation to evaporative dolomite genesis.** In: ZENGER, D.H., DUNHAM, J.B. & ETHINGTON, R.L. (eds) **Concepts and Models of Dolomitization: Society of Economic Paleontologists and Mineralogists, Special Publications**, v. 28, p. 11-30.
- Meng, F., Ni, P., Schiffbauer, J.D., Yuan, X., Zhou, C., Wang, Y., Xia, M., 2011, **Ediacaran seawater temperature: Evidence from inclusions of Sinian halite:** *Precambrian Research*, v. 184, p. 63–69.
- Meng, X., Liu, L., Balsam, W., Li, S., He, T., Chen, J., Ji, J., 2015, **Dolomite abundance in Chinese loess deposits: A new proxy of monsoon precipitation intensity:** *Geophysical Research Letters*, v. 42.
- Mercedes-Martín, R., Rogerson, M., Brasier, A., Vonhof, H., Prior, T., Fellows, S., Reijmer, J.J.G., Billing, I., Pedley, H.M., 2016, **Growing spherulitic calcite grains in saline, hyperalkaline lakes: Experimental evaluation of the effects of Mg-clays and organic acids:** *Sedimentary Geology*, v. 335, p. 93-102.
- Morrow, D.W., Ricketts, B.D., 1988, **Experimental investigation of sulfate inhibition of dolomite and its mineral analogues:** *Society of Economical Paleontology Mineralogy*, v. 43, p. 25-38.
- Norris, S. E., 1957, **Characteristics of Limestone and Dolomite Aquifers in Western Ohio:** *Journal - American Water Works Association*, v. 49, p. 464–468.
- Ohnemueller, F., Prave, A.R., Fallick, A.E., Kasemann, S.A., 2014, **Ocean acidification in the aftermath of the Marinoan glaciation:** *Geology*, v. 42, p. 1103–1106.
- Ohnemüller, F., 2014, **Reconstruction of Ediacaran to early Cambrian Ocean pH and weathering conditions:** *Dissertation. Universität Bremen.* [https://doi.org/\[http://\]http://nbn-resolving.de/urn:nbn:de:gbv:46-00103948-13](https://doi.org/[http://]http://nbn-resolving.de/urn:nbn:de:gbv:46-00103948-13).
- Pace, A., Bourillot, R., Bouton, A., Vennin, E., Galaup, S., Bundeleva, I., Patrier, P., Dupraz, C., Thomazo, C., Sansjofre, P., Yokoyama, Y., Franceschi, M., Anguy, Y., Pigot, L., Virgone, A., Visscher, P. T., 2016, **Microbial and diagenetic steps leading to the mineralisation of Great Salt Lake microbialites:** *Scientific Reports*, v. 6.
- Parkhurst, D.L., Appelo, C.A.J., 2013, **Description of input and examples for PHREEQC Version 3 – a computer program for speciation, batch-reaction, one-dimensional transport, and inverse geochemical calculations:** *U.S. Geological Survey Techniques and Methods*, book 6, chap. A43, p. 497.
- Paula-Santos, G.M., Caetano-Filho, S., Enzweiler, J., Navarro, M.S., Babinski, M., Guacaneme, C., Kuchenbecker, M., Reis, H., Trindade, R.I., 2020, **Rare earth elements in the terminal Ediacaran Bambuí Group carbonate rocks (Brazil): evidence for high seawater alkalinity during rise of early animals:** *Precambrian Research*, v. 336, p. 105506.

- Peng, H., Liu, S., Song, J., Sun, W., Ding, Y., Yin, K., 2014, **Characteristics of microbial carbonate rocks in upper Sinian Dengying Formation of Micang Mountains, North Sichuan, China (Chinese version):** *Journal of Chengdu University of Technology (Science and Technology Edition)*, v. 41, p. 181-191.
- Penman, D.E., Rooney, A.D., 2019, **Coupled carbon and silica cycle perturbations during the Marinoan snowball Earth deglaciation:** *Geology*, v. 47, p. 317–320.
- Peters, S. E., Husson, J. M., Wilcots, J., 2017, **The rise and fall of stromatolites in shallow marine environment:** *Geology*, v. 45, p. 487-490.
- Petrash, D.A., Bialik, O.M., Bontognali, T.R., Vasconcelos, C., Roberts, J.A., Mckenzie, J.A., and Konhauser, K.O., 2017, **Microbially catalyzed dolomite formation: From near-surface to burial:** *Earth-Science Reviews*, v. 171, p. 558–582.
- Plummer, L.N., Parkhurst, D.L., Fleming, G.W., Dunkle, S.A., 1988, **A computer program Incorporating Pitzer's equations for calculations of geochemical reactions in brines:** *U.S Geological Survey Water-Resources Investigations Report*, p. 88-4153.
- Roberts, J. A., Bennett, P. C., González, L. A., Macpherson, G., Milliken, K. L., 2004, **Microbial precipitation of dolomite in methanogenic groundwater:** *Geology*, v. 32, p. 277.
- Roberts, J. A., Kenward, P. A., Fowle, D. A., Goldstein, R. H., González, L. A., Moore, D.S., 2013, **Surface chemistry allows for abiotic precipitation of dolomite at low temperature:** *Proceedings of the National Academy of Sciences*, v. 110, p. 14540-14545.
- Rodriguez-Colon, B.J., Roberts, J.A., Baker, G.S., Ramírez-Martínez, W.R., Chabrier-Alpi, A., Hiripitiyage, Y., Duckett, M., Sturm, B., 2019, **Unveiling the Occurrence of Microbialite Formations in the Southwest of Puerto Rico:** *Astrobiology Science Conference 2019, Abstract #482874*.
- Samylyna, O. S., Zaytseva, L. V., 2018, **Characterization of modern dolomite stromatolites from hypersaline Petukhovskoe Soda Lake, Russia:** *Lethaia*, v. 52, p. 1–13.
- Sánchez-Román, M., Mckenzie, J.A., Wagener, A.D.L.R., Rivadeneyra, M.A. Vasconcelos, C., 2009, **Presence of sulfate does not inhibit low-temperature dolomite precipitation:** *Earth and Planetary Science Letters*, v. 285, p. 131–139.
- Sánchez-Román, M.C.B., Vasconcelos, C., Warthmann, R., Rivadeneyra, M., Mckenzie, J.A., 2009, **Microbial Dolomite Precipitation under Aerobic Conditions: Results from Brejo do Espinho Lagoon (Brazil) and Culture Experiments:** *Perspectives in Carbonate Geology*, v. 41, p. 167–178.
- Sanz-Montero, M. E., Cabestrero, Ó., Sánchez-Román, M., 2019, **Microbial Mg-rich Carbonates in an Extreme Alkaline Lake (Las Eras, Central Spain):** *Frontiers in Microbiology*, v. 10.
- Seilacher, A., Grazhdankin, D. Legouta, A., 2003, **Ediacaran biota: The dawn of animal life in the shadow of giant protists:** *Paleontological Research*, v. 7, p. 43–54.
- Shan, X., Zhang, J., Zhang, B., Liu, J., Zhou, H., Wang, Y., Fu, Z., 2017, **Characteristics of dolomite karstic reservoir in the Sinian Dengying Formation, Sichuan Basin:** *Petroleum Research*, v. 2, p. 13–24.
- Shen, A., Zheng, J., Chen, Y., Ni, X., Huang, L., 2016, **Characteristics, origin and distribution of dolomite reservoirs in Lower-Middle Cambrian, Tarim Basin, NW China:** *Petroleum Exploration and Development*, v. 43, p. 375–385.
- Siever, R., 1992, **The silica cycle in the Precambrian:** *Geochimica et Cosmochimica Acta*, v. 56, p. 3265–3272.

- Tarhan, L.G., Hood, A.V., Droser, M.L., Gehling, J.G., Briggs, D.E., 2016, **Exceptional Preservation of Soft-Bodied Ediacara Biota Promoted by Silica-Rich Oceans:** *Geology*, v. 44, p. 951-954.
- Tosca, N. J., Masterson, A. L., 2014, **Chemical controls on incipient Mg-silicate crystallization at 25°C: Implications for early and late diagenesis:** *Clay Minerals*, v. 49, p. 165-194.
- Tosca, N. J., Wright, V. P., 2015, **Diagenetic pathways linked to labile Mg-clays in lacustrine carbonate reservoirs: A model for the origin of secondary porosity in the Cretaceous pre-salt Barra Velha Formation, offshore Brazil:** *Geological Society, London, Special Publications*, v. 435, p. 33-46.
- Tucker, M.E., 1992, **The Precambrian–Cambrian boundary: seawater chemistry, ocean circulation and nutrient supply in metazoan evolution, extinction and biomineralization:** *Journal of the Geological Society*, v. 149, p. 655–668.
- Tutolo, B. M., Tosca, N. J., 2018, **Experimental Examination of the Mg-Silicate System at Ambient Temperature: Implications for Alkaline Chemical Sedimentation and Lacustrine Carbonate Formation:** *Geochimica et Cosmochimica Acta*, v. 225, p. 80-101.
- Van Gemerden, H. 1993, **Microbial mats: a joint venture:** *Mar Geol*, v. 113, p. 3– 25.
- Vandeginste, V., John, C. M., 2012, **Influence of climate and dolomite composition on dedolomitization: insights from a multi-proxy study in the central Oman Mountains:** *Journal of Sedimentary Research*, v. 82, p. 177–195.
- Vasconcelos, C., McKenzie, J. A., 1997, **Microbial mediation of modern dolomite precipitation and diagenesis under anoxic conditions (Lagoa Vermelha, Rio De Janeiro, Brazil):** *Journal of Sedimentary Petrology*, v. 67, p. 378–390.
- Vasconcelos, C., Mckenzie, J. A., Warthmann, R., Bernasconi, S. M., 2005, **Calibration of the $\delta^{18}\text{O}$ paleothermometer for dolomite precipitated in microbial cultures and natural environments:** *Geology*, v. 33, p. 317.
- Vasconcelos, C., Mckenzie, J.A., Bernasconi, S., Grujic, D., Tiens, A.J., 1995, **Microbial mediation as a possible mechanism for natural dolomiteformation at low temperatures:** *Nature*, v. 377, p. 220–222.
- Visscher, P.T., Stolz, J.F., 2005, **Microbial mats as bioreactors: populations, processes, and products:** *Palaeogeography, Palaeoclimatology, Palaeoecology* v. 219, p. 87-100.
- Walker, J. C., Hays, P. B., Kasting, J. F., 1981, **A negative feedback mechanism for the long-term stabilization of Earth's surface temperature:** *Journal of Geophysical Research*, v. 86, p. 9776.
- Walker, J.D., Geissman, J.W., Bowring, S.A., Babcock, L.E., compilers, 2018, **Geologic Time Scale v. 5.0:** *Geological Society of America*, <https://doi.org/10.1130/2018.CTS005R3C>.
- Walton, W. C., Neill, J. C., 1963, **Statistical analysis of specific-capacity data for a dolomite aquifer:** *Journal of Geophysical Research*, v. 68, p. 2251–2262.
- Wang, J., He, Z., Zhu, D., Liu, Q., Ding, Q., Li, S., Zhang, D., 2020, **Petrological and geochemical characteristics of the botryoidal dolomite of Dengying Formation in the Yangtze Craton, South China: Constraints on terminal Ediacaran “dolomite seas”:** *Sedimentary Geology*, v. 406, p. 105722.
- Warren, J. K., 1990, **Sedimentology and Mineralogy of Dolomitic Coorong Lakes, South Australia:** *SEPM Journal of Sedimentary Research*, v. 60.

- Wilkinson, B.H., Given, R.K., 1986, **Secular variation in abiotic marine carbonates: Constraints on Phanerozoic atmospheric carbon dioxide contents and oceanic Mg/Ca ratios:** *The Journal of Geology*, v. 94, p. 321-333.
- Williams, G., 1979, **Sedimentology, stable-isotope geochemistry and palaeoenvironment of dolostones capping Late Precambrian glacial sequences in Australia:** *Journal of the Geological Society of Australia*, v. 26, p. 377-386.
- Wright, D. T., 1999, **The role of sulphate-reducing bacteria and cyanobacteria in dolomite formation in distal ephemeral lakes of the Coorong region, South Australia:** *Sedimentary Geology*, v. 126, p. 147-157.
- Wright, D.T., Wacey, D., 2005, **Precipitation of dolomite using sulphate-reducing bacteria from the Coorong Region, South Australia: significance and implications:** *Sedimentology*, v. 52, p. 987-1008.
- Wright, V. P., 2012, **Lacustrine carbonates in rift settings: The interaction of volcanic and microbial processes on carbonate deposition:** *Geological Society, London, Special Publications*, v. 370, p. 39-47.
- Yang, J., Jansen, M. F., Macdonald, F. A., Abbot, D. S., 2017, **Persistence of a freshwater surface ocean after a snowball Earth:** *Geology*, v. 45, p. 615-618.
- Yang, Z., Sun, Z., Yang, T., Pei, J., 2004, **A long connection (750-380 Ma) between South China and Australia: Paleomagnetic constraints:** *Earth and Planetary Science Letters*, v. 220, p. 423-434.
- Yoerg, A., 2018, **Carboxylated Organic Matter Influences Magnesium Uptake in Three Low-Temperature Dolomite Models:** *Master's thesis, University of Kansas.*
<http://hdl.handle.net/1808/29562>
- You, X.L., Sun, S., Lin, C.S., Zhu, J.Q., 2018, **Microbial dolomite in the sabkha environment of the middle Cambrian in the Tarim Basin, NW China:** *Australian Journal of Earth Sciences*, v. 65, p. 109-120.
- Yu, W., Algeo, T. J., Zhou, Q., Du, Y., Wang, P., 2020, **Cryogenian cap carbonate models: A review and critical assessment:** *Palaeogeography, Palaeoclimatology, Palaeoecology*, v. 552.
- Zhang, F., Xiao, S., Kendall, B., Romaniello, S. J., Cui, H., Meyer, M., Gilleaudeau, G.J., Kaufman, A.J., Anbar, A. D., 2018, **Extensive marine anoxia during the terminal Ediacaran Period:** *Science Advances*, v. 4, p. 1-11.
- Zhang, J., Zhang, B., Shan, X., 2017, **Review and Significance of Microbial Carbonate Reservoirs in China:** *Acta Geologica Sinica - English Edition*, v. 91, p. 157-158.
- Zhou, C., Guan, C., Cui, H., Ouyang, Q., Wang, W., 2016, **Methane-derived authigenic carbonate from the lower Doushantuo Formation of South China: Implications for seawater sulfate concentration and global carbon cycle in the early Ediacaran ocean:** *Palaeogeography, Palaeoclimatology, Palaeoecology*, v. 461, p. 145-155.

Appendix A

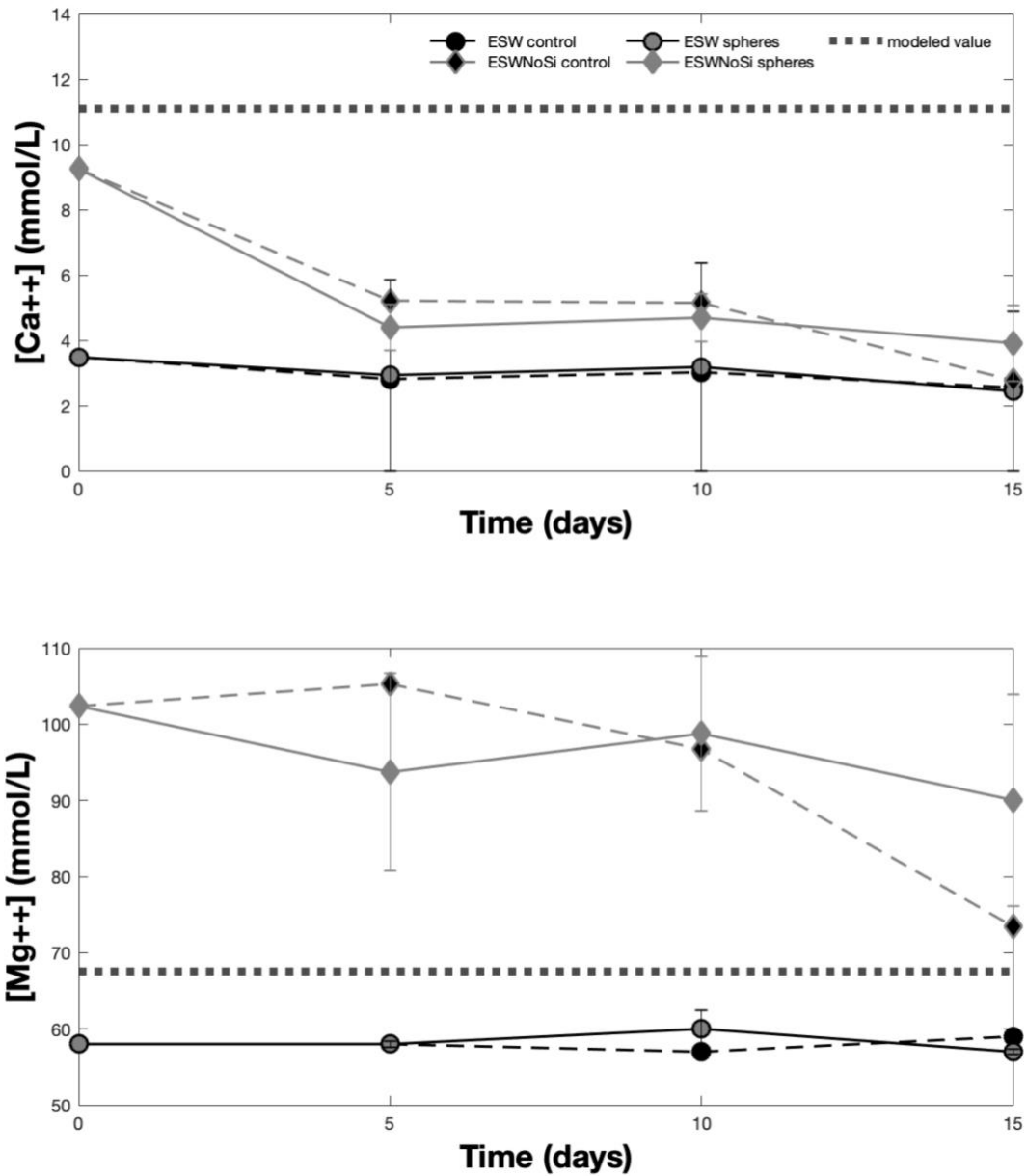


Figure Ap.1 | Calcium and magnesium evolution through the 15-day batch experiments.

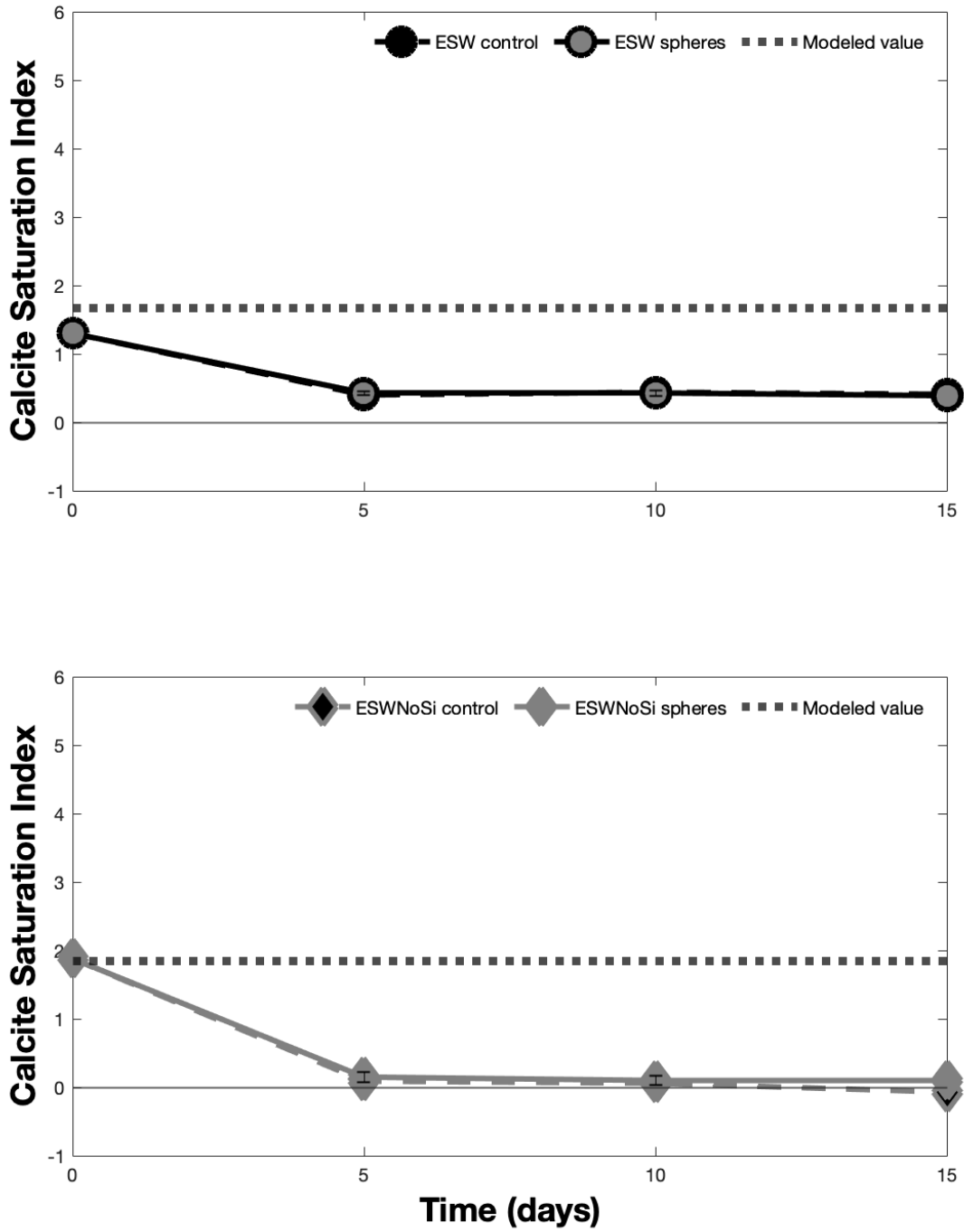


Figure Ap.2 | Saturation Indices of calcite (15 days) through time.

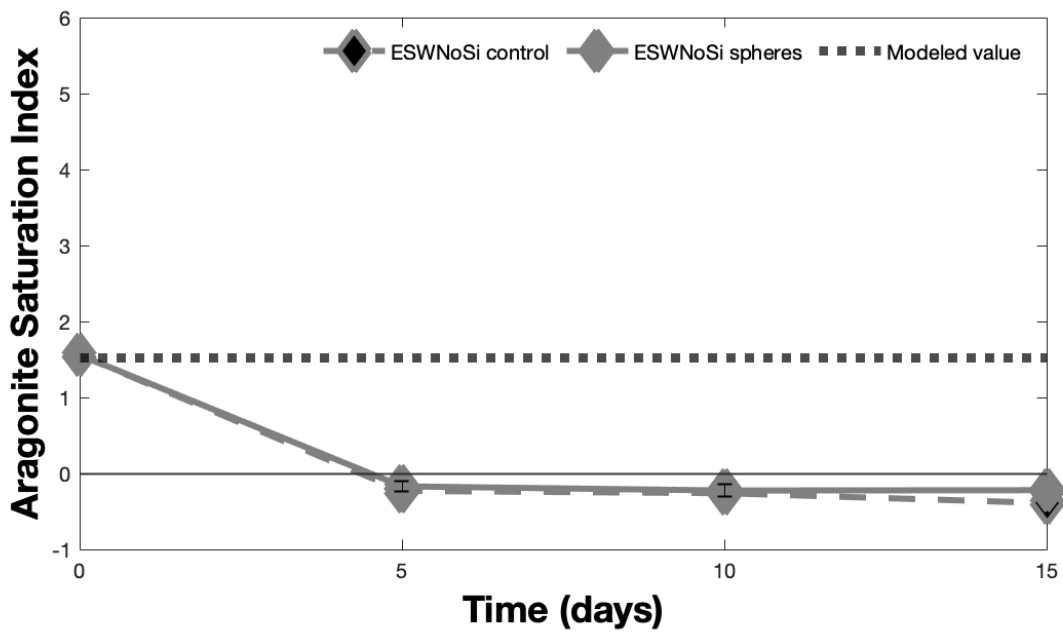
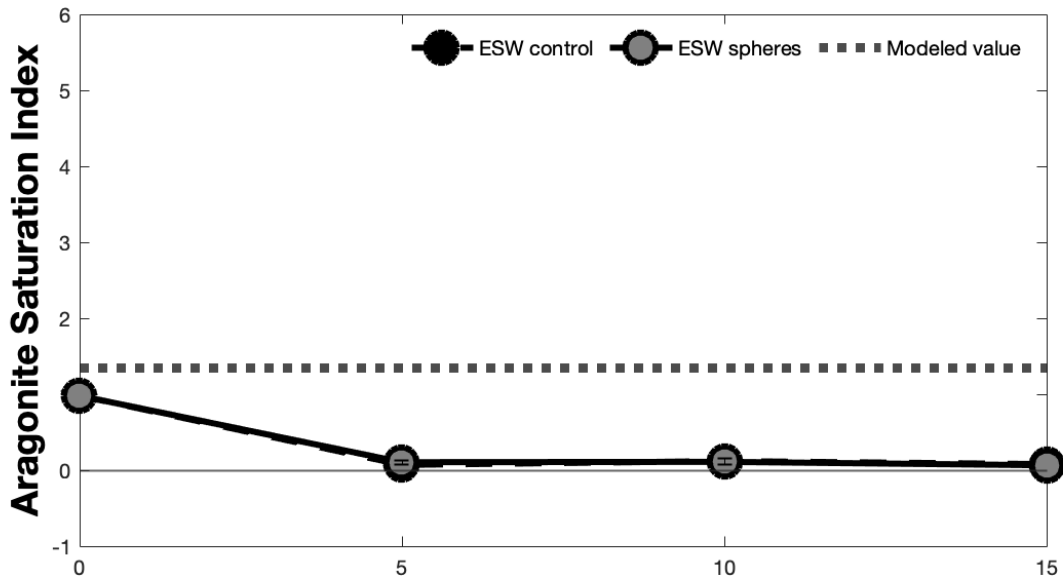


Figure Ap.3 | Saturation Indices of aragonite (15 days) through time.

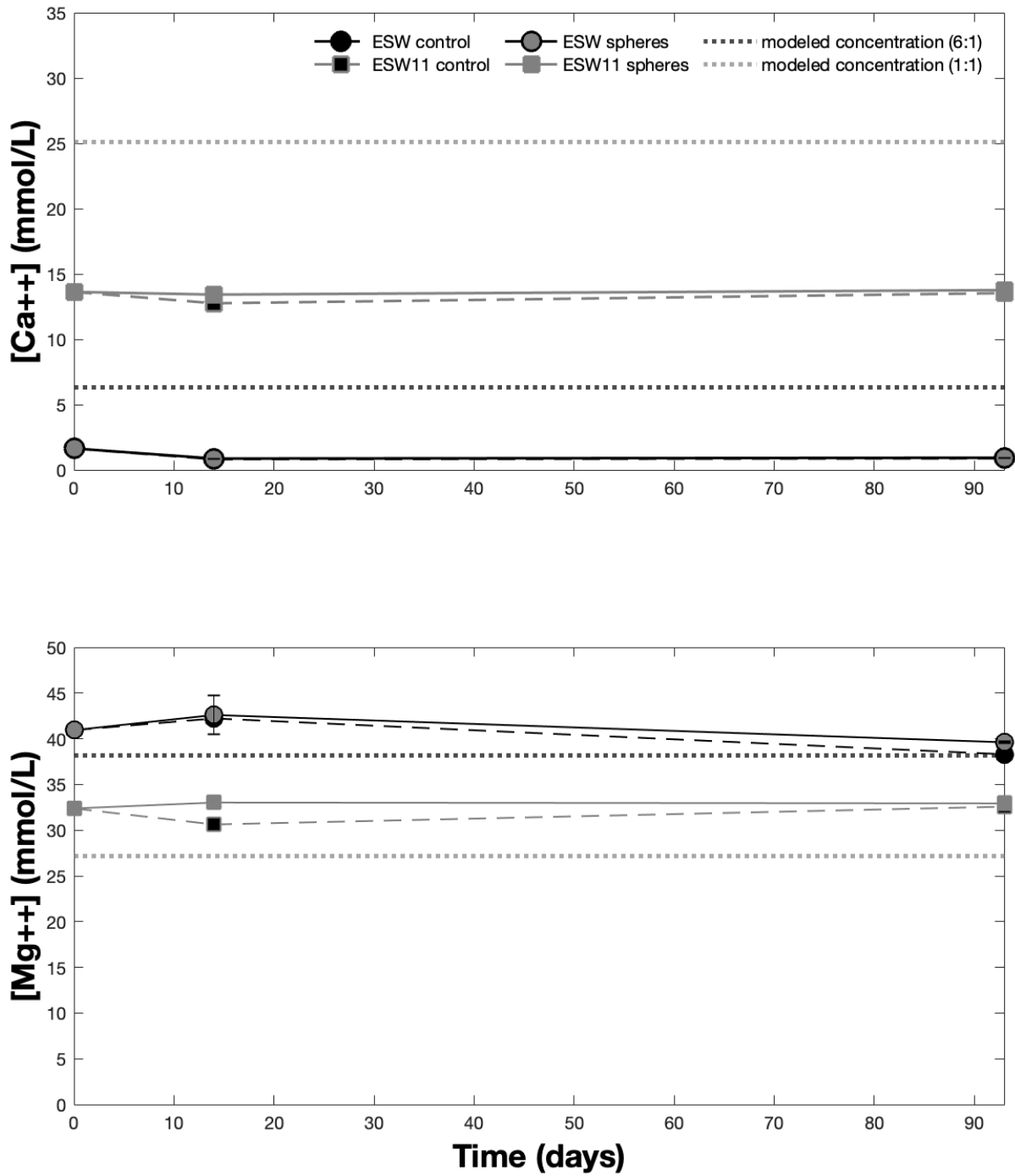


Figure Ap.4 | Calcium and magnesium evolution through the 93-day batch experiments.

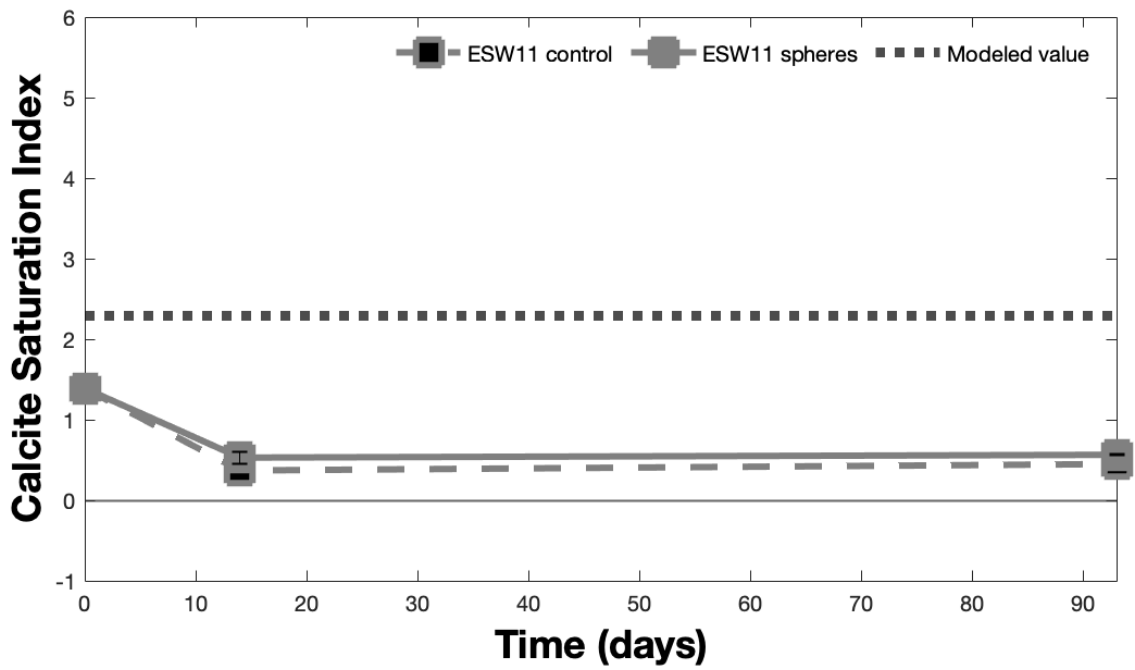
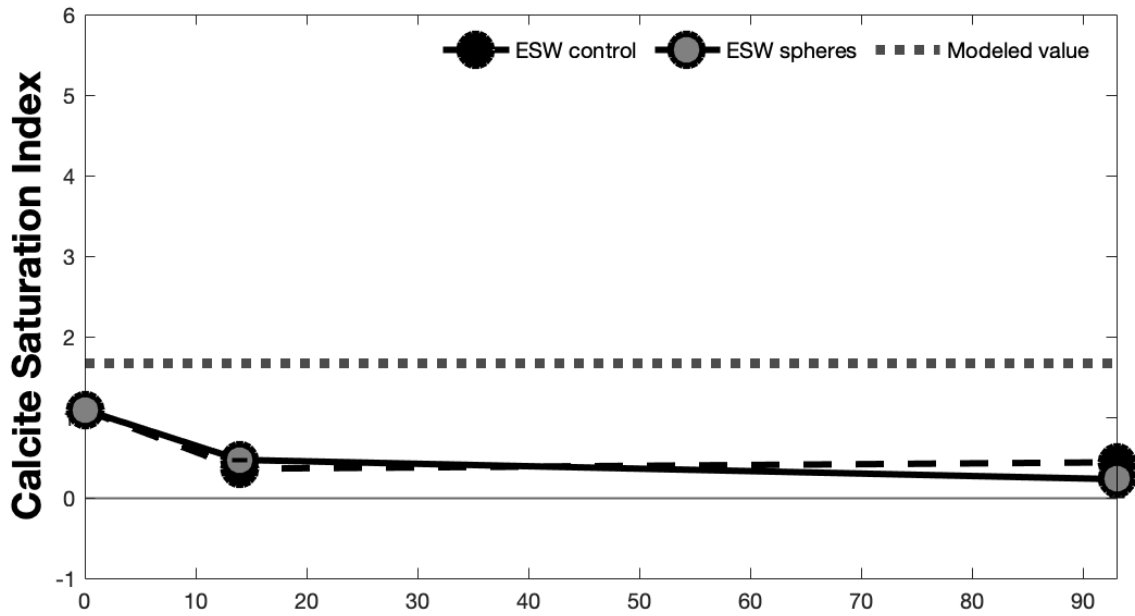


Figure Ap.5 | Saturation Indices of calcite (93-days) through time.

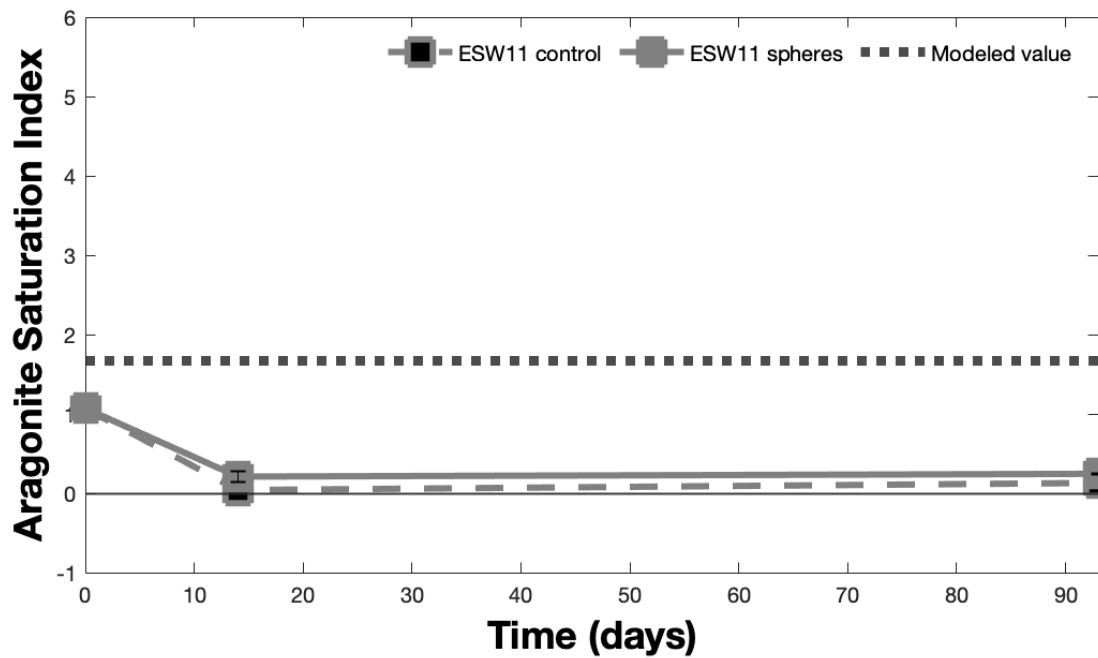
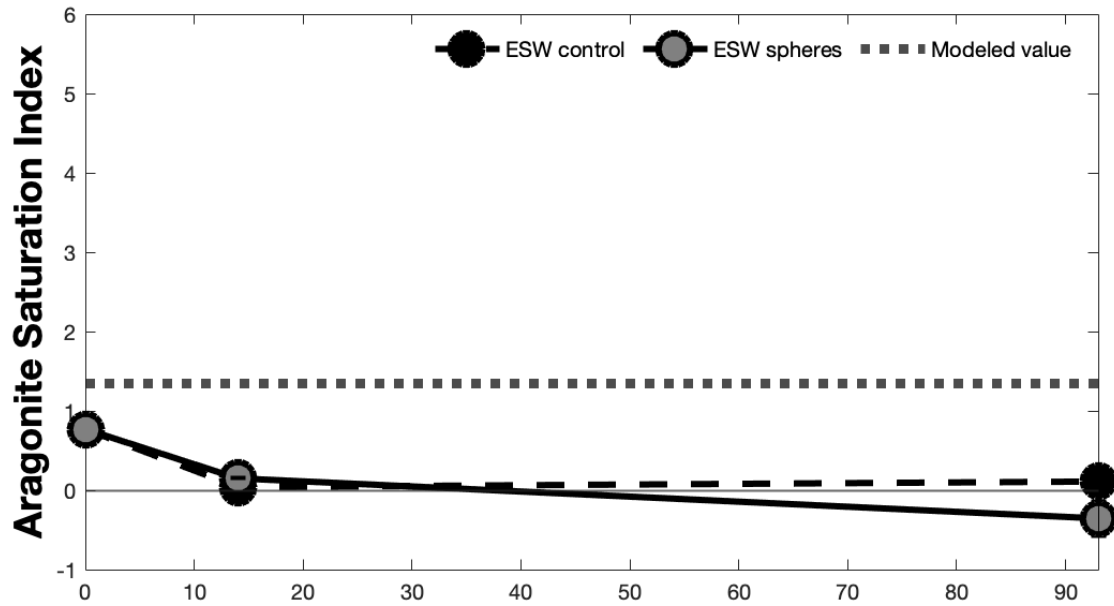


Figure Ap.6 | Saturation Indices of aragonite (93 days) through time.

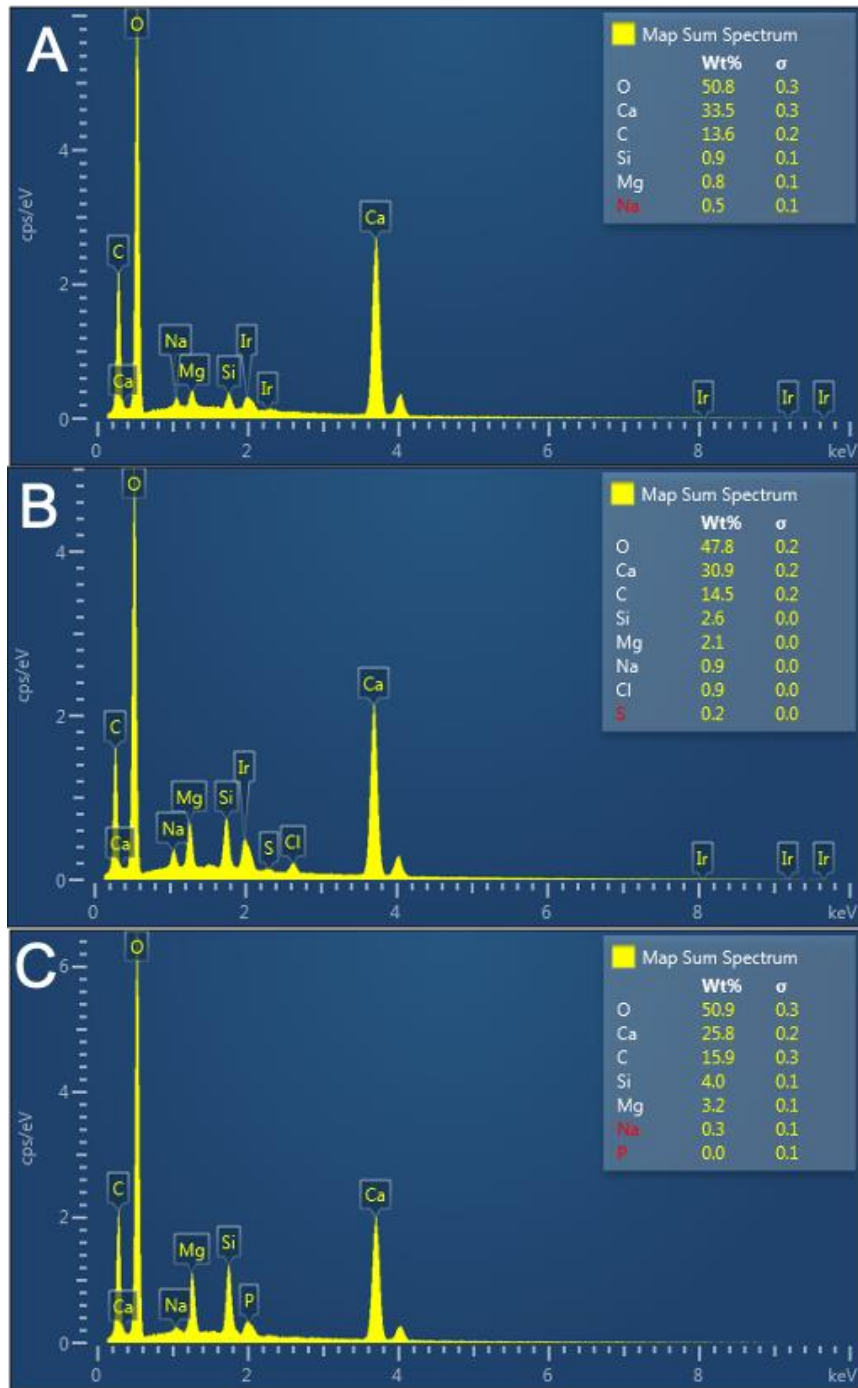


Figure Ap.7 | EDS spectra for Figure 8.

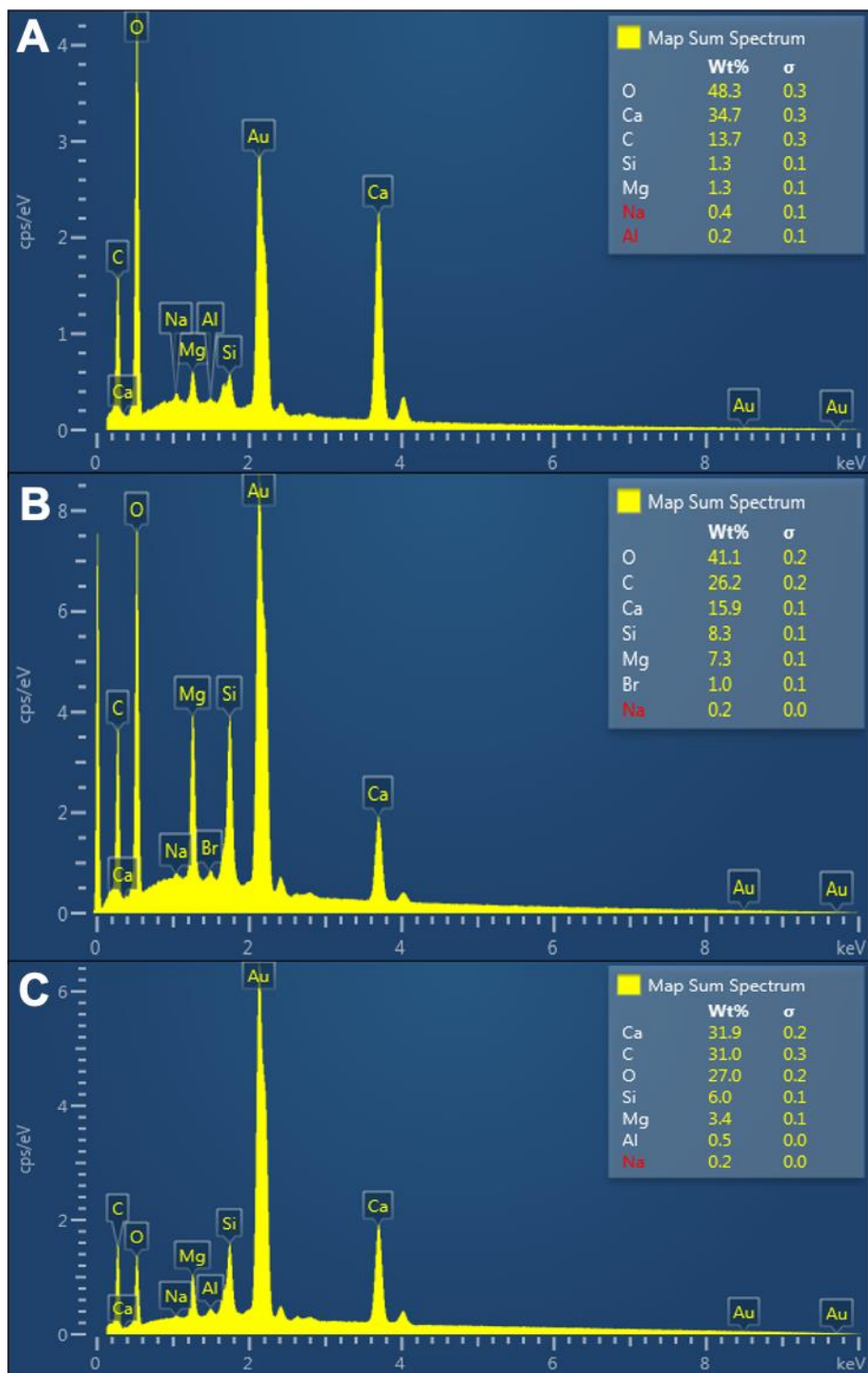


Figure Ap.8 | Elemental spectra for ESW control (Figure 9; A-14 days, B-93 days) and (C) experimental solution precipitates (Figure 16).

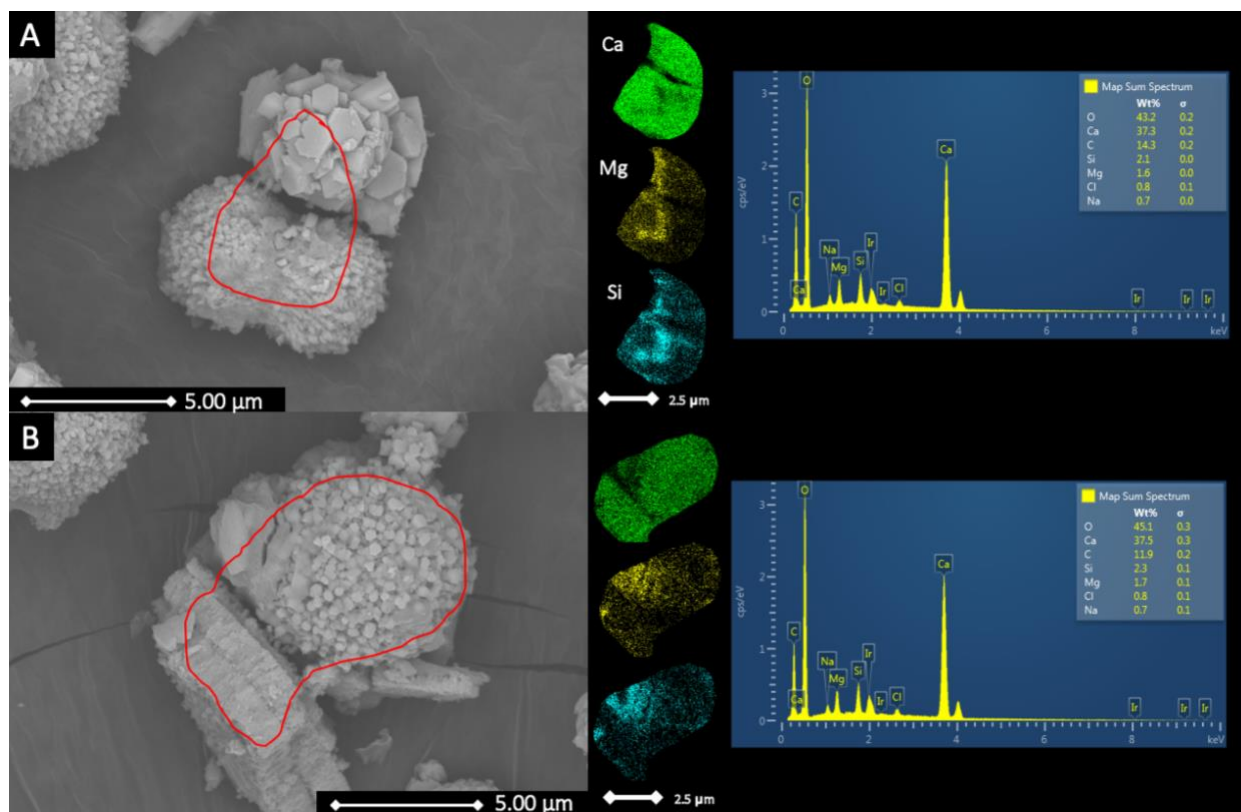


Figure Ap.9 | ESW precipitates after 10 days of incubation.

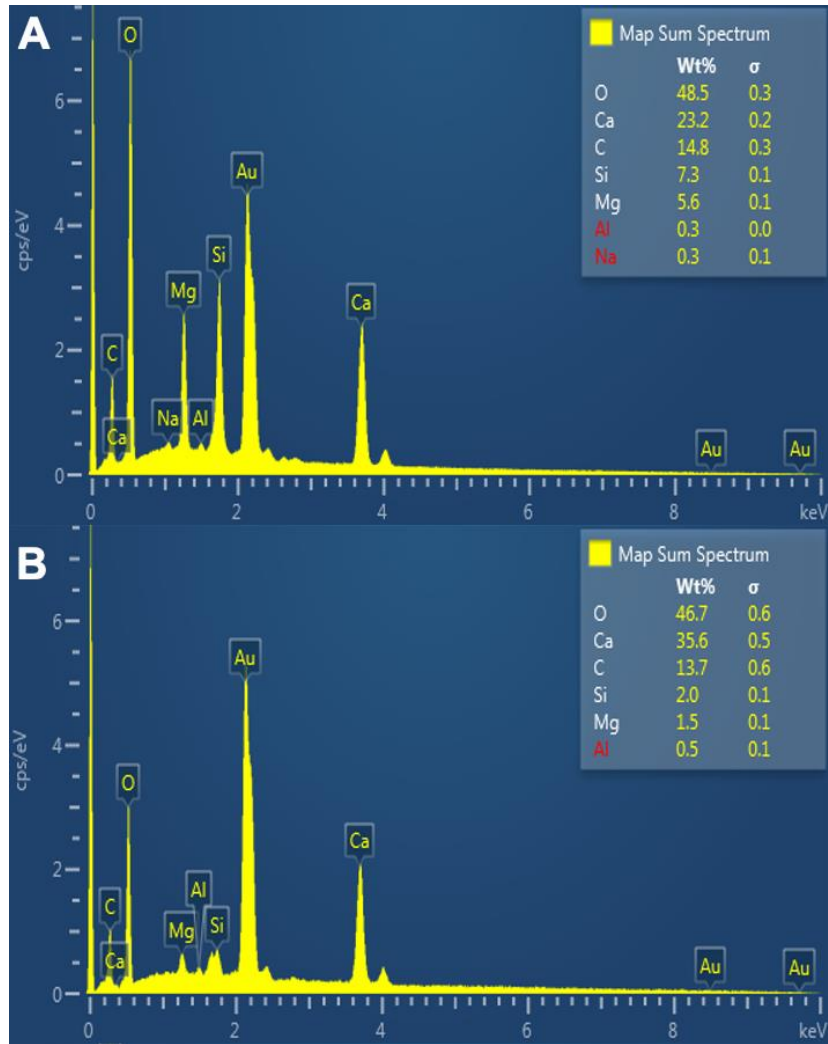


Figure Ap.10 | Elemental spectra for the SW11 control (Figure 11; A-14 days, B-3 days).

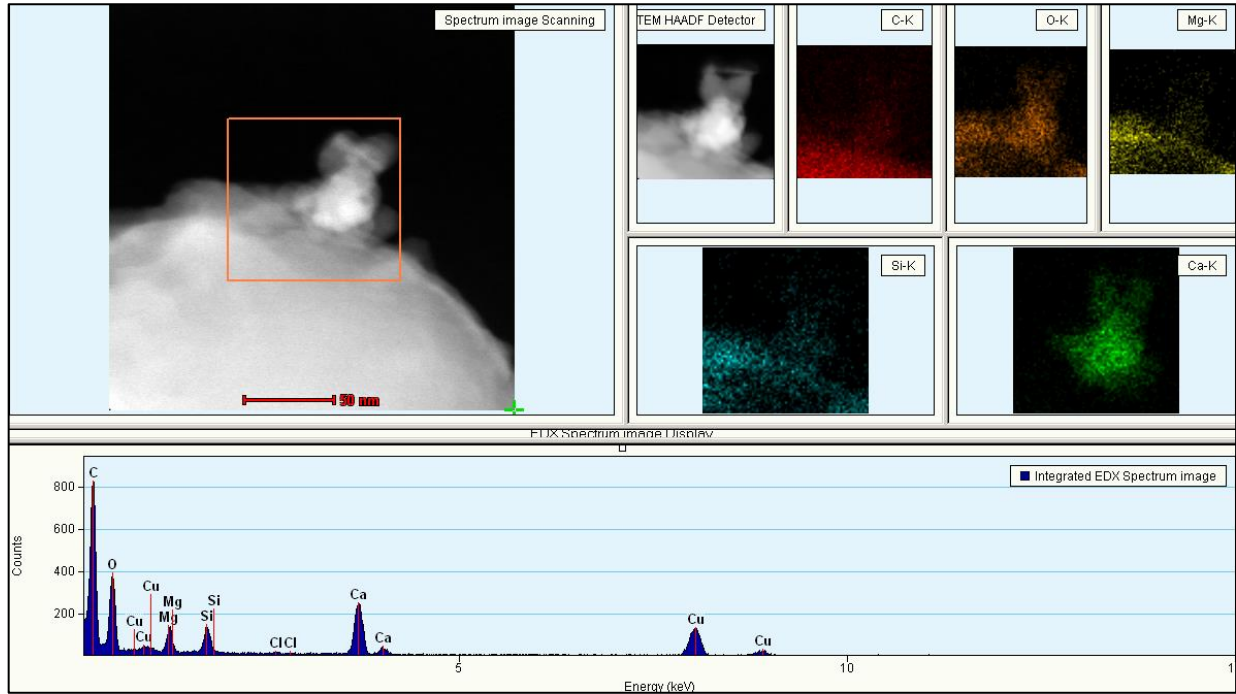


Figure Ap.11 | Elemental spectra for the TEM data (Figure 17)

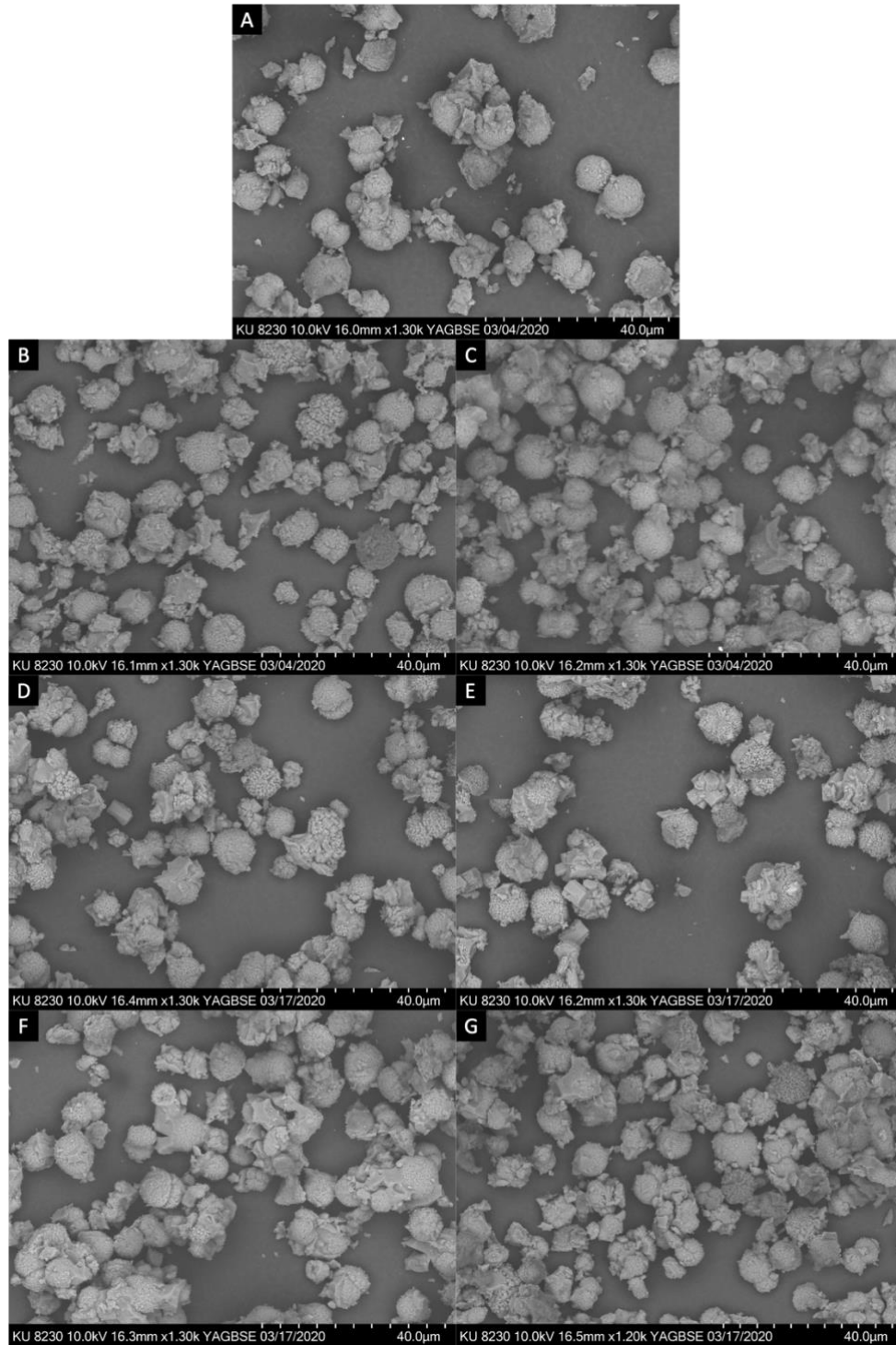


Figure Ap.12 | SEM captures of ESW precipitates. (A) T=0, (B-C) T = 5 days control and experimental (D-E) T = 10 days control and experimental and (F-G) T = 15 days control and experimental.

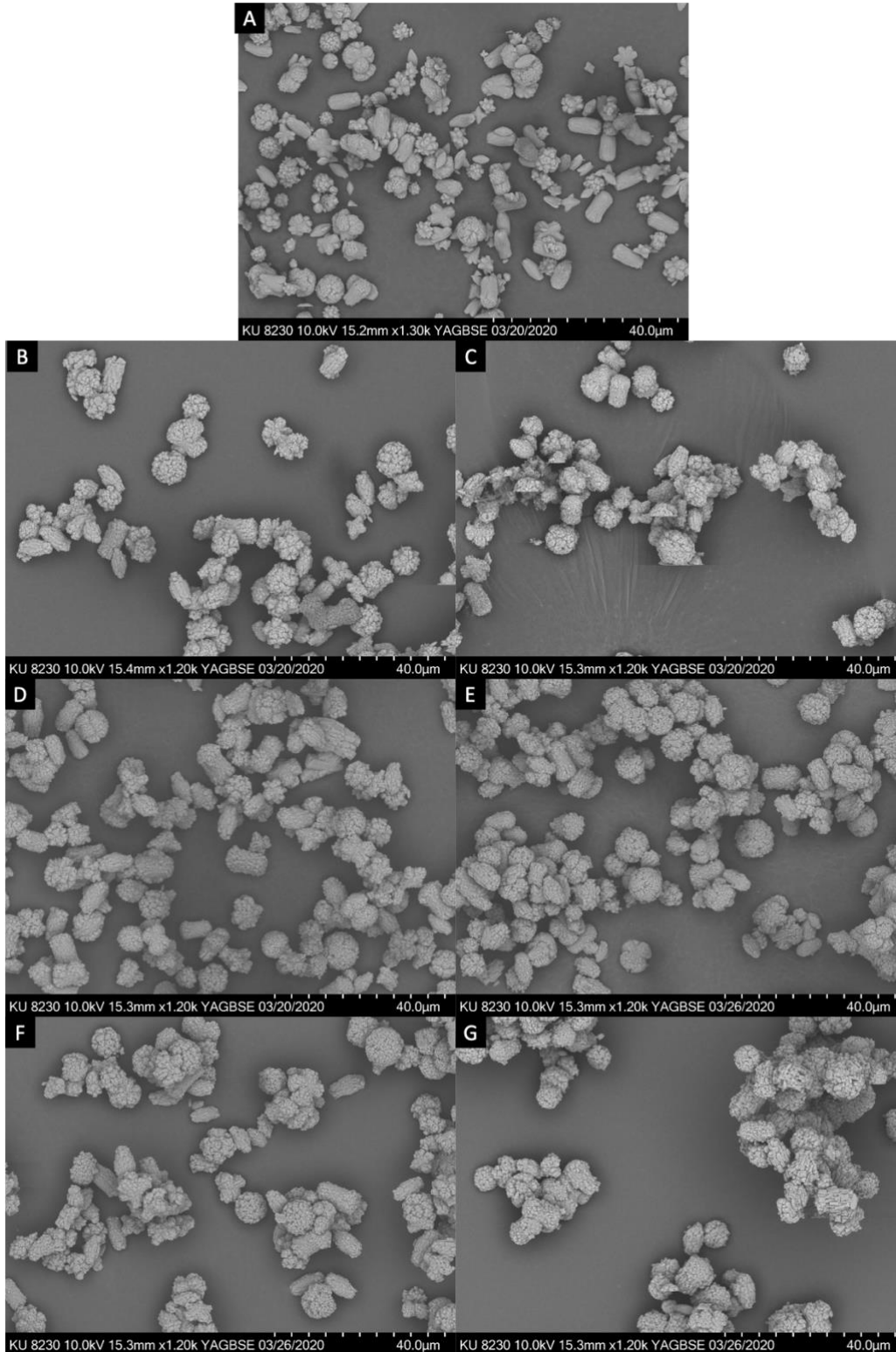


Figure Ap.13 | SEM captures of ESW non-silica batch precipitates. (A) T=0, (B-C) T = 5 days control and experimental (D-E) T = 10 days control and experimental and (F-G) T = 15 days control and experimental.

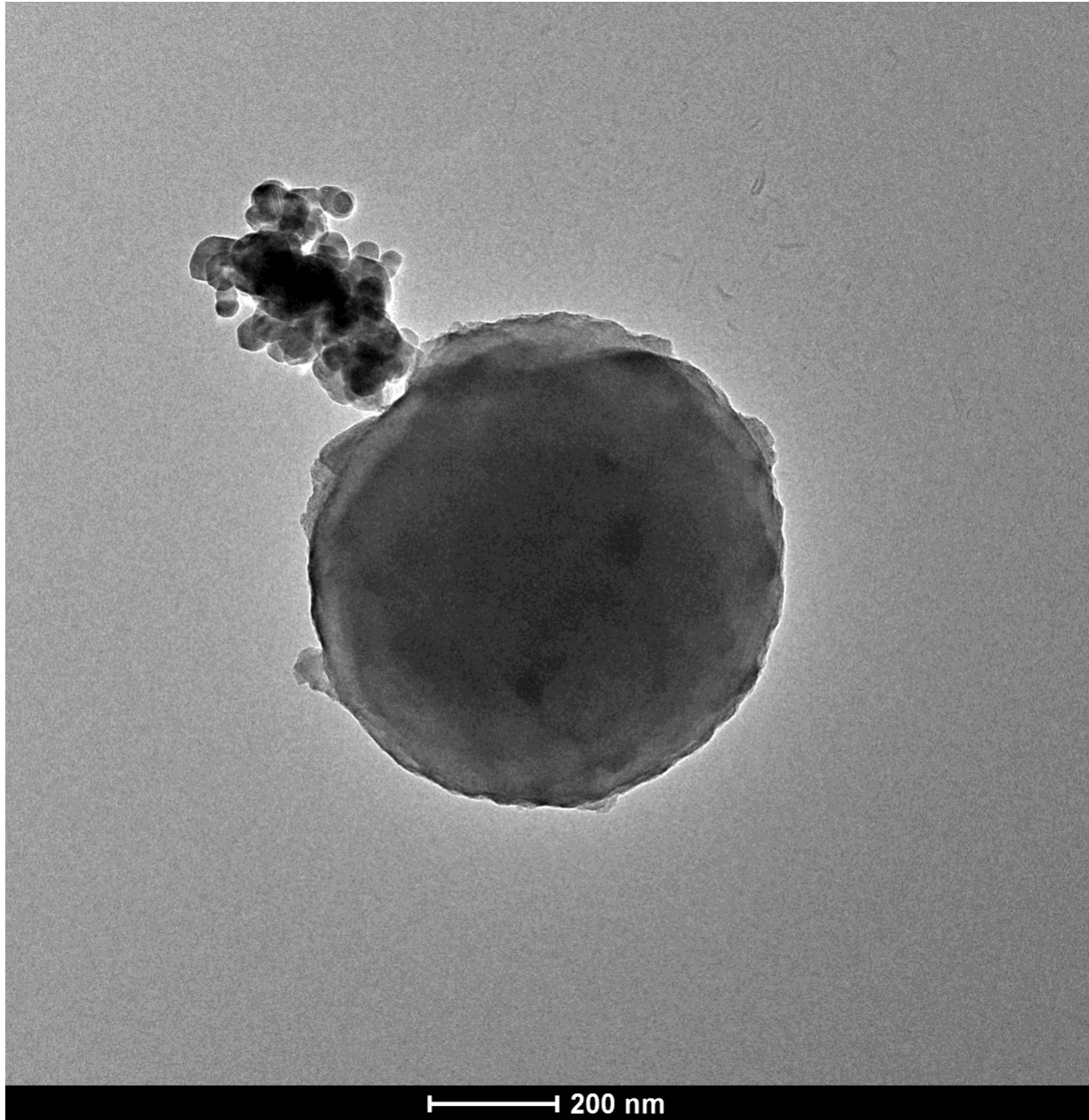


Figure Ap.14 | TEM captures of spheres with precipitates in the surface on ESW 6:1 solution. No EDX was able to be performed on this image given instrumentation constrains.

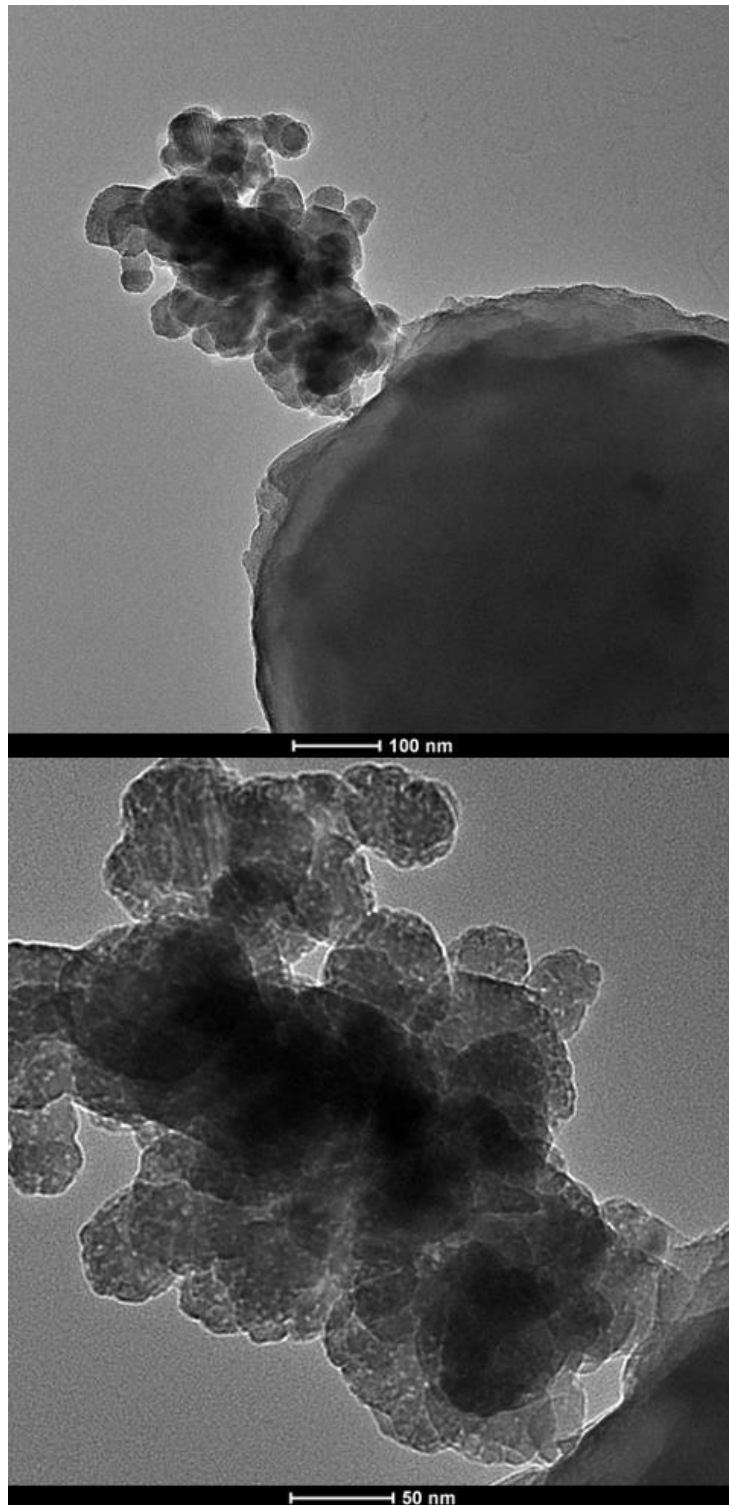


Figure Ap.15 | Close up of TEM captures (Figure Ap.14) of spheres with precipitates in the surface on ESW 6:1 solution. No EDX was able to be performed on this image given instrumentation constrains.

Appendix B: PhreeqC models

Model for ESW original solution chemistry

#This fluid recipe is will modeled the aqueous conditions of Late Neoproterozoic (Ediacaran) seawater.

#This is 6.1:1 Ca/Mg ratio (based on digital calculator). EWS

#grams per liter:

#grams of $\text{CaCl}_2 \cdot 2\text{H}_2\text{O}$ -> 1.63 gram

#grams of $\text{MgCl}_2 \cdot 6\text{H}_2\text{O}$ -> 13.75 grams

#grams of NaCl -> 70 grams

#grams of Na_2CO_3 -> 1 gram

#grams of Na_2SO_4 -> 2.75 grams

#grams of Na_4SiO_3 -> 0.4 grams

#Alkalinity is ~9 mmol (566 mg/L ad CO_3 ; using calculator), which was done by adding 1 gram of NaCO_3 .

#Horita et al. 2002. Geochimica et Cosmochimica Acta (Mg:Ca ratios and Sulfate conc.). S(6) is the sulfur concentration in late neoproterozoic seawater, which is 23.1 mmol.

#Meng et al. 2010. Precambrian Research (Temperatures).

#Bongtonali et al. 2010. and Paul et al., 2016 Sedimentology (pH values from modern microbial mats and modern seawater).

#Salinity is slightly higher than modern normal seawater. Modern seawater is 3.5 wt % whereas this solution is 8.3 wt % (based on digital calculator).

#Ionic Strength, based on digital calculator, is ~1.41

#Dissolved silica is present, as SiO_3 . Here, is Si.

Reading data base.

SOLUTION_MASTER_SPECIES
SOLUTION_SPECIES
PHASES
PITZER

EXCHANGE_MASTER_SPECIES
 EXCHANGE_SPECIES
 SURFACE_MASTER_SPECIES
 SURFACE_SPECIES
 END

 Reading input data for simulation 1.

TITLE Bryan Rodriguez's Solution - Dengying Formation (summer 2019)
 SOLUTION 1

pH	8.5
Temp	40
	Units mg/L
Ca	444
Mg	1644
Na	29234
Cl	48044
S(6)	2219
Si	61
Alkalinity	566 as CO3

SAVE SOLUTION 1

 TITLE

Bryan Rodriguez's Solution - Dengying Formation (summer 2019)

 Beginning of initial solution calculations.

Initial solution 1.

-----Solution composition-----

Elements	Molality	Moles
Alkalinity	1.028e-02	1.028e-02
Ca	1.207e-02	1.207e-02
Cl	1.477e+00	1.477e+00
Mg	7.370e-02	7.370e-02
Na	1.386e+00	1.386e+00
S(6)	2.517e-02	2.517e-02
Si	1.106e-03	1.106e-03

-----Description of solution-----

pH = 8.500
 pe = 4.000
 Specific Conductance ($\mu\text{S}/\text{cm}$, 40°C) = 147337
 Density (g/cm^3) = 1.05124
 Volume (L) = 1.03636
 Activity of water = 0.950
 Ionic strength (mol/kgw) = 1.656e+00
 Mass of water (kg) = 1.000e+00
 Total carbon (mol/kg) = 7.740e-03
 Total CO2 (mol/kg) = 7.740e-03
 Temperature ($^\circ\text{C}$) = 40.00
 Electrical balance (eq) = 1.990e-02
 Percent error, $100 \cdot (\text{Cat} - |\text{An}|) / (\text{Cat} + |\text{An}|)$ = 0.64
 Iterations = 18
 Gamma iterations = 5
 Osmotic coefficient = 0.96379
 Density of water = 0.99221
 Total H = 1.110221e+02
 Total O = 5.563458e+01

-----Distribution of species-----

Species	MacInnes		MacInnes		mole V Gamma	cm \geq /mol
	Molality	Activity	Log Molality	Log Activity		
OH-	1.975e-05	8.792e-06	-4.705	-5.056	-0.351	-0.62
H+	2.968e-09	3.162e-09	-8.528	-8.500	0.028	0.00
H2O	5.551e+01	9.496e-01	1.744	-0.022	0.000	18.16
C(4)	7.740e-03					
HCO3-	5.461e-03	2.520e-03	-2.263	-2.599	-0.336	29.15
CO3-2	1.204e-03	4.669e-05	-2.919	-4.331	-1.412	2.74
MgCO3	1.062e-03	1.062e-03	-2.974	-2.974	0.000	-17.10
CO2	1.259e-05	1.625e-05	-4.900	-4.789	0.111	35.16
Ca	1.207e-02					
Ca+2	1.207e-02	3.240e-03	-1.918	-2.489	-0.571	-15.79
Cl	1.477e+00					
Cl-	1.477e+00	8.641e-01	0.169	-0.063	-0.233	19.49
Mg	7.370e-02					
Mg+2	7.260e-02	2.154e-02	-1.139	-1.667	-0.528	-20.17
MgCO3	1.062e-03	1.062e-03	-2.974	-2.974	0.000	-17.10
MgOH+	3.389e-05	3.493e-05	-4.470	-4.457	0.013	(0)
Na	1.386e+00					
Na+	1.386e+00	1.039e+00	0.142	0.016	-0.125	0.47

S(6)	2.517e-02						
SO4-2	2.517e-02	1.000e-03	-1.599	-3.000	-1.401	21.48	
H2SO4	8.317e-10	4.619e-10	-9.080	-9.335	-0.255	42.17	
Si	1.106e-03						
H4SiO4	8.778e-04	1.046e-03	-3.057	-2.981	0.076	51.03	
H3SiO4-	2.281e-04	7.835e-05	-3.642	-4.106	-0.464	29.51	
H2SiO4-2	2.930e-07	4.119e-09	-6.533	-8.385	-1.852	(0)	

-----Saturation indices-----

Phase	SI**	log IAP	log K(313 K, 1 atm)	
Akermanite	-4.39	38.42	42.80	Ca2MgSi2O7
Anhydrite	-1.03	-5.49	-4.45	CaSO4
Anthophyllite	20.92	83.67	62.75	Mg7Si8O22(OH)2
Antigorite	185.45	634.41	448.96	Mg48Si34O85(OH)62
Aragonite	1.51	-6.82	-8.33	CaCO3
Artinite	0.89	19.46	18.57	Mg2CO3(OH)2:3H2O
Bischofite	-6.34	-1.93	4.41	MgCl2:6H2O
Bloedite	-5.38	-7.72	-2.35	Na2Mg(SO4)2:4H2O
Brucite	-1.07	-11.78	-10.71	Mg(OH)2
Burkeite	-9.46	-10.23	-0.77	Na6CO3(SO4)2
Calcite	1.83	-6.82	-8.65	CaCO3
Chalcedony	0.45	-2.94	-3.38	SiO2
Chrysotile	9.59	40.02	30.43	Mg3Si2O5(OH)4
CO2(g)	-3.16	-4.79	-1.63	CO2
Diopside	4.09	23.93	19.84	CaMgSi2O6
Dolomite	4.60	-12.82	-17.41	CaMg(CO3)2
Enstatite	1.74	12.38	10.63	MgSiO3
Epsomite	-3.07	-4.82	-1.75	MgSO4:7H2O
Forsterite	1.55	27.69	26.13	Mg2SiO4
Gaylussite	-1.81	-11.23	-9.42	CaNa2(CO3)2:5H2O
Glauberite	-2.94	-8.46	-5.52	Na2Ca(SO4)2
Gypsum	-0.91	-5.53	-4.63	CaSO4:2H2O
H2O(g)	-1.16	-0.02	1.14	H2O
Halite	-1.65	-0.05	1.61	NaCl
Hexahydrite	-3.19	-4.80	-1.61	MgSO4:6H2O
Huntite	7.43	16.12	8.69	CaMg3(CO3)4
Kieserite	-4.14	-4.69	-0.55	MgSO4:H2O
Labile_S	-5.80	-11.47	-5.67	Na4Ca(SO4)3:2H2O
Leonhardite	-3.87	-4.76	-0.89	MgSO4:4H2O
Magnesite	1.89	-6.00	-7.89	MgCO3
MgCl2_2H2O	-15.21	-1.84	13.37	MgCl2:2H2O
MgCl2_4H2O	-8.56	-1.88	6.68	MgCl2:4H2O
Mirabilite	-2.52	-3.19	-0.67	Na2SO4:10H2O
Nahcolite	-2.07	-12.81	-10.74	NaHCO3

Natron	-3.70	-4.52	-0.82	Na2CO3:10H2O
Nesquehonite	-0.90	-6.06	-5.17	MgCO3:3H2O
Pentahydrate	-3.49	-4.78	-1.28	MgSO4:5H2O
Pirssonite	-1.93	-11.16	-9.23	Na2Ca(CO3)2:2H2O
Portlandite	-7.41	-12.60	-5.19	Ca(OH)2
Quartz	0.83	-2.94	-3.77	SiO2
Sepiolite	6.35	21.74	15.38	Mg2Si3O7.5OH:3H2O
Sepiolite(d)	3.08	21.74	18.66	Mg2Si3O7.5OH:3H2O
SiO2(a)	-0.40	-2.94	-2.54	SiO2
Talc	14.40	34.17	19.77	Mg3Si4O10(OH)2
Thenardite	-2.59	-2.97	-0.37	Na2SO4
Trona	-5.77	-17.16	-11.38	Na3H(CO3)2:2H2O

**For a gas, SI = log10(fugacity). Fugacity = pressure * phi / 1 atm.
 For ideal gases, phi = 1.

 End of simulation.

 Reading input data for simulation 2.

 End of Run after 0.010414 Seconds.

ESW Before:

 Reading data base.

```

SOLUTION_MASTER_SPECIES
SOLUTION_SPECIES
PHASES
PITZER
EXCHANGE_MASTER_SPECIES
EXCHANGE_SPECIES
SURFACE_MASTER_SPECIES
SURFACE_SPECIES
END

```

 Reading input data for simulation 1.

TITLE Bryan Rodriguez's Solution - Dengying Formation (summer 2019)

SOLUTION 1

pH	8.52
Temp	40
	Units mg/L
Ca	139
Mg	1408
Na	29234
Cl	48044
S(6)	2219
Si	61
Alkalinity	497 as CO3

SAVE SOLUTION 1

TITLE

Bryan Rodriguez's Solution - Dengying Formation (summer 2019)

Beginning of initial solution calculations.

Initial solution 1.

-----Solution composition-----

Elements	Molality	Moles
Alkalinity	9.018e-03	9.018e-03
Ca	3.776e-03	3.776e-03
Cl	1.476e+00	1.476e+00
Mg	6.308e-02	6.308e-02
Na	1.385e+00	1.385e+00
S(6)	2.515e-02	2.515e-02
Si	1.105e-03	1.105e-03

-----Description of solution-----

pH = 8.520
pe = 4.000
Specific Conductance ($\mu\text{S}/\text{cm}$, 40°C) = 147010
Density (g/cm^3) = 1.05029
Volume (L) = 1.03663

Activity of water = 0.950
 Ionic strength (mol/kgw) = 1.617e+00
 Mass of water (kg) = 1.000e+00
 Total carbon (mol/kg) = 6.828e-03
 Total CO2 (mol/kg) = 6.828e-03
 Temperature (∞C) = 40.00
 Electrical balance (eq) = -1.657e-02
 Percent error, 100*(Cat-|An|)/(Cat+|An|) = -0.54
 Iterations = 17
 Gamma iterations = 5
 Osmotic coefficient = 0.96196
 Density of water = 0.99221
 Total H = 1.110216e+02
 Total O = 5.563177e+01

-----Distribution of species-----

Species	MacInnes		MacInnes		mole V Gamma	cm ³ /mol
	Molality	Activity	Log Molality	Log Activity		
OH-	2.006e-05	9.211e-06	-4.698	-5.036	-0.338	-0.68
H+	2.853e-09	3.020e-09	-8.545	-8.520	0.025	0.00
H2O	5.551e+01	9.500e-01	1.744	-0.022	0.000	18.16
C(4)	6.828e-03					
HCO3-	4.899e-03	2.266e-03	-2.310	-2.645	-0.335	29.08
CO3-2	1.056e-03	4.398e-05	-2.976	-4.357	-1.381	2.67
MgCO3	8.625e-04	8.625e-04	-3.064	-3.064	0.000	-17.10
CO2	1.089e-05	1.395e-05	-4.963	-4.855	0.108	35.16
Ca	3.776e-03					
Ca+2	3.776e-03	1.018e-03	-2.423	-2.992	-0.569	-15.81
Cl	1.476e+00					
Cl-	1.476e+00	8.646e-01	0.169	-0.063	-0.232	19.48
Mg	6.308e-02					
Mg+2	6.218e-02	1.857e-02	-1.206	-1.731	-0.525	-20.19
MgCO3	8.625e-04	8.625e-04	-3.064	-3.064	0.000	-17.10
MgOH+	3.030e-05	3.155e-05	-4.519	-4.501	0.017	(0)
Na	1.385e+00					
Na+	1.385e+00	1.032e+00	0.141	0.014	-0.128	0.46
S(6)	2.515e-02					
SO4-2	2.515e-02	1.037e-03	-1.599	-2.984	-1.385	21.41
HSO4-	8.256e-10	4.574e-10	-9.083	-9.340	-0.256	42.15
Si	1.105e-03					
H4SiO4	8.748e-04	1.033e-03	-3.058	-2.986	0.072	51.03
H3SiO4-	2.303e-04	8.104e-05	-3.638	-4.091	-0.454	29.49
H2SiO4-2	2.994e-07	4.461e-09	-6.524	-8.351	-1.827	(0)

-----Saturation indices-----

Phase	SI**	log IAP	log K(313 K, 1 atm)	
Akermanite	-5.35	37.45	42.80	Ca ₂ MgSi ₂ O ₇
Anhydrite	-1.52	-5.98	-4.45	CaSO ₄
Anthophyllite	20.71	83.45	62.75	Mg ₇ Si ₈ O ₂₂ (OH) ₂
Antigorite	184.09	633.06	448.96	Mg ₄₈ Si ₃₄ O ₈₅ (OH) ₆₂
Aragonite	0.98	-7.35	-8.33	CaCO ₃
Artinite	0.77	19.34	18.57	Mg ₂ CO ₃ (OH) ₂ :3H ₂ O
Bischofite	-6.40	-1.99	4.41	MgCl ₂ :6H ₂ O
Bloedite	-5.41	-7.76	-2.35	Na ₂ Mg(SO ₄) ₂ :4H ₂ O
Brucite	-1.09	-11.80	-10.71	Mg(OH) ₂
Burkeite	-9.47	-10.24	-0.77	Na ₆ CO ₃ (SO ₄) ₂
Calcite	1.30	-7.35	-8.65	CaCO ₃
Chalcedony	0.44	-2.94	-3.38	SiO ₂
Chrysotile	9.50	39.93	30.43	Mg ₃ Si ₂ O ₅ (OH) ₄
CO ₂ (g)	-3.23	-4.86	-1.63	CO ₂
Diopside	3.59	23.43	19.84	CaMgSi ₂ O ₆
Dolomite	3.98	-13.44	-17.41	CaMg(CO ₃) ₂
Enstatite	1.71	12.35	10.63	MgSiO ₃
Epsomite	-3.12	-4.87	-1.75	MgSO ₄ :7H ₂ O
Forsterite	1.50	27.63	26.13	Mg ₂ SiO ₄
Gaylussite	-2.37	-11.79	-9.42	CaNa ₂ (CO ₃) ₂ :5H ₂ O
Glauberite	-3.42	-8.93	-5.52	Na ₂ Ca(SO ₄) ₂
Gypsum	-1.39	-6.02	-4.63	CaSO ₄ :2H ₂ O
H ₂ O(g)	-1.16	-0.02	1.14	H ₂ O
Halite	-1.66	-0.05	1.61	NaCl
Hexahydrite	-3.24	-4.85	-1.61	MgSO ₄ :6H ₂ O
Huntite	6.63	15.32	8.69	CaMg ₃ (CO ₃) ₄
Kieserite	-4.19	-4.74	-0.55	MgSO ₄ :H ₂ O
Labile_S	-6.26	-11.93	-5.67	Na ₄ Ca(SO ₄) ₃ :2H ₂ O
Leonhardite	-3.92	-4.80	-0.89	MgSO ₄ :4H ₂ O
Magnesite	1.80	-6.09	-7.89	MgCO ₃
MgCl ₂ _2H ₂ O	-15.27	-1.90	13.37	MgCl ₂ :2H ₂ O
MgCl ₂ _4H ₂ O	-8.62	-1.95	6.68	MgCl ₂ :4H ₂ O
Mirabilite	-2.51	-3.18	-0.67	Na ₂ SO ₄ :10H ₂ O
Nahcolite	-2.12	-12.86	-10.74	NaHCO ₃
Natron	-3.73	-4.55	-0.82	Na ₂ CO ₃ :10H ₂ O
Nesquehonite	-0.99	-6.15	-5.17	MgCO ₃ :3H ₂ O
Pentahydrite	-3.54	-4.83	-1.28	MgSO ₄ :5H ₂ O
Pirssonite	-2.49	-11.72	-9.23	Na ₂ Ca(CO ₃) ₂ :2H ₂ O
Portlandite	-7.87	-13.06	-5.19	Ca(OH) ₂
Quartz	0.83	-2.94	-3.77	SiO ₂
Sepiolite	6.29	21.67	15.38	Mg ₂ Si ₃ O ₇ .5OH:3H ₂ O

Sepiolite(d)	3.01	21.67	18.66	Mg ₂ Si ₃ O ₇ .5OH:3H ₂ O
SiO ₂ (a)	-0.40	-2.94	-2.54	SiO ₂
Talc	14.30	34.07	19.77	Mg ₃ Si ₄ O ₁₀ (OH) ₂
Thenardite	-2.58	-2.96	-0.37	Na ₂ SO ₄
Trona	-5.85	-17.24	-11.38	Na ₃ H(CO ₃) ₂ :2H ₂ O

**For a gas, SI = log₁₀(fugacity). Fugacity = pressure * phi / 1 atm.
 For ideal gases, phi = 1.

 End of simulation.

 Reading input data for simulation 2.

 End of Run after 0.009717 Seconds.

ESW experimental (T=5, 10, 15)

 Reading data base.

SOLUTION_MASTER_SPECIES
 SOLUTION_SPECIES
 PHASES
 PITZER
 EXCHANGE_MASTER_SPECIES
 EXCHANGE_SPECIES
 SURFACE_MASTER_SPECIES
 SURFACE_SPECIES
 END

 Reading input data for simulation 1.

TITLE Bryan Rodriguez's Solution - Dengying Formation (summer 2019)
 SOLUTION 1
 pH 7.54
 Temp 40
 Units mg/L
 Ca 113

Mg 1399
 Na 29234
 Cl 48044
 S(6) 2219
 Si 61
 Alkalinity 425 as CO3

SAVE SOLUTION 1

 TITLE

Bryan Rodriguez's Solution - Dengying Formation (summer 2019)

 Beginning of initial solution calculations.

Initial solution 1.

-----Solution composition-----

Elements	Molality	Moles
Alkalinity	7.710e-03	7.710e-03
Ca	3.070e-03	3.070e-03
Cl	1.475e+00	1.475e+00
Mg	6.267e-02	6.267e-02
Na	1.384e+00	1.384e+00
S(6)	2.515e-02	2.515e-02
Si	1.105e-03	1.105e-03

-----Description of solution-----

pH = 7.540
 pe = 4.000
 Specific Conductance ($\mu\text{S}/\text{cm}$, 40°C) = 146989
 Density (g/cm^3) = 1.05020
 Volume (L) = 1.03671
 Activity of water = 0.950
 Ionic strength (mol/kgw) = 1.615e+00
 Mass of water (kg) = 1.000e+00
 Total carbon (mol/kg) = 7.534e-03
 Total CO2 (mol/kg) = 7.534e-03
 Temperature (°C) = 40.00
 Electrical balance (eq) = -1.749e-02
 Percent error, $100 \cdot (\text{Cat} - |\text{An}|) / (\text{Cat} + |\text{An}|)$ = -0.57

Iterations = 16
 Gamma iterations = 5
 Osmotic coefficient = 0.96208
 Density of water = 0.99221
 Total H = 1.110239e+02
 Total O = 5.563369e+01

-----Distribution of species-----

Species	MacInnes		MacInnes		mole V Gamma	cm ³ /mol
	Molality	Activity	Log Molality	Log Activity		
OH-	2.099e-06	9.645e-07	-5.678	-6.016	-0.338	-0.68
H+	2.723e-08	2.884e-08	-7.565	-7.540	0.025	0.00
H2O	5.551e+01	9.500e-01	1.744	-0.022	0.000	18.16
C(4)	7.534e-03					
HCO3-	7.092e-03	3.279e-03	-2.149	-2.484	-0.335	29.08
CO3-2	1.600e-04	6.662e-06	-3.796	-5.176	-1.381	2.66
CO2	1.504e-04	1.927e-04	-3.823	-3.715	0.108	35.16
MgCO3	1.318e-04	1.318e-04	-3.880	-3.880	0.000	-17.10
Ca	3.070e-03					
Ca+2	3.070e-03	8.331e-04	-2.513	-3.079	-0.566	-15.81
Cl	1.475e+00					
Cl-	1.475e+00	8.646e-01	0.169	-0.063	-0.232	19.48
Mg	6.267e-02					
Mg+2	6.253e-02	1.874e-02	-1.204	-1.727	-0.523	-20.19
MgCO3	1.318e-04	1.318e-04	-3.880	-3.880	0.000	-17.10
MgOH+	3.198e-06	3.333e-06	-5.495	-5.477	0.018	(0)
Na	1.384e+00					
Na+	1.384e+00	1.032e+00	0.141	0.014	-0.128	0.46
S(6)	2.515e-02					
SO4-2	2.515e-02	1.037e-03	-1.599	-2.984	-1.385	21.41
HSO4-	7.886e-09	4.369e-09	-8.103	-8.360	-0.256	42.15
Si	1.105e-03					
H4SiO4	1.076e-03	1.270e-03	-2.968	-2.896	0.072	51.03
H3SiO4-	2.964e-05	1.043e-05	-4.528	-4.982	-0.454	29.49
H2SiO4-2	4.035e-09	6.013e-11	-8.394	-10.221	-1.827	(0)

-----Saturation indices-----

Phase	SI**	log IAP	log K(313 K, 1 atm)
Akermanite	-11.22	31.58	42.80 Ca ₂ MgSi ₂ O ₇
Anhydrite	-1.61	-6.06	-4.45 CaSO ₄
Anthophyllite	7.73	70.48	62.75 Mg ₇ Si ₈ O ₂₂ (OH) ₂

Antigorite	93.25	542.21	448.96	Mg ₄₈ Si ₃₄ O ₈₅ (OH) ₆₂
Aragonite	0.07	-8.26	-8.33	CaCO ₃
Artinite	-2.00	16.57	18.57	Mg ₂ CO ₃ (OH) ₂ :3H ₂ O
Bischofite	-6.39	-1.99	4.41	MgCl ₂ :6H ₂ O
Bloedite	-5.41	-7.76	-2.35	Na ₂ Mg(SO ₄) ₂ :4H ₂ O
Brucite	-3.05	-13.76	-10.71	Mg(OH) ₂
Burkeite	-10.29	-11.06	-0.77	Na ₆ CO ₃ (SO ₄) ₂
Calcite	0.40	-8.26	-8.65	CaCO ₃
Chalcedony	0.53	-2.85	-3.38	SiO ₂
Chrysotile	3.82	34.24	30.43	Mg ₃ Si ₂ O ₅ (OH) ₄
CO ₂ (g)	-2.09	-3.72	-1.63	CO ₂
Diopside	-0.23	19.61	19.84	CaMgSi ₂ O ₆
Dolomite	2.25	-15.16	-17.41	CaMg(CO ₃) ₂
Enstatite	-0.15	10.48	10.63	MgSiO ₃
Epsomite	-3.12	-4.87	-1.75	MgSO ₄ :7H ₂ O
Forsterite	-2.32	23.81	26.13	Mg ₂ SiO ₄
Gaylussite	-4.10	-13.52	-9.42	CaNa ₂ (CO ₃) ₂ :5H ₂ O
Glauberite	-3.50	-9.02	-5.52	Na ₂ Ca(SO ₄) ₂
Gypsum	-1.48	-6.11	-4.63	CaSO ₄ :2H ₂ O
H ₂ O(g)	-1.16	-0.02	1.14	H ₂ O
Halite	-1.66	-0.05	1.61	NaCl
Hexahydrate	-3.24	-4.85	-1.61	MgSO ₄ :6H ₂ O
Huntite	3.28	11.96	8.69	CaMg ₃ (CO ₃) ₄
Kieserite	-4.18	-4.73	-0.55	MgSO ₄ :H ₂ O
Labile_S	-6.35	-12.02	-5.67	Na ₄ Ca(SO ₄) ₃ :2H ₂ O
Leonhardite	-3.91	-4.80	-0.89	MgSO ₄ :4H ₂ O
Magnesite	0.98	-6.90	-7.89	MgCO ₃
MgCl ₂ _2H ₂ O	-15.27	-1.90	13.37	MgCl ₂ :2H ₂ O
MgCl ₂ _4H ₂ O	-8.62	-1.94	6.68	MgCl ₂ :4H ₂ O
Mirabilite	-2.51	-3.18	-0.67	Na ₂ SO ₄ :10H ₂ O
Nahcolite	-1.96	-12.70	-10.74	NaHCO ₃
Natron	-4.55	-5.37	-0.82	Na ₂ CO ₃ :10H ₂ O
Nesquehonite	-1.80	-6.97	-5.17	MgCO ₃ :3H ₂ O
Pentahydrate	-3.54	-4.82	-1.28	MgSO ₄ :5H ₂ O
Pirssonite	-4.22	-13.45	-9.23	Na ₂ Ca(CO ₃) ₂ :2H ₂ O
Portlandite	-9.92	-15.11	-5.19	Ca(OH) ₂
Quartz	0.92	-2.85	-3.77	SiO ₂
Sepiolite	2.64	18.03	15.38	Mg ₂ Si ₃ O ₇ .5OH:3H ₂ O
Sepiolite(d)	-0.63	18.03	18.66	Mg ₂ Si ₃ O ₇ .5OH:3H ₂ O
SiO ₂ (a)	-0.31	-2.85	-2.54	SiO ₂
Talc	8.79	28.56	19.77	Mg ₃ Si ₄ O ₁₀ (OH) ₂
Thenardite	-2.58	-2.96	-0.37	Na ₂ SO ₄
Trona	-6.51	-17.90	-11.38	Na ₃ H(CO ₃) ₂ :2H ₂ O

**For a gas, SI = log₁₀(fugacity). Fugacity = pressure * phi / 1 atm.
For ideal gases, phi = 1.

End of simulation.

Reading input data for simulation 2.

End of Run after 0.009346 Seconds.

Reading data base.

SOLUTION_MASTER_SPECIES
SOLUTION_SPECIES
PHASES
PITZER
EXCHANGE_MASTER_SPECIES
EXCHANGE_SPECIES
SURFACE_MASTER_SPECIES
SURFACE_SPECIES
END

Reading input data for simulation 1.

TITLE Bryan Rodriguez's Solution - Dengying Formation (summer 2019)

SOLUTION 1

pH	7.56
Temp	40
	Units mg/L
Ca	124
Mg	1410
Na	29234
Cl	48044
S(6)	2219
Si	61
Alkalinity	425 as CO3

SAVE SOLUTION 1

TITLE

Beginning of initial solution calculations.

Initial solution 1.

-----Solution composition-----

Elements	Molality	Moles
Alkalinity	7.711e-03	7.711e-03
Ca	3.368e-03	3.368e-03
Cl	1.475e+00	1.475e+00
Mg	6.316e-02	6.316e-02
Na	1.384e+00	1.384e+00
S(6)	2.515e-02	2.515e-02
Si	1.105e-03	1.105e-03

-----Description of solution-----

pH = 7.560
pe = 4.000
Specific Conductance ($\mu\text{S}/\text{cm}$, 40°C) = 147001
Density (g/cm^3) = 1.05024
Volume (L) = 1.03670
Activity of water = 0.950
Ionic strength (mol/kgw) = 1.617e+00
Mass of water (kg) = 1.000e+00
Total carbon (mol/kg) = 7.511e-03
Total CO2 (mol/kg) = 7.511e-03
Temperature (°C) = 40.00
Electrical balance (eq) = -1.590e-02
Percent error, $100 * (\text{Cat} - |\text{An}|) / (\text{Cat} + |\text{An}|)$ = -0.52
Iterations = 16
Gamma iterations = 5
Osmotic coefficient = 0.96216
Density of water = 0.99221
Total H = 1.110239e+02
Total O = 5.563363e+01

-----Distribution of species-----

	MacInnes	MacInnes	MacInnes	Log	Log	Log	mole V
--	----------	----------	----------	-----	-----	-----	--------

Species	Molality	Activity	Molality	Activity	Gamma	cm ³ /mol
OH-	2.201e-06	1.010e-06	-5.657	-5.996	-0.338	-0.68
H+	2.600e-08	2.754e-08	-7.585	-7.560	0.025	0.00
H2O	5.551e+01	9.500e-01	1.744	-0.022	0.000	18.16
C(4)	7.511e-03					
HCO3-	7.062e-03	3.264e-03	-2.151	-2.486	-0.335	29.08
CO3-2	1.673e-04	6.945e-06	-3.777	-5.158	-1.382	2.67
CO2	1.430e-04	1.833e-04	-3.845	-3.737	0.108	35.16
MgCO3	1.385e-04	1.385e-04	-3.859	-3.859	0.000	-17.10
Ca	3.368e-03					
Ca+2	3.368e-03	9.140e-04	-2.473	-3.039	-0.566	-15.81
Cl	1.475e+00					
Cl-	1.475e+00	8.646e-01	0.169	-0.063	-0.232	19.48
Mg	6.316e-02					
Mg+2	6.302e-02	1.888e-02	-1.201	-1.724	-0.523	-20.19
MgCO3	1.385e-04	1.385e-04	-3.859	-3.859	0.000	-17.10
MgOH+	3.375e-06	3.516e-06	-5.472	-5.454	0.018	(0)
Na	1.384e+00					
Na+	1.384e+00	1.032e+00	0.141	0.014	-0.128	0.46
S(6)	2.515e-02					
SO4-2	2.515e-02	1.036e-03	-1.599	-2.985	-1.385	21.41
HSO4-	7.519e-09	4.166e-09	-8.124	-8.380	-0.256	42.15
Si	1.105e-03					
H4SiO4	1.074e-03	1.268e-03	-2.969	-2.897	0.072	51.03
H3SiO4-	3.104e-05	1.091e-05	-4.508	-4.962	-0.454	29.49
H2SiO4-2	4.432e-09	6.588e-11	-8.353	-10.181	-1.828	(0)

-----Saturation indices-----

Phase	SI**	log IAP	log K(313 K, 1 atm)	
Akermanite	-11.02	31.79	42.80	Ca ₂ MgSi ₂ O ₇
Anhydrite	-1.57	-6.02	-4.45	CaSO ₄
Anthophyllite	8.03	70.78	62.75	Mg ₇ Si ₈ O ₂₂ (OH) ₂
Antigorite	95.31	544.27	448.96	Mg ₄₈ Si ₃₄ O ₈₅ (OH) ₆₂
Aragonite	0.13	-8.20	-8.33	CaCO ₃
Artinite	-1.93	16.63	18.57	Mg ₂ CO ₃ (OH) ₂ :3H ₂ O
Bischofite	-6.39	-1.98	4.41	MgCl ₂ :6H ₂ O
Bloedite	-5.41	-7.76	-2.35	Na ₂ Mg(SO ₄) ₂ :4H ₂ O
Brucite	-3.01	-13.72	-10.71	Mg(OH) ₂
Burkeite	-10.27	-11.05	-0.77	Na ₆ CO ₃ (SO ₄) ₂
Calcite	0.45	-8.20	-8.65	CaCO ₃
Chalcedony	0.53	-2.85	-3.38	SiO ₂
Chrysotile	3.94	34.37	30.43	Mg ₃ Si ₂ O ₅ (OH) ₄
CO ₂ (g)	-2.11	-3.74	-1.63	CO ₂

Diopside	-0.11	19.73	19.84	CaMgSi2O6
Dolomite	2.33	-15.08	-17.41	CaMg(CO3)2
Enstatite	-0.11	10.52	10.63	MgSiO3
Epsomite	-3.12	-4.86	-1.75	MgSO4:7H2O
Forsterite	-2.24	23.90	26.13	Mg2SiO4
Gaylussite	-4.02	-13.44	-9.42	CaNa2(CO3)2:5H2O
Glauberite	-3.47	-8.98	-5.52	Na2Ca(SO4)2
Gypsum	-1.44	-6.07	-4.63	CaSO4:2H2O
H2O(g)	-1.16	-0.02	1.14	H2O
Halite	-1.66	-0.05	1.61	NaCl
Hexahydrate	-3.23	-4.84	-1.61	MgSO4:6H2O
Huntite	3.40	12.08	8.69	CaMg3(CO3)4
Kieserite	-4.18	-4.73	-0.55	MgSO4:H2O
Labile_S	-6.31	-11.98	-5.67	Na4Ca(SO4)3:2H2O
Leonhardite	-3.91	-4.80	-0.89	MgSO4:4H2O
Magnesite	1.00	-6.88	-7.89	MgCO3
MgCl2_2H2O	-15.26	-1.89	13.37	MgCl2:2H2O
MgCl2_4H2O	-8.62	-1.94	6.68	MgCl2:4H2O
Mirabilite	-2.51	-3.18	-0.67	Na2SO4:10H2O
Nahcolite	-1.96	-12.70	-10.74	NaHCO3
Natron	-4.53	-5.35	-0.82	Na2CO3:10H2O
Nesquehonite	-1.78	-6.95	-5.17	MgCO3:3H2O
Pentahydrate	-3.54	-4.82	-1.28	MgSO4:5H2O
Pirssonite	-4.14	-13.37	-9.23	Na2Ca(CO3)2:2H2O
Portlandite	-9.84	-15.03	-5.19	Ca(OH)2
Quartz	0.92	-2.85	-3.77	SiO2
Sepiolite	2.73	18.11	15.38	Mg2Si3O7.5OH:3H2O
Sepiolite(d)	-0.55	18.11	18.66	Mg2Si3O7.5OH:3H2O
SiO2(a)	-0.31	-2.85	-2.54	SiO2
Talc	8.92	28.69	19.77	Mg3Si4O10(OH)2
Thenardite	-2.59	-2.96	-0.37	Na2SO4
Trona	-6.50	-17.88	-11.38	Na3H(CO3)2:2H2O

**For a gas, SI = log10(fugacity). Fugacity = pressure * phi / 1 atm.

For ideal gases, phi = 1.

End of simulation.

Reading input data for simulation 2.

End of Run after 0.008495 Seconds.

Reading data base.

SOLUTION_MASTER_SPECIES
SOLUTION_SPECIES
PHASES
PITZER
EXCHANGE_MASTER_SPECIES
EXCHANGE_SPECIES
SURFACE_MASTER_SPECIES
SURFACE_SPECIES
END

Reading input data for simulation 1.

TITLE Bryan Rodriguez's Solution - Dengying Formation (summer 2019)
SOLUTION 1
pH 7.57
Temp 40
Units mg/L
Ca 111
Mg 1394
Na 29234
Cl 48044
S(6) 2219
Si 61
Alkalinity 416 as CO3
SAVE SOLUTION 1

TITLE

Bryan Rodriguez's Solution - Dengying Formation (summer 2019)

Beginning of initial solution calculations.

Initial solution 1.

-----Solution composition-----

Elements	Molality	Moles
----------	----------	-------

Alkalinity	7.547e-03	7.547e-03
Ca	3.015e-03	3.015e-03
Cl	1.475e+00	1.475e+00
Mg	6.244e-02	6.244e-02
Na	1.384e+00	1.384e+00
S(6)	2.515e-02	2.515e-02
Si	1.105e-03	1.105e-03

-----Description of solution-----

pH = 7.570
 pe = 4.000
 Specific Conductance ($\mu\text{S}/\text{cm}$, 40 ∞C) = 146982
 Density (g/cm^3) = 1.05019
 Volume (L) = 1.03671
 Activity of water = 0.950
 Ionic strength (mol/kgw) = 1.615e+00
 Mass of water (kg) = 1.000e+00
 Total carbon (mol/kg) = 7.343e-03
 Total CO2 (mol/kg) = 7.343e-03
 Temperature (∞C) = 40.00
 Electrical balance (eq) = -1.788e-02
 Percent error, $100 \cdot (\text{Cat} - |\text{An}|) / (\text{Cat} + |\text{An}|)$ = -0.59
 Iterations = 16
 Gamma iterations = 5
 Osmotic coefficient = 0.96206
 Density of water = 0.99221
 Total H = 1.110237e+02
 Total O = 5.563313e+01

-----Distribution of species-----

Species	MacInnes		MacInnes		mole V Gamma	cm \geq /mol
	Molality	Activity	Log Molality	Log Activity		
OH-	2.248e-06	1.033e-06	-5.648	-5.986	-0.338	-0.68
H+	2.542e-08	2.692e-08	-7.595	-7.570	0.025	0.00
H2O	5.551e+01	9.500e-01	1.744	-0.022	0.000	18.16
C(4)	7.343e-03					
HCO3-	6.902e-03	3.191e-03	-2.161	-2.496	-0.335	29.08
CO3-2	1.667e-04	6.948e-06	-3.778	-5.158	-1.380	2.66
MgCO3	1.370e-04	1.370e-04	-3.863	-3.863	0.000	-17.10
CO2	1.367e-04	1.751e-04	-3.864	-3.757	0.108	35.16
Ca	3.015e-03					

Ca+2	3.015e-03	8.182e-04	-2.521	-3.087	-0.566	-15.81
Cl	1.475e+00					
Cl-	1.475e+00	8.646e-01	0.169	-0.063	-0.232	19.48
Mg	6.244e-02					
Mg+2	6.230e-02	1.867e-02	-1.205	-1.729	-0.523	-20.20
MgCO3	1.370e-04	1.370e-04	-3.863	-3.863	0.000	-17.10
MgOH+	3.414e-06	3.559e-06	-5.467	-5.449	0.018	(0)
Na	1.384e+00					
Na+	1.384e+00	1.032e+00	0.141	0.014	-0.128	0.46
S(6)	2.515e-02					
SO4-2	2.515e-02	1.038e-03	-1.599	-2.984	-1.384	21.41
HSO4-	7.364e-09	4.080e-09	-8.133	-8.389	-0.256	42.15
Si	1.105e-03					
H4SiO4	1.074e-03	1.267e-03	-2.969	-2.897	0.072	51.03
H3SiO4-	3.168e-05	1.116e-05	-4.499	-4.953	-0.453	29.49
H2SiO4-2	4.619e-09	6.890e-11	-8.335	-10.162	-1.826	(0)

-----Saturation indices-----

Phase	SI**	log IAP	log K(313 K, 1 atm)	
Akermanite	-11.06	31.74	42.80	Ca2MgSi2O7
Anhydrite	-1.62	-6.07	-4.45	CaSO4
Anthophyllite	8.13	70.88	62.75	Mg7Si8O22(OH)2
Antigorite	96.03	544.99	448.96	Mg48Si34O85(OH)62
Aragonite	0.08	-8.25	-8.33	CaCO3
Artinite	-1.92	16.65	18.57	Mg2CO3(OH)2:3H2O
Bischofite	-6.40	-1.99	4.41	MgCl2:6H2O
Bloedite	-5.41	-7.76	-2.35	Na2Mg(SO4)2:4H2O
Brucite	-2.99	-13.70	-10.71	Mg(OH)2
Burkeite	-10.27	-11.04	-0.77	Na6CO3(SO4)2
Calcite	0.41	-8.25	-8.65	CaCO3
Chalcedony	0.53	-2.85	-3.38	SiO2
Chrysotile	3.99	34.42	30.43	Mg3Si2O5(OH)4
CO2(g)	-2.13	-3.76	-1.63	CO2
Diopside	-0.12	19.71	19.84	CaMgSi2O6
Dolomite	2.28	-15.13	-17.41	CaMg(CO3)2
Enstatite	-0.10	10.54	10.63	MgSiO3
Epsomite	-3.12	-4.87	-1.75	MgSO4:7H2O
Forsterite	-2.21	23.93	26.13	Mg2SiO4
Gaylussite	-4.07	-13.49	-9.42	CaNa2(CO3)2:5H2O
Glauberite	-3.51	-9.03	-5.52	Na2Ca(SO4)2
Gypsum	-1.49	-6.12	-4.63	CaSO4:2H2O
H2O(g)	-1.16	-0.02	1.14	H2O
Halite	-1.66	-0.05	1.61	NaCl
Hexahydrite	-3.24	-4.85	-1.61	MgSO4:6H2O

Huntite	3.34	12.02	8.69	CaMg ₃ (CO ₃) ₄
Kieserite	-4.18	-4.73	-0.55	MgSO ₄ :H ₂ O
Labile_S	-6.36	-12.03	-5.67	Na ₄ Ca(SO ₄) ₃ :2H ₂ O
Leonhardite	-3.91	-4.80	-0.89	MgSO ₄ :4H ₂ O
Magnesite	1.00	-6.89	-7.89	MgCO ₃
MgCl ₂ _2H ₂ O	-15.27	-1.90	13.37	MgCl ₂ :2H ₂ O
MgCl ₂ _4H ₂ O	-8.62	-1.94	6.68	MgCl ₂ :4H ₂ O
Mirabilite	-2.51	-3.18	-0.67	Na ₂ SO ₄ :10H ₂ O
Nahcolite	-1.97	-12.71	-10.74	NaHCO ₃
Natron	-4.53	-5.35	-0.82	Na ₂ CO ₃ :10H ₂ O
Nesquehonite	-1.79	-6.95	-5.17	MgCO ₃ :3H ₂ O
Pentahydrate	-3.54	-4.82	-1.28	MgSO ₄ :5H ₂ O
Pirssonite	-4.19	-13.42	-9.23	Na ₂ Ca(CO ₃) ₂ :2H ₂ O
Portlandite	-9.87	-15.06	-5.19	Ca(OH) ₂
Quartz	0.92	-2.85	-3.77	SiO ₂
Sepiolite	2.76	18.14	15.38	Mg ₂ Si ₃ O ₇ .5OH:3H ₂ O
Sepiolite(d)	-0.52	18.14	18.66	Mg ₂ Si ₃ O ₇ .5OH:3H ₂ O
SiO ₂ (a)	-0.31	-2.85	-2.54	SiO ₂
Talc	8.96	28.73	19.77	Mg ₃ Si ₄ O ₁₀ (OH) ₂
Thenardite	-2.58	-2.96	-0.37	Na ₂ SO ₄
Trona	-6.51	-17.89	-11.38	Na ₃ H(CO ₃) ₂ :2H ₂ O

**For a gas, SI = log₁₀(fugacity). Fugacity = pressure * phi / 1 atm.
For ideal gases, phi = 1.

End of simulation.

Reading input data for simulation 2.

End of Run after 0.008329 Seconds.

T = 10

Reading data base.

SOLUTION_MASTER_SPECIES
SOLUTION_SPECIES
PHASES
PITZER
EXCHANGE_MASTER_SPECIES

EXCHANGE_SPECIES
SURFACE_MASTER_SPECIES
SURFACE_SPECIES
END

Reading input data for simulation 1.

TITLE Bryan Rodriguez's Solution - Dengying Formation (summer 2019)

SOLUTION 1

pH	7.56
Temp	40
	Units mg/L
Ca	121
Mg	1392
Na	29234
Cl	48044
S(6)	2219
Si	61
Alkalinity	421 as CO3

SAVE SOLUTION 1

TITLE

Bryan Rodriguez's Solution - Dengying Formation (summer 2019)

Beginning of initial solution calculations.

Initial solution 1.

-----Solution composition-----

Elements	Molality	Moles
Alkalinity	7.638e-03	7.638e-03
Ca	3.287e-03	3.287e-03
Cl	1.475e+00	1.475e+00
Mg	6.235e-02	6.235e-02
Na	1.384e+00	1.384e+00
S(6)	2.515e-02	2.515e-02
Si	1.105e-03	1.105e-03

-----Description of solution-----

pH = 7.560
 pe = 4.000
 Specific Conductance ($\mu\text{S}/\text{cm}$, 40°C) = 146989
 Density (g/cm^3) = 1.05020
 Volume (L) = 1.03671
 Activity of water = 0.950
 Ionic strength (mol/kgw) = 1.615e+00
 Mass of water (kg) = 1.000e+00
 Total carbon (mol/kg) = 7.442e-03
 Total CO2 (mol/kg) = 7.442e-03
 Temperature ($^\circ\text{C}$) = 40.00
 Electrical balance (eq) = -1.760e-02
 Percent error, $100 \cdot (\text{Cat} - |\text{An}|) / (\text{Cat} + |\text{An}|)$ = -0.58
 Iterations = 16
 Gamma iterations = 5
 Osmotic coefficient = 0.96207
 Density of water = 0.99221
 Total H = 1.110238e+02
 Total O = 5.563342e+01

-----Distribution of species-----

Species	MacInnes		MacInnes		mole V Gamma	cm \geq /mol
	Molality	Activity	Log Molality	Log Activity		
OH-	2.198e-06	1.010e-06	-5.658	-5.996	-0.338	-0.68
H+	2.601e-08	2.754e-08	-7.585	-7.560	0.025	0.00
H2O	5.551e+01	9.500e-01	1.744	-0.022	0.000	18.16
C(4)	7.442e-03					
HCO3-	6.999e-03	3.237e-03	-2.155	-2.490	-0.335	29.08
CO3-2	1.653e-04	6.887e-06	-3.782	-5.162	-1.380	2.66
CO2	1.418e-04	1.817e-04	-3.848	-3.741	0.108	35.16
MgCO3	1.356e-04	1.356e-04	-3.868	-3.868	0.000	-17.10
Ca	3.287e-03					
Ca+2	3.287e-03	8.920e-04	-2.483	-3.050	-0.566	-15.81
Cl	1.475e+00					
Cl-	1.475e+00	8.646e-01	0.169	-0.063	-0.232	19.48
Mg	6.235e-02					
Mg+2	6.221e-02	1.864e-02	-1.206	-1.729	-0.523	-20.19
MgCO3	1.356e-04	1.356e-04	-3.868	-3.868	0.000	-17.10
MgOH+	3.332e-06	3.473e-06	-5.477	-5.459	0.018	(0)
Na	1.384e+00					
Na+	1.384e+00	1.032e+00	0.141	0.014	-0.128	0.46
S(6)	2.515e-02					

SO4-2	2.515e-02	1.037e-03	-1.599	-2.984	-1.385	21.41
HSO4-	7.531e-09	4.173e-09	-8.123	-8.380	-0.256	42.15
Si	1.105e-03					
H4SiO4	1.074e-03	1.268e-03	-2.969	-2.897	0.072	51.03
H3SiO4-	3.099e-05	1.091e-05	-4.509	-4.962	-0.453	29.49
H2SiO4-2	4.417e-09	6.585e-11	-8.355	-10.181	-1.827	(0)

-----Saturation indices-----

Phase	SI**	log IAP	log K(313 K, 1 atm)	
Akermanite	-11.05	31.76	42.80	Ca ₂ MgSi ₂ O ₇
Anhydrite	-1.58	-6.03	-4.45	CaSO ₄
Anthophyllite	7.99	70.74	62.75	Mg ₇ Si ₈ O ₂₂ (OH) ₂
Antigorite	95.05	544.01	448.96	Mg ₄₈ Si ₃₄ O ₈₅ (OH) ₆₂
Aragonite	0.12	-8.21	-8.33	CaCO ₃
Artinite	-1.95	16.62	18.57	Mg ₂ CO ₃ (OH) ₂ :3H ₂ O
Bischofite	-6.40	-1.99	4.41	MgCl ₂ :6H ₂ O
Bloedite	-5.41	-7.76	-2.35	Na ₂ Mg(SO ₄) ₂ :4H ₂ O
Brucite	-3.01	-13.72	-10.71	Mg(OH) ₂
Burkeite	-10.28	-11.05	-0.77	Na ₆ CO ₃ (SO ₄) ₂
Calcite	0.44	-8.21	-8.65	CaCO ₃
Chalcedony	0.53	-2.85	-3.38	SiO ₂
Chrysotile	3.93	34.36	30.43	Mg ₃ Si ₂ O ₅ (OH) ₄
CO ₂ (g)	-2.12	-3.74	-1.63	CO ₂
Diopside	-0.12	19.71	19.84	CaMgSi ₂ O ₆
Dolomite	2.31	-15.10	-17.41	CaMg(CO ₃) ₂
Enstatite	-0.12	10.52	10.63	MgSiO ₃
Epsomite	-3.12	-4.87	-1.75	MgSO ₄ :7H ₂ O
Forsterite	-2.25	23.88	26.13	Mg ₂ SiO ₄
Gaylussite	-4.04	-13.46	-9.42	CaNa ₂ (CO ₃) ₂ :5H ₂ O
Glauberite	-3.48	-8.99	-5.52	Na ₂ Ca(SO ₄) ₂
Gypsum	-1.45	-6.08	-4.63	CaSO ₄ :2H ₂ O
H ₂ O(g)	-1.16	-0.02	1.14	H ₂ O
Halite	-1.66	-0.05	1.61	NaCl
Hexahydrite	-3.24	-4.85	-1.61	MgSO ₄ :6H ₂ O
Huntite	3.36	12.04	8.69	CaMg ₃ (CO ₃) ₄
Kieserite	-4.18	-4.74	-0.55	MgSO ₄ :H ₂ O
Labile_S	-6.32	-11.99	-5.67	Na ₄ Ca(SO ₄) ₃ :2H ₂ O
Leonhardite	-3.92	-4.80	-0.89	MgSO ₄ :4H ₂ O
Magnesite	0.99	-6.89	-7.89	MgCO ₃
MgCl ₂ _2H ₂ O	-15.27	-1.90	13.37	MgCl ₂ :2H ₂ O
MgCl ₂ _4H ₂ O	-8.62	-1.94	6.68	MgCl ₂ :4H ₂ O
Mirabilite	-2.51	-3.18	-0.67	Na ₂ SO ₄ :10H ₂ O
Nahcolite	-1.97	-12.71	-10.74	NaHCO ₃
Natron	-4.53	-5.36	-0.82	Na ₂ CO ₃ :10H ₂ O

Nesquehonite	-1.79	-6.96	-5.17	MgCO3:3H2O
Pentahydrate	-3.54	-4.82	-1.28	MgSO4:5H2O
Pirssonite	-4.16	-13.39	-9.23	Na2Ca(CO3)2:2H2O
Portlandite	-9.85	-15.04	-5.19	Ca(OH)2
Quartz	0.92	-2.85	-3.77	SiO2
Sepiolite	2.72	18.10	15.38	Mg2Si3O7.5OH:3H2O
Sepiolite(d)	-0.56	18.10	18.66	Mg2Si3O7.5OH:3H2O
SiO2(a)	-0.31	-2.85	-2.54	SiO2
Talc	8.90	28.67	19.77	Mg3Si4O10(OH)2
Thenardite	-2.58	-2.96	-0.37	Na2SO4
Trona	-6.50	-17.89	-11.38	Na3H(CO3)2:2H2O

**For a gas, SI = log10(fugacity). Fugacity = pressure * phi / 1 atm.
 For ideal gases, phi = 1.

 End of simulation.

 Reading input data for simulation 2.

 End of Run after 0.009312 Seconds.

 Reading data base.

SOLUTION_MASTER_SPECIES
 SOLUTION_SPECIES
 PHASES
 PITZER
 EXCHANGE_MASTER_SPECIES
 EXCHANGE_SPECIES
 SURFACE_MASTER_SPECIES
 SURFACE_SPECIES
 END

 Reading input data for simulation 1.

TITLE Bryan Rodriguez's Solution - Dengying Formation (summer 2019)
 SOLUTION 1

pH 7.53
 Temp 40
 Units mg/L
 Ca 136
 Mg 1508
 Na 29234
 Cl 48044
 S(6) 2219
 Si 61
 Alkalinity 424 as CO3
 SAVE SOLUTION 1

 TITLE

Bryan Rodriguez's Solution - Dengying Formation (summer 2019)

 Beginning of initial solution calculations.

Initial solution 1.

-----Solution composition-----

Elements	Molality	Moles
Alkalinity	7.693e-03	7.693e-03
Ca	3.695e-03	3.695e-03
Cl	1.476e+00	1.476e+00
Mg	6.756e-02	6.756e-02
Na	1.385e+00	1.385e+00
S(6)	2.515e-02	2.515e-02
Si	1.105e-03	1.105e-03

-----Description of solution-----

pH = 7.530
 pe = 4.000
 Specific Conductance ($\mu\text{S}/\text{cm}$, 40°C) = 147054
 Density (g/cm^3) = 1.05045
 Volume (L) = 1.03662
 Activity of water = 0.950
 Ionic strength (mol/kgw) = 1.627e+00
 Mass of water (kg) = 1.000e+00
 Total carbon (mol/kg) = 7.515e-03

Total CO2 (mol/kg) = 7.515e-03
 Temperature (°C) = 40.00
 Electrical balance (eq) = -6.453e-03
 Percent error, 100*(Cat-|An|)/(Cat+|An|) = -0.21
 Iterations = 17
 Gamma iterations = 5
 Osmotic coefficient = 0.96270
 Density of water = 0.99221
 Total H = 1.110239e+02
 Total O = 5.563365e+01

-----Distribution of species-----

Species	MacInnes		MacInnes		mole V Gamma	cm ³ /mol
	Molality	Activity	Log Molality	Log Activity		
OH-	2.068e-06	9.424e-07	-5.684	-6.026	-0.341	-0.67
H+	2.781e-08	2.951e-08	-7.556	-7.530	0.026	0.00
H2O	5.551e+01	9.499e-01	1.744	-0.022	0.000	18.16
C(4)	7.515e-03					
HCO3-	7.066e-03	3.255e-03	-2.151	-2.487	-0.337	29.10
CO3-2	1.586e-04	6.464e-06	-3.800	-5.189	-1.390	2.68
CO2	1.525e-04	1.959e-04	-3.817	-3.708	0.109	35.16
MgCO3	1.377e-04	1.377e-04	-3.861	-3.861	0.000	-17.10
Ca	3.695e-03					
Ca+2	3.695e-03	1.001e-03	-2.432	-2.999	-0.567	-15.80
Cl	1.476e+00					
Cl-	1.476e+00	8.644e-01	0.169	-0.063	-0.232	19.48
Mg	6.756e-02					
Mg+2	6.742e-02	2.017e-02	-1.171	-1.695	-0.524	-20.19
MgCO3	1.377e-04	1.377e-04	-3.861	-3.861	0.000	-17.10
MgOH+	3.372e-06	3.506e-06	-5.472	-5.455	0.017	(0)
Na	1.385e+00					
Na+	1.385e+00	1.034e+00	0.141	0.014	-0.127	0.46
S(6)	2.515e-02					
SO4-2	2.515e-02	1.028e-03	-1.599	-2.988	-1.389	21.43
HSO4-	7.988e-09	4.429e-09	-8.098	-8.354	-0.256	42.16
Si	1.105e-03					
H4SiO4	1.076e-03	1.274e-03	-2.968	-2.895	0.073	51.03
H3SiO4-	2.927e-05	1.023e-05	-4.534	-4.990	-0.457	29.50
H2SiO4-2	3.935e-09	5.761e-11	-8.405	-10.240	-1.834	(0)

-----Saturation indices-----

Phase SI** log IAP log K(313 K, 1 atm)

Akermanite	-11.09	31.72	42.80	Ca ₂ MgSi ₂ O ₇
Anhydrite	-1.53	-5.99	-4.45	CaSO ₄
Anthophyllite	7.82	70.57	62.75	Mg ₇ Si ₈ O ₂₂ (OH) ₂
Antigorite	93.87	542.83	448.96	Mg ₄₈ Si ₃₄ O ₈₅ (OH) ₆₂
Aragonite	0.14	-8.19	-8.33	CaCO ₃
Artinite	-1.97	16.60	18.57	Mg ₂ CO ₃ (OH) ₂ :3H ₂ O
Bischofite	-6.36	-1.96	4.41	MgCl ₂ :6H ₂ O
Bloedite	-5.39	-7.73	-2.35	Na ₂ Mg(SO ₄) ₂ :4H ₂ O
Brucite	-3.04	-13.75	-10.71	Mg(OH) ₂
Burkeite	-10.31	-11.08	-0.77	Na ₆ CO ₃ (SO ₄) ₂
Calcite	0.46	-8.19	-8.65	CaCO ₃
Chalcedony	0.53	-2.85	-3.38	SiO ₂
Chrysotile	3.85	34.28	30.43	Mg ₃ Si ₂ O ₅ (OH) ₄
CO ₂ (g)	-2.08	-3.71	-1.63	CO ₂
Diopside	-0.16	19.68	19.84	CaMgSi ₂ O ₆
Dolomite	2.34	-15.07	-17.41	CaMg(CO ₃) ₂
Enstatite	-0.14	10.49	10.63	MgSiO ₃
Epsomite	-3.09	-4.84	-1.75	MgSO ₄ :7H ₂ O
Forsterite	-2.30	23.83	26.13	Mg ₂ SiO ₄
Gaylussite	-4.04	-13.46	-9.42	CaNa ₂ (CO ₃) ₂ :5H ₂ O
Glauberite	-3.43	-8.95	-5.52	Na ₂ Ca(SO ₄) ₂
Gypsum	-1.40	-6.03	-4.63	CaSO ₄ :2H ₂ O
H ₂ O(g)	-1.16	-0.02	1.14	H ₂ O
Halite	-1.66	-0.05	1.61	NaCl
Hexahydrite	-3.21	-4.82	-1.61	MgSO ₄ :6H ₂ O
Huntite	3.40	12.09	8.69	CaMg ₃ (CO ₃) ₄
Kieserite	-4.15	-4.71	-0.55	MgSO ₄ :H ₂ O
Labile_S	-6.28	-11.95	-5.67	Na ₄ Ca(SO ₄) ₃ :2H ₂ O
Leonhardite	-3.89	-4.77	-0.89	MgSO ₄ :4H ₂ O
Magnesite	1.00	-6.88	-7.89	MgCO ₃
MgCl ₂ _2H ₂ O	-15.23	-1.87	13.37	MgCl ₂ :2H ₂ O
MgCl ₂ _4H ₂ O	-8.59	-1.91	6.68	MgCl ₂ :4H ₂ O
Mirabilite	-2.52	-3.18	-0.67	Na ₂ SO ₄ :10H ₂ O
Nahcolite	-1.96	-12.71	-10.74	NaHCO ₃
Natron	-4.56	-5.38	-0.82	Na ₂ CO ₃ :10H ₂ O
Nesquehonite	-1.78	-6.95	-5.17	MgCO ₃ :3H ₂ O
Pentahydrite	-3.51	-4.80	-1.28	MgSO ₄ :5H ₂ O
Pirssonite	-4.16	-13.39	-9.23	Na ₂ Ca(CO ₃) ₂ :2H ₂ O
Portlandite	-9.86	-15.05	-5.19	Ca(OH) ₂
Quartz	0.92	-2.85	-3.77	SiO ₂
Sepiolite	2.67	18.06	15.38	Mg ₂ Si ₃ O ₇ .5OH:3H ₂ O
Sepiolite(d)	-0.60	18.06	18.66	Mg ₂ Si ₃ O ₇ .5OH:3H ₂ O
SiO ₂ (a)	-0.31	-2.85	-2.54	SiO ₂
Talc	8.83	28.60	19.77	Mg ₃ Si ₄ O ₁₀ (OH) ₂
Thenardite	-2.59	-2.96	-0.37	Na ₂ SO ₄

Trona -6.53 -17.91 -11.38 Na3H(CO3)2:2H2O

**For a gas, SI = log10(fugacity). Fugacity = pressure * phi / 1 atm.
For ideal gases, phi = 1.

End of simulation.

Reading input data for simulation 2.

End of Run after 0.010572 Seconds.

Reading data base.

SOLUTION_MASTER_SPECIES
SOLUTION_SPECIES
PHASES
PITZER
EXCHANGE_MASTER_SPECIES
EXCHANGE_SPECIES
SURFACE_MASTER_SPECIES
SURFACE_SPECIES
END

Reading input data for simulation 1.

TITLE Bryan Rodriguez's Solution - Dengying Formation (summer 2019)
SOLUTION 1

pH	7.53
Temp	40
	Units mg/L
Ca	119
Mg	1425
Na	29234
Cl	48044
S(6)	2219
Si	61

Alkalinity 421 as CO3
SAVE SOLUTION 1

TITLE

Bryan Rodriguez's Solution - Dengying Formation (summer 2019)

Beginning of initial solution calculations.

Initial solution 1.

-----Solution composition-----

Elements	Molality	Moles
Alkalinity	7.638e-03	7.638e-03
Ca	3.233e-03	3.233e-03
Cl	1.475e+00	1.475e+00
Mg	6.383e-02	6.383e-02
Na	1.384e+00	1.384e+00
S(6)	2.515e-02	2.515e-02
Si	1.105e-03	1.105e-03

-----Description of solution-----

pH = 7.530
pe = 4.000
Specific Conductance ($\mu\text{S}/\text{cm}$, 40°C) = 147003
Density (g/cm^3) = 1.05026
Volume (L) = 1.03669
Activity of water = 0.950
Ionic strength (mol/kgw) = 1.618e+00
Mass of water (kg) = 1.000e+00
Total carbon (mol/kg) = 7.471e-03
Total CO2 (mol/kg) = 7.471e-03
Temperature (°C) = 40.00
Electrical balance (eq) = -1.476e-02
Percent error, $100 \cdot (\text{Cat} - |\text{An}|) / (\text{Cat} + |\text{An}|)$ = -0.48
Iterations = 16
Gamma iterations = 5
Osmotic coefficient = 0.96223
Density of water = 0.99221
Total H = 1.110239e+02

Total O = 5.563350e+01

-----Distribution of species-----

Species	MacInnes		MacInnes		mole V Gamma	cm ³ /mol
	Molality	Activity	Log Molality	Log Activity		
OH-	2.055e-06	9.425e-07	-5.687	-6.026	-0.339	-0.68
H+	2.785e-08	2.951e-08	-7.555	-7.530	0.025	0.00
H2O	5.551e+01	9.500e-01	1.744	-0.022	0.000	18.16
C(4)	7.471e-03					
HCO3-	7.032e-03	3.248e-03	-2.153	-2.488	-0.335	29.08
CO3-2	1.557e-04	6.450e-06	-3.808	-5.190	-1.383	2.67
CO2	1.524e-04	1.954e-04	-3.817	-3.709	0.108	35.16
MgCO3	1.300e-04	1.300e-04	-3.886	-3.886	0.000	-17.10
Ca	3.233e-03					
Ca+2	3.233e-03	8.770e-04	-2.490	-3.057	-0.567	-15.81
Cl	1.475e+00					
Cl-	1.475e+00	8.645e-01	0.169	-0.063	-0.232	19.48
Mg	6.383e-02					
Mg+2	6.370e-02	1.908e-02	-1.196	-1.719	-0.523	-20.19
MgCO3	1.300e-04	1.300e-04	-3.886	-3.886	0.000	-17.10
MgOH+	3.184e-06	3.317e-06	-5.497	-5.479	0.018	(0)
Na	1.384e+00					
Na+	1.384e+00	1.032e+00	0.141	0.014	-0.128	0.46
S(6)	2.515e-02					
SO4-2	2.515e-02	1.035e-03	-1.599	-2.985	-1.386	21.41
HSO4-	8.050e-09	4.461e-09	-8.094	-8.351	-0.256	42.15
Si	1.105e-03					
H4SiO4	1.076e-03	1.271e-03	-2.968	-2.896	0.072	51.03
H3SiO4-	2.905e-05	1.021e-05	-4.537	-4.991	-0.454	29.49
H2SiO4-2	3.875e-09	5.750e-11	-8.412	-10.240	-1.829	(0)

-----Saturation indices-----

Phase	SI**	log IAP	log K(313 K, 1 atm)	
Akermanite	-11.23	31.58	42.80	Ca2MgSi2O7
Anhydrite	-1.59	-6.04	-4.45	CaSO4
Anthrophyllite	7.65	70.40	62.75	Mg7Si8O22(OH)2
Antigorite	92.69	541.65	448.96	Mg48Si34O85(OH)62
Aragonite	0.08	-8.25	-8.33	CaCO3
Artinite	-2.02	16.55	18.57	Mg2CO3(OH)2:3H2O
Bischofite	-6.39	-1.98	4.41	MgCl2:6H2O
Bloedite	-5.40	-7.75	-2.35	Na2Mg(SO4)2:4H2O

Brucite	-3.06	-13.77	-10.71	Mg(OH) ₂
Burkeite	-10.31	-11.08	-0.77	Na ₆ CO ₃ (SO ₄) ₂
Calcite	0.40	-8.25	-8.65	CaCO ₃
Chalcedony	0.53	-2.85	-3.38	SiO ₂
Chrysotile	3.78	34.21	30.43	Mg ₃ Si ₂ O ₅ (OH) ₄
CO ₂ (g)	-2.08	-3.71	-1.63	CO ₂
Diopside	-0.24	19.60	19.84	CaMgSi ₂ O ₆
Dolomite	2.26	-15.16	-17.41	CaMg(CO ₃) ₂
Enstatite	-0.17	10.47	10.63	MgSiO ₃
Epsomite	-3.11	-4.86	-1.75	MgSO ₄ :7H ₂ O
Forsterite	-2.35	23.79	26.13	Mg ₂ SiO ₄
Gaylussite	-4.10	-13.52	-9.42	CaNa ₂ (CO ₃) ₂ :5H ₂ O
Glauberite	-3.48	-9.00	-5.52	Na ₂ Ca(SO ₄) ₂
Gypsum	-1.46	-6.09	-4.63	CaSO ₄ :2H ₂ O
H ₂ O(g)	-1.16	-0.02	1.14	H ₂ O
Halite	-1.66	-0.05	1.61	NaCl
Hexahydrite	-3.23	-4.84	-1.61	MgSO ₄ :6H ₂ O
Huntite	3.27	11.95	8.69	CaMg ₃ (CO ₃) ₄
Kieserite	-4.18	-4.73	-0.55	MgSO ₄ :H ₂ O
Labile_S	-6.33	-12.00	-5.67	Na ₄ Ca(SO ₄) ₃ :2H ₂ O
Leonhardite	-3.91	-4.79	-0.89	MgSO ₄ :4H ₂ O
Magnesite	0.98	-6.91	-7.89	MgCO ₃
MgCl ₂ _2H ₂ O	-15.26	-1.89	13.37	MgCl ₂ :2H ₂ O
MgCl ₂ _4H ₂ O	-8.61	-1.93	6.68	MgCl ₂ :4H ₂ O
Mirabilite	-2.51	-3.18	-0.67	Na ₂ SO ₄ :10H ₂ O
Nahcolite	-1.96	-12.71	-10.74	NaHCO ₃
Natron	-4.56	-5.39	-0.82	Na ₂ CO ₃ :10H ₂ O
Nesquehonite	-1.81	-6.98	-5.17	MgCO ₃ :3H ₂ O
Pentahydrite	-3.53	-4.82	-1.28	MgSO ₄ :5H ₂ O
Pirssonite	-4.22	-13.45	-9.23	Na ₂ Ca(CO ₃) ₂ :2H ₂ O
Portlandite	-9.92	-15.11	-5.19	Ca(OH) ₂
Quartz	0.92	-2.85	-3.77	SiO ₂
Sepiolite	2.62	18.00	15.38	Mg ₂ Si ₃ O ₇ .5OH:3H ₂ O
Sepiolite(d)	-0.66	18.00	18.66	Mg ₂ Si ₃ O ₇ .5OH:3H ₂ O
SiO ₂ (a)	-0.31	-2.85	-2.54	SiO ₂
Talc	8.76	28.53	19.77	Mg ₃ Si ₄ O ₁₀ (OH) ₂
Thenardite	-2.59	-2.96	-0.37	Na ₂ SO ₄
Trona	-6.53	-17.91	-11.38	Na ₃ H(CO ₃) ₂ :2H ₂ O

**For a gas, SI = log₁₀(fugacity). Fugacity = pressure * phi / 1 atm.
For ideal gases, phi = 1.

End of simulation.

Reading input data for simulation 2.

End of Run after 0.009781 Seconds.

T=15

Reading data base.

SOLUTION_MASTER_SPECIES
SOLUTION_SPECIES
PHASES
PITZER
EXCHANGE_MASTER_SPECIES
EXCHANGE_SPECIES
SURFACE_MASTER_SPECIES
SURFACE_SPECIES
END

Reading input data for simulation 1.

TITLE Bryan Rodriguez's Solution - Dengying Formation (summer 2019)
SOLUTION 1
pH 7.63
Temp 40
Units mg/L
Ca 102
Mg 1430
Na 29234
Cl 48044
S(6) 2219
Si 61
Alkalinity 400 as CO3
SAVE SOLUTION 1

TITLE

Bryan Rodriguez's Solution - Dengying Formation (summer 2019)

Beginning of initial solution calculations.

Initial solution 1.

-----Solution composition-----

Elements	Molality	Moles
Alkalinity	7.257e-03	7.257e-03
Ca	2.771e-03	2.771e-03
Cl	1.475e+00	1.475e+00
Mg	6.406e-02	6.406e-02
Na	1.384e+00	1.384e+00
S(6)	2.515e-02	2.515e-02
Si	1.105e-03	1.105e-03

-----Description of solution-----

pH = 7.630
pe = 4.000
Specific Conductance ($\mu\text{S}/\text{cm}$, 40°C) = 146987
Density (g/cm^3) = 1.05023
Volume (L) = 1.03667
Activity of water = 0.950
Ionic strength (mol/kgw) = 1.617e+00
Mass of water (kg) = 1.000e+00
Total carbon (mol/kg) = 6.992e-03
Total CO2 (mol/kg) = 6.992e-03
Temperature (°C) = 40.00
Electrical balance (eq) = -1.485e-02
Percent error, $100 \cdot (\text{Cat} - |\text{An}|) / (\text{Cat} + |\text{An}|)$ = -0.49
Iterations = 16
Gamma iterations = 5
Osmotic coefficient = 0.96223
Density of water = 0.99221
Total H = 1.110234e+02
Total O = 5.563210e+01

-----Distribution of species-----

Species	MacInnes		MacInnes		mole V Gamma	cm ³ /mol
	MacInnes Molality	Activity	Log Molality	Log Activity		
OH-	2.586e-06	1.187e-06	-5.587	-5.926	-0.338	-0.68

H+	2.212e-08	2.344e-08	-7.655	-7.630	0.025	0.00
H2O	5.551e+01	9.500e-01	1.744	-0.022	0.000	18.16
C(4)	6.992e-03					
HCO3-	6.544e-03	3.022e-03	-2.184	-2.520	-0.336	29.08
CO3-2	1.821e-04	7.554e-06	-3.740	-5.122	-1.382	2.67
MgCO3	1.527e-04	1.527e-04	-3.816	-3.816	0.000	-17.10
CO2	1.126e-04	1.444e-04	-3.948	-3.840	0.108	35.16
Ca	2.771e-03					
Ca+2	2.771e-03	7.512e-04	-2.557	-3.124	-0.567	-15.81
Cl	1.475e+00					
Cl-	1.475e+00	8.645e-01	0.169	-0.063	-0.232	19.48
Mg	6.406e-02					
Mg+2	6.390e-02	1.914e-02	-1.195	-1.718	-0.523	-20.19
MgCO3	1.527e-04	1.527e-04	-3.816	-3.816	0.000	-17.10
MgOH+	4.020e-06	4.189e-06	-5.396	-5.378	0.018	(0)
Na	1.384e+00					
Na+	1.384e+00	1.032e+00	0.141	0.014	-0.128	0.46
S(6)	2.515e-02					
SO4-2	2.515e-02	1.036e-03	-1.599	-2.985	-1.385	21.41
HSO4-	6.401e-09	3.547e-09	-8.194	-8.450	-0.256	42.15
Si	1.105e-03					
H4SiO4	1.069e-03	1.262e-03	-2.971	-2.899	0.072	51.03
H3SiO4-	3.631e-05	1.276e-05	-4.440	-4.894	-0.454	29.49
H2SiO4-2	6.093e-09	9.050e-11	-8.215	-10.043	-1.828	(0)

-----Saturation indices-----

Phase	SI**	log IAP	log K(313 K, 1 atm)	
Akermanite	-10.77	32.04	42.80	Ca ₂ MgSi ₂ O ₇
Anhydrite	-1.65	-6.11	-4.45	CaSO ₄
Anthophyllite	9.03	71.78	62.75	Mg ₇ Si ₈ O ₂₂ (OH) ₂
Antigorite	102.25	551.21	448.96	Mg ₄₈ Si ₃₄ O ₈₅ (OH) ₆₂
Aragonite	0.08	-8.25	-8.33	CaCO ₃
Artinite	-1.75	16.82	18.57	Mg ₂ CO ₃ (OH) ₂ :3H ₂ O
Bischofite	-6.39	-1.98	4.41	MgCl ₂ :6H ₂ O
Bloedite	-5.40	-7.75	-2.35	Na ₂ Mg(SO ₄) ₂ :4H ₂ O
Brucite	-2.86	-13.57	-10.71	Mg(OH) ₂
Burkeite	-10.24	-11.01	-0.77	Na ₆ CO ₃ (SO ₄) ₂
Calcite	0.41	-8.25	-8.65	CaCO ₃
Chalcedony	0.53	-2.85	-3.38	SiO ₂
Chrysotile	4.38	34.81	30.43	Mg ₃ Si ₂ O ₅ (OH) ₄
CO ₂ (g)	-2.22	-3.84	-1.63	CO ₂
Diopside	0.09	19.92	19.84	CaMgSi ₂ O ₆
Dolomite	2.33	-15.09	-17.41	CaMg(CO ₃) ₂
Enstatite	0.03	10.67	10.63	MgSiO ₃

Epsomite	-3.11	-4.86	-1.75	MgSO4:7H2O
Forsterite	-1.95	24.19	26.13	Mg2SiO4
Gaylussite	-4.03	-13.45	-9.42	CaNa2(CO3)2:5H2O
Glauberite	-3.55	-9.07	-5.52	Na2Ca(SO4)2
Gypsum	-1.52	-6.15	-4.63	CaSO4:2H2O
H2O(g)	-1.16	-0.02	1.14	H2O
Halite	-1.66	-0.05	1.61	NaCl
Hexahydrite	-3.23	-4.84	-1.61	MgSO4:6H2O
Huntite	3.48	12.16	8.69	CaMg3(CO3)4
Kieserite	-4.17	-4.72	-0.55	MgSO4:H2O
Labile_S	-6.40	-12.07	-5.67	Na4Ca(SO4)3:2H2O
Leonhardite	-3.90	-4.79	-0.89	MgSO4:4H2O
Magnesite	1.05	-6.84	-7.89	MgCO3
MgCl2_2H2O	-15.26	-1.89	13.37	MgCl2:2H2O
MgCl2_4H2O	-8.61	-1.93	6.68	MgCl2:4H2O
Mirabilite	-2.51	-3.18	-0.67	Na2SO4:10H2O
Nahcolite	-2.00	-12.74	-10.74	NaHCO3
Natron	-4.49	-5.32	-0.82	Na2CO3:10H2O
Nesquehonite	-1.74	-6.91	-5.17	MgCO3:3H2O
Pentahydrite	-3.53	-4.81	-1.28	MgSO4:5H2O
Pirssonite	-4.15	-13.39	-9.23	Na2Ca(CO3)2:2H2O
Portlandite	-9.79	-14.98	-5.19	Ca(OH)2
Quartz	0.92	-2.85	-3.77	SiO2
Sepiolite	3.01	18.40	15.38	Mg2Si3O7.5OH:3H2O
Sepiolite(d)	-0.26	18.40	18.66	Mg2Si3O7.5OH:3H2O
SiO2(a)	-0.32	-2.85	-2.54	SiO2
Talc	9.35	29.12	19.77	Mg3Si4O10(OH)2
Thenardite	-2.58	-2.96	-0.37	Na2SO4
Trona	-6.49	-17.88	-11.38	Na3H(CO3)2:2H2O

**For a gas, SI = log10(fugacity). Fugacity = pressure * phi / 1 atm.
For ideal gases, phi = 1.

End of simulation.

Reading input data for simulation 2.

End of Run after 0.009556 Seconds.

Reading data base.

SOLUTION_MASTER_SPECIES
SOLUTION_SPECIES
PHASES
PITZER
EXCHANGE_MASTER_SPECIES
EXCHANGE_SPECIES
SURFACE_MASTER_SPECIES
SURFACE_SPECIES
END

Reading input data for simulation 1.

TITLE Bryan Rodriguez's Solution - Dengying Formation (summer 2019)

SOLUTION 1

pH	7.61
Temp	40
	Units mg/L
Ca	100
Mg	1389
Na	29234
Cl	48044
S(6)	2219
Si	61
Alkalinity	405 as CO3

SAVE SOLUTION 1

TITLE

Bryan Rodriguez's Solution - Dengying Formation (summer 2019)

Beginning of initial solution calculations.

Initial solution 1.

-----Solution composition-----

Elements	Molality	Moles
----------	----------	-------

Alkalinity	7.347e-03	7.347e-03
Ca	2.716e-03	2.716e-03
Cl	1.475e+00	1.475e+00
Mg	6.222e-02	6.222e-02
Na	1.384e+00	1.384e+00
S(6)	2.515e-02	2.515e-02
Si	1.105e-03	1.105e-03

-----Description of solution-----

pH = 7.610
 pe = 4.000
 Specific Conductance ($\mu\text{S}/\text{cm}$, 40°C) = 146968
 Density (g/cm^3) = 1.05015
 Volume (L) = 1.03671
 Activity of water = 0.950
 Ionic strength (mol/kgw) = 1.613e+00
 Mass of water (kg) = 1.000e+00
 Total carbon (mol/kg) = 7.106e-03
 Total CO2 (mol/kg) = 7.106e-03
 Temperature (°C) = 40.00
 Electrical balance (eq) = -1.872e-02
 Percent error, $100 \cdot (\text{Cat} - |\text{An}|) / (\text{Cat} + |\text{An}|)$ = -0.61
 Iterations = 16
 Gamma iterations = 5
 Osmotic coefficient = 0.96201
 Density of water = 0.99221
 Total H = 1.110235e+02
 Total O = 5.563243e+01

-----Distribution of species-----

Species	MacInnes		MacInnes		mole V Gamma	cm ³ /mol
	Molality	Activity	Log Molality	Log Activity		
OH-	2.463e-06	1.133e-06	-5.609	-5.946	-0.337	-0.69
H+	2.318e-08	2.455e-08	-7.635	-7.610	0.025	0.00
H2O	5.551e+01	9.500e-01	1.744	-0.022	0.000	18.16
C(4)	7.106e-03					
HCO3-	6.665e-03	3.082e-03	-2.176	-2.511	-0.335	29.07
CO3-2	1.761e-04	7.357e-06	-3.754	-5.133	-1.379	2.66
MgCO3	1.445e-04	1.445e-04	-3.840	-3.840	0.000	-17.10
CO2	1.204e-04	1.542e-04	-3.919	-3.812	0.108	35.16
Ca	2.716e-03					
Ca+2	2.716e-03	7.369e-04	-2.566	-3.133	-0.567	-15.81

Cl	1.475e+00						
Cl-	1.475e+00	8.646e-01	0.169	-0.063	-0.232	19.48	
Mg	6.222e-02						
Mg+2	6.207e-02	1.860e-02	-1.207	-1.730	-0.523	-20.20	
MgCO3	1.445e-04	1.445e-04	-3.840	-3.840	0.000	-17.10	
MgOH+	3.728e-06	3.888e-06	-5.429	-5.410	0.018	(0)	
Na	1.384e+00						
Na+	1.384e+00	1.031e+00	0.141	0.013	-0.128	0.46	
S(6)	2.515e-02						
SO4-2	2.515e-02	1.039e-03	-1.600	-2.983	-1.384	21.41	
HSO4-	6.725e-09	3.726e-09	-8.172	-8.429	-0.256	42.15	
Si	1.105e-03						
H4SiO4	1.071e-03	1.263e-03	-2.970	-2.899	0.072	51.03	
H3SiO4-	3.461e-05	1.219e-05	-4.461	-4.914	-0.453	29.49	
H2SiO4-2	5.527e-09	8.259e-11	-8.258	-10.083	-1.826	(0)	

-----Saturation indices-----

Phase	SI**	log IAP	log K(313 K, 1 atm)	
Akermanite	-10.92	31.89	42.80	Ca ₂ MgSi ₂ O ₇
Anhydrite	-1.66	-6.12	-4.45	CaSO ₄
Anthophyllite	8.67	71.42	62.75	Mg ₇ Si ₈ O ₂₂ (OH) ₂
Antigorite	99.75	548.71	448.96	Mg ₄₈ Si ₃₄ O ₈₅ (OH) ₆₂
Aragonite	0.06	-8.27	-8.33	CaCO ₃
Artinite	-1.82	16.75	18.57	Mg ₂ CO ₃ (OH) ₂ :3H ₂ O
Bischofite	-6.40	-1.99	4.41	MgCl ₂ :6H ₂ O
Bloedite	-5.41	-7.76	-2.35	Na ₂ Mg(SO ₄) ₂ :4H ₂ O
Brucite	-2.91	-13.62	-10.71	Mg(OH) ₂
Burkeite	-10.25	-11.02	-0.77	Na ₆ CO ₃ (SO ₄) ₂
Calcite	0.39	-8.27	-8.65	CaCO ₃
Chalcedony	0.53	-2.85	-3.38	SiO ₂
Chrysotile	4.22	34.65	30.43	Mg ₃ Si ₂ O ₅ (OH) ₄
CO ₂ (g)	-2.19	-3.81	-1.63	CO ₂
Diopside	-0.01	19.82	19.84	CaMgSi ₂ O ₆
Dolomite	2.28	-15.13	-17.41	CaMg(CO ₃) ₂
Enstatite	-0.02	10.61	10.63	MgSiO ₃
Epsomite	-3.12	-4.87	-1.75	MgSO ₄ :7H ₂ O
Forsterite	-2.05	24.08	26.13	Mg ₂ SiO ₄
Gaylussite	-4.06	-13.48	-9.42	CaNa ₂ (CO ₃) ₂ :5H ₂ O
Glauberite	-3.56	-9.07	-5.52	Na ₂ Ca(SO ₄) ₂
Gypsum	-1.53	-6.16	-4.63	CaSO ₄ :2H ₂ O
H ₂ O(g)	-1.16	-0.02	1.14	H ₂ O
Halite	-1.66	-0.05	1.61	NaCl
Hexahydrite	-3.24	-4.85	-1.61	MgSO ₄ :6H ₂ O
Huntite	3.39	12.07	8.69	CaMg ₃ (CO ₃) ₄

Kieserite	-4.18	-4.74	-0.55	MgSO4:H2O
Labile_S	-6.40	-12.07	-5.67	Na4Ca(SO4)3:2H2O
Leonhardite	-3.92	-4.80	-0.89	MgSO4:4H2O
Magnesite	1.02	-6.86	-7.89	MgCO3
MgCl2_2H2O	-15.27	-1.90	13.37	MgCl2:2H2O
MgCl2_4H2O	-8.62	-1.95	6.68	MgCl2:4H2O
Mirabilite	-2.51	-3.18	-0.67	Na2SO4:10H2O
Nahcolite	-1.99	-12.73	-10.74	NaHCO3
Natron	-4.50	-5.33	-0.82	Na2CO3:10H2O
Nesquehonite	-1.76	-6.93	-5.17	MgCO3:3H2O
Pentahydrate	-3.54	-4.83	-1.28	MgSO4:5H2O
Pirssonite	-4.18	-13.42	-9.23	Na2Ca(CO3)2:2H2O
Portlandite	-9.83	-15.02	-5.19	Ca(OH)2
Quartz	0.92	-2.85	-3.77	SiO2
Sepiolite	2.91	18.29	15.38	Mg2Si3O7.5OH:3H2O
Sepiolite(d)	-0.37	18.29	18.66	Mg2Si3O7.5OH:3H2O
SiO2(a)	-0.32	-2.85	-2.54	SiO2
Talc	9.19	28.96	19.77	Mg3Si4O10(OH)2
Thenardite	-2.58	-2.96	-0.37	Na2SO4
Trona	-6.50	-17.88	-11.38	Na3H(CO3)2:2H2O

**For a gas, SI = log10(fugacity). Fugacity = pressure * phi / 1 atm.
 For ideal gases, phi = 1.

 End of simulation.

 Reading input data for simulation 2.

 End of Run after 0.009687 Seconds.

 Reading data base.

SOLUTION_MASTER_SPECIES
 SOLUTION_SPECIES
 PHASES
 PITZER
 EXCHANGE_MASTER_SPECIES
 EXCHANGE_SPECIES

SURFACE_MASTER_SPECIES
SURFACE_SPECIES
END

Reading input data for simulation 1.

TITLE Bryan Rodriguez's Solution - Dengying Formation (summer 2019)
SOLUTION 1

pH	7.64
Temp	40
	Units mg/L
Ca	95
Mg	1376
Na	29234
Cl	48044
S(6)	2219
Si	61
Alkalinity	403 as CO3

SAVE SOLUTION 1

TITLE

Bryan Rodriguez's Solution - Dengying Formation (summer 2019)

Beginning of initial solution calculations.

Initial solution 1.

-----Solution composition-----

Elements	Molality	Moles
Alkalinity	7.311e-03	7.311e-03
Ca	2.580e-03	2.580e-03
Cl	1.475e+00	1.475e+00
Mg	6.163e-02	6.163e-02
Na	1.384e+00	1.384e+00
S(6)	2.515e-02	2.515e-02
Si	1.105e-03	1.105e-03

-----Description of solution-----

pH = 7.640
 pe = 4.000
 Specific Conductance ($\mu\text{S}/\text{cm}$, 40°C) = 146958
 Density (g/cm^3) = 1.05012
 Volume (L) = 1.03672
 Activity of water = 0.950
 Ionic strength (mol/kgw) = 1.612e+00
 Mass of water (kg) = 1.000e+00
 Total carbon (mol/kg) = 7.040e-03
 Total CO2 (mol/kg) = 7.040e-03
 Temperature ($^\circ\text{C}$) = 40.00
 Electrical balance (eq) = -2.012e-02
 Percent error, $100 \cdot (\text{Cat} - |\text{An}|) / (\text{Cat} + |\text{An}|)$ = -0.66
 Iterations = 18
 Gamma iterations = 5
 Osmotic coefficient = 0.96193
 Density of water = 0.99221
 Total H = 1.110234e+02
 Total O = 5.563224e+01

-----Distribution of species-----

Species	MacInnes		MacInnes		mole V Gamma	cm \geq /mol
	Molality	Activity	Log Molality	Log Activity		
OH-	2.636e-06	1.214e-06	-5.579	-5.916	-0.337	-0.69
H+	2.164e-08	2.291e-08	-7.665	-7.640	0.025	0.00
H2O	5.551e+01	9.500e-01	1.744	-0.022	0.000	18.16
C(4)	7.040e-03					
HCO3-	6.591e-03	3.049e-03	-2.181	-2.516	-0.335	29.07
CO3-2	1.861e-04	7.799e-06	-3.730	-5.108	-1.378	2.66
MgCO3	1.518e-04	1.518e-04	-3.819	-3.819	0.000	-17.10
CO2	1.112e-04	1.424e-04	-3.954	-3.847	0.107	35.16
Ca	2.580e-03					
Ca+2	2.580e-03	7.001e-04	-2.588	-3.155	-0.567	-15.81
Cl	1.475e+00					
Cl-	1.475e+00	8.646e-01	0.169	-0.063	-0.232	19.48
Mg	6.163e-02					
Mg+2	6.148e-02	1.843e-02	-1.211	-1.734	-0.523	-20.20
MgCO3	1.518e-04	1.518e-04	-3.819	-3.819	0.000	-17.10
MgOH+	3.956e-06	4.127e-06	-5.403	-5.384	0.018	(0)
Na	1.384e+00					
Na+	1.384e+00	1.031e+00	0.141	0.013	-0.128	0.46
S(6)	2.515e-02					
SO4-2	2.515e-02	1.040e-03	-1.600	-2.983	-1.383	21.40

HSO4-	6.285e-09	3.482e-09	-8.202	-8.458	-0.257	42.15
Si	1.105e-03					
H4SiO4	1.068e-03	1.260e-03	-2.971	-2.900	0.072	51.03
H3SiO4-	3.696e-05	1.303e-05	-4.432	-4.885	-0.453	29.49
H2SiO4-2	6.315e-09	9.458e-11	-8.200	-10.024	-1.825	(0)

-----Saturation indices-----

Phase	SI**	log IAP	log K(313 K, 1 atm)	
Akermanite	-10.79	32.02	42.80	Ca ₂ MgSi ₂ O ₇
Anhydrite	-1.68	-6.14	-4.45	CaSO ₄
Anthophyllite	9.05	71.80	62.75	Mg ₇ Si ₈ O ₂₂ (OH) ₂
Antigorite	102.39	551.35	448.96	Mg ₄₈ Si ₃₄ O ₈₅ (OH) ₆₂
Aragonite	0.07	-8.26	-8.33	CaCO ₃
Artinite	-1.75	16.82	18.57	Mg ₂ CO ₃ (OH) ₂ :3H ₂ O
Bischofite	-6.40	-1.99	4.41	MgCl ₂ :6H ₂ O
Bloedite	-5.42	-7.76	-2.35	Na ₂ Mg(SO ₄) ₂ :4H ₂ O
Brucite	-2.86	-13.57	-10.71	Mg(OH) ₂
Burkeite	-10.22	-10.99	-0.77	Na ₆ CO ₃ (SO ₄) ₂
Calcite	0.39	-8.26	-8.65	CaCO ₃
Chalcedony	0.53	-2.86	-3.38	SiO ₂
Chrysotile	4.39	34.82	30.43	Mg ₃ Si ₂ O ₅ (OH) ₄
CO ₂ (g)	-2.22	-3.85	-1.63	CO ₂
Diopside	0.08	19.92	19.84	CaMgSi ₂ O ₆
Dolomite	2.31	-15.11	-17.41	CaMg(CO ₃) ₂
Enstatite	0.03	10.67	10.63	MgSiO ₃
Epsomite	-3.12	-4.87	-1.75	MgSO ₄ :7H ₂ O
Forsterite	-1.94	24.19	26.13	Mg ₂ SiO ₄
Gaylussite	-4.03	-13.46	-9.42	CaNa ₂ (CO ₃) ₂ :5H ₂ O
Glauberite	-3.58	-9.09	-5.52	Na ₂ Ca(SO ₄) ₂
Gypsum	-1.55	-6.18	-4.63	CaSO ₄ :2H ₂ O
H ₂ O(g)	-1.16	-0.02	1.14	H ₂ O
Halite	-1.66	-0.05	1.61	NaCl
Hexahydrate	-3.24	-4.85	-1.61	MgSO ₄ :6H ₂ O
Huntite	3.45	12.14	8.69	CaMg ₃ (CO ₃) ₄
Kieserite	-4.19	-4.74	-0.55	MgSO ₄ :H ₂ O
Labile_S	-6.42	-12.09	-5.67	Na ₄ Ca(SO ₄) ₃ :2H ₂ O
Leonhardite	-3.92	-4.81	-0.89	MgSO ₄ :4H ₂ O
Magnesite	1.04	-6.84	-7.89	MgCO ₃
MgCl ₂ _2H ₂ O	-15.27	-1.91	13.37	MgCl ₂ :2H ₂ O
MgCl ₂ _4H ₂ O	-8.63	-1.95	6.68	MgCl ₂ :4H ₂ O
Mirabilite	-2.51	-3.18	-0.67	Na ₂ SO ₄ :10H ₂ O
Nahcolite	-1.99	-12.73	-10.74	NaHCO ₃
Natron	-4.48	-5.30	-0.82	Na ₂ CO ₃ :10H ₂ O
Nesquehonite	-1.74	-6.91	-5.17	MgCO ₃ :3H ₂ O

Pentahydrate	-3.54	-4.83	-1.28	MgSO4:5H2O
Pirssonite	-4.15	-13.39	-9.23	Na2Ca(CO3)2:2H2O
Portlandite	-9.80	-14.99	-5.19	Ca(OH)2
Quartz	0.91	-2.86	-3.77	SiO2
Sepiolite	3.02	18.40	15.38	Mg2Si3O7.5OH:3H2O
Sepiolite(d)	-0.26	18.40	18.66	Mg2Si3O7.5OH:3H2O
SiO2(a)	-0.32	-2.86	-2.54	SiO2
Talc	9.36	29.13	19.77	Mg3Si4O10(OH)2
Thenardite	-2.58	-2.96	-0.37	Na2SO4
Trona	-6.48	-17.86	-11.38	Na3H(CO3)2:2H2O

**For a gas, SI = log10(fugacity). Fugacity = pressure * phi / 1 atm.
For ideal gases, phi = 1.

End of simulation.

Reading input data for simulation 2.

End of Run after 0.009234 Seconds.

ESW NoSi solution chemistry:

Input file: /Users/bryanrodriguez/OneDrive - The University of Kansas/Bryan-MASTERS/PHREEQC/Phreeqc-Fluids/Summer2019/EWS/Bryan-ChinaFluid-EWS_NoSi.txt

Output file: /Users/bryanrodriguez/OneDrive - The University of Kansas/Bryan-MASTERS/PHREEQC/Phreeqc-Fluids/Summer2019/EWS/Bryan-ChinaFluid-EWS_NoSi.txt.out

Database file: /Users/bryanrodriguez/OneDrive - The University of Kansas/Bryan-MASTERS/PHREEQC/phreeqc-3.5.0-14000/database/pitzer.dat

#This fluid recipe is will modeled the aqueous conditions of Late Neoproterozoic (Ediacaran) seawater.

#This is 6.1:1 Ca/Mg ratio (based on digital calculator). EWS-NoSi

#grams per liter:

#grams of CaCl2*2H2O -> 1.63 gram

#grams of MgCL2*6H2O -> 13.75 grams

#grams of NaCl -> 70 grams

#grams of Na₂CO₃ -> 1 gram
#grams of Na₂SO₄ -> 2.75 grams

#Alkalinity is ~9 mmol (566 mg/L ad CO₃; using calculator), which was done by adding 1 gram of NaCO₃.

#Horita et al. 2002. Geochimica et Cosmochimica Acta (Mg:Ca ratios and Sulfate conc.). S(6) is the sulfur concentration in late neoproterozoic seawater, which is 23.1 mmol.

#Meng et al. 2010. Precambrian Research (Temperatures).

#Bongtonali et al. 2010. and Paul et al., 2016 Sedimentology (pH values from modern microbial mats and modern seawater).

#Salinity is slightly higher than modern normal seawater. Modern seawater is 3.5 wt % whereas this solution is 8.3 wt % (based on digital calculator).

#Ionic Strength, based on digital calculator, is ~1.40

Reading data base.

SOLUTION_MASTER_SPECIES
SOLUTION_SPECIES
PHASES
PITZER
EXCHANGE_MASTER_SPECIES
EXCHANGE_SPECIES
SURFACE_MASTER_SPECIES
SURFACE_SPECIES
END

Reading input data for simulation 1.

TITLE Bryan Rodriguez's Solution - Dengying Formation (summer 2019)
SOLUTION 1
pH 8.5
Temp 40
Units mg/L
Ca 444
Mg 1644

Na 29034
 Cl 48044
 S(6) 2219
 Alkalinity 566 as CO3

SAVE SOLUTION 1

 TITLE

Bryan Rodriguez's Solution - Dengying Formation (summer 2019)

 Beginning of initial solution calculations.

Initial solution 1.

-----Solution composition-----

Elements	Molality	Moles
Alkalinity	1.027e-02	1.027e-02
Ca	1.207e-02	1.207e-02
Cl	1.476e+00	1.476e+00
Mg	7.368e-02	7.368e-02
Na	1.376e+00	1.376e+00
S(6)	2.516e-02	2.516e-02

-----Description of solution-----

pH = 8.500
 pe = 4.000
 Specific Conductance ($\mu\text{S}/\text{cm}$, 40°C) = 147083
 Density (g/cm^3) = 1.05098
 Volume (L) = 1.03630
 Activity of water = 0.950
 Ionic strength (mol/kgw) = 1.651e+00
 Mass of water (kg) = 1.000e+00
 Total carbon (mol/kg) = 7.912e-03
 Total CO2 (mol/kg) = 7.912e-03
 Temperature (°C) = 40.00
 Electrical balance (eq) = 1.042e-02
 Percent error, $100 \cdot (\text{Cat} - |\text{An}|) / (\text{Cat} + |\text{An}|)$ = 0.34
 Iterations = 16
 Gamma iterations = 4
 Osmotic coefficient = 0.96349

Density of water = 0.99221
 Total H = 1.110181e+02
 Total O = 5.563064e+01

-----Distribution of species-----

Species	MacInnes		MacInnes		mole V Gamma	cm ³ /mol
	Molality	Activity	Log Molality	Log Activity		
OH-	1.975e-05	8.794e-06	-4.704	-5.056	-0.351	-0.63
H+	2.972e-09	3.162e-09	-8.527	-8.500	0.027	0.00
H2O	5.551e+01	9.498e-01	1.744	-0.022	0.000	18.16
C(4)	7.912e-03					
HCO3-	5.578e-03	2.580e-03	-2.254	-2.588	-0.335	29.14
CO3-2	1.232e-03	4.780e-05	-2.909	-4.321	-1.411	2.73
MgCO3	1.089e-03	1.089e-03	-2.963	-2.963	0.000	-17.10
CO2	1.291e-05	1.663e-05	-4.889	-4.779	0.110	35.16
Ca	1.207e-02					
Ca+2	1.207e-02	3.244e-03	-1.918	-2.489	-0.570	-15.79
Cl	1.476e+00					
Cl-	1.476e+00	8.640e-01	0.169	-0.063	-0.233	19.49
Mg	7.368e-02					
Mg+2	7.256e-02	2.157e-02	-1.139	-1.666	-0.527	-20.17
MgCO3	1.089e-03	1.089e-03	-2.963	-2.963	0.000	-17.10
MgOH+	3.390e-05	3.498e-05	-4.470	-4.456	0.014	(0)
Na	1.376e+00					
Na+	1.376e+00	1.030e+00	0.139	0.013	-0.126	0.47
S(6)	2.516e-02					
SO4-2	2.516e-02	1.002e-03	-1.599	-2.999	-1.400	21.48
HSO4-	8.330e-10	4.629e-10	-9.079	-9.334	-0.255	42.16

-----Saturation indices-----

Phase	SI**	log IAP	log K(313 K, 1 atm)
Anhydrite	-1.03	-5.49	-4.45 CaSO4
Aragonite	1.52	-6.81	-8.33 CaCO3
Artinite	0.90	19.47	18.57 Mg2CO3(OH)2:3H2O
Bischofite	-6.33	-1.93	4.41 MgCl2:6H2O
Bloedite	-5.38	-7.73	-2.35 Na2Mg(SO4)2:4H2O
Brucite	-1.07	-11.78	-10.71 Mg(OH)2
Burkeite	-9.47	-10.24	-0.77 Na6CO3(SO4)2
Calcite	1.84	-6.81	-8.65 CaCO3
CO2(g)	-3.15	-4.78	-1.63 CO2
Dolomite	4.62	-12.80	-17.41 CaMg(CO3)2

Epsomite	-3.07	-4.82	-1.75	MgSO4:7H2O
Gaylussite	-1.79	-11.22	-9.42	CaNa2(CO3)2:5H2O
Glauberite	-2.95	-8.46	-5.52	Na2Ca(SO4)2
Gypsum	-0.90	-5.53	-4.63	CaSO4:2H2O
H2O(g)	-1.16	-0.02	1.14	H2O
Halite	-1.66	-0.05	1.61	NaCl
Hexahydrite	-3.19	-4.80	-1.61	MgSO4:6H2O
Huntite	7.47	16.16	8.69	CaMg3(CO3)4
Kieserite	-4.14	-4.69	-0.55	MgSO4:H2O
Labile_S	-5.81	-11.48	-5.67	Na4Ca(SO4)3:2H2O
Leonhardite	-3.87	-4.75	-0.89	MgSO4:4H2O
Magnesite	1.90	-5.99	-7.89	MgCO3
MgCl2_2H2O	-15.21	-1.84	13.37	MgCl2:2H2O
MgCl2_4H2O	-8.56	-1.88	6.68	MgCl2:4H2O
Mirabilite	-2.53	-3.20	-0.67	Na2SO4:10H2O
Nahcolite	-2.07	-12.81	-10.74	NaHCO3
Natron	-3.69	-4.52	-0.82	Na2CO3:10H2O
Nesquehonite	-0.89	-6.05	-5.17	MgCO3:3H2O
Pentahydrite	-3.49	-4.78	-1.28	MgSO4:5H2O
Pirssonite	-1.91	-11.15	-9.23	Na2Ca(CO3)2:2H2O
Portlandite	-7.41	-12.60	-5.19	Ca(OH)2
Thenardite	-2.60	-2.97	-0.37	Na2SO4
Trona	-5.76	-17.15	-11.38	Na3H(CO3)2:2H2O

**For a gas, SI = log10(fugacity). Fugacity = pressure * phi / 1 atm.
For ideal gases, phi = 1.

End of simulation.

Reading input data for simulation 2.

End of Run after 0.008949 Seconds.

T = Before

Reading data base.

SOLUTION_MASTER_SPECIES
SOLUTION_SPECIES

PHASES
 PITZER
 EXCHANGE_MASTER_SPECIES
 EXCHANGE_SPECIES
 SURFACE_MASTER_SPECIES
 SURFACE_SPECIES
 END

 Reading input data for simulation 1.

TITLE Bryan Rodriguez's Solution - Dengying Formation (summer 2019)
 SOLUTION 1

pH	8.51
Temp	40
	Units mg/L
Ca	371
Mg	2488
Na	29034
Cl	48044
S(6)	2219
Alkalinity	848 as CO3

SAVE SOLUTION 1

 TITLE

 Bryan Rodriguez's Solution - Dengying Formation (summer 2019)

 Beginning of initial solution calculations.

Initial solution 1.

-----Solution composition-----

Elements	Molality	Moles
Alkalinity	1.541e-02	1.541e-02
Ca	1.009e-02	1.009e-02
Cl	1.478e+00	1.478e+00
Mg	1.116e-01	1.116e-01
Na	1.377e+00	1.377e+00
S(6)	2.519e-02	2.519e-02

-----Description of solution-----

pH = 8.510
 pe = 4.000
 Specific Conductance ($\mu\text{S}/\text{cm}$, 40°C) = 147460
 Density (g/cm^3) = 1.05267
 Volume (L) = 1.03573
 Activity of water = 0.949
 Ionic strength (mol/kgw) = 1.724e+00
 Mass of water (kg) = 1.000e+00
 Total carbon (mol/kg) = 1.137e-02
 Total CO2 (mol/kg) = 1.137e-02
 Temperature ($^\circ\text{C}$) = 40.00
 Electrical balance (eq) = 7.707e-02
 Percent error, $100 \cdot (\text{Cat} - |\text{An}|) / (\text{Cat} + |\text{An}|)$ = 2.44
 Iterations = 17
 Gamma iterations = 4
 Osmotic coefficient = 0.96690
 Density of water = 0.99221
 Total H = 1.110199e+02
 Total O = 5.564114e+01

-----Distribution of species-----

Species	MacInnes		MacInnes		mole V Gamma	cm \geq /mol
	Molality	Activity	Log Molality	Log Activity		
OH-	2.119e-05	8.991e-06	-4.674	-5.046	-0.372	-0.52
H+	2.864e-09	3.090e-09	-8.543	-8.510	0.033	0.00
H2O	5.551e+01	9.489e-01	1.744	-0.023	0.000	18.16
C(4)	1.137e-02					
HCO3-	7.367e-03	3.308e-03	-2.133	-2.480	-0.348	29.27
MgCO3	2.136e-03	2.136e-03	-2.670	-2.670	0.000	-17.10
CO3-2	1.849e-03	6.274e-05	-2.733	-4.202	-1.469	2.86
CO2	1.598e-05	2.086e-05	-4.796	-4.681	0.116	35.16
Ca	1.009e-02					
Ca+2	1.009e-02	2.701e-03	-1.996	-2.569	-0.573	-15.75
Cl	1.478e+00					
Cl-	1.478e+00	8.632e-01	0.170	-0.064	-0.234	19.51
Mg	1.116e-01					
Mg+2	1.094e-01	3.224e-02	-0.961	-1.492	-0.531	-20.13
MgCO3	2.136e-03	2.136e-03	-2.670	-2.670	0.000	-17.10
MgOH+	5.265e-05	5.345e-05	-4.279	-4.272	0.007	(0)
Na	1.377e+00					
Na+	1.377e+00	1.044e+00	0.139	0.019	-0.120	0.49

S(6)	2.519e-02					
SO4-2	2.519e-02	9.511e-04	-1.599	-3.022	-1.423	21.61
HSO4-	7.683e-10	4.293e-10	-9.114	-9.367	-0.253	42.19

-----Saturation indices-----

Phase	SI**	log IAP	log K(313 K, 1 atm)	
Anhydrite	-1.14	-5.59	-4.45	CaSO4
Aragonite	1.56	-6.77	-8.33	CaCO3
Artinite	1.38	19.95	18.57	Mg2CO3(OH)2:3H2O
Bischofite	-6.16	-1.76	4.41	MgCl2:6H2O
Bloedite	-5.24	-7.59	-2.35	Na2Mg(SO4)2:4H2O
Brucite	-0.87	-11.58	-10.71	Mg(OH)2
Burkeite	-9.36	-10.13	-0.77	Na6CO3(SO4)2
Calcite	1.88	-6.77	-8.65	CaCO3
CO2(g)	-3.06	-4.68	-1.63	CO2
Dolomite	4.95	-12.47	-17.41	CaMg(CO3)2
Epsomite	-2.92	-4.67	-1.75	MgSO4:7H2O
Gaylussite	-1.63	-11.05	-9.42	CaNa2(CO3)2:5H2O
Glauberite	-3.06	-8.58	-5.52	Na2Ca(SO4)2
Gypsum	-1.01	-5.64	-4.63	CaSO4:2H2O
H2O(g)	-1.16	-0.02	1.14	H2O
Halite	-1.65	-0.05	1.61	NaCl
Hexahydrite	-3.04	-4.65	-1.61	MgSO4:6H2O
Huntite	8.39	17.08	8.69	CaMg3(CO3)4
Kieserite	-3.98	-4.54	-0.55	MgSO4:H2O
Labile_S	-5.93	-11.61	-5.67	Na4Ca(SO4)3:2H2O
Leonhardite	-3.72	-4.60	-0.89	MgSO4:4H2O
Magnesite	2.19	-5.69	-7.89	MgCO3
MgCl2_2H2O	-15.03	-1.66	13.37	MgCl2:2H2O
MgCl2_4H2O	-8.39	-1.71	6.68	MgCl2:4H2O
Mirabilite	-2.55	-3.21	-0.67	Na2SO4:10H2O
Nahcolite	-1.95	-12.69	-10.74	NaHCO3
Natron	-3.57	-4.39	-0.82	Na2CO3:10H2O
Nesquehonite	-0.60	-5.76	-5.17	MgCO3:3H2O
Pentahydrite	-3.34	-4.63	-1.28	MgSO4:5H2O
Pirssonite	-1.75	-10.98	-9.23	Na2Ca(CO3)2:2H2O
Portlandite	-7.47	-12.66	-5.19	Ca(OH)2
Thenardite	-2.61	-2.98	-0.37	Na2SO4
Trona	-5.52	-16.90	-11.38	Na3H(CO3)2:2H2O

**For a gas, SI = log10(fugacity). Fugacity = pressure * phi / 1 atm.
For ideal gases, phi = 1.

End of simulation.

Reading input data for simulation 2.

End of Run after 0.009586 Seconds.

T=5

Reading data base.

SOLUTION_MASTER_SPECIES
SOLUTION_SPECIES
PHASES
PITZER
EXCHANGE_MASTER_SPECIES
EXCHANGE_SPECIES
SURFACE_MASTER_SPECIES
SURFACE_SPECIES
END

Reading input data for simulation 1.

TITLE Bryan Rodriguez's Solution - Dengying Formation (summer 2019)
SOLUTION 1

pH	6.85
Temp	40
	Units mg/L
Ca	209
Mg	2559
Na	29034
Cl	48044
S(6)	2219
Alkalinity	543 as CO3

SAVE SOLUTION 1

TITLE

Bryan Rodriguez's Solution - Dengying Formation (summer 2019)

 Beginning of initial solution calculations.

Initial solution 1.

-----Solution composition-----

Elements	Molality	Moles
Alkalinity	9.863e-03	9.863e-03
Ca	5.684e-03	5.684e-03
Cl	1.477e+00	1.477e+00
Mg	1.148e-01	1.148e-01
Na	1.377e+00	1.377e+00
S(6)	2.518e-02	2.518e-02

-----Description of solution-----

pH = 6.850
 pe = 4.000
 Specific Conductance ($\mu\text{S}/\text{cm}$, 40°C) = 147345
 Density (g/cm^3) = 1.05240
 Volume (L) = 1.03581
 Activity of water = 0.949
 Ionic strength (mol/kgw) = 1.723e+00
 Mass of water (kg) = 1.000e+00
 Total carbon (mol/kg) = 1.069e-02
 Total CO2 (mol/kg) = 1.069e-02
 Temperature ($^\circ\text{C}$) = 40.00
 Electrical balance (eq) = 8.014e-02
 Percent error, $100 \cdot (\text{Cat} - |\text{An}|) / (\text{Cat} + |\text{An}|)$ = 2.54
 Iterations = 14
 Gamma iterations = 4
 Osmotic coefficient = 0.96750
 Density of water = 0.99221
 Total H = 1.110221e+02
 Total O = 5.563807e+01

-----Distribution of species-----

Species	MacInnes		MacInnes		mole V Gamma
	MacInnes Molality	Log Activity	Log Molality	Log Activity	
					cm^3/mol

OH-	4.633e-07	1.967e-07	-6.334	-6.706	-0.372	-0.52
H+	1.306e-07	1.413e-07	-6.884	-6.850	0.034	0.00
H2O	5.551e+01	9.489e-01	1.744	-0.023	0.000	18.16
C(4)	1.069e-02					
HCO3-	9.628e-03	4.295e-03	-2.016	-2.367	-0.351	29.27
CO2	9.485e-04	1.238e-03	-3.023	-2.907	0.116	35.16
MgCO3	6.399e-05	6.399e-05	-4.194	-4.194	0.000	-17.10
CO3-2	5.276e-05	1.782e-06	-4.278	-5.749	-1.471	2.85
Ca	5.684e-03					
Ca+2	5.684e-03	1.535e-03	-2.245	-2.814	-0.569	-15.75
Cl	1.477e+00					
Cl-	1.477e+00	8.628e-01	0.169	-0.064	-0.234	19.51
Mg	1.148e-01					
Mg+2	1.147e-01	3.401e-02	-0.940	-1.468	-0.528	-20.14
MgCO3	6.399e-05	6.399e-05	-4.194	-4.194	0.000	-17.10
MgOH+	1.212e-06	1.233e-06	-5.917	-5.909	0.008	(0)
Na	1.377e+00					
Na+	1.377e+00	1.044e+00	0.139	0.019	-0.120	0.49
S(6)	2.518e-02					
SO4-2	2.518e-02	9.522e-04	-1.599	-3.021	-1.422	21.60
HSO4-	3.514e-08	1.965e-08	-7.454	-7.707	-0.253	42.18

-----Saturation indices-----

Phase	SI**	log IAP	log K(313 K, 1 atm)
Anhydrite	-1.38	-5.84	-4.45 CaSO4
Aragonite	-0.23	-8.56	-8.33 CaCO3
Artinite	-3.44	15.13	18.57 Mg2CO3(OH)2:3H2O
Bischofite	-6.14	-1.73	4.41 MgCl2:6H2O
Bloedite	-5.22	-7.56	-2.35 Na2Mg(SO4)2:4H2O
Brucite	-4.17	-14.88	-10.71 Mg(OH)2
Burkeite	-10.91	-11.68	-0.77 Na6CO3(SO4)2
Calcite	0.09	-8.56	-8.65 CaCO3
CO2(g)	-1.28	-2.91	-1.63 CO2
Dolomite	1.63	-15.78	-17.41 CaMg(CO3)2
Epsomite	-2.90	-4.65	-1.75 MgSO4:7H2O
Gaylussite	-4.97	-14.39	-9.42 CaNa2(CO3)2:5H2O
Glauberite	-3.30	-8.82	-5.52 Na2Ca(SO4)2
Gypsum	-1.25	-5.88	-4.63 CaSO4:2H2O
H2O(g)	-1.16	-0.02	1.14 H2O
Halite	-1.65	-0.05	1.61 NaCl
Hexahydrate	-3.02	-4.63	-1.61 MgSO4:6H2O
Huntite	2.03	10.71	8.69 CaMg3(CO3)4
Kieserite	-3.96	-4.51	-0.55 MgSO4:H2O
Labile_S	-6.18	-11.85	-5.67 Na4Ca(SO4)3:2H2O

Leonhardite	-3.69	-4.58	-0.89	MgSO4:4H2O
Magnesite	0.67	-7.22	-7.89	MgCO3
MgCl2_2H2O	-15.01	-1.64	13.37	MgCl2:2H2O
MgCl2_4H2O	-8.36	-1.69	6.68	MgCl2:4H2O
Mirabilite	-2.54	-3.21	-0.67	Na2SO4:10H2O
Nahcolite	-1.84	-12.58	-10.74	NaHCO3
Natron	-5.11	-5.94	-0.82	Na2CO3:10H2O
Nesquehonite	-2.12	-7.29	-5.17	MgCO3:3H2O
Pentahydrate	-3.32	-4.60	-1.28	MgSO4:5H2O
Pirssonite	-5.09	-14.32	-9.23	Na2Ca(CO3)2:2H2O
Portlandite	-11.04	-16.23	-5.19	Ca(OH)2
Thenardite	-2.61	-2.98	-0.37	Na2SO4
Trona	-6.95	-18.34	-11.38	Na3H(CO3)2:2H2O

**For a gas, SI = log10(fugacity). Fugacity = pressure * phi / 1 atm.
For ideal gases, phi = 1.

End of simulation.

Reading input data for simulation 2.

End of Run after 0.008314 Seconds.

Input file: /Users/bryanrodriguez/OneDrive - The University of Kansas/Bryan-MASTERS/PHREEQC/Phreeqc-Fluids/Summer2019/Feb2020/ESW-NoSi/Bryan-ChinaFluid-ESW_NoSi-experimental-T5sp1.txt

Output file: /Users/bryanrodriguez/OneDrive - The University of Kansas/Bryan-MASTERS/PHREEQC/Phreeqc-Fluids/Summer2019/Feb2020/ESW-NoSi/ESW_NoSi-T5sp1.txt.out

Database file: /Users/bryanrodriguez/OneDrive - The University of Kansas/Bryan-MASTERS/PHREEQC/phreeqc-3.5.0-14000/database/pitzer.dat

Reading data base.

SOLUTION_MASTER_SPECIES
SOLUTION_SPECIES
PHASES
PITZER
EXCHANGE_MASTER_SPECIES

EXCHANGE_SPECIES
SURFACE_MASTER_SPECIES
SURFACE_SPECIES
END

Reading input data for simulation 1.

TITLE Bryan Rodriguez's Solution - Dengying Formation (summer 2019)
SOLUTION 1

pH	6.98
Temp	40
	Units mg/L
Ca	196
Mg	2501
Na	29034
Cl	48044
S(6)	2219
Alkalinity	562 as CO3

SAVE SOLUTION 1

TITLE

Bryan Rodriguez's Solution - Dengying Formation (summer 2019)

Beginning of initial solution calculations.

Initial solution 1.

-----Solution composition-----

Elements	Molality	Moles
Alkalinity	1.021e-02	1.021e-02
Ca	5.330e-03	5.330e-03
Cl	1.477e+00	1.477e+00
Mg	1.122e-01	1.122e-01
Na	1.377e+00	1.377e+00
S(6)	2.518e-02	2.518e-02

-----Description of solution-----

pH = 6.980

pe = 4.000
 Specific Conductance ($\mu\text{S}/\text{cm}$, 40°C) = 147318
 Density (g/cm^3) = 1.05228
 Volume (L) = 1.03586
 Activity of water = 0.949
 Ionic strength (mol/kgw) = 1.717e+00
 Mass of water (kg) = 1.000e+00
 Total carbon (mol/kg) = 1.077e-02
 Total CO2 (mol/kg) = 1.077e-02
 Temperature ($^\circ\text{C}$) = 40.00
 Electrical balance (eq) = 7.388e-02
 Percent error, $100 \cdot (\text{Cat} - |\text{An}|) / (\text{Cat} + |\text{An}|)$ = 2.35
 Iterations = 15
 Gamma iterations = 4
 Osmotic coefficient = 0.96718
 Density of water = 0.99221
 Total H = 1.110223e+02
 Total O = 5.563852e+01

-----Distribution of species-----

Species	MacInnes		MacInnes		mole V Gamma	cm \geq /mol
	Molality	Activity	Log Molality	Log Activity		
OH-	6.224e-07	2.653e-07	-6.206	-6.576	-0.370	-0.53
H+	9.697e-08	1.047e-07	-7.013	-6.980	0.033	0.00
H2O	5.551e+01	9.490e-01	1.744	-0.023	0.000	18.16
C(4)	1.077e-02					
HCO3-	9.887e-03	4.418e-03	-2.005	-2.355	-0.350	29.26
CO2	7.239e-04	9.440e-04	-3.140	-3.025	0.115	35.16
MgCO3	8.679e-05	8.679e-05	-4.062	-4.062	0.000	-17.10
CO3-2	7.242e-05	2.472e-06	-4.140	-5.607	-1.467	2.85
Ca	5.330e-03					
Ca+2	5.330e-03	1.440e-03	-2.273	-2.842	-0.568	-15.75
Cl	1.477e+00					
Cl-	1.477e+00	8.629e-01	0.169	-0.064	-0.233	19.51
Mg	1.122e-01					
Mg+2	1.121e-01	3.324e-02	-0.951	-1.478	-0.528	-20.14
MgCO3	8.679e-05	8.679e-05	-4.062	-4.062	0.000	-17.10
MgOH+	1.596e-06	1.627e-06	-5.797	-5.789	0.008	(0)
Na	1.377e+00					
Na+	1.377e+00	1.043e+00	0.139	0.018	-0.121	0.49
S(6)	2.518e-02					
SO4-2	2.518e-02	9.565e-04	-1.599	-3.019	-1.420	21.60
HSO4-	2.618e-08	1.463e-08	-7.582	-7.835	-0.253	42.18

-----Saturation indices-----

Phase	SI**	log IAP	log K(313 K, 1 atm)	
Anhydrite	-1.41	-5.86	-4.45	CaSO4
Aragonite	-0.12	-8.45	-8.33	CaCO3
Artinite	-3.05	15.51	18.57	Mg2CO3(OH)2:3H2O
Bischofite	-6.15	-1.74	4.41	MgCl2:6H2O
Bloedite	-5.22	-7.57	-2.35	Na2Mg(SO4)2:4H2O
Brucite	-3.92	-14.63	-10.71	Mg(OH)2
Burkeite	-10.76	-11.54	-0.77	Na6CO3(SO4)2
Calcite	0.20	-8.45	-8.65	CaCO3
CO2(g)	-1.40	-3.03	-1.63	CO2
Dolomite	1.88	-15.53	-17.41	CaMg(CO3)2
Epsomite	-2.91	-4.66	-1.75	MgSO4:7H2O
Gaylussite	-4.71	-14.13	-9.42	CaNa2(CO3)2:5H2O
Glauberite	-3.33	-8.84	-5.52	Na2Ca(SO4)2
Gypsum	-1.28	-5.91	-4.63	CaSO4:2H2O
H2O(g)	-1.16	-0.02	1.14	H2O
Halite	-1.65	-0.05	1.61	NaCl
Hexahydrate	-3.02	-4.63	-1.61	MgSO4:6H2O
Huntite	2.54	11.22	8.69	CaMg3(CO3)4
Kieserite	-3.97	-4.52	-0.55	MgSO4:H2O
Labile_S	-6.20	-11.87	-5.67	Na4Ca(SO4)3:2H2O
Leonhardite	-3.70	-4.59	-0.89	MgSO4:4H2O
Magnesite	0.80	-7.09	-7.89	MgCO3
MgCl2_2H2O	-15.02	-1.65	13.37	MgCl2:2H2O
MgCl2_4H2O	-8.37	-1.70	6.68	MgCl2:4H2O
Mirabilite	-2.54	-3.21	-0.67	Na2SO4:10H2O
Nahcolite	-1.83	-12.57	-10.74	NaHCO3
Natron	-4.97	-5.80	-0.82	Na2CO3:10H2O
Nesquehonite	-1.99	-7.15	-5.17	MgCO3:3H2O
Pentahydrate	-3.33	-4.61	-1.28	MgSO4:5H2O
Pirssonite	-4.83	-14.06	-9.23	Na2Ca(CO3)2:2H2O
Portlandite	-10.80	-15.99	-5.19	Ca(OH)2
Thenardite	-2.61	-2.98	-0.37	Na2SO4
Trona	-6.80	-18.18	-11.38	Na3H(CO3)2:2H2O

**For a gas, SI = log10(fugacity). Fugacity = pressure * phi / 1 atm.
For ideal gases, phi = 1.

End of simulation.

Reading input data for simulation 2.

End of Run after 0.008931 Seconds.

Input file: /Users/bryanrodriguez/OneDrive - The University of Kansas/Bryan-MASTERS/PHREEQC/Phreeqc-Fluids/Summer2019/Feb2020/ESW-NoSi/Bryan-ChinaFluid-ESW_NoSi-experimental-T5sp2.txt

Output file: /Users/bryanrodriguez/OneDrive - The University of Kansas/Bryan-MASTERS/PHREEQC/Phreeqc-Fluids/Summer2019/Feb2020/ESW-NoSi/ESW_NoSi-T5sp2.txt.out

Database file: /Users/bryanrodriguez/OneDrive - The University of Kansas/Bryan-MASTERS/PHREEQC/phreeqc-3.5.0-14000/database/pitzer.dat

Reading data base.

SOLUTION_MASTER_SPECIES
SOLUTION_SPECIES
PHASES
PITZER
EXCHANGE_MASTER_SPECIES
EXCHANGE_SPECIES
SURFACE_MASTER_SPECIES
SURFACE_SPECIES
END

Reading input data for simulation 1.

TITLE Bryan Rodriguez's Solution - Dengying Formation (summer 2019)

SOLUTION 1

pH	6.98
Temp	40
	Units mg/L
Ca	156
Mg	2054
Na	29034
Cl	48044
S(6)	2219
Alkalinity	550 as CO3

SAVE SOLUTION 1

TITLE

Bryan Rodriguez's Solution - Dengying Formation (summer 2019)

Beginning of initial solution calculations.

Initial solution 1.

-----Solution composition-----

Elements	Molality	Moles
Alkalinity	9.984e-03	9.984e-03
Ca	4.240e-03	4.240e-03
Cl	1.476e+00	1.476e+00
Mg	9.206e-02	9.206e-02
Na	1.376e+00	1.376e+00
S(6)	2.516e-02	2.516e-02

-----Description of solution-----

pH = 6.980
pe = 4.000
Specific Conductance ($\mu\text{S}/\text{cm}$, 40°C) = 147097
Density (g/cm^3) = 1.05135
Volume (L) = 1.03622
Activity of water = 0.949
Ionic strength (mol/kgw) = 1.674e+00
Mass of water (kg) = 1.000e+00
Total carbon (mol/kg) = 1.057e-02
Total CO2 (mol/kg) = 1.057e-02
Temperature (°C) = 40.00
Electrical balance (eq) = 3.181e-02
Percent error, $100 \cdot (\text{Cat} - |\text{An}|) / (\text{Cat} + |\text{An}|)$ = 1.02
Iterations = 14
Gamma iterations = 4
Osmotic coefficient = 0.96505
Density of water = 0.99221
Total H = 1.110221e+02
Total O = 5.563786e+01

-----Distribution of species-----

Species	MacInnes		MacInnes		mole V Gamma	cm ³ /mol
	Molality	Activity	Log Molality	Log Activity		
OH-	6.042e-07	2.655e-07	-6.219	-6.576	-0.357	-0.59
H+	9.783e-08	1.047e-07	-7.010	-6.980	0.030	0.00
H2O	5.551e+01	9.494e-01	1.744	-0.023	0.000	18.16
C(4)	1.057e-02					
HCO3-	9.707e-03	4.399e-03	-2.013	-2.357	-0.344	29.18
CO2	7.262e-04	9.395e-04	-3.139	-3.027	0.112	35.16
MgCO3	7.126e-05	7.126e-05	-4.147	-4.147	0.000	-17.10
CO3-2	6.661e-05	2.462e-06	-4.176	-5.609	-1.432	2.77
Ca	4.240e-03					
Ca+2	4.240e-03	1.150e-03	-2.373	-2.939	-0.567	-15.77
Cl	1.476e+00					
Cl-	1.476e+00	8.635e-01	0.169	-0.064	-0.233	19.50
Mg	9.206e-02					
Mg+2	9.199e-02	2.741e-02	-1.036	-1.562	-0.526	-20.16
MgCO3	7.126e-05	7.126e-05	-4.147	-4.147	0.000	-17.10
MgOH+	1.305e-06	1.342e-06	-5.884	-5.872	0.012	(0)
Na	1.376e+00					
Na+	1.376e+00	1.035e+00	0.139	0.015	-0.124	0.48
S(6)	2.516e-02					
SO4-2	2.516e-02	9.885e-04	-1.599	-3.005	-1.406	21.52
HSO4-	2.715e-08	1.512e-08	-7.566	-7.821	-0.254	42.17

-----Saturation indices-----

Phase	SI**	log IAP	log K(313 K, 1 atm)
Anhydrite	-1.49	-5.94	-4.45 CaSO4
Aragonite	-0.22	-8.55	-8.33 CaCO3
Artinite	-3.22	15.35	18.57 Mg2CO3(OH)2:3H2O
Bischofite	-6.23	-1.82	4.41 MgCl2:6H2O
Bloedite	-5.29	-7.63	-2.35 Na2Mg(SO4)2:4H2O
Brucite	-4.00	-14.71	-10.71 Mg(OH)2
Burkeite	-10.76	-11.53	-0.77 Na6CO3(SO4)2
Calcite	0.10	-8.55	-8.65 CaCO3
CO2(g)	-1.40	-3.03	-1.63 CO2
Dolomite	1.70	-15.72	-17.41 CaMg(CO3)2
Epsomite	-2.98	-4.72	-1.75 MgSO4:7H2O
Gaylussite	-4.82	-14.24	-9.42 CaNa2(CO3)2:5H2O
Glauberite	-3.40	-8.92	-5.52 Na2Ca(SO4)2
Gypsum	-1.36	-5.99	-4.63 CaSO4:2H2O
H2O(g)	-1.16	-0.02	1.14 H2O
Halite	-1.66	-0.05	1.61 NaCl

Hexahydrate	-3.09	-4.70	-1.61	MgSO4:6H2O
Huntite	2.18	10.87	8.69	CaMg3(CO3)4
Kieserite	-4.04	-4.59	-0.55	MgSO4:H2O
Labile_S	-6.27	-11.94	-5.67	Na4Ca(SO4)3:2H2O
Leonhardite	-3.77	-4.66	-0.89	MgSO4:4H2O
Magnesite	0.71	-7.17	-7.89	MgCO3
MgCl2_2H2O	-15.10	-1.73	13.37	MgCl2:2H2O
MgCl2_4H2O	-8.46	-1.78	6.68	MgCl2:4H2O
Mirabilite	-2.53	-3.20	-0.67	Na2SO4:10H2O
Nahcolite	-1.83	-12.57	-10.74	NaHCO3
Natron	-4.98	-5.80	-0.82	Na2CO3:10H2O
Nesquehonite	-2.07	-7.24	-5.17	MgCO3:3H2O
Pentahydrate	-3.39	-4.68	-1.28	MgSO4:5H2O
Pirssonite	-4.94	-14.17	-9.23	Na2Ca(CO3)2:2H2O
Portlandite	-10.90	-16.09	-5.19	Ca(OH)2
Thenardite	-2.60	-2.98	-0.37	Na2SO4
Trona	-6.81	-18.20	-11.38	Na3H(CO3)2:2H2O

**For a gas, SI = log10(fugacity). Fugacity = pressure * phi / 1 atm.
 For ideal gases, phi = 1.

 End of simulation.

 Reading input data for simulation 2.

 End of Run after 0.009384 Seconds.

T = 10

 Reading data base.

SOLUTION_MASTER_SPECIES
 SOLUTION_SPECIES
 PHASES
 PITZER
 EXCHANGE_MASTER_SPECIES
 EXCHANGE_SPECIES
 SURFACE_MASTER_SPECIES
 SURFACE_SPECIES

END

Reading input data for simulation 1.

TITLE Bryan Rodriguez's Solution - Dengying Formation (summer 2019)

SOLUTION 1

pH 6.83
Temp 40
Units mg/L
Ca 206
Mg 2351
Na 29034
Cl 48044
S(6) 2219
Alkalinity 537 as CO3

SAVE SOLUTION 1

TITLE

Bryan Rodriguez's Solution - Dengying Formation (summer 2019)

Beginning of initial solution calculations.

Initial solution 1.

-----Solution composition-----

Elements	Molality	Moles
Alkalinity	9.752e-03	9.752e-03
Ca	5.601e-03	5.601e-03
Cl	1.477e+00	1.477e+00
Mg	1.054e-01	1.054e-01
Na	1.376e+00	1.376e+00
S(6)	2.517e-02	2.517e-02

-----Description of solution-----

pH = 6.830
pe = 4.000
Specific Conductance ($\mu\text{S}/\text{cm}$, 40°C) = 147254
Density (g/cm^3) = 1.05199

Volume (L) = 1.03597
 Activity of water = 0.949
 Ionic strength (mol/kgw) = 1.704e+00
 Mass of water (kg) = 1.000e+00
 Total carbon (mol/kg) = 1.064e-02
 Total CO2 (mol/kg) = 1.064e-02
 Temperature (∞C) = 40.00
 Electrical balance (eq) = 6.141e-02
 Percent error, 100*(Cat-|An|)/(Cat+|An|) = 1.96
 Iterations = 14
 Gamma iterations = 4
 Osmotic coefficient = 0.96658
 Density of water = 0.99221
 Total H = 1.110220e+02
 Total O = 5.563784e+01

-----Distribution of species-----

Species	MacInnes		MacInnes		mole V Gamma	cm ³ /mol
	Molality	Log Activity	Log Molality	Log Activity		
OH-	4.368e-07	1.879e-07	-6.360	-6.726	-0.366	-0.55
H+	1.373e-07	1.479e-07	-6.862	-6.830	0.032	0.00
H2O	5.551e+01	9.491e-01	1.744	-0.023	0.000	18.16
C(4)	1.064e-02					
HCO3-	9.541e-03	4.285e-03	-2.020	-2.368	-0.348	29.23
CO2	9.941e-04	1.293e-03	-3.003	-2.888	0.114	35.16
MgCO3	5.611e-05	5.611e-05	-4.251	-4.251	0.000	-17.10
CO3-2	4.853e-05	1.698e-06	-4.314	-5.770	-1.456	2.82
Ca	5.601e-03					
Ca+2	5.601e-03	1.515e-03	-2.252	-2.820	-0.568	-15.76
Cl	1.477e+00					
Cl-	1.477e+00	8.631e-01	0.169	-0.064	-0.233	19.51
Mg	1.054e-01					
Mg+2	1.054e-01	3.129e-02	-0.977	-1.505	-0.527	-20.15
MgCO3	5.611e-05	5.611e-05	-4.251	-4.251	0.000	-17.10
MgOH+	1.061e-06	1.084e-06	-5.974	-5.965	0.009	(0)
Na	1.376e+00					
Na+	1.376e+00	1.040e+00	0.139	0.017	-0.122	0.49
S(6)	2.517e-02					
SO4-2	2.517e-02	9.658e-04	-1.599	-3.015	-1.416	21.57
HSO4-	3.738e-08	2.086e-08	-7.427	-7.681	-0.253	42.18

-----Saturation indices-----

Phase	SI**	log IAP	log K(313 K, 1 atm)	
Anhydrite	-1.38	-5.83	-4.45	CaSO4
Aragonite	-0.26	-8.59	-8.33	CaCO3
Artinite	-3.57	15.00	18.57	Mg2CO3(OH)2:3H2O
Bischofite	-6.18	-1.77	4.41	MgCl2:6H2O
Bloedite	-5.24	-7.59	-2.35	Na2Mg(SO4)2:4H2O
Brucite	-4.25	-14.96	-10.71	Mg(OH)2
Burkeite	-10.93	-11.70	-0.77	Na6CO3(SO4)2
Calcite	0.06	-8.59	-8.65	CaCO3
CO2(g)	-1.26	-2.89	-1.63	CO2
Dolomite	1.55	-15.86	-17.41	CaMg(CO3)2
Epsomite	-2.93	-4.68	-1.75	MgSO4:7H2O
Gaylussite	-5.02	-14.44	-9.42	CaNa2(CO3)2:5H2O
Glauberite	-3.30	-8.82	-5.52	Na2Ca(SO4)2
Gypsum	-1.25	-5.88	-4.63	CaSO4:2H2O
H2O(g)	-1.16	-0.02	1.14	H2O
Halite	-1.65	-0.05	1.61	NaCl
Hexahydrite	-3.05	-4.66	-1.61	MgSO4:6H2O
Huntite	1.83	10.51	8.69	CaMg3(CO3)4
Kieserite	-3.99	-4.54	-0.55	MgSO4:H2O
Labile_S	-6.17	-11.84	-5.67	Na4Ca(SO4)3:2H2O
Leonhardite	-3.72	-4.61	-0.89	MgSO4:4H2O
Magnesite	0.61	-7.27	-7.89	MgCO3
MgCl2_2H2O	-15.05	-1.68	13.37	MgCl2:2H2O
MgCl2_4H2O	-8.40	-1.72	6.68	MgCl2:4H2O
Mirabilite	-2.54	-3.21	-0.67	Na2SO4:10H2O
Nahcolite	-1.84	-12.58	-10.74	NaHCO3
Natron	-5.14	-5.96	-0.82	Na2CO3:10H2O
Nesquehonite	-2.18	-7.34	-5.17	MgCO3:3H2O
Pentahydrite	-3.35	-4.63	-1.28	MgSO4:5H2O
Pirssonite	-5.14	-14.37	-9.23	Na2Ca(CO3)2:2H2O
Portlandite	-11.08	-16.27	-5.19	Ca(OH)2
Thenardite	-2.61	-2.98	-0.37	Na2SO4
Trona	-6.98	-18.36	-11.38	Na3H(CO3)2:2H2O

**For a gas, SI = log10(fugacity). Fugacity = pressure * phi / 1 atm.
For ideal gases, phi = 1.

End of simulation.

Reading input data for simulation 2.

End of Run after 0.008012 Seconds.

Reading data base.

SOLUTION_MASTER_SPECIES
SOLUTION_SPECIES
PHASES
PITZER
EXCHANGE_MASTER_SPECIES
EXCHANGE_SPECIES
SURFACE_MASTER_SPECIES
SURFACE_SPECIES
END

Reading input data for simulation 1.

TITLE Bryan Rodriguez's Solution - Dengying Formation (summer 2019)
SOLUTION 1
pH 6.92
Temp 40
Units mg/L
Ca 209
Mg 2574
Na 29034
Cl 48044
S(6) 2219
Alkalinity 534 as CO3
SAVE SOLUTION 1

TITLE

Bryan Rodriguez's Solution - Dengying Formation (summer 2019)

Beginning of initial solution calculations.

Initial solution 1.

-----Solution composition-----

Elements	Molality	Moles
Alkalinity	9.700e-03	9.700e-03
Ca	5.684e-03	5.684e-03
Cl	1.477e+00	1.477e+00
Mg	1.154e-01	1.154e-01
Na	1.377e+00	1.377e+00
S(6)	2.518e-02	2.518e-02

-----Description of solution-----

pH = 6.920
 pe = 4.000
 Specific Conductance ($\mu\text{S}/\text{cm}$, 40°C) = 147348
 Density (g/cm^3) = 1.05242
 Volume (L) = 1.03579
 Activity of water = 0.949
 Ionic strength (mol/kgw) = 1.724e+00
 Mass of water (kg) = 1.000e+00
 Total carbon (mol/kg) = 1.035e-02
 Total CO2 (mol/kg) = 1.035e-02
 Temperature ($^\circ\text{C}$) = 40.00
 Electrical balance (eq) = 8.165e-02
 Percent error, $100 \cdot (\text{Cat} - |\text{An}|) / (\text{Cat} + |\text{An}|)$ = 2.59
 Iterations = 15
 Gamma iterations = 4
 Osmotic coefficient = 0.96756
 Density of water = 0.99221
 Total H = 1.110219e+02
 Total O = 5.563721e+01

-----Distribution of species-----

Species	MacInnes		MacInnes		mole V Gamma	cm \geq /mol
	Molality	Activity	Log Molality	Log Activity		
OH-	5.448e-07	2.311e-07	-6.264	-6.636	-0.372	-0.52
H+	1.112e-07	1.202e-07	-6.954	-6.920	0.034	0.00
H2O	5.551e+01	9.489e-01	1.744	-0.023	0.000	18.16
C(4)	1.035e-02					
HCO3-	9.428e-03	4.204e-03	-2.026	-2.376	-0.351	29.27
CO2	7.900e-04	1.031e-03	-3.102	-2.987	0.116	35.16
MgCO3	7.400e-05	7.400e-05	-4.131	-4.131	0.000	-17.10
CO3-2	6.081e-05	2.049e-06	-4.216	-5.688	-1.472	2.86

Ca	5.684e-03						
Ca+2	5.684e-03	1.534e-03	-2.245	-2.814	-0.569	-15.75	
Cl	1.477e+00						
Cl-	1.477e+00	8.628e-01	0.169	-0.064	-0.234	19.51	
Mg	1.154e-01						
Mg+2	1.154e-01	3.420e-02	-0.938	-1.466	-0.528	-20.13	
MgCO3	7.400e-05	7.400e-05	-4.131	-4.131	0.000	-17.10	
MgOH+	1.432e-06	1.457e-06	-5.844	-5.836	0.008	(0)	
Na	1.377e+00						
Na+	1.377e+00	1.044e+00	0.139	0.019	-0.120	0.49	
S(6)	2.518e-02						
SO4-2	2.518e-02	9.514e-04	-1.599	-3.022	-1.423	21.61	
HSO4-	2.988e-08	1.671e-08	-7.525	-7.777	-0.253	42.19	

-----Saturation indices-----

Phase	SI**	log IAP	log K(313 K, 1 atm)	
Anhydrite	-1.38	-5.84	-4.45	CaSO4
Aragonite	-0.17	-8.50	-8.33	CaCO3
Artinite	-3.23	15.34	18.57	Mg2CO3(OH)2:3H2O
Bischofite	-6.14	-1.73	4.41	MgCl2:6H2O
Bloedite	-5.22	-7.56	-2.35	Na2Mg(SO4)2:4H2O
Brucite	-4.03	-14.74	-10.71	Mg(OH)2
Burkeite	-10.85	-11.62	-0.77	Na6CO3(SO4)2
Calcite	0.15	-8.50	-8.65	CaCO3
CO2(g)	-1.36	-2.99	-1.63	CO2
Dolomite	1.76	-15.66	-17.41	CaMg(CO3)2
Epsomite	-2.90	-4.65	-1.75	MgSO4:7H2O
Gaylussite	-4.85	-14.27	-9.42	CaNa2(CO3)2:5H2O
Glauberite	-3.30	-8.82	-5.52	Na2Ca(SO4)2
Gypsum	-1.25	-5.88	-4.63	CaSO4:2H2O
H2O(g)	-1.16	-0.02	1.14	H2O
Halite	-1.65	-0.05	1.61	NaCl
Hexahydrate	-3.01	-4.62	-1.61	MgSO4:6H2O
Huntite	2.28	10.96	8.69	CaMg3(CO3)4
Kieserite	-3.96	-4.51	-0.55	MgSO4:H2O
Labile_S	-6.18	-11.85	-5.67	Na4Ca(SO4)3:2H2O
Leonhardite	-3.69	-4.58	-0.89	MgSO4:4H2O
Magnesite	0.73	-7.15	-7.89	MgCO3
MgCl2_2H2O	-15.01	-1.64	13.37	MgCl2:2H2O
MgCl2_4H2O	-8.36	-1.69	6.68	MgCl2:4H2O
Mirabilite	-2.54	-3.21	-0.67	Na2SO4:10H2O
Nahcolite	-1.85	-12.59	-10.74	NaHCO3
Natron	-5.05	-5.88	-0.82	Na2CO3:10H2O
Nesquehonite	-2.06	-7.22	-5.17	MgCO3:3H2O

Pentahydrate	-3.32	-4.60	-1.28	MgSO4:5H2O
Pirssonite	-4.96	-14.20	-9.23	Na2Ca(CO3)2:2H2O
Portlandite	-10.90	-16.09	-5.19	Ca(OH)2
Thenardite	-2.61	-2.98	-0.37	Na2SO4
Trona	-6.90	-18.29	-11.38	Na3H(CO3)2:2H2O

**For a gas, SI = log10(fugacity). Fugacity = pressure * phi / 1 atm.
 For ideal gases, phi = 1.

 End of simulation.

 Reading input data for simulation 2.

 End of Run after 0.008667 Seconds.

 Reading data base.

SOLUTION_MASTER_SPECIES
 SOLUTION_SPECIES
 PHASES
 PITZER
 EXCHANGE_MASTER_SPECIES
 EXCHANGE_SPECIES
 SURFACE_MASTER_SPECIES
 SURFACE_SPECIES
 END

 Reading input data for simulation 1.

TITLE Bryan Rodriguez's Solution - Dengying Formation (summer 2019)
 SOLUTION 1

pH	6.91
Temp	40
	Units mg/L
Ca	167
Mg	2227
Na	29034
Cl	48044

S(6) 2219
Alkalinity 532 as CO3
SAVE SOLUTION 1

TITLE

Bryan Rodriguez's Solution - Dengying Formation (summer 2019)

Beginning of initial solution calculations.

Initial solution 1.

-----Solution composition-----

Elements	Molality	Moles
Alkalinity	9.659e-03	9.659e-03
Ca	4.540e-03	4.540e-03
Cl	1.477e+00	1.477e+00
Mg	9.984e-02	9.984e-02
Na	1.376e+00	1.376e+00
S(6)	2.517e-02	2.517e-02

-----Description of solution-----

pH = 6.910
pe = 4.000
Specific Conductance ($\mu\text{S}/\text{cm}$, 40°C) = 147174
Density (g/cm^3) = 1.05169
Volume (L) = 1.03607
Activity of water = 0.949
Ionic strength (mol/kgw) = 1.690e+00
Mass of water (kg) = 1.000e+00
Total carbon (mol/kg) = 1.036e-02
Total CO2 (mol/kg) = 1.036e-02
Temperature ($^\circ\text{C}$) = 40.00
Electrical balance (eq) = 4.825e-02
Percent error, $100 \cdot (\text{Cat} - |\text{An}|) / (\text{Cat} + |\text{An}|)$ = 1.55
Iterations = 14
Gamma iterations = 4
Osmotic coefficient = 0.96591
Density of water = 0.99221
Total H = 1.110219e+02

Total O = 5.563715e+01

-----Distribution of species-----

Species	MacInnes		MacInnes		mole V Gamma	cm ³ /mol
	Molality	Activity	Log Molality	Log Activity		
OH-	5.201e-07	2.259e-07	-6.284	-6.646	-0.362	-0.57
H+	1.145e-07	1.230e-07	-6.941	-6.910	0.031	0.00
H2O	5.551e+01	9.493e-01	1.744	-0.023	0.000	18.16
C(4)	1.036e-02					
HCO3-	9.418e-03	4.245e-03	-2.026	-2.372	-0.346	29.21
CO2	8.209e-04	1.065e-03	-3.086	-2.973	0.113	35.16
MgCO3	6.336e-05	6.336e-05	-4.198	-4.198	0.000	-17.10
CO3-2	5.638e-05	2.022e-06	-4.249	-5.694	-1.445	2.79
Ca	4.540e-03					
Ca+2	4.540e-03	1.229e-03	-2.343	-2.911	-0.568	-15.77
Cl	1.477e+00					
Cl-	1.477e+00	8.633e-01	0.169	-0.064	-0.233	19.50
Mg	9.984e-02					
Mg+2	9.977e-02	2.968e-02	-1.001	-1.528	-0.527	-20.15
MgCO3	6.336e-05	6.336e-05	-4.198	-4.198	0.000	-17.10
MgOH+	1.207e-06	1.236e-06	-5.918	-5.908	0.011	(0)
Na	1.376e+00					
Na+	1.376e+00	1.038e+00	0.139	0.016	-0.122	0.48
S(6)	2.517e-02					
SO4-2	2.517e-02	9.763e-04	-1.599	-3.010	-1.411	21.54
HSO4-	3.146e-08	1.754e-08	-7.502	-7.756	-0.254	42.18

-----Saturation indices-----

Phase	SI**	log IAP	log K(313 K, 1 atm)
Anhydrite	-1.47	-5.92	-4.45 CaSO4
Aragonite	-0.28	-8.60	-8.33 CaCO3
Artinite	-3.38	15.19	18.57 Mg2CO3(OH)2:3H2O
Bischofite	-6.20	-1.79	4.41 MgCl2:6H2O
Bloedite	-5.26	-7.61	-2.35 Na2Mg(SO4)2:4H2O
Brucite	-4.11	-14.82	-10.71 Mg(OH)2
Burkeite	-10.85	-11.62	-0.77 Na6CO3(SO4)2
Calcite	0.05	-8.60	-8.65 CaCO3
CO2(g)	-1.35	-2.97	-1.63 CO2
Dolomite	1.59	-15.83	-17.41 CaMg(CO3)2
Epsomite	-2.95	-4.70	-1.75 MgSO4:7H2O
Gaylussite	-4.96	-14.38	-9.42 CaNa2(CO3)2:5H2O

Glauberite	-3.38	-8.90	-5.52	Na ₂ Ca(SO ₄) ₂
Gypsum	-1.34	-5.97	-4.63	CaSO ₄ :2H ₂ O
H ₂ O(g)	-1.16	-0.02	1.14	H ₂ O
Halite	-1.65	-0.05	1.61	NaCl
Hexahydrate	-3.06	-4.67	-1.61	MgSO ₄ :6H ₂ O
Huntite	1.97	10.66	8.69	CaMg ₃ (CO ₃) ₄
Kieserite	-4.01	-4.56	-0.55	MgSO ₄ :H ₂ O
Labile_S	-6.25	-11.92	-5.67	Na ₄ Ca(SO ₄) ₃ :2H ₂ O
Leonhardite	-3.74	-4.63	-0.89	MgSO ₄ :4H ₂ O
Magnesite	0.66	-7.22	-7.89	MgCO ₃
MgCl ₂ _2H ₂ O	-15.07	-1.70	13.37	MgCl ₂ :2H ₂ O
MgCl ₂ _4H ₂ O	-8.42	-1.75	6.68	MgCl ₂ :4H ₂ O
Mirabilite	-2.54	-3.20	-0.67	Na ₂ SO ₄ :10H ₂ O
Nahcolite	-1.85	-12.59	-10.74	NaHCO ₃
Natron	-5.06	-5.89	-0.82	Na ₂ CO ₃ :10H ₂ O
Nesquehonite	-2.12	-7.29	-5.17	MgCO ₃ :3H ₂ O
Pentahydrate	-3.37	-4.65	-1.28	MgSO ₄ :5H ₂ O
Pirssonite	-5.08	-14.31	-9.23	Na ₂ Ca(CO ₃) ₂ :2H ₂ O
Portlandite	-11.01	-16.20	-5.19	Ca(OH) ₂
Thenardite	-2.61	-2.98	-0.37	Na ₂ SO ₄
Trona	-6.91	-18.30	-11.38	Na ₃ H(CO ₃) ₂ :2H ₂ O

**For a gas, SI = log₁₀(fugacity). Fugacity = pressure * phi / 1 atm.
For ideal gases, phi = 1.

End of simulation.

Reading input data for simulation 2.

End of Run after 0.0081 Seconds.

T = 15

Reading data base.

SOLUTION_MASTER_SPECIES
SOLUTION_SPECIES
PHASES
PITZER

EXCHANGE_MASTER_SPECIES
EXCHANGE_SPECIES
SURFACE_MASTER_SPECIES
SURFACE_SPECIES
END

Reading input data for simulation 1.

TITLE Bryan Rodriguez's Solution - Dengying Formation (summer 2019)
SOLUTION 1

pH	6.97
Temp	40
	Units mg/L
Ca	111
Mg	1785
Na	29034
Cl	48044
S(6)	2219
Alkalinity	521 as CO3

SAVE SOLUTION 1

TITLE

Bryan Rodriguez's Solution - Dengying Formation (summer 2019)

Beginning of initial solution calculations.

Initial solution 1.

-----Solution composition-----

Elements	Molality	Moles
Alkalinity	9.454e-03	9.454e-03
Ca	3.016e-03	3.016e-03
Cl	1.476e+00	1.476e+00
Mg	7.998e-02	7.998e-02
Na	1.375e+00	1.375e+00
S(6)	2.515e-02	2.515e-02

-----Description of solution-----

pH = 6.970
 pe = 4.000
 Specific Conductance ($\mu\text{S}/\text{cm}$, 40°C) = 146939
 Density (g/cm^3) = 1.05075
 Volume (L) = 1.03642
 Activity of water = 0.950
 Ionic strength (mol/kgw) = 1.646e+00
 Mass of water (kg) = 1.000e+00
 Total carbon (mol/kg) = 1.005e-02
 Total CO2 (mol/kg) = 1.005e-02
 Temperature ($^\circ\text{C}$) = 40.00
 Electrical balance (eq) = 5.776e-03
 Percent error, $100 \cdot (\text{Cat} - |\text{An}|) / (\text{Cat} + |\text{An}|)$ = 0.19
 Iterations = 14
 Gamma iterations = 4
 Osmotic coefficient = 0.96367
 Density of water = 0.99221
 Total H = 1.110217e+02
 Total O = 5.563627e+01

-----Distribution of species-----

Species	MacInnes		MacInnes		mole V Gamma	cm \geq /mol
	Molality	Activity	Log Molality	Log Activity		
OH-	5.792e-07	2.595e-07	-6.237	-6.586	-0.349	-0.64
H+	1.006e-07	1.072e-07	-6.997	-6.970	0.027	0.00
H2O	5.551e+01	9.498e-01	1.744	-0.022	0.000	18.16
C(4)	1.005e-02					
HCO3-	9.218e-03	4.213e-03	-2.035	-2.375	-0.340	29.13
CO2	7.149e-04	9.204e-04	-3.146	-3.036	0.110	35.16
CO3-2	5.924e-05	2.304e-06	-4.227	-5.638	-1.410	2.72
MgCO3	5.814e-05	5.814e-05	-4.236	-4.236	0.000	-17.10
Ca	3.016e-03					
Ca+2	3.016e-03	8.193e-04	-2.521	-3.087	-0.566	-15.79
Cl	1.476e+00					
Cl-	1.476e+00	8.639e-01	0.169	-0.064	-0.233	19.49
Mg	7.998e-02					
Mg+2	7.992e-02	2.389e-02	-1.097	-1.622	-0.524	-20.18
MgCO3	5.814e-05	5.814e-05	-4.236	-4.236	0.000	-17.10
MgOH+	1.106e-06	1.144e-06	-5.956	-5.942	0.015	(0)
Na	1.375e+00					
Na+	1.375e+00	1.030e+00	0.138	0.013	-0.126	0.47
S(6)	2.515e-02					
SO4-2	2.515e-02	1.010e-03	-1.599	-2.996	-1.396	21.47

HSO4- 2.845e-08 1.581e-08 -7.546 -7.801 -0.255 42.16

-----Saturation indices-----

Phase	SI**	log IAP	log K(313 K, 1 atm)
Anhydrite	-1.63	-6.08	-4.45 CaSO4
Aragonite	-0.39	-8.72	-8.33 CaCO3
Artinite	-3.39	15.18	18.57 Mg2CO3(OH)2:3H2O
Bischofite	-6.29	-1.88	4.41 MgCl2:6H2O
Bloedite	-5.33	-7.68	-2.35 Na2Mg(SO4)2:4H2O
Brucite	-4.08	-14.79	-10.71 Mg(OH)2
Burkeite	-10.78	-11.55	-0.77 Na6CO3(SO4)2
Calcite	-0.07	-8.72	-8.65 CaCO3
CO2(g)	-1.41	-3.04	-1.63 CO2
Dolomite	1.43	-15.98	-17.41 CaMg(CO3)2
Epsomite	-3.02	-4.77	-1.75 MgSO4:7H2O
Gaylussite	-5.03	-14.45	-9.42 CaNa2(CO3)2:5H2O
Glauberite	-3.54	-9.05	-5.52 Na2Ca(SO4)2
Gypsum	-1.50	-6.13	-4.63 CaSO4:2H2O
H2O(g)	-1.16	-0.02	1.14 H2O
Halite	-1.66	-0.05	1.61 NaCl
Hexahydrite	-3.14	-4.75	-1.61 MgSO4:6H2O
Huntite	1.74	10.43	8.69 CaMg3(CO3)4
Kieserite	-4.09	-4.64	-0.55 MgSO4:H2O
Labile_S	-6.39	-12.07	-5.67 Na4Ca(SO4)3:2H2O
Leonhardite	-3.82	-4.71	-0.89 MgSO4:4H2O
Magnesite	0.63	-7.26	-7.89 MgCO3
MgCl2_2H2O	-15.16	-1.79	13.37 MgCl2:2H2O
MgCl2_4H2O	-8.51	-1.84	6.68 MgCl2:4H2O
Mirabilite	-2.53	-3.19	-0.67 Na2SO4:10H2O
Nahcolite	-1.85	-12.59	-10.74 NaHCO3
Natron	-5.01	-5.84	-0.82 Na2CO3:10H2O
Nesquehonite	-2.16	-7.33	-5.17 MgCO3:3H2O
Pentahydrite	-3.44	-4.73	-1.28 MgSO4:5H2O
Pirssonite	-5.15	-14.38	-9.23 Na2Ca(CO3)2:2H2O
Portlandite	-11.07	-16.26	-5.19 Ca(OH)2
Thenardite	-2.60	-2.97	-0.37 Na2SO4
Trona	-6.87	-18.25	-11.38 Na3H(CO3)2:2H2O

**For a gas, SI = log10(fugacity). Fugacity = pressure * phi / 1 atm.
For ideal gases, phi = 1.

End of simulation.

Reading input data for simulation 2.

End of Run after 0.008946 Seconds.

Reading data base.

SOLUTION_MASTER_SPECIES
SOLUTION_SPECIES
PHASES
PITZER
EXCHANGE_MASTER_SPECIES
EXCHANGE_SPECIES
SURFACE_MASTER_SPECIES
SURFACE_SPECIES
END

Reading input data for simulation 1.

TITLE Bryan Rodriguez's Solution - Dengying Formation (summer 2019)
SOLUTION 1
pH 7.00
Temp 40
Units mg/L
Ca 189
Mg 2427
Na 29034
Cl 48044
S(6) 2219
Alkalinity 529 as CO3
SAVE SOLUTION 1

TITLE

Bryan Rodriguez's Solution - Dengying Formation (summer 2019)

Beginning of initial solution calculations.

Initial solution 1.

-----Solution composition-----

Elements	Molality	Moles
Alkalinity	9.607e-03	9.607e-03
Ca	5.139e-03	5.139e-03
Cl	1.477e+00	1.477e+00
Mg	1.088e-01	1.088e-01
Na	1.376e+00	1.376e+00
S(6)	2.517e-02	2.517e-02

-----Description of solution-----

pH = 7.000
 pe = 4.000
 Specific Conductance ($\mu\text{S}/\text{cm}$, 40°C) = 147272
 Density (g/cm^3) = 1.05211
 Volume (L) = 1.03590
 Activity of water = 0.949
 Ionic strength (mol/kgw) = 1.710e+00
 Mass of water (kg) = 1.000e+00
 Total carbon (mol/kg) = 1.010e-02
 Total CO2 (mol/kg) = 1.010e-02
 Temperature (°C) = 40.00
 Electrical balance (eq) = 6.745e-02
 Percent error, $100 \cdot (\text{Cat} - |\text{An}|) / (\text{Cat} + |\text{An}|)$ = 2.15
 Iterations = 15
 Gamma iterations = 4
 Osmotic coefficient = 0.96685
 Density of water = 0.99221
 Total H = 1.110217e+02
 Total O = 5.563658e+01

-----Distribution of species-----

Species	MacInnes		MacInnes		mole V Gamma	cm ³ /mol
	Molality	Activity	Log Molality	Log Activity		
OH-	6.485e-07	2.779e-07	-6.188	-6.556	-0.368	-0.54
H+	9.274e-08	1.000e-07	-7.033	-7.000	0.033	0.00
H2O	5.551e+01	9.490e-01	1.744	-0.023	0.000	18.16
C(4)	1.010e-02					

HCO3-	9.298e-03	4.164e-03	-2.032	-2.380	-0.349	29.25
CO2	6.525e-04	8.497e-04	-3.185	-3.071	0.115	35.16
MgCO3	8.317e-05	8.317e-05	-4.080	-4.080	0.000	-17.10
CO3-2	7.052e-05	2.440e-06	-4.152	-5.613	-1.461	2.83
Ca	5.139e-03					
Ca+2	5.139e-03	1.388e-03	-2.289	-2.857	-0.568	-15.75
Cl	1.477e+00					
Cl-	1.477e+00	8.630e-01	0.169	-0.064	-0.233	19.51
Mg	1.088e-01					
Mg+2	1.087e-01	3.227e-02	-0.964	-1.491	-0.528	-20.14
MgCO3	8.317e-05	8.317e-05	-4.080	-4.080	0.000	-17.10
MgOH+	1.621e-06	1.654e-06	-5.790	-5.781	0.009	(0)
Na	1.376e+00					
Na+	1.376e+00	1.041e+00	0.139	0.018	-0.121	0.49
S(6)	2.517e-02					
SO4-2	2.517e-02	9.620e-04	-1.599	-3.017	-1.418	21.58
HSO4-	2.516e-08	1.405e-08	-7.599	-7.852	-0.253	42.18

-----Saturation indices-----

Phase	SI**	log IAP	log K(313 K, 1 atm)	
Anhydrite	-1.42	-5.87	-4.45	CaSO4
Aragonite	-0.14	-8.47	-8.33	CaCO3
Artinite	-3.05	15.52	18.57	Mg2CO3(OH)2:3H2O
Bischofite	-6.16	-1.76	4.41	MgCl2:6H2O
Bloedite	-5.23	-7.58	-2.35	Na2Mg(SO4)2:4H2O
Brucite	-3.89	-14.60	-10.71	Mg(OH)2
Burkeite	-10.77	-11.54	-0.77	Na6CO3(SO4)2
Calcite	0.18	-8.47	-8.65	CaCO3
CO2(g)	-1.45	-3.07	-1.63	CO2
Dolomite	1.84	-15.57	-17.41	CaMg(CO3)2
Epsomite	-2.92	-4.67	-1.75	MgSO4:7H2O
Gaylussite	-4.74	-14.16	-9.42	CaNa2(CO3)2:5H2O
Glauberite	-3.34	-8.86	-5.52	Na2Ca(SO4)2
Gypsum	-1.29	-5.92	-4.63	CaSO4:2H2O
H2O(g)	-1.16	-0.02	1.14	H2O
Halite	-1.65	-0.05	1.61	NaCl
Hexahydrite	-3.03	-4.64	-1.61	MgSO4:6H2O
Huntite	2.46	11.15	8.69	CaMg3(CO3)4
Kieserite	-3.98	-4.53	-0.55	MgSO4:H2O
Labile_S	-6.21	-11.88	-5.67	Na4Ca(SO4)3:2H2O
Leonhardite	-3.71	-4.60	-0.89	MgSO4:4H2O
Magnesite	0.78	-7.10	-7.89	MgCO3
MgCl2_2H2O	-15.03	-1.66	13.37	MgCl2:2H2O
MgCl2_4H2O	-8.39	-1.71	6.68	MgCl2:4H2O

Mirabilite	-2.54	-3.21	-0.67	Na2SO4:10H2O
Nahcolite	-1.85	-12.59	-10.74	NaHCO3
Natron	-4.98	-5.80	-0.82	Na2CO3:10H2O
Nesquehonite	-2.00	-7.17	-5.17	MgCO3:3H2O
Pentahydrate	-3.34	-4.62	-1.28	MgSO4:5H2O
Pirssonite	-4.86	-14.09	-9.23	Na2Ca(CO3)2:2H2O
Portlandite	-10.78	-15.97	-5.19	Ca(OH)2
Thenardite	-2.61	-2.98	-0.37	Na2SO4
Trona	-6.83	-18.22	-11.38	Na3H(CO3)2:2H2O

**For a gas, SI = log10(fugacity). Fugacity = pressure * phi / 1 atm.
 For ideal gases, phi = 1.

 End of simulation.

 Reading input data for simulation 2.

 End of Run after 0.008063 Seconds.

 Reading data base.

SOLUTION_MASTER_SPECIES
 SOLUTION_SPECIES
 PHASES
 PITZER
 EXCHANGE_MASTER_SPECIES
 EXCHANGE_SPECIES
 SURFACE_MASTER_SPECIES
 SURFACE_SPECIES
 END

 Reading input data for simulation 1.

TITLE Bryan Rodriguez's Solution - Dengying Formation (summer 2019)
 SOLUTION 1
 pH 7.01
 Temp 40
 Units mg/L

Ca	124
Mg	1950
Na	29034
Cl	48044
S(6)	2219
Alkalinity	529 as CO3

SAVE SOLUTION 1

 TITLE

Bryan Rodriguez's Solution - Dengying Formation (summer 2019)

 Beginning of initial solution calculations.

Initial solution 1.

-----Solution composition-----

Elements	Molality	Moles
Alkalinity	9.601e-03	9.601e-03
Ca	3.370e-03	3.370e-03
Cl	1.476e+00	1.476e+00
Mg	8.739e-02	8.739e-02
Na	1.376e+00	1.376e+00
S(6)	2.516e-02	2.516e-02

-----Description of solution-----

pH = 7.010
 pe = 4.000
 Specific Conductance ($\mu\text{S}/\text{cm}$, 40°C) = 147024
 Density (g/cm^3) = 1.05109
 Volume (L) = 1.03630
 Activity of water = 0.950
 Ionic strength (mol/kgw) = 1.662e+00
 Mass of water (kg) = 1.000e+00
 Total carbon (mol/kg) = 1.012e-02
 Total CO2 (mol/kg) = 1.012e-02
 Temperature (°C) = 40.00
 Electrical balance (eq) = 2.113e-02
 Percent error, $100 \cdot (\text{Cat} - |\text{An}|) / (\text{Cat} + |\text{An}|)$ = 0.68
 Iterations = 14

Gamma iterations = 4
 Osmotic coefficient = 0.96449
 Density of water = 0.99221
 Total H = 1.110218e+02
 Total O = 5.563655e+01

-----Distribution of species-----

Species	MacInnes		MacInnes		mole V Gamma	cm ³ /mol
	Molality	Activity	Log Molality	Log Activity		
OH-	6.421e-07	2.845e-07	-6.192	-6.546	-0.354	-0.61
H+	9.150e-08	9.772e-08	-7.039	-7.010	0.029	0.00
H2O	5.551e+01	9.496e-01	1.744	-0.022	0.000	18.16
C(4)	1.012e-02					
HCO3-	9.325e-03	4.239e-03	-2.030	-2.373	-0.342	29.16
CO2	6.543e-04	8.447e-04	-3.184	-3.073	0.111	35.16
MgCO3	6.993e-05	6.993e-05	-4.155	-4.155	0.000	-17.10
CO3-2	6.733e-05	2.542e-06	-4.172	-5.595	-1.423	2.75
Ca	3.370e-03					
Ca+2	3.370e-03	9.141e-04	-2.472	-3.039	-0.567	-15.78
Cl	1.476e+00					
Cl-	1.476e+00	8.637e-01	0.169	-0.064	-0.233	19.49
Mg	8.739e-02					
Mg+2	8.732e-02	2.605e-02	-1.059	-1.584	-0.525	-20.17
MgCO3	6.993e-05	6.993e-05	-4.155	-4.155	0.000	-17.10
MgOH+	1.326e-06	1.367e-06	-5.877	-5.864	0.013	(0)
Na	1.376e+00					
Na+	1.376e+00	1.033e+00	0.138	0.014	-0.124	0.47
S(6)	2.516e-02					
SO4-2	2.516e-02	9.978e-04	-1.599	-3.001	-1.402	21.50
HSO4-	2.560e-08	1.424e-08	-7.592	-7.846	-0.255	42.17

-----Saturation indices-----

Phase	SI**	log IAP	log K(313 K, 1 atm)	
Anhydrite	-1.59	-6.04	-4.45	CaSO4
Aragonite	-0.30	-8.63	-8.33	CaCO3
Artinite	-3.19	15.38	18.57	Mg2CO3(OH)2:3H2O
Bischofite	-6.25	-1.85	4.41	MgCl2:6H2O
Bloedite	-5.30	-7.65	-2.35	Na2Mg(SO4)2:4H2O
Brucite	-3.97	-14.68	-10.71	Mg(OH)2
Burkeite	-10.74	-11.51	-0.77	Na6CO3(SO4)2
Calcite	0.02	-8.63	-8.65	CaCO3

CO2(g)	-1.45	-3.07	-1.63	CO2
Dolomite	1.60	-15.81	-17.41	CaMg(CO3)2
Epsomite	-2.99	-4.74	-1.75	MgSO4:7H2O
Gaylussite	-4.89	-14.31	-9.42	CaNa2(CO3)2:5H2O
Glauberite	-3.50	-9.01	-5.52	Na2Ca(SO4)2
Gypsum	-1.46	-6.08	-4.63	CaSO4:2H2O
H2O(g)	-1.16	-0.02	1.14	H2O
Halite	-1.66	-0.05	1.61	NaCl
Hexahydrate	-3.11	-4.72	-1.61	MgSO4:6H2O
Huntite	2.07	10.76	8.69	CaMg3(CO3)4
Kieserite	-4.06	-4.61	-0.55	MgSO4:H2O
Labile_S	-6.36	-12.03	-5.67	Na4Ca(SO4)3:2H2O
Leonhardite	-3.79	-4.67	-0.89	MgSO4:4H2O
Magnesite	0.71	-7.18	-7.89	MgCO3
MgCl2_2H2O	-15.12	-1.76	13.37	MgCl2:2H2O
MgCl2_4H2O	-8.48	-1.80	6.68	MgCl2:4H2O
Mirabilite	-2.53	-3.20	-0.67	Na2SO4:10H2O
Nahcolite	-1.85	-12.59	-10.74	NaHCO3
Natron	-4.97	-5.79	-0.82	Na2CO3:10H2O
Nesquehonite	-2.08	-7.25	-5.17	MgCO3:3H2O
Pentahydrate	-3.41	-4.70	-1.28	MgSO4:5H2O
Pirssonite	-5.01	-14.25	-9.23	Na2Ca(CO3)2:2H2O
Portlandite	-10.94	-16.13	-5.19	Ca(OH)2
Thenardite	-2.60	-2.97	-0.37	Na2SO4
Trona	-6.82	-18.20	-11.38	Na3H(CO3)2:2H2O

**For a gas, SI = log10(fugacity). Fugacity = pressure * phi / 1 atm.
For ideal gases, phi = 1.

End of simulation.

Reading input data for simulation 2.

End of Run after 0.008383 Seconds.

Model ESW** 93-day solution model:

TITLE Bryan Rodriguez's Solution - Dengying Formation (summer 2019)

#This fluid recipe is will modeled the aqueous conditions during the Late Neoproterozoic (Ediacaran) seawater.

#This is 6.07:1 Ca/Mg ratio (based on digital calculator). ESW**

#grams per liter:

#grams of $\text{CaCl}_2 \cdot 2\text{H}_2\text{O}$ -> 1 gram
#grams of $\text{MgCl}_2 \cdot 6\text{H}_2\text{O}$ -> 8.4 grams
#grams of NaCl -> 70 grams
#grams of Na_2CO_3 -> 1 gram
#grams of Na_2SO_4 -> 2.75 grams
#grams of Na_4SiO_3 -> 0.4 grams

#Alkalinity is ~9 mmol (566 mg/L ad CO_3 ; using calculator), which was done by adding 1 gram of NaCO_3 .

#Horita et al. 2002. *Geochimica et Cosmochimica Acta* (Mg:Ca ratios and Sulfate conc.). S(6) is the sulfur concentration in late neoproterozoic seawater, which is 23.1 mmol.

#Meng et al. 2010. *Precambrian Research* (Temperatures).

#Bongtonali et al. 2010. and Paul et al., 2016 *Sedimentology* (pH values from modern microbial mats and modern seawater).

#Salinity is slightly higher than modern normal seawater. Modern seawater is 3.5 wt % whereas this solution is 7.9 wt % (based on digital calculator).

#Ionic Strength, based on digital calculator, is ~1.35

#Dissolved silica is present, as SiO_3 . Here, is Si.

Reading data base.

SOLUTION_MASTER_SPECIES
SOLUTION_SPECIES
PHASES
PITZER

EXCHANGE_MASTER_SPECIES
EXCHANGE_SPECIES
SURFACE_MASTER_SPECIES
SURFACE_SPECIES
END

Reading input data for simulation 1.

TITLE Bryan Rodriguez's Solution - Dengying Formation (summer 2019)
SOLUTION 1

pH	8.5
Temp	40
	Units mg/L
Ca	273
Mg	1004
Na	29230
Cl	45874
S(6)	2219
Si	61
Alkalinity	566 as CO3

SAVE SOLUTION 1

TITLE

Bryan Rodriguez's Solution - Dengying Formation (summer 2019)

Beginning of initial solution calculations.

Initial solution 1.

-----Solution composition-----

Elements	Molality	Moles
Alkalinity	1.024e-02	1.024e-02
Ca	7.397e-03	7.397e-03
Cl	1.405e+00	1.405e+00
Mg	4.486e-02	4.486e-02
Na	1.381e+00	1.381e+00
S(6)	2.509e-02	2.509e-02
Si	1.103e-03	1.103e-03

-----Description of solution-----

pH = 8.500
 pe = 4.000
 Specific Conductance ($\mu\text{S}/\text{cm}$, 40°C) = 143308
 Density (g/cm^3) = 1.04869
 Volume (L) = 1.03554
 Activity of water = 0.952
 Ionic strength (mol/kgw) = 1.552e+00
 Mass of water (kg) = 1.000e+00
 Total carbon (mol/kg) = 8.103e-03
 Total CO2 (mol/kg) = 8.103e-03
 Temperature ($^\circ\text{C}$) = 40.00
 Electrical balance (eq) = 1.966e-02
 Percent error, $100 \cdot (\text{Cat} - |\text{An}|) / (\text{Cat} + |\text{An}|)$ = 0.67
 Iterations = 16
 Gamma iterations = 4
 Osmotic coefficient = 0.95764
 Density of water = 0.99221
 Total H = 1.110229e+02
 Total O = 5.563531e+01

-----Distribution of species-----

Species	MacInnes		MacInnes		mole V Gamma	cm \geq /mol
	Molality	Activity	Log Molality	Log Activity		
OH-	1.867e-05	8.812e-06	-4.729	-5.055	-0.326	-0.78
H+	3.056e-09	3.162e-09	-8.515	-8.500	0.015	0.00
H2O	5.551e+01	9.517e-01	1.744	-0.022	0.000	18.16
C(4)	8.103e-03					
HCO3-	6.189e-03	2.910e-03	-2.208	-2.536	-0.328	28.96
CO3-2	1.179e-03	5.392e-05	-2.929	-4.268	-1.340	2.55
MgCO3	7.200e-04	7.200e-04	-3.143	-3.143	0.000	-17.10
CO2	1.469e-05	1.872e-05	-4.833	-4.728	0.105	35.16
Ca	7.397e-03					
Ca+2	7.397e-03	1.928e-03	-2.131	-2.715	-0.584	-15.85
Cl	1.405e+00					
Cl-	1.405e+00	8.253e-01	0.148	-0.083	-0.231	19.46
Mg	4.486e-02					
Mg+2	4.412e-02	1.264e-02	-1.355	-1.898	-0.543	-20.23
MgCO3	7.200e-04	7.200e-04	-3.143	-3.143	0.000	-17.10
MgOH+	1.978e-05	2.055e-05	-4.704	-4.687	0.017	(0)
Na	1.381e+00					
Na+	1.381e+00	1.021e+00	0.140	0.009	-0.131	0.43

S(6)	2.509e-02						
SO4-2	2.509e-02	1.087e-03	-1.601	-2.964	-1.363	21.29	
HSO4-	9.043e-10	5.018e-10	-9.044	-9.299	-0.256	42.13	
Si	1.103e-03						
H4SiO4	8.854e-04	1.038e-03	-3.053	-2.984	0.069	51.03	
H3SiO4-	2.169e-04	7.777e-05	-3.664	-4.109	-0.445	29.46	
H2SiO4-2	2.553e-07	4.088e-09	-6.593	-8.388	-1.795	(0)	

-----Saturation indices-----

Phase	SI**	log IAP	log K(313 K, 1 atm)	
Akermanite	-5.08	37.73	42.80	Ca ₂ MgSi ₂ O ₇
Anhydrite	-1.22	-5.68	-4.45	CaSO ₄
Anthophyllite	19.27	82.01	62.75	Mg ₇ Si ₈ O ₂₂ (OH) ₂
Antigorite	174.24	623.20	448.96	Mg ₄₈ Si ₃₄ O ₈₅ (OH) ₆₂
Aragonite	1.35	-6.98	-8.33	CaCO ₃
Artinite	0.49	19.06	18.57	Mg ₂ CO ₃ (OH) ₂ :3H ₂ O
Bischofite	-6.60	-2.19	4.41	MgCl ₂ :6H ₂ O
Bloedite	-5.55	-7.89	-2.35	Na ₂ Mg(SO ₄) ₂ :4H ₂ O
Brucite	-1.30	-12.01	-10.71	Mg(OH) ₂
Burkeite	-9.37	-10.14	-0.77	Na ₆ CO ₃ (SO ₄) ₂
Calcite	1.67	-6.98	-8.65	CaCO ₃
Chalcedony	0.44	-2.94	-3.38	SiO ₂
Chrysotile	8.89	39.32	30.43	Mg ₃ Si ₂ O ₅ (OH) ₄
CO ₂ (g)	-3.10	-4.73	-1.63	CO ₂
Diopside	3.63	23.46	19.84	CaMgSi ₂ O ₆
Dolomite	4.26	-13.15	-17.41	CaMg(CO ₃) ₂
Enstatite	1.51	12.14	10.63	MgSiO ₃
Epsomite	-3.26	-5.01	-1.75	MgSO ₄ :7H ₂ O
Forsterite	1.09	27.22	26.13	Mg ₂ SiO ₄
Gaylussite	-1.92	-11.34	-9.42	CaNa ₂ (CO ₃) ₂ :5H ₂ O
Glauberite	-3.11	-8.63	-5.52	Na ₂ Ca(SO ₄) ₂
Gypsum	-1.09	-5.72	-4.63	CaSO ₄ :2H ₂ O
H ₂ O(g)	-1.16	-0.02	1.14	H ₂ O
Halite	-1.68	-0.07	1.61	NaCl
Hexahydrite	-3.38	-4.99	-1.61	MgSO ₄ :6H ₂ O
Huntite	6.76	15.45	8.69	CaMg ₃ (CO ₃) ₄
Kieserite	-4.33	-4.88	-0.55	MgSO ₄ :H ₂ O
Labile_S	-5.94	-11.61	-5.67	Na ₄ Ca(SO ₄) ₃ :2H ₂ O
Leonhardite	-4.06	-4.95	-0.89	MgSO ₄ :4H ₂ O
Magnesite	1.72	-6.17	-7.89	MgCO ₃
MgCl ₂ _2H ₂ O	-15.48	-2.11	13.37	MgCl ₂ :2H ₂ O
MgCl ₂ _4H ₂ O	-8.83	-2.15	6.68	MgCl ₂ :4H ₂ O
Mirabilite	-2.49	-3.16	-0.67	Na ₂ SO ₄ :10H ₂ O
Nahcolite	-2.02	-12.76	-10.74	NaHCO ₃

Natron	-3.64	-4.47	-0.82	Na ₂ CO ₃ :10H ₂ O
Nesquehonite	-1.06	-6.23	-5.17	MgCO ₃ :3H ₂ O
Pentahydrate	-3.68	-4.97	-1.28	MgSO ₄ :5H ₂ O
Pirssonite	-2.04	-11.28	-9.23	Na ₂ Ca(CO ₃) ₂ :2H ₂ O
Portlandite	-7.63	-12.82	-5.19	Ca(OH) ₂
Quartz	0.83	-2.94	-3.77	SiO ₂
Sepiolite	5.88	21.26	15.38	Mg ₂ Si ₃ O ₇ .5OH:3H ₂ O
Sepiolite(d)	2.60	21.26	18.66	Mg ₂ Si ₃ O ₇ .5OH:3H ₂ O
SiO ₂ (a)	-0.40	-2.94	-2.54	SiO ₂
Talc	13.68	33.46	19.77	Mg ₃ Si ₄ O ₁₀ (OH) ₂
Thenardite	-2.57	-2.95	-0.37	Na ₂ SO ₄
Trona	-5.67	-17.05	-11.38	Na ₃ H(CO ₃) ₂ :2H ₂ O

**For a gas, SI = log₁₀(fugacity). Fugacity = pressure * phi / 1 atm.
For ideal gases, phi = 1.

End of simulation.

Reading input data for simulation 2.

End of Run after 0.009596 Seconds.

ESW** solution model (control and experimental for 93 days):

Reading data base.

 SOLUTION_MASTER_SPECIES
 SOLUTION_SPECIES
 PHASES
 PITZER
 EXCHANGE_MASTER_SPECIES
 EXCHANGE_SPECIES
 SURFACE_MASTER_SPECIES
 SURFACE_SPECIES
 END

Reading input data for simulation 1.

TITLE Bryan Rodriguez's Solution - Dengying Formation (summer 2019)
#This fluid recipe is will modeled the aqueous conditions during the Late Neoproterozoic (Ediacaran) seawater over time by using the experimental data from ICP-OES (Ca & Mg concentrations in ppm). SW61

SW61-Before (T=0)

SOLUTION 1

pH	8.47
Temp	40
	Units mg/L
Ca	66
Mg	995
Na	28930
Cl	45874
S(6)	2219
Si	61
Alkalinity	634 as CO3

SAVE SOLUTION 1

SW61-2 weeks cc (T=14)

SOLUTION 2

pH	8.01
Temp	40
	Units mg/L
Ca	33
Mg	1026
Na	28930
Cl	45874
S(6)	2219
Si	61
Alkalinity	522 as CO3

SAVE SOLUTION 2

SW61-2 weeks sp1 (T=14)

SOLUTION 3

pH	8.08
Temp	40
	Units mg/L
Ca	35
Mg	999
Na	28930
Cl	45874
S(6)	2219
Si	61

Alkalinity 535 as CO3
SAVE SOLUTION 3

SW61-2 weeks sp2 (T=14)

SOLUTION 4

pH	8.11
Temp	40
	Units mg/L
Ca	35
Mg	1072
Na	28930
Cl	45874
S(6)	2219
Si	61
Alkalinity	540 as CO3

SAVE SOLUTION 4

SW61-3 months cc (T=93)

SOLUTION 5

pH	8.05
Temp	40
	Units mg/L
Ca	36
Mg	931
Na	28930
Cl	45874
S(6)	2219
Si	61
Alkalinity	517 as CO3

SAVE SOLUTION 5

SW61-3 months sp1 (T=93)

SOLUTION 6

pH	7.98
Temp	40
	Units mg/L
Ca	37
Mg	961
Na	28930
Cl	45874
S(6)	2219
Si	61
Alkalinity	522 as CO3

SAVE SOLUTION 6

SW61-3 months sp2 (T=93)

SOLUTION 7

pH	7.05
Temp	40
	Units mg/L
Ca	38
Mg	964
Na	28930
Cl	45874
S(6)	2219
Si	61
Alkalinity	524 as CO3

SAVE SOLUTION 7

TITLE

Bryan Rodriguez's Solution - Dengying Formation (summer 2019)

Beginning of initial solution calculations.

Initial solution 1.

-----Solution composition-----

Elements	Molality	Moles
Alkalinity	1.147e-02	1.147e-02
Ca	1.788e-03	1.788e-03
Cl	1.405e+00	1.405e+00
Mg	4.444e-02	4.444e-02
Na	1.366e+00	1.366e+00
S(6)	2.507e-02	2.507e-02
Si	1.102e-03	1.102e-03

-----Description of solution-----

pH = 8.470
pe = 4.000
Specific Conductance ($\mu\text{S}/\text{cm}$, 40°C) = 142790
Density (g/cm^3) = 1.04809
Volume (L) = 1.03563
Activity of water = 0.952
Ionic strength (mol/kgw) = 1.533e+00

Mass of water (kg) = 1.000e+00
 Total carbon (mol/kg) = 9.225e-03
 Total CO2 (mol/kg) = 9.225e-03
 Temperature (°C) = 40.00
 Electrical balance (eq) = -7.759e-03
 Percent error, 100*(Cat-|An|)/(Cat+|An|) = -0.27
 Iterations = 16
 Gamma iterations = 4
 Osmotic coefficient = 0.95665
 Density of water = 0.99221
 Total H = 1.110239e+02
 Total O = 5.563861e+01

-----Distribution of species-----

Species	MacInnes		MacInnes		mole V Gamma	cm ³ /mol
	Molality	Activity	Log Molality	Log Activity		
OH-	1.723e-05	8.227e-06	-4.764	-5.085	-0.321	-0.81
H+	3.288e-09	3.388e-09	-8.483	-8.470	0.013	0.00
H2O	5.551e+01	9.520e-01	1.744	-0.021	0.000	18.16
C(4)	9.225e-03					
HCO3-	7.183e-03	3.377e-03	-2.144	-2.471	-0.328	28.93
CO3-2	1.247e-03	5.841e-05	-2.904	-4.234	-1.329	2.51
MgCO3	7.763e-04	7.763e-04	-3.110	-3.110	0.000	-17.10
CO2	1.835e-05	2.328e-05	-4.736	-4.633	0.103	35.16
Ca	1.788e-03					
Ca+2	1.788e-03	4.690e-04	-2.748	-3.329	-0.581	-15.86
Cl	1.405e+00					
Cl-	1.405e+00	8.255e-01	0.148	-0.083	-0.231	19.45
Mg	4.444e-02					
Mg+2	4.364e-02	1.259e-02	-1.360	-1.900	-0.540	-20.24
MgCO3	7.763e-04	7.763e-04	-3.110	-3.110	0.000	-17.10
MgOH+	1.829e-05	1.909e-05	-4.738	-4.719	0.019	(0)
Na	1.366e+00					
Na+	1.366e+00	1.007e+00	0.135	0.003	-0.132	0.43
S(6)	2.507e-02					
SO4-2	2.507e-02	1.106e-03	-1.601	-2.956	-1.356	21.26
HSO4-	9.858e-10	5.472e-10	-9.006	-9.262	-0.256	42.13
Si	1.102e-03					
H4SiO4	8.995e-04	1.050e-03	-3.046	-2.979	0.067	51.03
H3SiO4-	2.024e-04	7.341e-05	-3.694	-4.134	-0.440	29.46
H2SiO4-2	2.186e-07	3.601e-09	-6.660	-8.444	-1.783	(0)

-----Saturation indices-----

Phase	SI**	log IAP	log K(313 K, 1 atm)	
Akermanite	-6.48	36.33	42.80	Ca ₂ MgSi ₂ O ₇
Anhydrite	-1.83	-6.29	-4.45	CaSO ₄
Anthophyllite	18.87	81.62	62.75	Mg ₇ Si ₈ O ₂₂ (OH) ₂
Antigorite	171.43	620.39	448.96	Mg ₄₈ Si ₃₄ O ₈₅ (OH) ₆₂
Aragonite	0.77	-7.56	-8.33	CaCO ₃
Artinite	0.46	19.03	18.57	Mg ₂ CO ₃ (OH) ₂ :3H ₂ O
Bischofite	-6.60	-2.19	4.41	MgCl ₂ :6H ₂ O
Bloedite	-5.55	-7.89	-2.35	Na ₂ Mg(SO ₄) ₂ :4H ₂ O
Brucite	-1.36	-12.07	-10.71	Mg(OH) ₂
Burkeite	-9.36	-10.13	-0.77	Na ₆ CO ₃ (SO ₄) ₂
Calcite	1.09	-7.56	-8.65	CaCO ₃
Chalcedony	0.45	-2.94	-3.38	SiO ₂
Chrysotile	8.71	39.14	30.43	Mg ₃ Si ₂ O ₅ (OH) ₄
CO ₂ (g)	-3.01	-4.63	-1.63	CO ₂
Diopside	2.90	22.74	19.84	CaMgSi ₂ O ₆
Dolomite	3.72	-13.70	-17.41	CaMg(CO ₃) ₂
Enstatite	1.45	12.08	10.63	MgSiO ₃
Epsomite	-3.26	-5.01	-1.75	MgSO ₄ :7H ₂ O
Forsterite	0.97	27.10	26.13	Mg ₂ SiO ₄
Gaylussite	-2.48	-11.90	-9.42	CaNa ₂ (CO ₃) ₂ :5H ₂ O
Glauberite	-3.72	-9.24	-5.52	Na ₂ Ca(SO ₄) ₂
Gypsum	-1.70	-6.33	-4.63	CaSO ₄ :2H ₂ O
H ₂ O(g)	-1.16	-0.02	1.14	H ₂ O
Halite	-1.69	-0.08	1.61	NaCl
Hexahydrate	-3.37	-4.98	-1.61	MgSO ₄ :6H ₂ O
Huntite	6.28	14.97	8.69	CaMg ₃ (CO ₃) ₄
Kieserite	-4.33	-4.88	-0.55	MgSO ₄ :H ₂ O
Labile_S	-6.56	-12.23	-5.67	Na ₄ Ca(SO ₄) ₃ :2H ₂ O
Leonhardite	-4.05	-4.94	-0.89	MgSO ₄ :4H ₂ O
Magnesite	1.75	-6.13	-7.89	MgCO ₃
MgCl ₂ _2H ₂ O	-15.48	-2.11	13.37	MgCl ₂ :2H ₂ O
MgCl ₂ _4H ₂ O	-8.83	-2.15	6.68	MgCl ₂ :4H ₂ O
Mirabilite	-2.50	-3.16	-0.67	Na ₂ SO ₄ :10H ₂ O
Nahcolite	-1.96	-12.70	-10.74	NaHCO ₃
Natron	-3.62	-4.44	-0.82	Na ₂ CO ₃ :10H ₂ O
Nesquehonite	-1.03	-6.20	-5.17	MgCO ₃ :3H ₂ O
Pentahydrate	-3.68	-4.96	-1.28	MgSO ₄ :5H ₂ O
Pirssonite	-2.60	-11.83	-9.23	Na ₂ Ca(CO ₃) ₂ :2H ₂ O
Portlandite	-8.31	-13.50	-5.19	Ca(OH) ₂
Quartz	0.83	-2.94	-3.77	SiO ₂
Sepiolite	5.77	21.15	15.38	Mg ₂ Si ₃ O ₇ .5OH:3H ₂ O
Sepiolite(d)	2.49	21.15	18.66	Mg ₂ Si ₃ O ₇ .5OH:3H ₂ O
SiO ₂ (a)	-0.40	-2.94	-2.54	SiO ₂

Talc	13.52	33.29	19.77	Mg ₃ Si ₄ O ₁₀ (OH) ₂
Thenardite	-2.58	-2.95	-0.37	Na ₂ SO ₄
Trona	-5.59	-16.97	-11.38	Na ₃ H(CO ₃) ₂ ·2H ₂ O

**For a gas, SI = log₁₀(fugacity). Fugacity = pressure * phi / 1 atm.
For ideal gases, phi = 1.

Initial solution 2.

-----Solution composition-----

Elements	Molality	Moles
Alkalinity	9.441e-03	9.441e-03
Ca	8.937e-04	8.937e-04
Cl	1.404e+00	1.404e+00
Mg	4.582e-02	4.582e-02
Na	1.366e+00	1.366e+00
S(6)	2.507e-02	2.507e-02
Si	1.102e-03	1.102e-03

-----Description of solution-----

pH = 8.010
 pe = 4.000
 Specific Conductance (μS/cm, 40°C) = 142761
 Density (g/cm³) = 1.04804
 Volume (L) = 1.03563
 Activity of water = 0.952
 Ionic strength (mol/kgw) = 1.533e+00
 Mass of water (kg) = 1.000e+00
 Total carbon (mol/kg) = 8.631e-03
 Total CO₂ (mol/kg) = 8.631e-03
 Temperature (°C) = 40.00
 Electrical balance (eq) = -4.751e-03
 Percent error, 100*(Cat-|An|)/(Cat+|An|) = -0.16
 Iterations = 15 (31 overall)
 Gamma iterations = 4
 Osmotic coefficient = 0.95696
 Density of water = 0.99221
 Total H = 1.110246e+02
 Total O = 5.563676e+01

-----Distribution of species-----

MacInnes MacInnes

Species	MacInnes Molality	Log Activity	Log Molality	Log Activity	mole V Gamma	cm ³ /mol
OH-	5.980e-06	2.852e-06	-5.223	-5.545	-0.322	-0.81
H+	9.471e-09	9.772e-09	-8.024	-8.010	0.014	0.00
H2O	5.551e+01	9.520e-01	1.744	-0.021	0.000	18.16
C(4)	8.631e-03					
HCO3-	7.798e-03	3.659e-03	-2.108	-2.437	-0.329	28.93
CO3-2	4.704e-04	2.194e-05	-3.328	-4.659	-1.331	2.51
MgCO3	3.049e-04	3.049e-04	-3.516	-3.516	0.000	-17.10
CO2	5.731e-05	7.273e-05	-4.242	-4.138	0.104	35.16
Ca	8.937e-04					
Ca+2	8.937e-04	2.353e-04	-3.049	-3.628	-0.580	-15.86
Cl	1.404e+00					
Cl-	1.404e+00	8.254e-01	0.147	-0.083	-0.231	19.45
Mg	4.582e-02					
Mg+2	4.551e-02	1.316e-02	-1.342	-1.881	-0.539	-20.24
MgCO3	3.049e-04	3.049e-04	-3.516	-3.516	0.000	-17.10
MgOH+	6.623e-06	6.921e-06	-5.179	-5.160	0.019	(0)
Na	1.366e+00					
Na+	1.366e+00	1.007e+00	0.135	0.003	-0.132	0.43
S(6)	2.507e-02					
SO4-2	2.507e-02	1.105e-03	-1.601	-2.957	-1.356	21.26
HSO4-	2.839e-09	1.577e-09	-8.547	-8.802	-0.256	42.13
Si	1.102e-03					
H4SiO4	1.022e-03	1.193e-03	-2.991	-2.923	0.067	51.03
H3SiO4-	7.988e-05	2.893e-05	-4.098	-4.539	-0.441	29.46
H2SiO4-2	2.998e-08	4.922e-10	-7.523	-9.308	-1.785	(0)

-----Saturation indices-----

Phase	SI**	log IAP	log K(313 K, 1 atm)	
Akermanite	-9.71	33.10	42.80	Ca2MgSi2O7
Anhydrite	-2.13	-6.59	-4.45	CaSO4
Anthophyllite	13.01	75.76	62.75	Mg7Si8O22(OH)2
Antigorite	130.09	579.05	448.96	Mg48Si34O85(OH)62
Aragonite	0.04	-8.29	-8.33	CaCO3
Artinite	-0.84	17.72	18.57	Mg2CO3(OH)2:3H2O
Bischofite	-6.58	-2.18	4.41	MgCl2:6H2O
Bloedite	-5.53	-7.87	-2.35	Na2Mg(SO4)2:4H2O
Brucite	-2.26	-12.97	-10.71	Mg(OH)2
Burkeite	-9.78	-10.55	-0.77	Na6CO3(SO4)2
Calcite	0.36	-8.29	-8.65	CaCO3
Chalcedony	0.50	-2.88	-3.38	SiO2
Chrysotile	6.12	36.55	30.43	Mg3Si2O5(OH)4

CO2(g)	-2.51	-4.14	-1.63	CO2
Diopside	0.89	20.73	19.84	CaMgSi2O6
Dolomite	2.59	-14.83	-17.41	CaMg(CO3)2
Enstatite	0.60	11.24	10.63	MgSiO3
Epsomite	-3.24	-4.99	-1.75	MgSO4:7H2O
Forsterite	-0.78	25.35	26.13	Mg2SiO4
Gaylussite	-3.63	-13.05	-9.42	CaNa2(CO3)2:5H2O
Glauberite	-4.02	-9.54	-5.52	Na2Ca(SO4)2
Gypsum	-2.00	-6.63	-4.63	CaSO4:2H2O
H2O(g)	-1.16	-0.02	1.14	H2O
Halite	-1.69	-0.08	1.61	NaCl
Hexahydrate	-3.36	-4.97	-1.61	MgSO4:6H2O
Huntite	4.34	13.02	8.69	CaMg3(CO3)4
Kieserite	-4.31	-4.86	-0.55	MgSO4:H2O
Labile_S	-6.86	-12.53	-5.67	Na4Ca(SO4)3:2H2O
Leonhardite	-4.04	-4.92	-0.89	MgSO4:4H2O
Magnesite	1.35	-6.54	-7.89	MgCO3
MgCl2_2H2O	-15.46	-2.09	13.37	MgCl2:2H2O
MgCl2_4H2O	-8.81	-2.13	6.68	MgCl2:4H2O
Mirabilite	-2.50	-3.16	-0.67	Na2SO4:10H2O
Nahcolite	-1.92	-12.67	-10.74	NaHCO3
Natron	-4.04	-4.87	-0.82	Na2CO3:10H2O
Nesquehonite	-1.44	-6.60	-5.17	MgCO3:3H2O
Pentahydrate	-3.66	-4.94	-1.28	MgSO4:5H2O
Pirssonite	-3.75	-12.98	-9.23	Na2Ca(CO3)2:2H2O
Portlandite	-9.53	-14.72	-5.19	Ca(OH)2
Quartz	0.89	-2.88	-3.77	SiO2
Sepiolite	4.13	19.52	15.38	Mg2Si3O7.5OH:3H2O
Sepiolite(d)	0.86	19.52	18.66	Mg2Si3O7.5OH:3H2O
SiO2(a)	-0.34	-2.88	-2.54	SiO2
Talc	11.04	30.81	19.77	Mg3Si4O10(OH)2
Thenardite	-2.58	-2.95	-0.37	Na2SO4
Trona	-5.98	-17.36	-11.38	Na3H(CO3)2:2H2O

**For a gas, SI = log10(fugacity). Fugacity = pressure * phi / 1 atm.
For ideal gases, phi = 1.

Initial solution 3.

-----Solution composition-----

Elements	Molality	Moles
Alkalinity	9.676e-03	9.676e-03
Ca	9.478e-04	9.478e-04
Cl	1.404e+00	1.404e+00

Mg	4.461e-02	4.461e-02
Na	1.366e+00	1.366e+00
S(6)	2.507e-02	2.507e-02
Si	1.102e-03	1.102e-03

-----Description of solution-----

pH = 8.080
 pe = 4.000
 Specific Conductance ($\mu\text{S}/\text{cm}$, 40°C) = 142750
 Density (g/cm^3) = 1.04800
 Volume (L) = 1.03565
 Activity of water = 0.952
 Ionic strength (mol/kgw) = 1.531e+00
 Mass of water (kg) = 1.000e+00
 Total carbon (mol/kg) = 8.721e-03
 Total CO2 (mol/kg) = 8.721e-03
 Temperature ($^\circ\text{C}$) = 40.00
 Electrical balance (eq) = -7.289e-03
 Percent error, $100 \cdot (\text{Cat} - |\text{An}|) / (\text{Cat} + |\text{An}|)$ = -0.25
 Iterations = 15 (46 overall)
 Gamma iterations = 4
 Osmotic coefficient = 0.95680
 Density of water = 0.99221
 Total H = 1.110245e+02
 Total O = 5.563704e+01

-----Distribution of species-----

Species	MacInnes		MacInnes		mole V Gamma	cm \geq /mol
	MacInnes Molality	Log Activity	Log Molality	Log Activity		
OH-	7.014e-06	3.351e-06	-5.154	-5.475	-0.321	-0.81
H+	8.066e-09	8.318e-09	-8.093	-8.080	0.013	0.00
H2O	5.551e+01	9.521e-01	1.744	-0.021	0.000	18.16
C(4)	8.721e-03					
HCO3-	7.775e-03	3.653e-03	-2.109	-2.437	-0.328	28.93
CO3-2	5.490e-04	2.573e-05	-3.260	-4.590	-1.329	2.51
MgCO3	3.478e-04	3.478e-04	-3.459	-3.459	0.000	-17.10
CO2	4.871e-05	6.179e-05	-4.312	-4.209	0.103	35.16
Ca	9.478e-04					
Ca+2	9.478e-04	2.495e-04	-3.023	-3.603	-0.580	-15.86
Cl	1.404e+00					
Cl-	1.404e+00	8.255e-01	0.147	-0.083	-0.231	19.45
Mg	4.461e-02					

Mg+2	4.426e-02	1.280e-02	-1.354	-1.893	-0.539	-20.24
MgCO3	3.478e-04	3.478e-04	-3.459	-3.459	0.000	-17.10
MgOH+	7.565e-06	7.909e-06	-5.121	-5.102	0.019	(0)
Na	1.366e+00					
Na+	1.366e+00	1.007e+00	0.135	0.003	-0.132	0.43
S(6)	2.507e-02					
SO4-2	2.507e-02	1.107e-03	-1.601	-2.956	-1.355	21.25
HSO4-	2.422e-09	1.345e-09	-8.616	-8.871	-0.256	42.13
Si	1.102e-03					
H4SiO4	1.009e-03	1.178e-03	-2.996	-2.929	0.067	51.03
H3SiO4-	9.249e-05	3.355e-05	-4.034	-4.474	-0.440	29.46
H2SiO4-2	4.069e-08	6.706e-10	-7.391	-9.174	-1.783	(0)

-----Saturation indices-----

Phase	SI**	log IAP	log K(313 K, 1 atm)	
Akermanite	-9.26	33.54	42.80	Ca ₂ MgSi ₂ O ₇
Anhydrite	-2.10	-6.56	-4.45	CaSO ₄
Anthophyllite	13.86	76.61	62.75	Mg ₇ Si ₈ O ₂₂ (OH) ₂
Antigorite	136.04	585.00	448.96	Mg ₄₈ Si ₃₄ O ₈₅ (OH) ₆₂
Aragonite	0.14	-8.19	-8.33	CaCO ₃
Artinite	-0.66	17.91	18.57	Mg ₂ CO ₃ (OH) ₂ :3H ₂ O
Bischofite	-6.59	-2.19	4.41	MgCl ₂ :6H ₂ O
Bloedite	-5.54	-7.88	-2.35	Na ₂ Mg(SO ₄) ₂ :4H ₂ O
Brucite	-2.13	-12.84	-10.71	Mg(OH) ₂
Burkeite	-9.71	-10.48	-0.77	Na ₆ CO ₃ (SO ₄) ₂
Calcite	0.46	-8.19	-8.65	CaCO ₃
Chalcedony	0.50	-2.89	-3.38	SiO ₂
Chrysotile	6.49	36.92	30.43	Mg ₃ Si ₂ O ₅ (OH) ₄
CO ₂ (g)	-2.58	-4.21	-1.63	CO ₂
Diopside	1.17	21.01	19.84	CaMgSi ₂ O ₆
Dolomite	2.74	-14.67	-17.41	CaMg(CO ₃) ₂
Enstatite	0.73	11.36	10.63	MgSiO ₃
Epsomite	-3.25	-5.00	-1.75	MgSO ₄ :7H ₂ O
Forsterite	-0.53	25.61	26.13	Mg ₂ SiO ₄
Gaylussite	-3.46	-12.88	-9.42	CaNa ₂ (CO ₃) ₂ :5H ₂ O
Glauberite	-3.99	-9.51	-5.52	Na ₂ Ca(SO ₄) ₂
Gypsum	-1.97	-6.60	-4.63	CaSO ₄ :2H ₂ O
H ₂ O(g)	-1.16	-0.02	1.14	H ₂ O
Halite	-1.69	-0.08	1.61	NaCl
Hexahydrite	-3.37	-4.98	-1.61	MgSO ₄ :6H ₂ O
Huntite	4.60	13.29	8.69	CaMg ₃ (CO ₃) ₄
Kieserite	-4.32	-4.87	-0.55	MgSO ₄ :H ₂ O
Labile_S	-6.83	-12.50	-5.67	Na ₄ Ca(SO ₄) ₃ :2H ₂ O
Leonhardite	-4.05	-4.93	-0.89	MgSO ₄ :4H ₂ O

Magnesite	1.40	-6.48	-7.89	MgCO ₃
MgCl ₂ ·2H ₂ O	-15.47	-2.10	13.37	MgCl ₂ :2H ₂ O
MgCl ₂ ·4H ₂ O	-8.82	-2.14	6.68	MgCl ₂ :4H ₂ O
Mirabilite	-2.50	-3.16	-0.67	Na ₂ SO ₄ :10H ₂ O
Nahcolite	-1.92	-12.67	-10.74	NaHCO ₃
Natron	-3.97	-4.80	-0.82	Na ₂ CO ₃ :10H ₂ O
Nesquehonite	-1.38	-6.55	-5.17	MgCO ₃ :3H ₂ O
Pentahydrate	-3.67	-4.96	-1.28	MgSO ₄ :5H ₂ O
Pirssonite	-3.58	-12.82	-9.23	Na ₂ Ca(CO ₃) ₂ :2H ₂ O
Portlandite	-9.36	-14.55	-5.19	Ca(OH) ₂
Quartz	0.88	-2.89	-3.77	SiO ₂
Sepiolite	4.37	19.76	15.38	Mg ₂ Si ₃ O ₇ ·5OH:3H ₂ O
Sepiolite(d)	1.10	19.76	18.66	Mg ₂ Si ₃ O ₇ ·5OH:3H ₂ O
SiO ₂ (a)	-0.35	-2.89	-2.54	SiO ₂
Talc	11.40	31.17	19.77	Mg ₃ Si ₄ O ₁₀ (OH) ₂
Thenardite	-2.58	-2.95	-0.37	Na ₂ SO ₄
Trona	-5.91	-17.29	-11.38	Na ₃ H(CO ₃) ₂ :2H ₂ O

**For a gas, SI = log₁₀(fugacity). Fugacity = pressure * phi / 1 atm.
For ideal gases, phi = 1.

Initial solution 4.

-----Solution composition-----

Elements	Molality	Moles
Alkalinity	9.767e-03	9.767e-03
Ca	9.479e-04	9.479e-04
Cl	1.405e+00	1.405e+00
Mg	4.788e-02	4.788e-02
Na	1.366e+00	1.366e+00
S(6)	2.507e-02	2.507e-02
Si	1.102e-03	1.102e-03

-----Description of solution-----

pH = 8.110
pe = 4.000
Specific Conductance (μS/cm, 40°C) = 142790
Density (g/cm³) = 1.04814
Volume (L) = 1.03559
Activity of water = 0.952
Ionic strength (mol/kgw) = 1.537e+00
Mass of water (kg) = 1.000e+00
Total carbon (mol/kg) = 8.715e-03

Total CO2 (mol/kg) = 8.715e-03
 Temperature (°C) = 40.00
 Electrical balance (eq) = -8.599e-04
 Percent error, 100*(Cat-|An|)/(Cat+|An|) = -0.03
 Iterations = 16 (62 overall)
 Gamma iterations = 4
 Osmotic coefficient = 0.95715
 Density of water = 0.99221
 Total H = 1.110244e+02
 Total O = 5.563703e+01

-----Distribution of species-----

Species	MacInnes		MacInnes		Log Activity	mole V Gamma	cm ³ /mol
	Molality	Activity	Log Molality	Log Activity			
OH-	7.551e-06	3.591e-06	-5.122	-5.445	-0.323	-0.80	
H+	7.518e-09	7.762e-09	-8.124	-8.110	0.014	0.00	
H2O	5.551e+01	9.520e-01	1.744	-0.021	0.000	18.16	
C(4)	8.715e-03						
HCO3-	7.689e-03	3.602e-03	-2.114	-2.443	-0.329	28.94	
CO3-2	5.878e-04	2.719e-05	-3.231	-4.566	-1.335	2.52	
MgCO3	3.938e-04	3.938e-04	-3.405	-3.405	0.000	-17.10	
CO2	4.478e-05	5.688e-05	-4.349	-4.245	0.104	35.16	
Ca	9.479e-04						
Ca+2	9.479e-04	2.493e-04	-3.023	-3.603	-0.580	-15.85	
Cl	1.405e+00						
Cl-	1.405e+00	8.253e-01	0.148	-0.083	-0.231	19.45	
Mg	4.788e-02						
Mg+2	4.747e-02	1.371e-02	-1.324	-1.863	-0.539	-20.24	
MgCO3	3.938e-04	3.938e-04	-3.405	-3.405	0.000	-17.10	
MgOH+	8.699e-06	9.080e-06	-5.061	-5.042	0.019	(0)	
Na	1.366e+00						
Na+	1.366e+00	1.008e+00	0.135	0.003	-0.132	0.43	
S(6)	2.507e-02						
SO4-2	2.507e-02	1.101e-03	-1.601	-2.958	-1.358	21.27	
HSO4-	2.247e-09	1.248e-09	-8.648	-8.904	-0.255	42.13	
Si	1.102e-03						
H4SiO4	1.003e-03	1.172e-03	-2.999	-2.931	0.068	51.03	
H3SiO4-	9.905e-05	3.578e-05	-4.004	-4.446	-0.442	29.46	
H2SiO4-2	4.699e-08	7.662e-10	-7.328	-9.116	-1.788	(0)	

-----Saturation indices-----

Phase SI** log IAP log K(313 K, 1 atm)

Akermanite	-9.06	33.75	42.80	Ca ₂ MgSi ₂ O ₇
Anhydrite	-2.11	-6.56	-4.45	CaSO ₄
Anthophyllite	14.47	77.22	62.75	Mg ₇ Si ₈ O ₂₂ (OH) ₂
Antigorite	140.29	589.25	448.96	Mg ₄₈ Si ₃₄ O ₈₅ (OH) ₆₂
Aragonite	0.16	-8.17	-8.33	CaCO ₃
Artinite	-0.52	18.05	18.57	Mg ₂ CO ₃ (OH) ₂ :3H ₂ O
Bischofite	-6.56	-2.16	4.41	MgCl ₂ :6H ₂ O
Bloedite	-5.51	-7.86	-2.35	Na ₂ Mg(SO ₄) ₂ :4H ₂ O
Brucite	-2.04	-12.75	-10.71	Mg(OH) ₂
Burkeite	-9.69	-10.46	-0.77	Na ₆ CO ₃ (SO ₄) ₂
Calcite	0.48	-8.17	-8.65	CaCO ₃
Chalcedony	0.50	-2.89	-3.38	SiO ₂
Chrysotile	6.76	37.19	30.43	Mg ₃ Si ₂ O ₅ (OH) ₄
CO ₂ (g)	-2.62	-4.25	-1.63	CO ₂
Diopside	1.32	21.15	19.84	CaMgSi ₂ O ₆
Dolomite	2.82	-14.60	-17.41	CaMg(CO ₃) ₂
Enstatite	0.81	11.45	10.63	MgSiO ₃
Epsomite	-3.22	-4.97	-1.75	MgSO ₄ :7H ₂ O
Forsterite	-0.35	25.78	26.13	Mg ₂ SiO ₄
Gaylussite	-3.41	-12.83	-9.42	CaNa ₂ (CO ₃) ₂ :5H ₂ O
Glauberite	-4.00	-9.51	-5.52	Na ₂ Ca(SO ₄) ₂
Gypsum	-1.98	-6.60	-4.63	CaSO ₄ :2H ₂ O
H ₂ O(g)	-1.16	-0.02	1.14	H ₂ O
Halite	-1.69	-0.08	1.61	NaCl
Hexahydrite	-3.34	-4.95	-1.61	MgSO ₄ :6H ₂ O
Huntite	4.79	13.47	8.69	CaMg ₃ (CO ₃) ₄
Kieserite	-4.29	-4.84	-0.55	MgSO ₄ :H ₂ O
Labile_S	-6.84	-12.51	-5.67	Na ₄ Ca(SO ₄) ₃ :2H ₂ O
Leonhardite	-4.02	-4.91	-0.89	MgSO ₄ :4H ₂ O
Magnesite	1.46	-6.43	-7.89	MgCO ₃
MgCl ₂ _2H ₂ O	-15.44	-2.07	13.37	MgCl ₂ :2H ₂ O
MgCl ₂ _4H ₂ O	-8.79	-2.12	6.68	MgCl ₂ :4H ₂ O
Mirabilite	-2.50	-3.17	-0.67	Na ₂ SO ₄ :10H ₂ O
Nahcolite	-1.93	-12.67	-10.74	NaHCO ₃
Natron	-3.95	-4.77	-0.82	Na ₂ CO ₃ :10H ₂ O
Nesquehonite	-1.33	-6.49	-5.17	MgCO ₃ :3H ₂ O
Pentahydrite	-3.64	-4.93	-1.28	MgSO ₄ :5H ₂ O
Pirssonite	-3.54	-12.77	-9.23	Na ₂ Ca(CO ₃) ₂ :2H ₂ O
Portlandite	-9.30	-14.49	-5.19	Ca(OH) ₂
Quartz	0.88	-2.89	-3.77	SiO ₂
Sepiolite	4.55	19.93	15.38	Mg ₂ Si ₃ O ₇ .5OH:3H ₂ O
Sepiolite(d)	1.27	19.93	18.66	Mg ₂ Si ₃ O ₇ .5OH:3H ₂ O
SiO ₂ (a)	-0.35	-2.89	-2.54	SiO ₂
Talc	11.66	31.43	19.77	Mg ₃ Si ₄ O ₁₀ (OH) ₂
Thenardite	-2.58	-2.95	-0.37	Na ₂ SO ₄

Trona -5.89 -17.27 -11.38 Na₃H(CO₃)₂·2H₂O

**For a gas, SI = log₁₀(fugacity). Fugacity = pressure * phi / 1 atm.
For ideal gases, phi = 1.

Initial solution 5.

-----Solution composition-----

Elements	Molality	Moles
Alkalinity	9.350e-03	9.350e-03
Ca	9.748e-04	9.748e-04
Cl	1.404e+00	1.404e+00
Mg	4.157e-02	4.157e-02
Na	1.366e+00	1.366e+00
S(6)	2.507e-02	2.507e-02
Si	1.102e-03	1.102e-03

-----Description of solution-----

pH = 8.050
pe = 4.000
Specific Conductance (μS/cm, 40°C) = 142710
Density (g/cm³) = 1.04786
Volume (L) = 1.03570
Activity of water = 0.952
Ionic strength (mol/kgw) = 1.524e+00
Mass of water (kg) = 1.000e+00
Total carbon (mol/kg) = 8.503e-03
Total CO₂ (mol/kg) = 8.503e-03
Temperature (°C) = 40.00
Electrical balance (eq) = -1.298e-02
Percent error, 100*(Cat-|An|)/(Cat+|An|) = -0.45
Iterations = 15 (77 overall)
Gamma iterations = 4
Osmotic coefficient = 0.95650
Density of water = 0.99221
Total H = 1.110244e+02
Total O = 5.563637e+01

-----Distribution of species-----

Species	MacInnes		MacInnes		mole V Gamma	cm ³ /mol
	Molality	Activity	Log Molality	Log Activity		

OH-	6.517e-06	3.128e-06	-5.186	-5.505	-0.319	-0.82
H+	8.652e-09	8.913e-09	-8.063	-8.050	0.013	0.00
H2O	5.551e+01	9.521e-01	1.744	-0.021	0.000	18.16
C(4)	8.503e-03					
HCO3-	7.653e-03	3.604e-03	-2.116	-2.443	-0.327	28.91
CO3-2	4.995e-04	2.370e-05	-3.301	-4.625	-1.324	2.50
MgCO3	2.989e-04	2.989e-04	-3.524	-3.524	0.000	-17.10
CO2	5.155e-05	6.533e-05	-4.288	-4.185	0.103	35.16
Ca	9.748e-04					
Ca+2	9.748e-04	2.568e-04	-3.011	-3.590	-0.579	-15.86
Cl	1.404e+00					
Cl-	1.404e+00	8.256e-01	0.147	-0.083	-0.231	19.45
Mg	4.157e-02					
Mg+2	4.127e-02	1.195e-02	-1.384	-1.923	-0.538	-20.25
MgCO3	2.989e-04	2.989e-04	-3.524	-3.524	0.000	-17.10
MgOH+	6.580e-06	6.891e-06	-5.182	-5.162	0.020	(0)
Na	1.366e+00					
Na+	1.366e+00	1.006e+00	0.135	0.003	-0.133	0.42
S(6)	2.507e-02					
SO4-2	2.507e-02	1.112e-03	-1.601	-2.954	-1.353	21.24
HSO4-	2.610e-09	1.448e-09	-8.583	-8.839	-0.256	42.13
Si	1.102e-03					
H4SiO4	1.015e-03	1.183e-03	-2.993	-2.927	0.066	51.03
H3SiO4-	8.635e-05	3.146e-05	-4.064	-4.502	-0.439	29.45
H2SiO4-2	3.524e-08	5.868e-10	-7.453	-9.232	-1.779	(0)

-----Saturation indices-----

Phase	SI**	log IAP	log K(313 K, 1 atm)	
Akermanite	-9.44	33.36	42.80	Ca ₂ MgSi ₂ O ₇
Anhydrite	-2.09	-6.54	-4.45	CaSO ₄
Anthophyllite	13.25	75.99	62.75	Mg ₇ Si ₈ O ₂₂ (OH) ₂
Antigorite	131.79	580.75	448.96	Mg ₄₈ Si ₃₄ O ₈₅ (OH) ₆₂
Aragonite	0.11	-8.22	-8.33	CaCO ₃
Artinite	-0.81	17.75	18.57	Mg ₂ CO ₃ (OH) ₂ :3H ₂ O
Bischofite	-6.62	-2.22	4.41	MgCl ₂ :6H ₂ O
Bloedite	-5.56	-7.91	-2.35	Na ₂ Mg(SO ₄) ₂ :4H ₂ O
Brucite	-2.22	-12.93	-10.71	Mg(OH) ₂
Burkeite	-9.75	-10.52	-0.77	Na ₆ CO ₃ (SO ₄) ₂
Calcite	0.44	-8.22	-8.65	CaCO ₃
Chalcedony	0.50	-2.88	-3.38	SiO ₂
Chrysotile	6.23	36.66	30.43	Mg ₃ Si ₂ O ₅ (OH) ₄
CO ₂ (g)	-2.56	-4.18	-1.63	CO ₂
Diopside	1.04	20.88	19.84	CaMgSi ₂ O ₆

Dolomite	2.65	-14.76	-17.41	CaMg(CO ₃) ₂
Enstatite	0.64	11.27	10.63	MgSiO ₃
Epsomite	-3.28	-5.03	-1.75	MgSO ₄ :7H ₂ O
Forsterite	-0.70	25.43	26.13	Mg ₂ SiO ₄
Gaylussite	-3.52	-12.94	-9.42	CaNa ₂ (CO ₃) ₂ :5H ₂ O
Glauberite	-3.98	-9.49	-5.52	Na ₂ Ca(SO ₄) ₂
Gypsum	-1.96	-6.59	-4.63	CaSO ₄ :2H ₂ O
H ₂ O(g)	-1.16	-0.02	1.14	H ₂ O
Halite	-1.69	-0.08	1.61	NaCl
Hexahydrite	-3.39	-5.00	-1.61	MgSO ₄ :6H ₂ O
Huntite	4.38	13.07	8.69	CaMg ₃ (CO ₃) ₄
Kieserite	-4.35	-4.90	-0.55	MgSO ₄ :H ₂ O
Labile_S	-6.81	-12.48	-5.67	Na ₄ Ca(SO ₄) ₃ :2H ₂ O
Leonhardite	-4.07	-4.96	-0.89	MgSO ₄ :4H ₂ O
Magnesite	1.34	-6.55	-7.89	MgCO ₃
MgCl ₂ _2H ₂ O	-15.50	-2.13	13.37	MgCl ₂ :2H ₂ O
MgCl ₂ _4H ₂ O	-8.85	-2.17	6.68	MgCl ₂ :4H ₂ O
Mirabilite	-2.49	-3.16	-0.67	Na ₂ SO ₄ :10H ₂ O
Nahcolite	-1.93	-12.67	-10.74	NaHCO ₃
Natron	-4.01	-4.83	-0.82	Na ₂ CO ₃ :10H ₂ O
Nesquehonite	-1.44	-6.61	-5.17	MgCO ₃ :3H ₂ O
Pentahydrite	-3.70	-4.98	-1.28	MgSO ₄ :5H ₂ O
Pirssonite	-3.64	-12.88	-9.23	Na ₂ Ca(CO ₃) ₂ :2H ₂ O
Portlandite	-9.41	-14.60	-5.19	Ca(OH) ₂
Quartz	0.89	-2.88	-3.77	SiO ₂
Sepiolite	4.20	19.58	15.38	Mg ₂ Si ₃ O ₇ .5OH:3H ₂ O
Sepiolite(d)	0.92	19.58	18.66	Mg ₂ Si ₃ O ₇ .5OH:3H ₂ O
SiO ₂ (a)	-0.35	-2.88	-2.54	SiO ₂
Talc	11.14	30.91	19.77	Mg ₃ Si ₄ O ₁₀ (OH) ₂
Thenardite	-2.58	-2.95	-0.37	Na ₂ SO ₄
Trona	-5.95	-17.34	-11.38	Na ₃ H(CO ₃) ₂ :2H ₂ O

**For a gas, SI = log₁₀(fugacity). Fugacity = pressure * phi / 1 atm.
For ideal gases, phi = 1.

Initial solution 6.

-----Solution composition-----

Elements	Molality	Moles
Alkalinity	9.440e-03	9.440e-03
Ca	1.002e-03	1.002e-03
Cl	1.404e+00	1.404e+00
Mg	4.291e-02	4.291e-02
Na	1.366e+00	1.366e+00

S(6) 2.507e-02 2.507e-02
 Si 1.102e-03 1.102e-03

-----Description of solution-----

pH = 7.980
 pe = 4.000
 Specific Conductance ($\mu\text{S}/\text{cm}$, 40°C) = 142729
 Density (g/cm^3) = 1.04792
 Volume (L) = 1.03568
 Activity of water = 0.952
 Ionic strength (mol/kgw) = 1.527e+00
 Mass of water (kg) = 1.000e+00
 Total carbon (mol/kg) = 8.703e-03
 Total CO2 (mol/kg) = 8.703e-03
 Temperature (°C) = 40.00
 Electrical balance (eq) = -1.034e-02
 Percent error, $100 \cdot (\text{Cat} - |\text{An}|) / (\text{Cat} + |\text{An}|)$ = -0.35
 Iterations = 15 (92 overall)
 Gamma iterations = 4
 Osmotic coefficient = 0.95665
 Density of water = 0.99221
 Total H = 1.110247e+02
 Total O = 5.563696e+01

-----Distribution of species-----

Species	MacInnes		MacInnes		mole V	Gamma	cm \geq /mol
	Molality	Activity	Log Molality	Log Activity			
OH-	5.559e-06	2.662e-06	-5.255	-5.575	-0.320	-0.82	
H+	1.016e-08	1.047e-08	-7.993	-7.980	0.013	0.00	
H2O	5.551e+01	9.521e-01	1.744	-0.021	0.000	18.16	
C(4)	8.703e-03						
HCO3-	7.926e-03	3.728e-03	-2.101	-2.428	-0.328	28.92	
CO3-2	4.424e-04	2.087e-05	-3.354	-4.681	-1.326	2.50	
MgCO3	2.719e-04	2.719e-04	-3.566	-3.566	0.000	-17.10	
CO2	6.263e-05	7.940e-05	-4.203	-4.100	0.103	35.16	
Ca	1.002e-03						
Ca+2	1.002e-03	2.640e-04	-2.999	-3.578	-0.579	-15.86	
Cl	1.404e+00						
Cl-	1.404e+00	8.255e-01	0.147	-0.083	-0.231	19.45	
Mg	4.291e-02						
Mg+2	4.263e-02	1.234e-02	-1.370	-1.909	-0.538	-20.24	
MgCO3	2.719e-04	2.719e-04	-3.566	-3.566	0.000	-17.10	

MgOH+	5.789e-06	6.058e-06	-5.237	-5.218	0.020	(0)
Na	1.366e+00					
Na+	1.366e+00	1.006e+00	0.135	0.003	-0.133	0.43
S(6)	2.507e-02					
SO4-2	2.507e-02	1.110e-03	-1.601	-2.955	-1.354	21.25
HSO4-	3.058e-09	1.697e-09	-8.515	-8.770	-0.256	42.13
Si	1.102e-03					
H4SiO4	1.027e-03	1.198e-03	-2.988	-2.922	0.067	51.03
H3SiO4-	7.455e-05	2.710e-05	-4.128	-4.567	-0.439	29.45
H2SiO4-2	2.597e-08	4.303e-10	-7.585	-9.366	-1.781	(0)

-----Saturation indices-----

Phase	SI**	log IAP	log K(313 K, 1 atm)	
Akermanite	-9.81	32.99	42.80	Ca ₂ MgSi ₂ O ₇
Anhydrite	-2.08	-6.53	-4.45	CaSO ₄
Anthophyllite	12.41	75.16	62.75	Mg ₇ Si ₈ O ₂₂ (OH) ₂
Antigorite	125.93	574.89	448.96	Mg ₄₈ Si ₃₄ O ₈₅ (OH) ₆₂
Aragonite	0.07	-8.26	-8.33	CaCO ₃
Artinite	-0.98	17.59	18.57	Mg ₂ CO ₃ (OH) ₂ :3H ₂ O
Bischofite	-6.61	-2.20	4.41	MgCl ₂ :6H ₂ O
Bloedite	-5.55	-7.90	-2.35	Na ₂ Mg(SO ₄) ₂ :4H ₂ O
Brucite	-2.35	-13.06	-10.71	Mg(OH) ₂
Burkeite	-9.80	-10.57	-0.77	Na ₆ CO ₃ (SO ₄) ₂
Calcite	0.39	-8.26	-8.65	CaCO ₃
Chalcedony	0.51	-2.88	-3.38	SiO ₂
Chrysotile	5.86	36.29	30.43	Mg ₃ Si ₂ O ₅ (OH) ₄
CO ₂ (g)	-2.48	-4.10	-1.63	CO ₂
Diopside	0.80	20.63	19.84	CaMgSi ₂ O ₆
Dolomite	2.57	-14.85	-17.41	CaMg(CO ₃) ₂
Enstatite	0.52	11.15	10.63	MgSiO ₃
Epsomite	-3.26	-5.01	-1.75	MgSO ₄ :7H ₂ O
Forsterite	-0.95	25.18	26.13	Mg ₂ SiO ₄
Gaylussite	-3.62	-13.04	-9.42	CaNa ₂ (CO ₃) ₂ :5H ₂ O
Glauberite	-3.97	-9.48	-5.52	Na ₂ Ca(SO ₄) ₂
Gypsum	-1.95	-6.58	-4.63	CaSO ₄ :2H ₂ O
H ₂ O(g)	-1.16	-0.02	1.14	H ₂ O
Halite	-1.69	-0.08	1.61	NaCl
Hexahydrite	-3.38	-4.99	-1.61	MgSO ₄ :6H ₂ O
Huntite	4.22	12.90	8.69	CaMg ₃ (CO ₃) ₄
Kieserite	-4.33	-4.88	-0.55	MgSO ₄ :H ₂ O
Labile_S	-6.80	-12.47	-5.67	Na ₄ Ca(SO ₄) ₃ :2H ₂ O
Leonhardite	-4.06	-4.95	-0.89	MgSO ₄ :4H ₂ O
Magnesite	1.30	-6.59	-7.89	MgCO ₃
MgCl ₂ _2H ₂ O	-15.49	-2.12	13.37	MgCl ₂ :2H ₂ O

MgCl2_4H2O	-8.84	-2.16	6.68	MgCl2:4H2O
Mirabilite	-2.50	-3.16	-0.67	Na2SO4:10H2O
Nahcolite	-1.92	-12.66	-10.74	NaHCO3
Natron	-4.06	-4.89	-0.82	Na2CO3:10H2O
Nesquehonite	-1.49	-6.65	-5.17	MgCO3:3H2O
Pentahydrate	-3.69	-4.97	-1.28	MgSO4:5H2O
Pirssonite	-3.74	-12.98	-9.23	Na2Ca(CO3)2:2H2O
Portlandite	-9.54	-14.73	-5.19	Ca(OH)2
Quartz	0.89	-2.88	-3.77	SiO2
Sepiolite	3.96	19.35	15.38	Mg2Si3O7.5OH:3H2O
Sepiolite(d)	0.69	19.35	18.66	Mg2Si3O7.5OH:3H2O
SiO2(a)	-0.34	-2.88	-2.54	SiO2
Talc	10.78	30.55	19.77	Mg3Si4O10(OH)2
Thenardite	-2.58	-2.95	-0.37	Na2SO4
Trona	-5.99	-17.38	-11.38	Na3H(CO3)2:2H2O

**For a gas, SI = log10(fugacity). Fugacity = pressure * phi / 1 atm.
For ideal gases, phi = 1.

Initial solution 7.

-----Solution composition-----

Elements	Molality	Moles
Alkalinity	9.477e-03	9.477e-03
Ca	1.029e-03	1.029e-03
Cl	1.404e+00	1.404e+00
Mg	4.305e-02	4.305e-02
Na	1.366e+00	1.366e+00
S(6)	2.507e-02	2.507e-02
Si	1.102e-03	1.102e-03

-----Description of solution-----

pH = 7.050
pe = 4.000
Specific Conductance ($\mu\text{S}/\text{cm}$, 40°C) = 142740
Density (g/cm^3) = 1.04794
Volume (L) = 1.03574
Activity of water = 0.952
Ionic strength (mol/kgw) = 1.528e+00
Mass of water (kg) = 1.000e+00
Total carbon (mol/kg) = 9.991e-03
Total CO2 (mol/kg) = 9.991e-03
Temperature (°C) = 40.00

Electrical balance (eq) = -1.005e-02
 Percent error, 100*(Cat-|An|)/(Cat+|An|) = -0.34
 Iterations = 15 (107 overall)
 Gamma iterations = 4
 Osmotic coefficient = 0.95677
 Density of water = 0.99221
 Total H = 1.110261e+02
 Total O = 5.564025e+01

-----Distribution of species-----

Species	MacInnes		MacInnes		mole V Gamma	cm ³ /mol
	Molality	Activity	Log Molality	Log Activity		
OH-	6.536e-07	3.128e-07	-6.185	-6.505	-0.320	-0.82
H+	8.644e-08	8.913e-08	-7.063	-7.050	0.013	0.00
H2O	5.551e+01	9.521e-01	1.744	-0.021	0.000	18.16
C(4)	9.991e-03					
HCO3-	9.269e-03	4.359e-03	-2.033	-2.361	-0.328	28.92
CO2	6.231e-04	7.901e-04	-3.205	-3.102	0.103	35.16
CO3-2	6.090e-05	2.866e-06	-4.215	-5.543	-1.327	2.50
MgCO3	3.773e-05	3.773e-05	-4.423	-4.423	0.000	-17.10
Ca	1.029e-03					
Ca+2	1.029e-03	2.721e-04	-2.988	-3.565	-0.578	-15.86
Cl	1.404e+00					
Cl-	1.404e+00	8.255e-01	0.147	-0.083	-0.231	19.45
Mg	4.305e-02					
Mg+2	4.301e-02	1.247e-02	-1.366	-1.904	-0.538	-20.24
MgCO3	3.773e-05	3.773e-05	-4.423	-4.423	0.000	-17.10
MgOH+	6.871e-07	7.190e-07	-6.163	-6.143	0.020	(0)
Na	1.366e+00					
Na+	1.366e+00	1.007e+00	0.135	0.003	-0.133	0.43
S(6)	2.507e-02					
SO4-2	2.507e-02	1.108e-03	-1.601	-2.955	-1.355	21.25
HSO4-	2.599e-08	1.443e-08	-7.585	-7.841	-0.256	42.13
Si	1.102e-03					
H4SiO4	1.093e-03	1.274e-03	-2.962	-2.895	0.067	51.03
H3SiO4-	9.323e-06	3.387e-06	-5.030	-5.470	-0.440	29.45
H2SiO4-2	3.821e-10	6.319e-12	-9.418	-11.199	-1.782	(0)

-----Saturation indices-----

Phase	SI**	log IAP	log K(313 K, 1 atm)
Akermanite	-15.31	27.50	42.80 Ca2MgSi2O7

Anhydrite	-2.07	-6.52	-4.45	CaSO ₄
Anthophyllite	-0.37	62.38	62.75	Mg ₇ Si ₈ O ₂₂ (OH) ₂
Antigorite	37.77	486.73	448.96	Mg ₄₈ Si ₃₄ O ₈₅ (OH) ₆₂
Aragonite	-0.78	-9.11	-8.33	CaCO ₃
Artinite	-3.70	14.87	18.57	Mg ₂ CO ₃ (OH) ₂ :3H ₂ O
Bischofite	-6.61	-2.20	4.41	MgCl ₂ :6H ₂ O
Bloedite	-5.55	-7.89	-2.35	Na ₂ Mg(SO ₄) ₂ :4H ₂ O
Brucite	-4.20	-14.91	-10.71	Mg(OH) ₂
Burkeite	-10.66	-11.44	-0.77	Na ₆ CO ₃ (SO ₄) ₂
Calcite	-0.46	-9.11	-8.65	CaCO ₃
Chalcedony	0.53	-2.85	-3.38	SiO ₂
Chrysotile	0.35	30.78	30.43	Mg ₃ Si ₂ O ₅ (OH) ₄
CO ₂ (g)	-1.48	-3.10	-1.63	CO ₂
Diopside	-2.85	16.98	19.84	CaMgSi ₂ O ₆
Dolomite	0.86	-16.56	-17.41	CaMg(CO ₃) ₂
Enstatite	-1.31	9.32	10.63	MgSiO ₃
Epsomite	-3.26	-5.01	-1.75	MgSO ₄ :7H ₂ O
Forsterite	-4.63	21.50	26.13	Mg ₂ SiO ₄
Gaylussite	-5.33	-14.75	-9.42	CaNa ₂ (CO ₃) ₂ :5H ₂ O
Glauberite	-3.95	-9.47	-5.52	Na ₂ Ca(SO ₄) ₂
Gypsum	-1.93	-6.56	-4.63	CaSO ₄ :2H ₂ O
H ₂ O(g)	-1.16	-0.02	1.14	H ₂ O
Halite	-1.69	-0.08	1.61	NaCl
Hexahydrite	-3.38	-4.99	-1.61	MgSO ₄ :6H ₂ O
Huntite	0.79	9.48	8.69	CaMg ₃ (CO ₃) ₄
Kieserite	-4.33	-4.88	-0.55	MgSO ₄ :H ₂ O
Labile_S	-6.79	-12.46	-5.67	Na ₄ Ca(SO ₄) ₃ :2H ₂ O
Leonhardite	-4.06	-4.95	-0.89	MgSO ₄ :4H ₂ O
Magnesite	0.44	-7.45	-7.89	MgCO ₃
MgCl ₂ _2H ₂ O	-15.48	-2.11	13.37	MgCl ₂ :2H ₂ O
MgCl ₂ _4H ₂ O	-8.83	-2.16	6.68	MgCl ₂ :4H ₂ O
Mirabilite	-2.50	-3.16	-0.67	Na ₂ SO ₄ :10H ₂ O
Nahcolite	-1.85	-12.59	-10.74	NaHCO ₃
Natron	-4.93	-5.75	-0.82	Na ₂ CO ₃ :10H ₂ O
Nesquehonite	-2.34	-7.51	-5.17	MgCO ₃ :3H ₂ O
Pentahydrite	-3.68	-4.97	-1.28	MgSO ₄ :5H ₂ O
Pirssonite	-5.45	-14.69	-9.23	Na ₂ Ca(CO ₃) ₂ :2H ₂ O
Portlandite	-11.38	-16.57	-5.19	Ca(OH) ₂
Quartz	0.92	-2.85	-3.77	SiO ₂
Sepiolite	0.33	15.72	15.38	Mg ₂ Si ₃ O ₇ .5OH:3H ₂ O
Sepiolite(d)	-2.94	15.72	18.66	Mg ₂ Si ₃ O ₇ .5OH:3H ₂ O
SiO ₂ (a)	-0.31	-2.85	-2.54	SiO ₂
Talc	5.32	25.09	19.77	Mg ₃ Si ₄ O ₁₀ (OH) ₂
Thenardite	-2.58	-2.95	-0.37	Na ₂ SO ₄
Trona	-6.79	-18.17	-11.38	Na ₃ H(CO ₃) ₂ :2H ₂ O

**For a gas, $SI = \log_{10}(\text{fugacity})$. Fugacity = pressure * phi / 1 atm.
For ideal gases, phi = 1.

End of simulation.

Reading input data for simulation 2.

End of Run after 0.01475 Seconds.

ESW11 solution model:

#This fluid recipe is will modeled the aqueous conditions during the Late Neoproterozoic (Ediacaran) seawater.

#This is 1.08 Ca/Mg ratio (based on digital calculator). ESW11

#grams per liter:

#grams of $\text{CaCl}_2 \cdot 2\text{H}_2\text{O}$ -> 4 gram
#grams of $\text{MgCl}_2 \cdot 6\text{H}_2\text{O}$ -> 6 grams
#grams of NaCl -> 70 grams
#grams of Na_2CO_3 -> 1 gram
#grams of Na_2SO_4 -> 2.75 grams
#grams of Na_4SiO_3 -> 0.4 grams

#Alkalinity is ~9 mmol (566 mg/L ad CO_3 ; using calculator), which was done by adding 1 gram of NaCO_3 .

#Horita et al. 2002. *Geochimica et Cosmochimica Acta* (Mg:Ca ratios and Sulfate conc.). S(6) is the sulfur concentration in late neoproterozoic seawater, which is 23.1 mmol.

#Meng et al. 2010. *Precambrian Research* (Temperatures).

#Bongtonali et al. 2010. and Paul et al., 2016 *Sedimentology* (pH values from modern microbial mats and modern seawater).

#Salinity is slightly higher than modern normal seawater. Modern seawater is 3.5 wt % whereas this solution is 8.1 wt % (based on digital calculator).

#Ionic Strength, based on digital calculator, is ~1.37

#Dissolved silica is present, as SiO_3 . Here, is Si.

Reading data base.

SOLUTION_MASTER_SPECIES
SOLUTION_SPECIES
PHASES
PITZER
EXCHANGE_MASTER_SPECIES
EXCHANGE_SPECIES
SURFACE_MASTER_SPECIES
SURFACE_SPECIES
END

Reading input data for simulation 1.

TITLE Bryan Rodriguez's Solution - Dengying Formation (summer 2019)
SOLUTION 1
pH 8.5
Temp 40
Units mg/L
Ca 1090
Mg 717
Na 29234
Cl 46484
S(6) 2219
Si 61
Alkalinity 566 as CO3
SAVE SOLUTION 1

TITLE

Bryan Rodriguez's Solution - Dengying Formation (summer 2019)

Beginning of initial solution calculations.

Initial solution 1.

-----Solution composition-----

Elements	Molality	Moles
----------	----------	-------

Alkalinity	1.026e-02	1.026e-02
Ca	2.957e-02	2.957e-02
Cl	1.426e+00	1.426e+00
Mg	3.208e-02	3.208e-02
Na	1.383e+00	1.383e+00
S(6)	2.512e-02	2.512e-02
Si	1.104e-03	1.104e-03

-----Description of solution-----

pH = 8.500
 pe = 4.000
 Specific Conductance ($\mu\text{S}/\text{cm}$, 40°C) = 144764
 Density (g/cm^3) = 1.04965
 Volume (L) = 1.03588
 Activity of water = 0.951
 Ionic strength (mol/kgw) = 1.583e+00
 Mass of water (kg) = 1.000e+00
 Total carbon (mol/kg) = 8.183e-03
 Total CO2 (mol/kg) = 8.183e-03
 Temperature (°C) = 40.00
 Electrical balance (eq) = 1.982e-02
 Percent error, $100 \cdot (\text{Cat} - |\text{An}|) / (\text{Cat} + |\text{An}|)$ = 0.66
 Iterations = 16
 Gamma iterations = 4
 Osmotic coefficient = 0.95889
 Density of water = 0.99221
 Total H = 1.110230e+02
 Total O = 5.563567e+01

-----Distribution of species-----

Species	MacInnes		MacInnes		mole V Gamma	cm ³ /mol
	Molality	Activity	Log Molality	Log Activity		
OH-	1.917e-05	8.806e-06	-4.717	-5.055	-0.338	-0.73
H+	3.037e-09	3.162e-09	-8.518	-8.500	0.018	0.00
H2O	5.551e+01	9.511e-01	1.744	-0.022	0.000	18.16
C(4)	8.183e-03					
HCO3-	6.333e-03	3.052e-03	-2.198	-2.515	-0.317	29.02
CO3-2	1.291e-03	5.655e-05	-2.889	-4.248	-1.359	2.60
MgCO3	5.432e-04	5.432e-04	-3.265	-3.265	0.000	-17.10
CO2	1.536e-05	1.965e-05	-4.814	-4.707	0.107	35.16
Ca	2.957e-02					

Ca+2	2.957e-02	7.755e-03	-1.529	-2.110	-0.581	-15.83
Cl	1.426e+00					
Cl-	1.426e+00	8.364e-01	0.154	-0.078	-0.232	19.47
Mg	3.208e-02					
Mg+2	3.152e-02	9.095e-03	-1.501	-2.041	-0.540	-20.21
MgCO3	5.432e-04	5.432e-04	-3.265	-3.265	0.000	-17.10
MgOH+	1.429e-05	1.477e-05	-4.845	-4.831	0.014	(0)
Na	1.383e+00					
Na+	1.383e+00	1.025e+00	0.141	0.011	-0.130	0.45
S(6)	2.512e-02					
SO4-2	2.512e-02	1.043e-03	-1.600	-2.982	-1.382	21.35
HSO4-	8.687e-10	4.816e-10	-9.061	-9.317	-0.256	42.14
Si	1.104e-03					
H4SiO4	8.839e-04	1.041e-03	-3.054	-2.983	0.071	51.03
H3SiO4-	2.198e-04	7.800e-05	-3.658	-4.108	-0.450	29.48
H2SiO4-2	2.647e-07	4.101e-09	-6.577	-8.387	-1.810	(0)

-----Saturation indices-----

Phase	SI**	log IAP	log K(313 K, 1 atm)	
Akermanite	-4.01	38.79	42.80	Ca2MgSi2O7
Anhydrite	-0.64	-5.09	-4.45	CaSO4
Anthophyllite	18.28	81.03	62.75	Mg7Si8O22(OH)2
Antigorite	167.41	616.37	448.96	Mg48Si34O85(OH)62
Aragonite	1.97	-6.36	-8.33	CaCO3
Artinite	0.22	18.79	18.57	Mg2CO3(OH)2:3H2O
Bischofite	-6.73	-2.33	4.41	MgCl2:6H2O
Bloedite	-5.72	-8.07	-2.35	Na2Mg(SO4)2:4H2O
Brucite	-1.44	-12.15	-10.71	Mg(OH)2
Burkeite	-9.37	-10.15	-0.77	Na6CO3(SO4)2
Calcite	2.29	-6.36	-8.65	CaCO3
Chalcedony	0.45	-2.94	-3.38	SiO2
Chrysotile	8.46	38.89	30.43	Mg3Si2O5(OH)4
CO2(g)	-3.08	-4.71	-1.63	CO2
Diopside	4.09	23.93	19.84	CaMgSi2O6
Dolomite	4.77	-12.65	-17.41	CaMg(CO3)2
Enstatite	1.36	12.00	10.63	MgSiO3
Epsomite	-3.43	-5.18	-1.75	MgSO4:7H2O
Forsterite	0.80	26.94	26.13	Mg2SiO4
Gaylussite	-1.27	-10.69	-9.42	CaNa2(CO3)2:5H2O
Glauberite	-2.54	-8.05	-5.52	Na2Ca(SO4)2
Gypsum	-0.51	-5.14	-4.63	CaSO4:2H2O
H2O(g)	-1.16	-0.02	1.14	H2O
Halite	-1.67	-0.07	1.61	NaCl
Hexahydrite	-3.54	-5.15	-1.61	MgSO4:6H2O

Huntite	7.02	15.70	8.69	CaMg ₃ (CO ₃) ₄
Kieserite	-4.49	-5.04	-0.55	MgSO ₄ :H ₂ O
Labile_S	-5.38	-11.06	-5.67	Na ₄ Ca(SO ₄) ₃ :2H ₂ O
Leonhardite	-4.22	-5.11	-0.89	MgSO ₄ :4H ₂ O
Magnesite	1.60	-6.29	-7.89	MgCO ₃
MgCl ₂ _2H ₂ O	-15.61	-2.24	13.37	MgCl ₂ :2H ₂ O
MgCl ₂ _4H ₂ O	-8.96	-2.28	6.68	MgCl ₂ :4H ₂ O
Mirabilite	-2.51	-3.18	-0.67	Na ₂ SO ₄ :10H ₂ O
Nahcolite	-1.99	-12.74	-10.74	NaHCO ₃
Natron	-3.62	-4.44	-0.82	Na ₂ CO ₃ :10H ₂ O
Nesquehonite	-1.19	-6.35	-5.17	MgCO ₃ :3H ₂ O
Pentahydrate	-3.85	-5.13	-1.28	MgSO ₄ :5H ₂ O
Pirssonite	-1.39	-10.63	-9.23	Na ₂ Ca(CO ₃) ₂ :2H ₂ O
Portlandite	-7.03	-12.22	-5.19	Ca(OH) ₂
Quartz	0.83	-2.94	-3.77	SiO ₂
Sepiolite	5.60	20.98	15.38	Mg ₂ Si ₃ O ₇ .5OH:3H ₂ O
Sepiolite(d)	2.32	20.98	18.66	Mg ₂ Si ₃ O ₇ .5OH:3H ₂ O
SiO ₂ (a)	-0.40	-2.94	-2.54	SiO ₂
Talc	13.26	33.03	19.77	Mg ₃ Si ₄ O ₁₀ (OH) ₂
Thenardite	-2.59	-2.96	-0.37	Na ₂ SO ₄
Trona	-5.62	-17.01	-11.38	Na ₃ H(CO ₃) ₂ :2H ₂ O

**For a gas, SI = log₁₀(fugacity). Fugacity = pressure * phi / 1 atm.
For ideal gases, phi = 1.

End of simulation.

Reading input data for simulation 2.

End of Run after 0.010833 Seconds.

ESW11 solution model (control and experimental 93 days):

#This fluid recipe is will modeled the aqueous conditions during the Late Neoproterozoic (Ediacaran) seawater over time by using the experimental data from ICP-OES (Ca & Mg concentrations in ppm). ESW11

Reading data base.

SOLUTION_MASTER_SPECIES
SOLUTION_SPECIES
PHASES
PITZER
EXCHANGE_MASTER_SPECIES
EXCHANGE_SPECIES
SURFACE_MASTER_SPECIES
SURFACE_SPECIES
END

Reading input data for simulation 1.

TITLE Bryan Rodriguez's Solution - Dengying Formation (summer 2019)

#SW11- Before (T=0)

SOLUTION 1

pH	8.39
Temp	40
	Units mg/L
Ca	546
Mg	787
Na	28930
Cl	45874
S(6)	2219
Si	61
Alkalinity	177 as CO3

SAVE SOLUTION 1

#SW11- cc 2 weeks (T=14)

SOLUTION 2

pH	8.01
Temp	40
	Units mg/L
Ca	33
Mg	1026
Na	28930
Cl	45874
S(6)	2219
Si	61
Alkalinity	522 as CO3

SAVE SOLUTION 2

#SW11- sp1 2 weeks (T=14)

SOLUTION 3

pH	8.08
Temp	40
	Units mg/L
Ca	35
Mg	999
Na	28930
Cl	45874
S(6)	2219
Si	61
Alkalinity	535 as CO3

SAVE SOLUTION 3

#SW11- sp2 2 weeks (T=14)

SOLUTION 4

pH	8.11
Temp	40
	Units mg/L
Ca	35
Mg	1072
Na	28930
Cl	45874
S(6)	2219
Si	61
Alkalinity	540 as CO3

SAVE SOLUTION 4

#SW11- cc 3 months(T=93)

SOLUTION 5

pH	8.05
Temp	40
	Units mg/L
Ca	36
Mg	931
Na	28930
Cl	45874
S(6)	2219
Si	61
Alkalinity	517 as CO3

SAVE SOLUTION 5

#SW11- sp1 3 months(T=93)

SOLUTION 6

pH	7.98
----	------

Temp	40
	Units mg/L
Ca	37
Mg	961
Na	28930
Cl	45874
S(6)	2219
Si	61
Alkalinity	522 as CO3

SAVE SOLUTION 6

#SW11- sp2 3 months(T=93)

SOLUTION 7

pH	7.05
Temp	40
	Units mg/L
Ca	38
Mg	964
Na	28930
Cl	45874
S(6)	2219
Si	61
Alkalinity	524 as CO3

SAVE SOLUTION 7

TITLE

Bryan Rodriguez's Solution - Dengying Formation (summer 2019)

Beginning of initial solution calculations.

Initial solution 1.

-----Solution composition-----

Elements	Molality	Moles
Alkalinity	3.201e-03	3.201e-03
Ca	1.478e-02	1.478e-02
Cl	1.404e+00	1.404e+00
Mg	3.514e-02	3.514e-02
Na	1.366e+00	1.366e+00
S(6)	2.507e-02	2.507e-02

Si 1.102e-03 1.102e-03

-----Description of solution-----

pH = 8.390
 pe = 4.000
 Specific Conductance ($\mu\text{S}/\text{cm}$, 40°C) = 142887
 Density (g/cm^3) = 1.04814
 Volume (L) = 1.03545
 Activity of water = 0.952
 Ionic strength (mol/kgw) = 1.536e+00
 Mass of water (kg) = 1.000e+00
 Total carbon (mol/kg) = 2.545e-03
 Total CO2 (mol/kg) = 2.545e-03
 Temperature ($^\circ\text{C}$) = 40.00
 Electrical balance (eq) = 7.927e-03
 Percent error, $100 \cdot (\text{Cat} - |\text{An}|) / (\text{Cat} + |\text{An}|)$ = 0.27
 Iterations = 15
 Gamma iterations = 4
 Osmotic coefficient = 0.95740
 Density of water = 0.99221
 Total H = 1.110188e+02
 Total O = 5.561856e+01

-----Distribution of species-----

Species	MacInnes		MacInnes		mole V Gamma	cm \geq /mol
	Molality	Activity	Log Molality	Log Activity		
OH-	1.451e-05	6.843e-06	-4.838	-5.165	-0.326	-0.80
H+	3.943e-09	4.074e-09	-8.404	-8.390	0.014	0.00
H2O	5.551e+01	9.521e-01	1.744	-0.021	0.000	18.16
C(4)	2.545e-03					
HCO3-	2.079e-03	9.935e-04	-2.682	-3.003	-0.321	28.93
CO3-2	3.081e-04	1.429e-05	-3.511	-4.845	-1.334	2.52
MgCO3	1.523e-04	1.523e-04	-3.817	-3.817	0.000	-17.10
CO2	6.478e-06	8.232e-06	-5.189	-5.084	0.104	35.16
Ca	1.478e-02					
Ca+2	1.478e-02	3.854e-03	-1.830	-2.414	-0.584	-15.86
Cl	1.404e+00					
Cl-	1.404e+00	8.252e-01	0.147	-0.083	-0.231	19.45
Mg	3.514e-02					
Mg+2	3.498e-02	1.009e-02	-1.456	-1.996	-0.540	-20.24
MgCO3	1.523e-04	1.523e-04	-3.817	-3.817	0.000	-17.10
MgOH+	1.219e-05	1.273e-05	-4.914	-4.895	0.019	(0)

Na	1.366e+00					
Na+	1.366e+00	1.009e+00	0.135	0.004	-0.132	0.43
S(6)	2.507e-02					
SO4-2	2.507e-02	1.090e-03	-1.601	-2.963	-1.362	21.26
HSO4-	1.167e-09	6.485e-10	-8.933	-9.188	-0.255	42.13
Si	1.102e-03					
H4SiO4	9.271e-04	1.084e-03	-3.033	-2.965	0.068	51.03
H3SiO4-	1.746e-04	6.306e-05	-3.758	-4.200	-0.442	29.46
H2SiO4-2	1.575e-07	2.573e-09	-6.803	-8.590	-1.787	(0)

-----Saturation indices-----

Phase	SI**	log IAP	log K(313 K, 1 atm)	
Akermanite	-5.20	37.61	42.80	Ca2MgSi2O7
Anhydrite	-0.92	-5.38	-4.45	CaSO4
Anthophyllite	17.19	79.94	62.75	Mg7Si8O22(OH)2
Antigorite	159.62	608.58	448.96	Mg48Si34O85(OH)62
Aragonite	1.07	-7.26	-8.33	CaCO3
Artinite	-0.50	18.07	18.57	Mg2CO3(OH)2:3H2O
Bischofite	-6.70	-2.29	4.41	MgCl2:6H2O
Bloedite	-5.65	-8.00	-2.35	Na2Mg(SO4)2:4H2O
Brucite	-1.62	-12.33	-10.71	Mg(OH)2
Burkeite	-9.98	-10.75	-0.77	Na6CO3(SO4)2
Calcite	1.39	-7.26	-8.65	CaCO3
Chalcedony	0.46	-2.92	-3.38	SiO2
Chrysotile	7.97	38.40	30.43	Mg3Si2O5(OH)4
CO2(g)	-3.46	-5.08	-1.63	CO2
Diopside	3.43	23.26	19.84	CaMgSi2O6
Dolomite	3.31	-14.10	-17.41	CaMg(CO3)2
Enstatite	1.21	11.84	10.63	MgSiO3
Epsomite	-3.36	-5.11	-1.75	MgSO4:7H2O
Forsterite	0.47	26.60	26.13	Mg2SiO4
Gaylussite	-2.78	-12.20	-9.42	CaNa2(CO3)2:5H2O
Glauberite	-2.82	-8.33	-5.52	Na2Ca(SO4)2
Gypsum	-0.79	-5.42	-4.63	CaSO4:2H2O
H2O(g)	-1.16	-0.02	1.14	H2O
Halite	-1.69	-0.08	1.61	NaCl
Hexahydrite	-3.48	-5.09	-1.61	MgSO4:6H2O
Huntite	4.46	13.15	8.69	CaMg3(CO3)4
Kieserite	-4.43	-4.98	-0.55	MgSO4:H2O
Labile_S	-5.66	-11.33	-5.67	Na4Ca(SO4)3:2H2O
Leonhardite	-4.16	-5.04	-0.89	MgSO4:4H2O
Magnesite	1.04	-6.84	-7.89	MgCO3
MgCl2_2H2O	-15.57	-2.21	13.37	MgCl2:2H2O
MgCl2_4H2O	-8.92	-2.25	6.68	MgCl2:4H2O

Mirabilite	-2.50	-3.17	-0.67	Na2SO4:10H2O
Nahcolite	-2.49	-13.23	-10.74	NaHCO3
Natron	-4.23	-5.05	-0.82	Na2CO3:10H2O
Nesquehonite	-1.74	-6.91	-5.17	MgCO3:3H2O
Pentahydrate	-3.78	-5.07	-1.28	MgSO4:5H2O
Pirssonite	-2.91	-12.14	-9.23	Na2Ca(CO3)2:2H2O
Portlandite	-7.55	-12.74	-5.19	Ca(OH)2
Quartz	0.85	-2.92	-3.77	SiO2
Sepiolite	5.30	20.68	15.38	Mg2Si3O7.5OH:3H2O
Sepiolite(d)	2.02	20.68	18.66	Mg2Si3O7.5OH:3H2O
SiO2(a)	-0.38	-2.92	-2.54	SiO2
Talc	12.81	32.58	19.77	Mg3Si4O10(OH)2
Thenardite	-2.58	-2.96	-0.37	Na2SO4
Trona	-6.73	-18.11	-11.38	Na3H(CO3)2:2H2O

**For a gas, SI = log10(fugacity). Fugacity = pressure * phi / 1 atm.
For ideal gases, phi = 1.

Initial solution 2.

-----Solution composition-----

Elements	Molality	Moles
Alkalinity	9.441e-03	9.441e-03
Ca	8.937e-04	8.937e-04
Cl	1.404e+00	1.404e+00
Mg	4.582e-02	4.582e-02
Na	1.366e+00	1.366e+00
S(6)	2.507e-02	2.507e-02
Si	1.102e-03	1.102e-03

-----Description of solution-----

pH = 8.010
pe = 4.000
Specific Conductance (μS/cm, 40°C) = 142761
Density (g/cm³) = 1.04804
Volume (L) = 1.03563
Activity of water = 0.952
Ionic strength (mol/kgw) = 1.533e+00
Mass of water (kg) = 1.000e+00
Total carbon (mol/kg) = 8.631e-03
Total CO2 (mol/kg) = 8.631e-03
Temperature (°C) = 40.00
Electrical balance (eq) = -4.751e-03

Percent error, $100 \cdot (\text{Cat} - |\text{An}|) / (\text{Cat} + |\text{An}|) = -0.16$

Iterations = 15 (30 overall)

Gamma iterations = 4

Osmotic coefficient = 0.95696

Density of water = 0.99221

Total H = 1.110246e+02

Total O = 5.563676e+01

-----Distribution of species-----

Species	MacInnes		MacInnes		mole V Gamma	cm \geq /mol
	Molality	Activity	Log Molality	Log Activity		
OH-	5.980e-06	2.852e-06	-5.223	-5.545	-0.322	-0.81
H+	9.471e-09	9.772e-09	-8.024	-8.010	0.014	0.00
H2O	5.551e+01	9.520e-01	1.744	-0.021	0.000	18.16
C(4)	8.631e-03					
HCO3-	7.798e-03	3.659e-03	-2.108	-2.437	-0.329	28.93
CO3-2	4.704e-04	2.194e-05	-3.328	-4.659	-1.331	2.51
MgCO3	3.049e-04	3.049e-04	-3.516	-3.516	0.000	-17.10
CO2	5.731e-05	7.273e-05	-4.242	-4.138	0.104	35.16
Ca	8.937e-04					
Ca+2	8.937e-04	2.353e-04	-3.049	-3.628	-0.580	-15.86
Cl	1.404e+00					
Cl-	1.404e+00	8.254e-01	0.147	-0.083	-0.231	19.45
Mg	4.582e-02					
Mg+2	4.551e-02	1.316e-02	-1.342	-1.881	-0.539	-20.24
MgCO3	3.049e-04	3.049e-04	-3.516	-3.516	0.000	-17.10
MgOH+	6.623e-06	6.921e-06	-5.179	-5.160	0.019	(0)
Na	1.366e+00					
Na+	1.366e+00	1.007e+00	0.135	0.003	-0.132	0.43
S(6)	2.507e-02					
SO4-2	2.507e-02	1.105e-03	-1.601	-2.957	-1.356	21.26
HSO4-	2.839e-09	1.577e-09	-8.547	-8.802	-0.256	42.13
Si	1.102e-03					
H4SiO4	1.022e-03	1.193e-03	-2.991	-2.923	0.067	51.03
H3SiO4-	7.988e-05	2.893e-05	-4.098	-4.539	-0.441	29.46
H2SiO4-2	2.998e-08	4.922e-10	-7.523	-9.308	-1.785	(0)

-----Saturation indices-----

Phase	SI**	log IAP	log K(313 K, 1 atm)
Akermanite	-9.71	33.10	42.80 Ca ₂ MgSi ₂ O ₇
Anhydrite	-2.13	-6.59	-4.45 CaSO ₄

Anthophyllite	13.01	75.76	62.75	Mg ₇ Si ₈ O ₂₂ (OH) ₂
Antigorite	130.09	579.05	448.96	Mg ₄₈ Si ₃₄ O ₈₅ (OH) ₆₂
Aragonite	0.04	-8.29	-8.33	CaCO ₃
Artinite	-0.84	17.72	18.57	Mg ₂ CO ₃ (OH) ₂ :3H ₂ O
Bischofite	-6.58	-2.18	4.41	MgCl ₂ :6H ₂ O
Bloedite	-5.53	-7.87	-2.35	Na ₂ Mg(SO ₄) ₂ :4H ₂ O
Brucite	-2.26	-12.97	-10.71	Mg(OH) ₂
Burkeite	-9.78	-10.55	-0.77	Na ₆ CO ₃ (SO ₄) ₂
Calcite	0.36	-8.29	-8.65	CaCO ₃
Chalcedony	0.50	-2.88	-3.38	SiO ₂
Chrysotile	6.12	36.55	30.43	Mg ₃ Si ₂ O ₅ (OH) ₄
CO ₂ (g)	-2.51	-4.14	-1.63	CO ₂
Diopside	0.89	20.73	19.84	CaMgSi ₂ O ₆
Dolomite	2.59	-14.83	-17.41	CaMg(CO ₃) ₂
Enstatite	0.60	11.24	10.63	MgSiO ₃
Epsomite	-3.24	-4.99	-1.75	MgSO ₄ :7H ₂ O
Forsterite	-0.78	25.35	26.13	Mg ₂ SiO ₄
Gaylussite	-3.63	-13.05	-9.42	CaNa ₂ (CO ₃) ₂ :5H ₂ O
Glauberite	-4.02	-9.54	-5.52	Na ₂ Ca(SO ₄) ₂
Gypsum	-2.00	-6.63	-4.63	CaSO ₄ :2H ₂ O
H ₂ O(g)	-1.16	-0.02	1.14	H ₂ O
Halite	-1.69	-0.08	1.61	NaCl
Hexahydrite	-3.36	-4.97	-1.61	MgSO ₄ :6H ₂ O
Huntite	4.34	13.02	8.69	CaMg ₃ (CO ₃) ₄
Kieserite	-4.31	-4.86	-0.55	MgSO ₄ :H ₂ O
Labile_S	-6.86	-12.53	-5.67	Na ₄ Ca(SO ₄) ₃ :2H ₂ O
Leonhardite	-4.04	-4.92	-0.89	MgSO ₄ :4H ₂ O
Magnesite	1.35	-6.54	-7.89	MgCO ₃
MgCl ₂ _2H ₂ O	-15.46	-2.09	13.37	MgCl ₂ :2H ₂ O
MgCl ₂ _4H ₂ O	-8.81	-2.13	6.68	MgCl ₂ :4H ₂ O
Mirabilite	-2.50	-3.16	-0.67	Na ₂ SO ₄ :10H ₂ O
Nahcolite	-1.92	-12.67	-10.74	NaHCO ₃
Natron	-4.04	-4.87	-0.82	Na ₂ CO ₃ :10H ₂ O
Nesquehonite	-1.44	-6.60	-5.17	MgCO ₃ :3H ₂ O
Pentahydrite	-3.66	-4.94	-1.28	MgSO ₄ :5H ₂ O
Pirssonite	-3.75	-12.98	-9.23	Na ₂ Ca(CO ₃) ₂ :2H ₂ O
Portlandite	-9.53	-14.72	-5.19	Ca(OH) ₂
Quartz	0.89	-2.88	-3.77	SiO ₂
Sepiolite	4.13	19.52	15.38	Mg ₂ Si ₃ O ₇ .5OH:3H ₂ O
Sepiolite(d)	0.86	19.52	18.66	Mg ₂ Si ₃ O ₇ .5OH:3H ₂ O
SiO ₂ (a)	-0.34	-2.88	-2.54	SiO ₂
Talc	11.04	30.81	19.77	Mg ₃ Si ₄ O ₁₀ (OH) ₂
Thenardite	-2.58	-2.95	-0.37	Na ₂ SO ₄
Trona	-5.98	-17.36	-11.38	Na ₃ H(CO ₃) ₂ :2H ₂ O

**For a gas, SI = log₁₀(fugacity). Fugacity = pressure * phi / 1 atm.

For ideal gases, $\phi = 1$.

Initial solution 3.

-----Solution composition-----

Elements	Molality	Moles
Alkalinity	9.676e-03	9.676e-03
Ca	9.478e-04	9.478e-04
Cl	1.404e+00	1.404e+00
Mg	4.461e-02	4.461e-02
Na	1.366e+00	1.366e+00
S(6)	2.507e-02	2.507e-02
Si	1.102e-03	1.102e-03

-----Description of solution-----

$\text{pH} = 8.080$
 $\text{pe} = 4.000$
 Specific Conductance ($\mu\text{S}/\text{cm}$, 40°C) = 142750
 Density (g/cm^3) = 1.04800
 Volume (L) = 1.03565
 Activity of water = 0.952
 Ionic strength (mol/kgw) = 1.531e+00
 Mass of water (kg) = 1.000e+00
 Total carbon (mol/kg) = 8.721e-03
 Total CO2 (mol/kg) = 8.721e-03
 Temperature ($^\circ\text{C}$) = 40.00
 Electrical balance (eq) = -7.289e-03
 Percent error, $100 \cdot (\text{Cat} - |\text{An}|) / (\text{Cat} + |\text{An}|) = -0.25$
 Iterations = 15 (45 overall)
 Gamma iterations = 4
 Osmotic coefficient = 0.95680
 Density of water = 0.99221
 Total H = 1.110245e+02
 Total O = 5.563704e+01

-----Distribution of species-----

Species	MacInnes		MacInnes		mole V Gamma	cm \geq /mol
	MacInnes Molality	MacInnes Activity	Log Molality	Log Activity		
OH-	7.014e-06	3.351e-06	-5.154	-5.475	-0.321	-0.81
H+	8.066e-09	8.318e-09	-8.093	-8.080	0.013	0.00

H2O	5.551e+01	9.521e-01	1.744	-0.021	0.000	18.16
C(4)	8.721e-03					
HCO3-	7.775e-03	3.653e-03	-2.109	-2.437	-0.328	28.93
CO3-2	5.490e-04	2.573e-05	-3.260	-4.590	-1.329	2.51
MgCO3	3.478e-04	3.478e-04	-3.459	-3.459	0.000	-17.10
CO2	4.871e-05	6.179e-05	-4.312	-4.209	0.103	35.16
Ca	9.478e-04					
Ca+2	9.478e-04	2.495e-04	-3.023	-3.603	-0.580	-15.86
Cl	1.404e+00					
Cl-	1.404e+00	8.255e-01	0.147	-0.083	-0.231	19.45
Mg	4.461e-02					
Mg+2	4.426e-02	1.280e-02	-1.354	-1.893	-0.539	-20.24
MgCO3	3.478e-04	3.478e-04	-3.459	-3.459	0.000	-17.10
MgOH+	7.565e-06	7.909e-06	-5.121	-5.102	0.019	(0)
Na	1.366e+00					
Na+	1.366e+00	1.007e+00	0.135	0.003	-0.132	0.43
S(6)	2.507e-02					
SO4-2	2.507e-02	1.107e-03	-1.601	-2.956	-1.355	21.25
HSO4-	2.422e-09	1.345e-09	-8.616	-8.871	-0.256	42.13
Si	1.102e-03					
H4SiO4	1.009e-03	1.178e-03	-2.996	-2.929	0.067	51.03
H3SiO4-	9.249e-05	3.355e-05	-4.034	-4.474	-0.440	29.46
H2SiO4-2	4.069e-08	6.706e-10	-7.391	-9.174	-1.783	(0)

-----Saturation indices-----

Phase	SI**	log IAP	log K(313 K, 1 atm)	
Akermanite	-9.26	33.54	42.80	Ca2MgSi2O7
Anhydrite	-2.10	-6.56	-4.45	CaSO4
Anthophyllite	13.86	76.61	62.75	Mg7Si8O22(OH)2
Antigorite	136.04	585.00	448.96	Mg48Si34O85(OH)62
Aragonite	0.14	-8.19	-8.33	CaCO3
Artinite	-0.66	17.91	18.57	Mg2CO3(OH)2:3H2O
Bischofite	-6.59	-2.19	4.41	MgCl2:6H2O
Bloedite	-5.54	-7.88	-2.35	Na2Mg(SO4)2:4H2O
Brucite	-2.13	-12.84	-10.71	Mg(OH)2
Burkeite	-9.71	-10.48	-0.77	Na6CO3(SO4)2
Calcite	0.46	-8.19	-8.65	CaCO3
Chalcedony	0.50	-2.89	-3.38	SiO2
Chrysotile	6.49	36.92	30.43	Mg3Si2O5(OH)4
CO2(g)	-2.58	-4.21	-1.63	CO2
Diopside	1.17	21.01	19.84	CaMgSi2O6
Dolomite	2.74	-14.67	-17.41	CaMg(CO3)2
Enstatite	0.73	11.36	10.63	MgSiO3
Epsomite	-3.25	-5.00	-1.75	MgSO4:7H2O

Forsterite	-0.53	25.61	26.13	Mg ₂ SiO ₄
Gaylussite	-3.46	-12.88	-9.42	CaNa ₂ (CO ₃) ₂ ·5H ₂ O
Glauberite	-3.99	-9.51	-5.52	Na ₂ Ca(SO ₄) ₂
Gypsum	-1.97	-6.60	-4.63	CaSO ₄ ·2H ₂ O
H ₂ O(g)	-1.16	-0.02	1.14	H ₂ O
Halite	-1.69	-0.08	1.61	NaCl
Hexahydrite	-3.37	-4.98	-1.61	MgSO ₄ ·6H ₂ O
Huntite	4.60	13.29	8.69	CaMg ₃ (CO ₃) ₄
Kieserite	-4.32	-4.87	-0.55	MgSO ₄ ·H ₂ O
Labile_S	-6.83	-12.50	-5.67	Na ₄ Ca(SO ₄) ₃ ·2H ₂ O
Leonhardite	-4.05	-4.93	-0.89	MgSO ₄ ·4H ₂ O
Magnesite	1.40	-6.48	-7.89	MgCO ₃
MgCl ₂ ·2H ₂ O	-15.47	-2.10	13.37	MgCl ₂ ·2H ₂ O
MgCl ₂ ·4H ₂ O	-8.82	-2.14	6.68	MgCl ₂ ·4H ₂ O
Mirabilite	-2.50	-3.16	-0.67	Na ₂ SO ₄ ·10H ₂ O
Nahcolite	-1.92	-12.67	-10.74	NaHCO ₃
Natron	-3.97	-4.80	-0.82	Na ₂ CO ₃ ·10H ₂ O
Nesquehonite	-1.38	-6.55	-5.17	MgCO ₃ ·3H ₂ O
Pentahydrite	-3.67	-4.96	-1.28	MgSO ₄ ·5H ₂ O
Pirssonite	-3.58	-12.82	-9.23	Na ₂ Ca(CO ₃) ₂ ·2H ₂ O
Portlandite	-9.36	-14.55	-5.19	Ca(OH) ₂
Quartz	0.88	-2.89	-3.77	SiO ₂
Sepiolite	4.37	19.76	15.38	Mg ₂ Si ₃ O ₇ ·5OH·3H ₂ O
Sepiolite(d)	1.10	19.76	18.66	Mg ₂ Si ₃ O ₇ ·5OH·3H ₂ O
SiO ₂ (a)	-0.35	-2.89	-2.54	SiO ₂
Talc	11.40	31.17	19.77	Mg ₃ Si ₄ O ₁₀ (OH) ₂
Thenardite	-2.58	-2.95	-0.37	Na ₂ SO ₄
Trona	-5.91	-17.29	-11.38	Na ₃ H(CO ₃) ₂ ·2H ₂ O

**For a gas, SI = log₁₀(fugacity). Fugacity = pressure * phi / 1 atm.
For ideal gases, phi = 1.

Initial solution 4.

-----Solution composition-----

Elements	Molality	Moles
Alkalinity	9.767e-03	9.767e-03
Ca	9.479e-04	9.479e-04
Cl	1.405e+00	1.405e+00
Mg	4.788e-02	4.788e-02
Na	1.366e+00	1.366e+00
S(6)	2.507e-02	2.507e-02
Si	1.102e-03	1.102e-03

-----Description of solution-----

pH = 8.110
 pe = 4.000
 Specific Conductance ($\mu\text{S}/\text{cm}$, 40°C) = 142790
 Density (g/cm^3) = 1.04814
 Volume (L) = 1.03559
 Activity of water = 0.952
 Ionic strength (mol/kgw) = 1.537e+00
 Mass of water (kg) = 1.000e+00
 Total carbon (mol/kg) = 8.715e-03
 Total CO2 (mol/kg) = 8.715e-03
 Temperature ($^\circ\text{C}$) = 40.00
 Electrical balance (eq) = -8.599e-04
 Percent error, $100 \cdot (\text{Cat} - |\text{An}|) / (\text{Cat} + |\text{An}|)$ = -0.03
 Iterations = 16 (61 overall)
 Gamma iterations = 4
 Osmotic coefficient = 0.95715
 Density of water = 0.99221
 Total H = 1.110244e+02
 Total O = 5.563703e+01

-----Distribution of species-----

Species	MacInnes		MacInnes		mole V Gamma	cm \geq /mol
	Molality	Activity	Log Molality	Log Activity		
OH-	7.551e-06	3.591e-06	-5.122	-5.445	-0.323	-0.80
H+	7.518e-09	7.762e-09	-8.124	-8.110	0.014	0.00
H2O	5.551e+01	9.520e-01	1.744	-0.021	0.000	18.16
C(4)	8.715e-03					
HCO3-	7.689e-03	3.602e-03	-2.114	-2.443	-0.329	28.94
CO3-2	5.878e-04	2.719e-05	-3.231	-4.566	-1.335	2.52
MgCO3	3.938e-04	3.938e-04	-3.405	-3.405	0.000	-17.10
CO2	4.478e-05	5.688e-05	-4.349	-4.245	0.104	35.16
Ca	9.479e-04					
Ca+2	9.479e-04	2.493e-04	-3.023	-3.603	-0.580	-15.85
Cl	1.405e+00					
Cl-	1.405e+00	8.253e-01	0.148	-0.083	-0.231	19.45
Mg	4.788e-02					
Mg+2	4.747e-02	1.371e-02	-1.324	-1.863	-0.539	-20.24
MgCO3	3.938e-04	3.938e-04	-3.405	-3.405	0.000	-17.10
MgOH+	8.699e-06	9.080e-06	-5.061	-5.042	0.019	(0)
Na	1.366e+00					
Na+	1.366e+00	1.008e+00	0.135	0.003	-0.132	0.43

S(6)	2.507e-02						
SO4-2	2.507e-02	1.101e-03	-1.601	-2.958	-1.358	21.27	
H2SO4-	2.247e-09	1.248e-09	-8.648	-8.904	-0.255	42.13	
Si	1.102e-03						
H4SiO4	1.003e-03	1.172e-03	-2.999	-2.931	0.068	51.03	
H3SiO4-	9.905e-05	3.578e-05	-4.004	-4.446	-0.442	29.46	
H2SiO4-2	4.699e-08	7.662e-10	-7.328	-9.116	-1.788	(0)	

-----Saturation indices-----

Phase	SI**	log IAP	log K(313 K, 1 atm)	
Akermanite	-9.06	33.75	42.80	Ca2MgSi2O7
Anhydrite	-2.11	-6.56	-4.45	CaSO4
Anthophyllite	14.47	77.22	62.75	Mg7Si8O22(OH)2
Antigorite	140.29	589.25	448.96	Mg48Si34O85(OH)62
Aragonite	0.16	-8.17	-8.33	CaCO3
Artinite	-0.52	18.05	18.57	Mg2CO3(OH)2:3H2O
Bischofite	-6.56	-2.16	4.41	MgCl2:6H2O
Bloedite	-5.51	-7.86	-2.35	Na2Mg(SO4)2:4H2O
Brucite	-2.04	-12.75	-10.71	Mg(OH)2
Burkeite	-9.69	-10.46	-0.77	Na6CO3(SO4)2
Calcite	0.48	-8.17	-8.65	CaCO3
Chalcedony	0.50	-2.89	-3.38	SiO2
Chrysotile	6.76	37.19	30.43	Mg3Si2O5(OH)4
CO2(g)	-2.62	-4.25	-1.63	CO2
Diopside	1.32	21.15	19.84	CaMgSi2O6
Dolomite	2.82	-14.60	-17.41	CaMg(CO3)2
Enstatite	0.81	11.45	10.63	MgSiO3
Epsomite	-3.22	-4.97	-1.75	MgSO4:7H2O
Forsterite	-0.35	25.78	26.13	Mg2SiO4
Gaylussite	-3.41	-12.83	-9.42	CaNa2(CO3)2:5H2O
Glauberite	-4.00	-9.51	-5.52	Na2Ca(SO4)2
Gypsum	-1.98	-6.60	-4.63	CaSO4:2H2O
H2O(g)	-1.16	-0.02	1.14	H2O
Halite	-1.69	-0.08	1.61	NaCl
Hexahydrite	-3.34	-4.95	-1.61	MgSO4:6H2O
Huntite	4.79	13.47	8.69	CaMg3(CO3)4
Kieserite	-4.29	-4.84	-0.55	MgSO4:H2O
Labile_S	-6.84	-12.51	-5.67	Na4Ca(SO4)3:2H2O
Leonhardite	-4.02	-4.91	-0.89	MgSO4:4H2O
Magnesite	1.46	-6.43	-7.89	MgCO3
MgCl2_2H2O	-15.44	-2.07	13.37	MgCl2:2H2O
MgCl2_4H2O	-8.79	-2.12	6.68	MgCl2:4H2O
Mirabilite	-2.50	-3.17	-0.67	Na2SO4:10H2O
Nahcolite	-1.93	-12.67	-10.74	NaHCO3

Natron	-3.95	-4.77	-0.82	Na ₂ CO ₃ :10H ₂ O
Nesquehonite	-1.33	-6.49	-5.17	MgCO ₃ :3H ₂ O
Pentahydrate	-3.64	-4.93	-1.28	MgSO ₄ :5H ₂ O
Pirssonite	-3.54	-12.77	-9.23	Na ₂ Ca(CO ₃) ₂ :2H ₂ O
Portlandite	-9.30	-14.49	-5.19	Ca(OH) ₂
Quartz	0.88	-2.89	-3.77	SiO ₂
Sepiolite	4.55	19.93	15.38	Mg ₂ Si ₃ O ₇ .5OH:3H ₂ O
Sepiolite(d)	1.27	19.93	18.66	Mg ₂ Si ₃ O ₇ .5OH:3H ₂ O
SiO ₂ (a)	-0.35	-2.89	-2.54	SiO ₂
Talc	11.66	31.43	19.77	Mg ₃ Si ₄ O ₁₀ (OH) ₂
Thenardite	-2.58	-2.95	-0.37	Na ₂ SO ₄
Trona	-5.89	-17.27	-11.38	Na ₃ H(CO ₃) ₂ :2H ₂ O

**For a gas, SI = log₁₀(fugacity). Fugacity = pressure * phi / 1 atm.
For ideal gases, phi = 1.

Initial solution 5.

-----Solution composition-----

Elements	Molality	Moles
Alkalinity	9.350e-03	9.350e-03
Ca	9.748e-04	9.748e-04
Cl	1.404e+00	1.404e+00
Mg	4.157e-02	4.157e-02
Na	1.366e+00	1.366e+00
S(6)	2.507e-02	2.507e-02
Si	1.102e-03	1.102e-03

-----Description of solution-----

pH = 8.050
pe = 4.000
Specific Conductance (μS/cm, 40°C) = 142710
Density (g/cm³) = 1.04786
Volume (L) = 1.03570
Activity of water = 0.952
Ionic strength (mol/kgw) = 1.524e+00
Mass of water (kg) = 1.000e+00
Total carbon (mol/kg) = 8.503e-03
Total CO₂ (mol/kg) = 8.503e-03
Temperature (°C) = 40.00
Electrical balance (eq) = -1.298e-02
Percent error, 100*(Cat-|An|)/(Cat+|An|) = -0.45
Iterations = 15 (76 overall)

Gamma iterations = 4
 Osmotic coefficient = 0.95650
 Density of water = 0.99221
 Total H = 1.110244e+02
 Total O = 5.563637e+01

-----Distribution of species-----

Species	MacInnes		MacInnes		mole V Gamma	cm ³ /mol
	Molality	Activity	Log Molality	Log Activity		
OH-	6.517e-06	3.128e-06	-5.186	-5.505	-0.319	-0.82
H+	8.652e-09	8.913e-09	-8.063	-8.050	0.013	0.00
H2O	5.551e+01	9.521e-01	1.744	-0.021	0.000	18.16
C(4)	8.503e-03					
HCO3-	7.653e-03	3.604e-03	-2.116	-2.443	-0.327	28.91
CO3-2	4.995e-04	2.370e-05	-3.301	-4.625	-1.324	2.50
MgCO3	2.989e-04	2.989e-04	-3.524	-3.524	0.000	-17.10
CO2	5.155e-05	6.533e-05	-4.288	-4.185	0.103	35.16
Ca	9.748e-04					
Ca+2	9.748e-04	2.568e-04	-3.011	-3.590	-0.579	-15.86
Cl	1.404e+00					
Cl-	1.404e+00	8.256e-01	0.147	-0.083	-0.231	19.45
Mg	4.157e-02					
Mg+2	4.127e-02	1.195e-02	-1.384	-1.923	-0.538	-20.25
MgCO3	2.989e-04	2.989e-04	-3.524	-3.524	0.000	-17.10
MgOH+	6.580e-06	6.891e-06	-5.182	-5.162	0.020	(0)
Na	1.366e+00					
Na+	1.366e+00	1.006e+00	0.135	0.003	-0.133	0.42
S(6)	2.507e-02					
SO4-2	2.507e-02	1.112e-03	-1.601	-2.954	-1.353	21.24
HSO4-	2.610e-09	1.448e-09	-8.583	-8.839	-0.256	42.13
Si	1.102e-03					
H4SiO4	1.015e-03	1.183e-03	-2.993	-2.927	0.066	51.03
H3SiO4-	8.635e-05	3.146e-05	-4.064	-4.502	-0.439	29.45
H2SiO4-2	3.524e-08	5.868e-10	-7.453	-9.232	-1.779	(0)

-----Saturation indices-----

Phase	SI**	log IAP	log K(313 K, 1 atm)	
Akermanite	-9.44	33.36	42.80	Ca2MgSi2O7
Anhydrite	-2.09	-6.54	-4.45	CaSO4
Anthophyllite	13.25	75.99	62.75	Mg7Si8O22(OH)2
Antigorite	131.79	580.75	448.96	Mg48Si34O85(OH)62

Aragonite	0.11	-8.22	-8.33	CaCO ₃
Artinite	-0.81	17.75	18.57	Mg ₂ CO ₃ (OH) ₂ :3H ₂ O
Bischofite	-6.62	-2.22	4.41	MgCl ₂ :6H ₂ O
Bloedite	-5.56	-7.91	-2.35	Na ₂ Mg(SO ₄) ₂ :4H ₂ O
Brucite	-2.22	-12.93	-10.71	Mg(OH) ₂
Burkeite	-9.75	-10.52	-0.77	Na ₆ CO ₃ (SO ₄) ₂
Calcite	0.44	-8.22	-8.65	CaCO ₃
Chalcedony	0.50	-2.88	-3.38	SiO ₂
Chrysotile	6.23	36.66	30.43	Mg ₃ Si ₂ O ₅ (OH) ₄
CO ₂ (g)	-2.56	-4.18	-1.63	CO ₂
Diopside	1.04	20.88	19.84	CaMgSi ₂ O ₆
Dolomite	2.65	-14.76	-17.41	CaMg(CO ₃) ₂
Enstatite	0.64	11.27	10.63	MgSiO ₃
Epsomite	-3.28	-5.03	-1.75	MgSO ₄ :7H ₂ O
Forsterite	-0.70	25.43	26.13	Mg ₂ SiO ₄
Gaylussite	-3.52	-12.94	-9.42	CaNa ₂ (CO ₃) ₂ :5H ₂ O
Glauberite	-3.98	-9.49	-5.52	Na ₂ Ca(SO ₄) ₂
Gypsum	-1.96	-6.59	-4.63	CaSO ₄ :2H ₂ O
H ₂ O(g)	-1.16	-0.02	1.14	H ₂ O
Halite	-1.69	-0.08	1.61	NaCl
Hexahydrate	-3.39	-5.00	-1.61	MgSO ₄ :6H ₂ O
Huntite	4.38	13.07	8.69	CaMg ₃ (CO ₃) ₄
Kieserite	-4.35	-4.90	-0.55	MgSO ₄ :H ₂ O
Labile_S	-6.81	-12.48	-5.67	Na ₄ Ca(SO ₄) ₃ :2H ₂ O
Leonhardite	-4.07	-4.96	-0.89	MgSO ₄ :4H ₂ O
Magnesite	1.34	-6.55	-7.89	MgCO ₃
MgCl ₂ _2H ₂ O	-15.50	-2.13	13.37	MgCl ₂ :2H ₂ O
MgCl ₂ _4H ₂ O	-8.85	-2.17	6.68	MgCl ₂ :4H ₂ O
Mirabilite	-2.49	-3.16	-0.67	Na ₂ SO ₄ :10H ₂ O
Nahcolite	-1.93	-12.67	-10.74	NaHCO ₃
Natron	-4.01	-4.83	-0.82	Na ₂ CO ₃ :10H ₂ O
Nesquehonite	-1.44	-6.61	-5.17	MgCO ₃ :3H ₂ O
Pentahydrate	-3.70	-4.98	-1.28	MgSO ₄ :5H ₂ O
Pirssonite	-3.64	-12.88	-9.23	Na ₂ Ca(CO ₃) ₂ :2H ₂ O
Portlandite	-9.41	-14.60	-5.19	Ca(OH) ₂
Quartz	0.89	-2.88	-3.77	SiO ₂
Sepiolite	4.20	19.58	15.38	Mg ₂ Si ₃ O ₇ .5OH:3H ₂ O
Sepiolite(d)	0.92	19.58	18.66	Mg ₂ Si ₃ O ₇ .5OH:3H ₂ O
SiO ₂ (a)	-0.35	-2.88	-2.54	SiO ₂
Talc	11.14	30.91	19.77	Mg ₃ Si ₄ O ₁₀ (OH) ₂
Thenardite	-2.58	-2.95	-0.37	Na ₂ SO ₄
Trona	-5.95	-17.34	-11.38	Na ₃ H(CO ₃) ₂ :2H ₂ O

**For a gas, SI = log₁₀(fugacity). Fugacity = pressure * phi / 1 atm.
For ideal gases, phi = 1.

Initial solution 6.

-----Solution composition-----

Elements	Molality	Moles
Alkalinity	9.440e-03	9.440e-03
Ca	1.002e-03	1.002e-03
Cl	1.404e+00	1.404e+00
Mg	4.291e-02	4.291e-02
Na	1.366e+00	1.366e+00
S(6)	2.507e-02	2.507e-02
Si	1.102e-03	1.102e-03

-----Description of solution-----

pH = 7.980
 pe = 4.000
 Specific Conductance ($\mu\text{S}/\text{cm}$, 40°C) = 142729
 Density (g/cm^3) = 1.04792
 Volume (L) = 1.03568
 Activity of water = 0.952
 Ionic strength (mol/kgw) = 1.527e+00
 Mass of water (kg) = 1.000e+00
 Total carbon (mol/kg) = 8.703e-03
 Total CO2 (mol/kg) = 8.703e-03
 Temperature (°C) = 40.00
 Electrical balance (eq) = -1.034e-02
 Percent error, $100 * (\text{Cat} - |\text{An}|) / (\text{Cat} + |\text{An}|)$ = -0.35
 Iterations = 15 (91 overall)
 Gamma iterations = 4
 Osmotic coefficient = 0.95665
 Density of water = 0.99221
 Total H = 1.110247e+02
 Total O = 5.563696e+01

-----Distribution of species-----

Species	MacInnes		MacInnes		mole V Gamma	cm ³ /mol
	Molality	Activity	Log Molality	Log Activity		
OH-	5.559e-06	2.662e-06	-5.255	-5.575	-0.320	-0.82
H+	1.016e-08	1.047e-08	-7.993	-7.980	0.013	0.00
H2O	5.551e+01	9.521e-01	1.744	-0.021	0.000	18.16
C(4)	8.703e-03					

HCO3-	7.926e-03	3.728e-03	-2.101	-2.428	-0.328	28.92
CO3-2	4.424e-04	2.087e-05	-3.354	-4.681	-1.326	2.50
MgCO3	2.719e-04	2.719e-04	-3.566	-3.566	0.000	-17.10
CO2	6.263e-05	7.940e-05	-4.203	-4.100	0.103	35.16
Ca	1.002e-03					
Ca+2	1.002e-03	2.640e-04	-2.999	-3.578	-0.579	-15.86
Cl	1.404e+00					
Cl-	1.404e+00	8.255e-01	0.147	-0.083	-0.231	19.45
Mg	4.291e-02					
Mg+2	4.263e-02	1.234e-02	-1.370	-1.909	-0.538	-20.24
MgCO3	2.719e-04	2.719e-04	-3.566	-3.566	0.000	-17.10
MgOH+	5.789e-06	6.058e-06	-5.237	-5.218	0.020	(0)
Na	1.366e+00					
Na+	1.366e+00	1.006e+00	0.135	0.003	-0.133	0.43
S(6)	2.507e-02					
SO4-2	2.507e-02	1.110e-03	-1.601	-2.955	-1.354	21.25
HSO4-	3.058e-09	1.697e-09	-8.515	-8.770	-0.256	42.13
Si	1.102e-03					
H4SiO4	1.027e-03	1.198e-03	-2.988	-2.922	0.067	51.03
H3SiO4-	7.455e-05	2.710e-05	-4.128	-4.567	-0.439	29.45
H2SiO4-2	2.597e-08	4.303e-10	-7.585	-9.366	-1.781	(0)

-----Saturation indices-----

Phase	SI**	log IAP	log K(313 K, 1 atm)
Akermanite	-9.81	32.99	42.80 Ca2MgSi2O7
Anhydrite	-2.08	-6.53	-4.45 CaSO4
Anthophyllite	12.41	75.16	62.75 Mg7Si8O22(OH)2
Antigorite	125.93	574.89	448.96 Mg48Si34O85(OH)62
Aragonite	0.07	-8.26	-8.33 CaCO3
Artinite	-0.98	17.59	18.57 Mg2CO3(OH)2:3H2O
Bischofite	-6.61	-2.20	4.41 MgCl2:6H2O
Bloedite	-5.55	-7.90	-2.35 Na2Mg(SO4)2:4H2O
Brucite	-2.35	-13.06	-10.71 Mg(OH)2
Burkeite	-9.80	-10.57	-0.77 Na6CO3(SO4)2
Calcite	0.39	-8.26	-8.65 CaCO3
Chalcedony	0.51	-2.88	-3.38 SiO2
Chrysotile	5.86	36.29	30.43 Mg3Si2O5(OH)4
CO2(g)	-2.48	-4.10	-1.63 CO2
Diopside	0.80	20.63	19.84 CaMgSi2O6
Dolomite	2.57	-14.85	-17.41 CaMg(CO3)2
Enstatite	0.52	11.15	10.63 MgSiO3
Epsomite	-3.26	-5.01	-1.75 MgSO4:7H2O
Forsterite	-0.95	25.18	26.13 Mg2SiO4
Gaylussite	-3.62	-13.04	-9.42 CaNa2(CO3)2:5H2O

Glauberite	-3.97	-9.48	-5.52	Na ₂ Ca(SO ₄) ₂
Gypsum	-1.95	-6.58	-4.63	CaSO ₄ :2H ₂ O
H ₂ O(g)	-1.16	-0.02	1.14	H ₂ O
Halite	-1.69	-0.08	1.61	NaCl
Hexahydrite	-3.38	-4.99	-1.61	MgSO ₄ :6H ₂ O
Huntite	4.22	12.90	8.69	CaMg ₃ (CO ₃) ₄
Kieserite	-4.33	-4.88	-0.55	MgSO ₄ :H ₂ O
Labile_S	-6.80	-12.47	-5.67	Na ₄ Ca(SO ₄) ₃ :2H ₂ O
Leonhardite	-4.06	-4.95	-0.89	MgSO ₄ :4H ₂ O
Magnesite	1.30	-6.59	-7.89	MgCO ₃
MgCl ₂ _2H ₂ O	-15.49	-2.12	13.37	MgCl ₂ :2H ₂ O
MgCl ₂ _4H ₂ O	-8.84	-2.16	6.68	MgCl ₂ :4H ₂ O
Mirabilite	-2.50	-3.16	-0.67	Na ₂ SO ₄ :10H ₂ O
Nahcolite	-1.92	-12.66	-10.74	NaHCO ₃
Natron	-4.06	-4.89	-0.82	Na ₂ CO ₃ :10H ₂ O
Nesquehonite	-1.49	-6.65	-5.17	MgCO ₃ :3H ₂ O
Pentahydrite	-3.69	-4.97	-1.28	MgSO ₄ :5H ₂ O
Pirssonite	-3.74	-12.98	-9.23	Na ₂ Ca(CO ₃) ₂ :2H ₂ O
Portlandite	-9.54	-14.73	-5.19	Ca(OH) ₂
Quartz	0.89	-2.88	-3.77	SiO ₂
Sepiolite	3.96	19.35	15.38	Mg ₂ Si ₃ O ₇ .5OH:3H ₂ O
Sepiolite(d)	0.69	19.35	18.66	Mg ₂ Si ₃ O ₇ .5OH:3H ₂ O
SiO ₂ (a)	-0.34	-2.88	-2.54	SiO ₂
Talc	10.78	30.55	19.77	Mg ₃ Si ₄ O ₁₀ (OH) ₂
Thenardite	-2.58	-2.95	-0.37	Na ₂ SO ₄
Trona	-5.99	-17.38	-11.38	Na ₃ H(CO ₃) ₂ :2H ₂ O

**For a gas, SI = log₁₀(fugacity). Fugacity = pressure * phi / 1 atm.
For ideal gases, phi = 1.

Initial solution 7.

-----Solution composition-----

Elements	Molality	Moles
Alkalinity	9.477e-03	9.477e-03
Ca	1.029e-03	1.029e-03
Cl	1.404e+00	1.404e+00
Mg	4.305e-02	4.305e-02
Na	1.366e+00	1.366e+00
S(6)	2.507e-02	2.507e-02
Si	1.102e-03	1.102e-03

-----Description of solution-----

pH = 7.050
 pe = 4.000
 Specific Conductance ($\mu\text{S}/\text{cm}$, 40°C) = 142740
 Density (g/cm^3) = 1.04794
 Volume (L) = 1.03574
 Activity of water = 0.952
 Ionic strength (mol/kgw) = 1.528e+00
 Mass of water (kg) = 1.000e+00
 Total carbon (mol/kg) = 9.991e-03
 Total CO2 (mol/kg) = 9.991e-03
 Temperature ($^\circ\text{C}$) = 40.00
 Electrical balance (eq) = -1.005e-02
 Percent error, $100 \cdot (\text{Cat} - |\text{An}|) / (\text{Cat} + |\text{An}|)$ = -0.34
 Iterations = 15 (106 overall)
 Gamma iterations = 4
 Osmotic coefficient = 0.95677
 Density of water = 0.99221
 Total H = 1.110261e+02
 Total O = 5.564025e+01

-----Distribution of species-----

Species	MacInnes		MacInnes		mole V Gamma	cm \geq /mol
	Molality	Activity	Log Molality	Log Activity		
OH-	6.536e-07	3.128e-07	-6.185	-6.505	-0.320	-0.82
H+	8.644e-08	8.913e-08	-7.063	-7.050	0.013	0.00
H2O	5.551e+01	9.521e-01	1.744	-0.021	0.000	18.16
C(4)	9.991e-03					
HCO3-	9.269e-03	4.359e-03	-2.033	-2.361	-0.328	28.92
CO2	6.231e-04	7.901e-04	-3.205	-3.102	0.103	35.16
CO3-2	6.090e-05	2.866e-06	-4.215	-5.543	-1.327	2.50
MgCO3	3.773e-05	3.773e-05	-4.423	-4.423	0.000	-17.10
Ca	1.029e-03					
Ca+2	1.029e-03	2.721e-04	-2.988	-3.565	-0.578	-15.86
Cl	1.404e+00					
Cl-	1.404e+00	8.255e-01	0.147	-0.083	-0.231	19.45
Mg	4.305e-02					
Mg+2	4.301e-02	1.247e-02	-1.366	-1.904	-0.538	-20.24
MgCO3	3.773e-05	3.773e-05	-4.423	-4.423	0.000	-17.10
MgOH+	6.871e-07	7.190e-07	-6.163	-6.143	0.020	(0)
Na	1.366e+00					
Na+	1.366e+00	1.007e+00	0.135	0.003	-0.133	0.43
S(6)	2.507e-02					
SO4-2	2.507e-02	1.108e-03	-1.601	-2.955	-1.355	21.25

HSO4-	2.599e-08	1.443e-08	-7.585	-7.841	-0.256	42.13
Si	1.102e-03					
H4SiO4	1.093e-03	1.274e-03	-2.962	-2.895	0.067	51.03
H3SiO4-	9.323e-06	3.387e-06	-5.030	-5.470	-0.440	29.45
H2SiO4-2	3.821e-10	6.319e-12	-9.418	-11.199	-1.782	(0)

-----Saturation indices-----

Phase	SI**	log IAP	log K(313 K, 1 atm)	
Akermanite	-15.31	27.50	42.80	Ca ₂ MgSi ₂ O ₇
Anhydrite	-2.07	-6.52	-4.45	CaSO ₄
Anthophyllite	-0.37	62.38	62.75	Mg ₇ Si ₈ O ₂₂ (OH) ₂
Antigorite	37.77	486.73	448.96	Mg ₄₈ Si ₃₄ O ₈₅ (OH) ₆₂
Aragonite	-0.78	-9.11	-8.33	CaCO ₃
Artinite	-3.70	14.87	18.57	Mg ₂ CO ₃ (OH) ₂ :3H ₂ O
Bischofite	-6.61	-2.20	4.41	MgCl ₂ :6H ₂ O
Bloedite	-5.55	-7.89	-2.35	Na ₂ Mg(SO ₄) ₂ :4H ₂ O
Brucite	-4.20	-14.91	-10.71	Mg(OH) ₂
Burkeite	-10.66	-11.44	-0.77	Na ₆ CO ₃ (SO ₄) ₂
Calcite	-0.46	-9.11	-8.65	CaCO ₃
Chalcedony	0.53	-2.85	-3.38	SiO ₂
Chrysotile	0.35	30.78	30.43	Mg ₃ Si ₂ O ₅ (OH) ₄
CO ₂ (g)	-1.48	-3.10	-1.63	CO ₂
Diopside	-2.85	16.98	19.84	CaMgSi ₂ O ₆
Dolomite	0.86	-16.56	-17.41	CaMg(CO ₃) ₂
Enstatite	-1.31	9.32	10.63	MgSiO ₃
Epsomite	-3.26	-5.01	-1.75	MgSO ₄ :7H ₂ O
Forsterite	-4.63	21.50	26.13	Mg ₂ SiO ₄
Gaylussite	-5.33	-14.75	-9.42	CaNa ₂ (CO ₃) ₂ :5H ₂ O
Glauberite	-3.95	-9.47	-5.52	Na ₂ Ca(SO ₄) ₂
Gypsum	-1.93	-6.56	-4.63	CaSO ₄ :2H ₂ O
H ₂ O(g)	-1.16	-0.02	1.14	H ₂ O
Halite	-1.69	-0.08	1.61	NaCl
Hexahydrite	-3.38	-4.99	-1.61	MgSO ₄ :6H ₂ O
Huntite	0.79	9.48	8.69	CaMg ₃ (CO ₃) ₄
Kieserite	-4.33	-4.88	-0.55	MgSO ₄ :H ₂ O
Labile_S	-6.79	-12.46	-5.67	Na ₄ Ca(SO ₄) ₃ :2H ₂ O
Leonhardite	-4.06	-4.95	-0.89	MgSO ₄ :4H ₂ O
Magnesite	0.44	-7.45	-7.89	MgCO ₃
MgCl ₂ _2H ₂ O	-15.48	-2.11	13.37	MgCl ₂ :2H ₂ O
MgCl ₂ _4H ₂ O	-8.83	-2.16	6.68	MgCl ₂ :4H ₂ O
Mirabilite	-2.50	-3.16	-0.67	Na ₂ SO ₄ :10H ₂ O
Nahcolite	-1.85	-12.59	-10.74	NaHCO ₃
Natron	-4.93	-5.75	-0.82	Na ₂ CO ₃ :10H ₂ O
Nesquehonite	-2.34	-7.51	-5.17	MgCO ₃ :3H ₂ O

Pentahydrate	-3.68	-4.97	-1.28	MgSO4:5H2O
Pirssonite	-5.45	-14.69	-9.23	Na2Ca(CO3)2:2H2O
Portlandite	-11.38	-16.57	-5.19	Ca(OH)2
Quartz	0.92	-2.85	-3.77	SiO2
Sepiolite	0.33	15.72	15.38	Mg2Si3O7.5OH:3H2O
Sepiolite(d)	-2.94	15.72	18.66	Mg2Si3O7.5OH:3H2O
SiO2(a)	-0.31	-2.85	-2.54	SiO2
Talc	5.32	25.09	19.77	Mg3Si4O10(OH)2
Thenardite	-2.58	-2.95	-0.37	Na2SO4
Trona	-6.79	-18.17	-11.38	Na3H(CO3)2:2H2O

**For a gas, $SI = \log_{10}(\text{fugacity})$. Fugacity = pressure * ϕ / 1 atm.
 For ideal gases, $\phi = 1$.

 End of simulation.

 Reading input data for simulation 2.

 End of Run after 0.014397 Seconds.
